ISSN 2188-286X

マス・フォア・インダストリ研究　No.2

Collaboration Between Theory and Practice in Inverse Problems

Institute of Mathematics for Industry
Kyushu University

編　集　滝口 孝志
　　　　藤原 宏志

九州大学マス・フォア・インダストリ研究所

Collaboration between theory and practice in inverse problems

Editors :
Takashi Takiguchi
National Defense Academy of Japan
and
Hiroshi Fujiwara
Kyoto University

About the Mathematics for Industry Research

The Mathematics for Industry Research was founded on the occasion of the certification of the Institute of Mathematics for Industry (IMI), established in April 2011, as a MEXT Joint Usage/Research Center – the Joint Research Center for Advanced and Fundamental Mathematics for Industry – by the Ministry of Education, Culture, Sports, Science and Technology (MEXT) in April 2013. This series publishes mainly proceedings of workshops and conferences on Mathematics for Industry (MfI). Each volume includes surveys and reviews of MfI from new viewpoints as well as up-to-date research studies to support the development of MfI.

October 2014
Yasuhide Fukumoto
Director
Institute of Mathematics for Industry

Collaboration between theory and practice in inverse problems

Mathematics for Industry Research No.2, Institute of Mathematics for Industry, Kyushu University

ISSN 2188-286X

Editors: Takashi Takiguchi, Hiroshi Fujiwara

Date of issue: 12 March 2015

Publisher:

Institute of Mathematics for Industry, Kyushu University

Motooka 744, Nishi-ku, Fukuoka, 819-0395, JAPAN

Tel +81-(0)92-802-4402, Fax +81-(0)92-802-4405

URL http://www.imi.kyushu-u.ac.jp/

Printed by

Social Welfare Service Corporation Fukuoka Colony

1-11-1, Midorigahama, Shingu-machi Kasuya-gun, Fukuoka, 811-0119, Japan

TEL +81-(0)92-962-0764 FAX +81-(0)92-962-0768

Preface

These are the proceedings of the conference “Collaboration between theory and practice in inverse problems”, held at IMI, Kyushu University, from December sixteenth to December ninteenth, 2014. The main topic in this conference was “Rearrangement of the infrastructure”. During the conference, the following problems and invetigations on them were reported and lively dicussions were had on them. We had the following talks during the conference. Remark that they are brief explanations of the talks, not the titles.

- Mr. Kenji Hashizume : Orginally developed inspection techniques and unsolved problems for maintenance of the expressways.
- Prof. Kil Hyun Kwon : Sampling theory in relation with the frame theory.
- Prof. Cheng Hua : Evaluation of cracks in view of fracture mechanics and mechanics of materials.
- Prof. Noriyuki Mita : Basic propertiers of concrete and its non destructive testing with application of acoustic tomography.
- Prof. Yuko Hatano : Mathematical model for migration of radionuclides near Fukushima.
- Prof. Kohji Ohtsuka : Mathematical treatment of perturbation of singular points in continuum mechanics and its application to shape optimization.

On the first day of the conference, Mister Kenji Hashizume gave a talk to introduce the techniques for the inspection of the expressways developed by West Nippon Expressway Shikoku Company Limited. He also posed several open problems for the development of the non-destructive testing of the tunnels and bridges of the expressways, which have a lot to do with mathematical ideas, integral geometry, propagation of cracks in elastic bodies and so on as well as the concrete structures. In response to his talk, we discussed how to give mathematical models for the problems posed by Mr. Hashizume and how to solve them.

On the second day, in the morning, Professor Kil Hyun Kwon gave a talk on sampling theory based on the theory of the frame theory, which will be made use of for the implimentation of the research results applying numerical calculatoin by computers. In the afternoon, Professor Cheng Hua gave a talk on the cracks in the elastic body, from the viewpoint of mechanics and engineering science. His lecture will be of help to give mathematical formulations of the problems posed by Mr. Hashizume. In the afternoon, Professor Cheng Hua gave a talk on how to describe the propagation of cracks in view of fracture mechanics and mechanics of materials. After thier talks, lively dicussions were had on them.

In the morning on December 18th, Professor Noriyuki Mita talked on basic propertiers of concrete and its non destructive testing with application of acoustic tomography. No determinate non-destrucive testing method for concrete structures being known for the time being, it is very important for rearrangement of infrastracture to study the problem to establish a determinate non-deestrucive testing method posed in this talk. During his talk, a number of questiones were asked and we had vigorous dicussions. In the afternoon, Professor Yuko Hatano gave a talk on very important problems. She introduced some mathematical models to describe the migration of radionuclides near Fukushima area. She also posed several problems how to predict migration of radionuclides, which is essentially important for reconstruction of infrastructure and rearrangement of environment in Fukushima prefecture. During her talk, there were many questions asked by the audience and many problems, including a modification of the introduced mathematical models to describe migration of radionuclides, were discussed.

On the final day, Professor Kohji Ohtsuka introduced theory on the progation of the cracks in relation with its application to fracture mechanics and shape optimization. It is very interesting and important in view of its application for the testing methods of concrete structures. It is also intersting from the viewpoint of mathematics. After his talk, an application of microlocal approach to the model for crack propagation was discussed, in addition to which, many queations in view of engineering appraoch were asked and suggestive and fruitful discussions were had on his talk.

We wish that we would have more opportunities to hold such conferences to discuss important problems in the rearrangement of infrastructure based on the collaboration between theory and practice, and that this kind of collaboration would be more popular in mathematics, engineering and pracitical industry.

At the end of Preface, we would express our gratefulness to Ms. Kyoko Sakaguchi and Ms. Kazuko Ito, the secretaries of this conference, for their faithful help.

January 31, 2015

Takashi Takiguchi
Hiroshi Fujiwara

Collaboration between theory and practice in inverse problems

December 16-19, 2014

IMI, Ito Campus, Kyushu Univeristy
Seminar Room 7, Faculty of Mathematics building
744 Motooka, Nishi-ku Fukuoka 819-0395, Japan

December 16, Tuesday

13:50 Opening

(Chair: T. Takiguchi)

14:00-15:00 Kenji Hashizume
(West Nippon Expressway Shikoku Company Limited, Japan)
Inspection of bridges, tunnels, and pavement by using cameras

15:30-16:30 Discussion

December 17, Wednesday

(Chair: A. Kaneko)

11:00-12:30 Kil Hyun Kwon (KAIST, Korea)
Beyond Shannon: Generalized Sampling

14:00-15:30 Cheng Hua (Fudan University, China)
Evaluation of crack tip fields and role of fracture mechanics

15:30-16:30 Discussion

December 18, Thursday

(Chair: H. Fujiwara)

11:00-12:30 Noriyuki Mita (Polytechnic University of Japan) and
Takashi Takiguchi (National Defense Academy of Japan)
Basic propertiers of concrete and its non destructive testing

14:00-15:30 Yuko Hatano (Tsukuba University, Japan)
Modeling of atmospheric- and underground migration of radionuclides
in the 100 km vicinity of Fukushima

15:30-16:30 Discussion

December 19, Friday

(Chair: C. Hua)

11:00-12:30 Kohji Ohtsuka (Hiroshima Kokusai Gakuin University, Japan)
Mathematical theory on perturbation of singular points in continuum mechanics and its application to fracture and shape optimization

13:30 Closing

Organizers:

Hiroshi Fujiwara (Kyoto University, Japan)
Takashi Takiguchi (National Defense Academy of Japan)

Supported by:

IMI, Kyushu University
JSPS Grant-in-Aid for Scientific Research Research (C) 26400184 and (C) 26400198

Table of contents

Inspection of bridges, tunnels, and pavement by using cameras

Kenji Hashizume

West Nippon Expressway Shikoku Company Limited

I. Outline

A lot of resources and costs would be necessary for infrastructure developments and rehabilitations. So the followings are very important: (i) managing, repairing, and renewing the developed infrastructures efficiently and effectively, and (ii) eliminating serious accidents triggered by the deteriorations and damages, and realizing the society without any anxiety. This is necessary for the utilization of the limited resources and the sustainable development of the society. For the given purpose, the efficient and effective inspections and maintenance practice shall be necessary. The inspection method using cameras for the bridges, tunnels, and pavements inspections with objective evaluations and keeping their records is now proposed.

II. Bridge Inspections

We now explain the “J-System” (Figure-1) for the inspection method using the infrared cameras.

The reinforced concrete fulfill its role with the joint functioning of rebar and concrete for the concrete structure. When the rebar gathers rust in the concrete, cracks appear on the concrete surface along the rebar, the surface concrete spalls, and so its durability is to be reduced. We have been inspecting the cracks triggered by the concrete delaminations along the rebar through the hammering. The infrared cameras inspection is the new one detecting the damaged areas such as concrete delaminations and cracks through photographing the concrete surface by using infrared cameras from remote palaces, and keeping the records of the concrete surface conditions using digital cameras. The inspections of bridges surface by infrared cameras are done by the passive method, and the followings are the important elements;

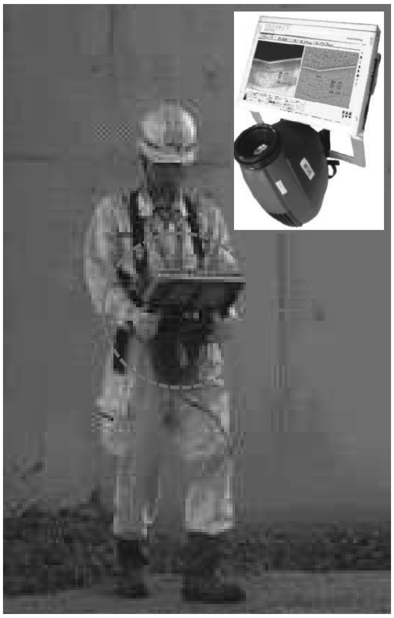

figure -1　J-system

i. **Cameras Quality (Is the cameras suitable for the inspection environment?)**

Inspections are done basically during night, so it is important to extend the surveillance hours of the day and increase the annual surveillance days by using the camera with a short- wave type which has no the environmental reflections during night and with a enforcing-cooling- system type with a small thermal resolution.

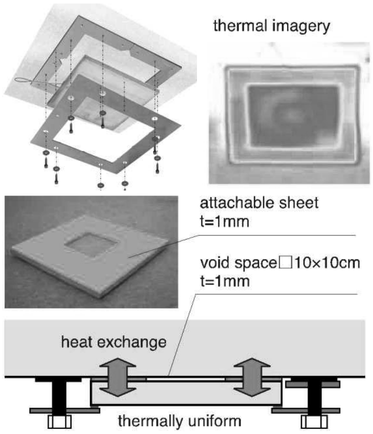

figure -2 J-system EM(S)

ii. **judgment on time zone of the day when inspections can be done (Do we inspect at a suitable time ?)**

We implement the night- time inspection basically, because there are various bridge types and bridge members which are not suitable to inspect during daytime. The time zone of the day when inspection is possible is based on data of the EMS (Environment Measuring System)(Figure-2) mounted on the inspection bridges.

iii. **Simple and Objective Evaluation Method**
(Is it possible and easy to evaluate objectively?)

There could be, for individuals, differences among the inspection judgments because it is sometime impossible to judge the damage evaluation such as delamination and spalling for the bridge members and damaged parts only by looking at the infrared images. It is also impossible to judge the crack's depth along the rebar. However, the red, yellow, and blue cracks' judgment- images at the 1, 2, 3 cm depth from the surface are shown at the camera monitor (Figure -3).

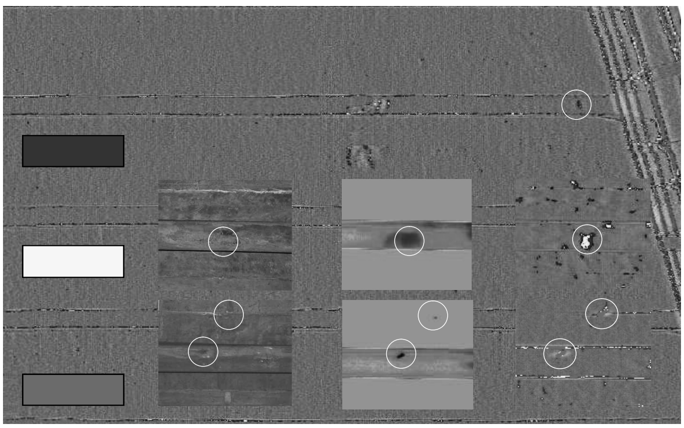
figure -3 J-System Monitor Image

III. Tunnel and Pavement Inspection

We now explain the “L & L System” (Figure-4) inspection method which uses the Line Censor Camera and Laser Marker. Line Censor cameras mount the visual image censors, and can photograph seamless and continuous imageries. They can also be applied for the tunnel and pavement inspections.

Light Cutting method is photographing the laser marker images from a upper and oblique position by using the laser which is irradiated vertically down on measuring surfaces and obtain the object shape. This method is used for road surface profile measuring.

figure -4　L&L　System

i. Tunnel Inspection

It is possible to obtain the fine and colorful continuous images (Figure-5) of tunnel lining by using Line Censor cameras mounted on the inspection cars with high speed (less than 100km/h). The cracks of tunnel lining can be detected up to 0.2mm, and water leakage and lime isolation can be also found. The damage spreading drawings and their diagonal charts can easily be produced based on the captive pictures, and so we inspect only the areas where further close and detail investigations are necessary. And we can clearly watch the conditions of rusted accessories in tunnels, and so it is now possible to apply them for the accessories inspections.

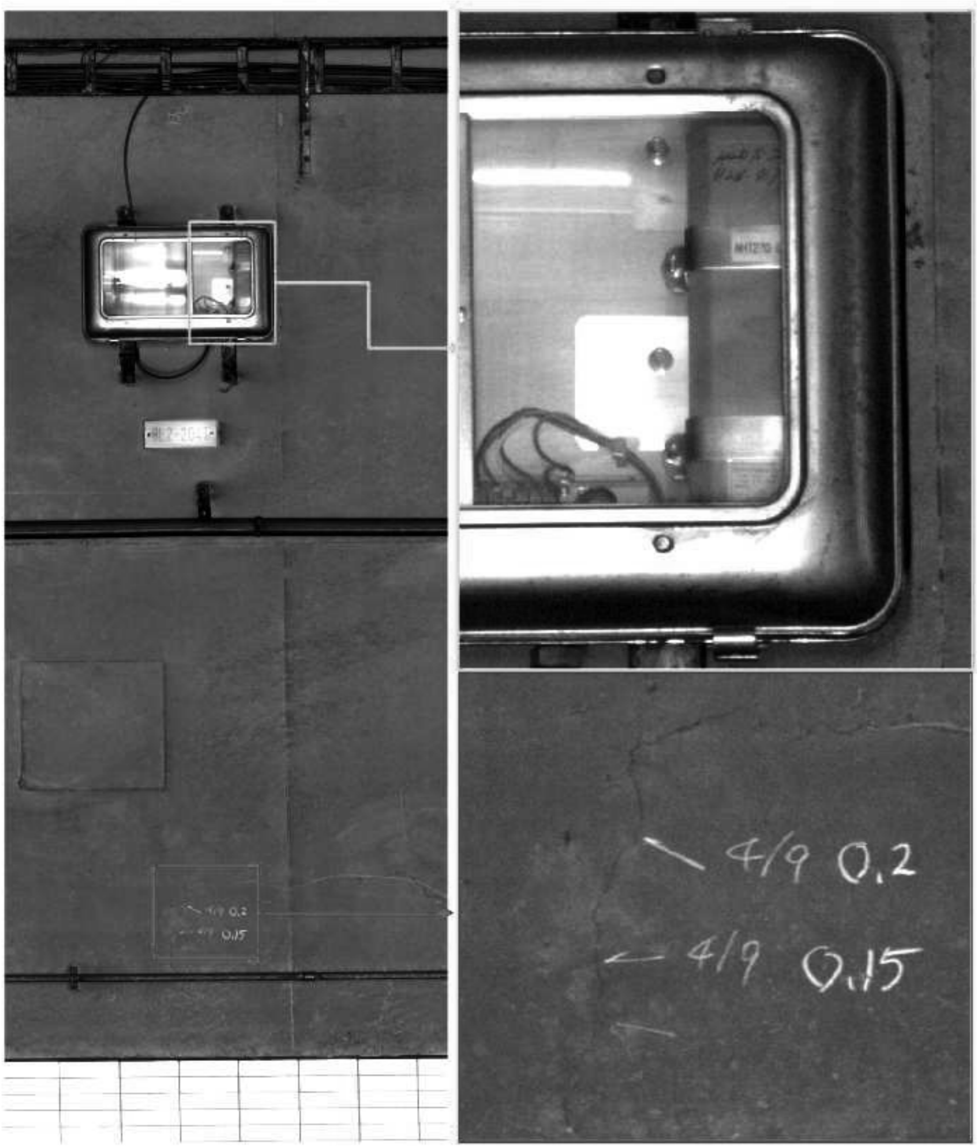

figure -5　Visual image with cracks and the accessories

ii. Pavement Inspection

We can inspect the pavement conditions such as cracks and potholes, and conditions of bridge expansion joints by using Line Censer cameras mounted on the vehicle with high speed (less than 100km/h). At the same time, we can also measure rutting, bumps, and upheaval through using laser cameras, and measure road surface profile such as height, and also evaluate the evenness, bump and IRI values.

We can also display the grade evaluation for the cracks, rutting, bumps, evenness, and IRI values obtained by the road surface measurements, and we can also easily sort and extract some of the data with abnormal ranges which show more than a certain threshold (Figure-6). Thus, the repairing and renewal plans of road pavement and the bumps will be made easier.

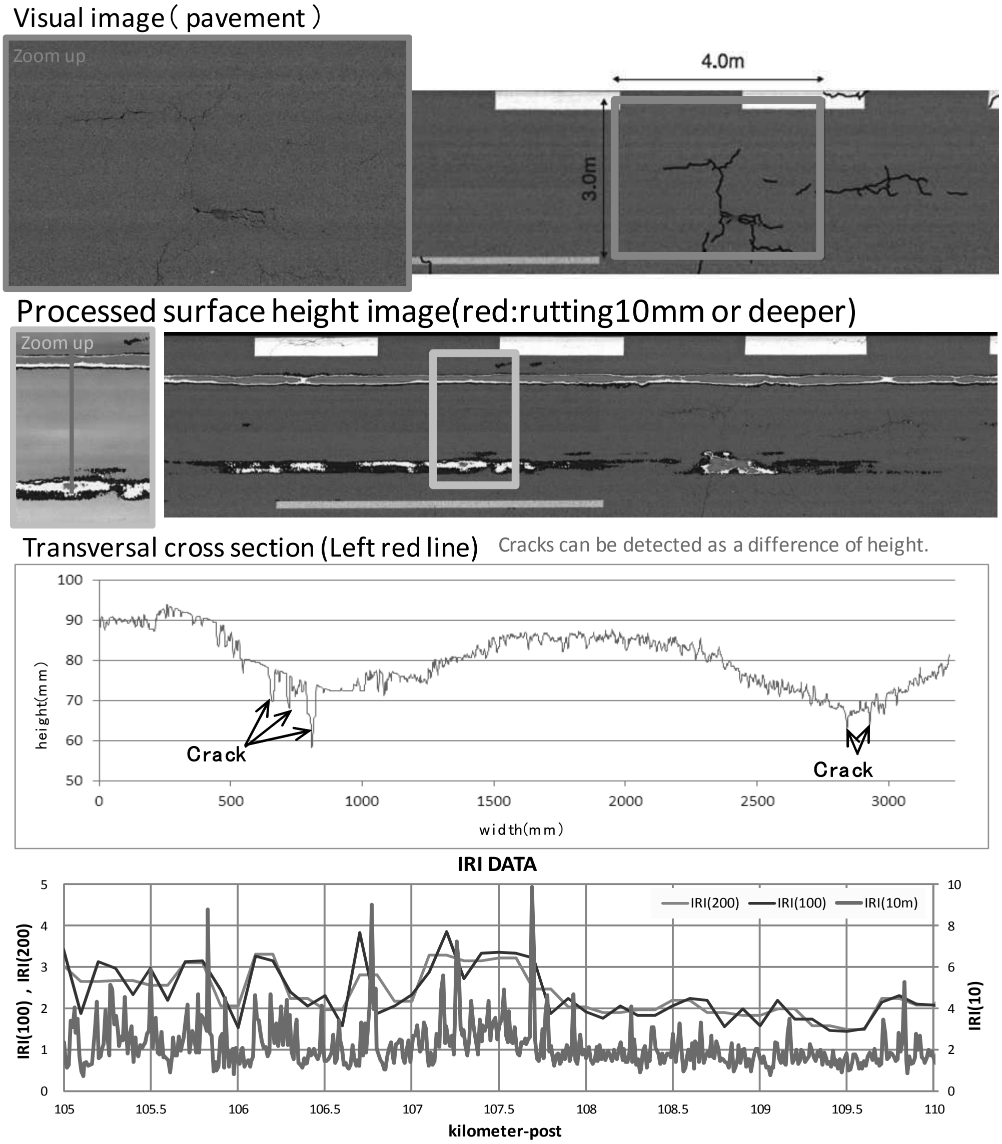

figure -6　Pavement evaluation

Also, we can measure the inner damages such as layer delamination and cracks of pavement by using infrared cameras (Figure-7).

Cracks Image　IR Raw Image　IR Prosess Image

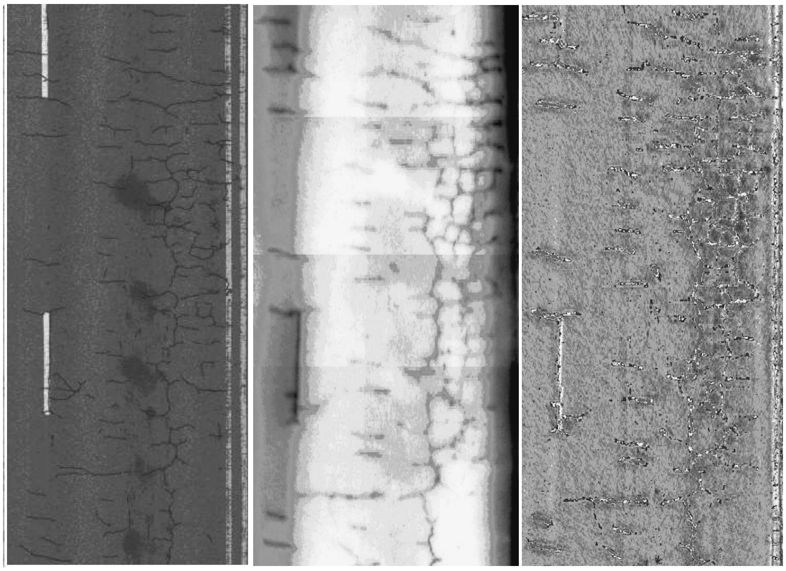

figure -7　Pavement IR evaluation

IV. Conclusion

The bridges, tunnels, and pavement inspections by cameras can be used for the assistances for the on-site inspections or their alternatives, and we can maintain the objective evaluations and predict the future damages through their annual transitions. Also the repairing plan can be made easily and efficiently.

The proposed inspection method using the cameras makes it possible to use, select and combine those inspection tools economically and effectively in accordance with budges and utilizations patterns of each organization based on their different road structure maintenance and repairing standards.

Finally, we show the demonstration of the inspection technology implemented at Singapore in February 2014. We inspected the bridges using infrared cameras. For the pavement inspections, we used the Deck Top Scanning System which combines the photographing by Line Censer cameras mounted on the high-speed vehicles and the repairing survey of the pavement by infrared cameras(Figure-8). A lot of participants welcomed and evaluated our technology in good favors at the exhibition.

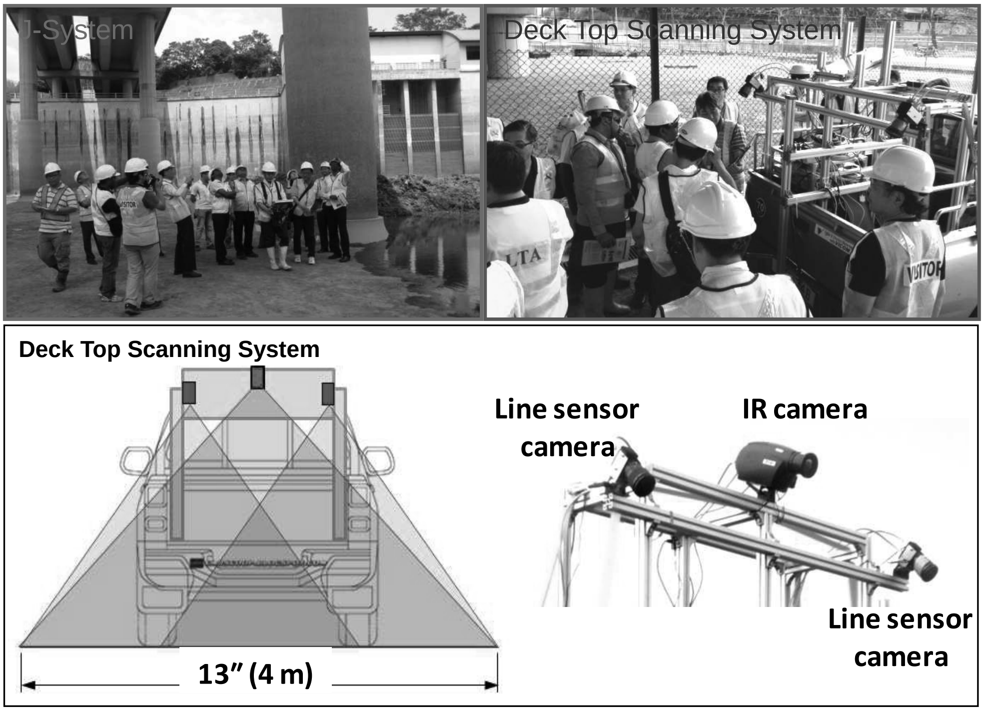

figure-8 Situation of the Demonstration

References (in Japanese)

1. 福田泰樹, 貝戸清之, 橋爪謙治, 横山和明,
"RC床版の統計的劣化予想と補修効果の事後評価",
コンクリート工学年次論文集, Vol.33, No.2, pp.1495-1500.(2011)

2. 貝戸清之, 起塚亮輔, 伊藤哲男, 橋爪謙治, 出口宗浩,
"床版かぶりコンクリートの剥離・剥落発生リスクと最適点検政策",
土木学会論文集F4, Vol.68, No.1, pp.11-27.(2012)

3. 貝戸清之, 福田泰樹, 起塚亮輔, 橋爪謙治, 出口宗浩, 横山和昭,
"遊離石灰法に基づくRC床版の劣化予測および補修優先順位の決定",
土木学会論文集F4, Vol.68, No.3, pp.123-140.(2012)

4. 橋爪謙治, 橋本和明, 全邦釘,
"同時生起行列を用いた赤外線サーモグラフィ法
自動診断支援システムの基礎研究",
コンクリート工学年次論文集, Vol. 36, No.2, pp.2002-2007. (2014)

5. 橋爪謙治, 橋本和明, 明石行雄, 全邦釘,
"排水性舗装の基層以深の劣化を要因としたポットホール発生予測手法の一提案",
土木学会論文集E1, Vol. 70, No. 3, pp.I_17-I_24. (2014)

Appendix

About unsolved problems in the maintenance of the expressways

By Takashi Takiguchi

In the first day of the conference, Mr Kenji Hashizume gave a very interesting talk on the testing techniques originally developed by West Nippon Expressway Shikoku Company Limited, which was introduced in the main part of this paper. The organizers of this conference were suprized and moved very much at the orinigality and creativity of the West Nippon Expressway Shikoku Company Limited to develop both the devises and the ideas for the inspection of the expressways.

Although Mr. Hashizume would have not mentioned them in the main part of this paper, he introduced a number of unsolved problems in the maintenance of the expressways in his talk. Since they are interesting and important in view of rearrangement of infrastructure, the main topic of this conference, the author of this appendix would summarize some of them, as an organizer of this conference. Among the problems Mr. Hashizume introduced were

- How to predict and prevent the concrete flaking accsident of tunnels (unreinforced concrete structures).
- How to predict and prevent the concrete flaking accsident of expressway bridges (reinforced concrete structures).
- How to predict and prevent the pot holes on the pavements

For the first and second problems, confer the references 1 ～ 5.

For the last one, confer the reference 6.

The main part of this paper were devoted to introduce the devices and the testing techniques originally developed by West Nippon Expressway Shikoku Company Limited, however, Mr. Hashizume mentioned a number of unsolved problems left to be solved for further development which would be very important not only for the maintenance of expressway but for the maintenance of a lot of concrete structures, especially in view of the rearrangement of infrastructure. For their solution, it is very important to study the cracks, for which confer the papers in these proceedings by Professor Cheng Hua (Fudan University, China) in view of fracture mechanics and mechanics of materials, and by Professor Kohji Ohtsuka (Hiroshima Kokusai Gakuin University, Japan) from mathematical approach. Since it is very difficult to describe the propagation of cracks, together with many other reasons, there are many unsolved problems for the inspection of flaking phenomena of the concrete structures.

The author of this appendix is very sorry that we cannot mention the open problems mentioned above in detail because of some restriction. Instead, let us introduce another problem possibly essentially important for the maintenance of a lot of concrete structures in view of the rearrangement of infrastructure. West Nippon Expressway Shikoku Company Limited, Professor Noriyuki Mita (Polytechnic University of Japan) and the author of this appendix are collaborating to develop a determinate non-destructing testing method applying acoustic tomography, for which confer the paper in this proceedings by Prof. Mita and the author of this appendix.

The author of this appendix hopes not only that his collaboration with West Nippon Expressway Shikoku Company Limited would make important contribution to develop determinate testing methods for the maintenance of expressways, but that we would make a breakthrough in the study of concrete structure through this collaboration.

Beyond Shannon: Generalized Sampling

Sinuk Kang[1], Kil Hyun Kwon[2], and Dae Gwan Lee[2]

Abstract

We give an expository account on the classical sampling theorem and its generalizations. We first introduce the classical Shannon sampling theorem on Paley-Wiener spaces with two different proofs. We then treat some extensions of the theorem from Paley-Wiener spaces to shift invariant spaces. Generalized sampling such as regular, irregular, multi-channel, average sampling in shift invariant spaces are considered. We also cover the topics of consistent sampling in abstract Hilbert spaces and oversampling in MRA.

It is not enough for you to have a good product to sell; you must package it right and advertise it properly. Otherwise, you will go out of business.

from Personal Opinion by Gian-Carlos Rota, Notices of AMS, Dec. 1992.

1 Introduction

Think analog. But act digital.

In signal processing, "sampling" is the reduction of a continuous-time signal (analog signal) $f(t)$ into a discrete-time signal $\{\, f(t_n)\}_{n\in\mathbb{Z}}$ (discrete signal). Then our goal is to recover $f(t)$ by $\{\, f(t_n)\}_{n\in\mathbb{Z}}$ as

$$f(t) = \sum_{n\in\mathbb{Z}} f(t_n)\, S_n(t) \ \Big(\text{or } f(t) = \sum_j \sum_n \mathcal{L}_j(f)(t_{j,n})\, S_{j,n}(t) \Big)$$

where $\{S_n(t)\}_{n\in\mathbb{Z}}$ are reconstruction functions, which are independent of individual signals.

Two fundamental questions are i) what class of analog signals admits such sampling series? and ii) how one can take sample points $\{t_n\}$ and reconstruction functions $\{S_n(t)\}$?

As extreme examples we have: any straight line can be completely recovered by its values at two distinct points, say at $t = 0, 1$ as

$$f(t) = at + b = f(0)\,(1-t) + f(1)\,t,$$

and any entire analytic function can be completely recovered by its successive derivatives at $z = 0$ as

$$f(z) = \sum_{n=0}^{\infty} \frac{1}{n!} f^{(n)}(0) z^n.$$

A signal $f(t)$ of finite energy (i.e., $f(t) \in L^2(\mathbb{R})$) is band-limited if its Fourier transform (frequency spectrum) $\hat{f}(\xi) = \int_{-\infty}^{\infty} f(t)e^{-it\xi}dt$ has compact support.

For any $B > 0$, Paley-Wiener space is defined as

$$\begin{aligned} PW_B &:= \{f(t) \in L^2(\mathbb{R}) : \text{supp } \hat{f}(\xi) \subseteq [-B, B]\} \\ &= \{f(z) \in E_B : f(t) \in L^2(\mathbb{R})\} \end{aligned}$$

where E_B is the space of entire analytic functions of exponential type $\leq B$.

Two early main contributors in signal processing are electrical engineer H. Nyquist and applied mathematician C. E. Shannon. H. Nyquist ([21]) showed that for a complete recovery, one should sample at a rate at least twice the bandwidth of a signal. C. E. Shannon introduced, among others, the now everyday word 'bit' (binary digit) and the information theory. See [28] for an excellent survey on the development of the sampling theory.

Figure 1: H. Nyquist (left) and C. E. Shannon (right)

Theorem 1 (Whittaker-Shannon-Kotel'nikov-Someya sampling theorem)([24, 25])**.** *Any signal $f(t)$ in PW_B can be reconstructed by its uniform sample values as a cardinal series:*

$$f(t) = \sum_{n\in\mathbb{Z}} f\left(n\frac{\pi}{\tilde{B}}\right) \text{sinc}\left(\frac{\tilde{B}}{\pi}t - n\right) \quad \textit{for any } \tilde{B} \geq B$$

which converges both in $L^2(\mathbb{R})$ and absolutely and uniformly on $\mathbb{R}$. Here $\text{sinc}t = \frac{\sin \pi t}{\pi t}$ *is the cardinal sine function and $\frac{\tilde{B}}{\pi}$ (samples/sec) is the sampling rate and $\frac{B}{\pi}$ is the Nyquist rate, the smallest possible sampling rate.*

1st proof: For simplicity, assume $\tilde{B} = B = \pi$ so that $f(t) \in PW_\pi$. Then $\hat{f}(\xi) \in L^2(\mathbb{R})$ and $\hat{f}(\xi) = 0$ a.e. for $|\xi| > \pi$ so that

$$\hat{f}(\xi) = \frac{1}{2\pi} \sum_{n\in\mathbb{Z}} \langle \hat{f}(\xi), e^{-in\xi} \rangle_{L^2[-\pi,\pi]} e^{-in\xi} = \sum_{n\in\mathbb{Z}} f(n) e^{-in\xi} \text{ in } L^2[-\pi, \pi]$$

and so

$$\hat{f}(\xi) \;=\; \sum_{n\in\mathbb{Z}} f(n)e^{-in\xi}\chi_{[-\pi,\pi]}(\xi).$$

Taking its inverse Fourier transform gives

$$f(t) = \sum_{n\in\mathbb{Z}} f(n)\frac{\sin\pi(t-n)}{\pi(t-n)} = \sum_{n\in\mathbb{Z}} f(n)\mathrm{sinc}(t-n).$$

$\square$

2nd proof: For any $\tilde{B}$ ($\geq B$), consider the impulse train

$$f_d(t) \;:=\; \sum_{n\in\mathbb{Z}} f\left(n\frac{\pi}{\tilde{B}}\right)\delta\left(t-n\frac{\pi}{\tilde{B}}\right).$$

Then by the Poisson summation formula, we have

$$\hat{f}_d(\xi) \;=\; \sum_{n\in\mathbb{Z}} f\left(n\frac{\pi}{\tilde{B}}\right)e^{-in\frac{\pi}{\tilde{B}}\xi} \;=\; \frac{\tilde{B}}{\pi}\sum_{n\in\mathbb{Z}}\hat{f}\left(\xi+2\tilde{B}n\right). \tag{1}$$

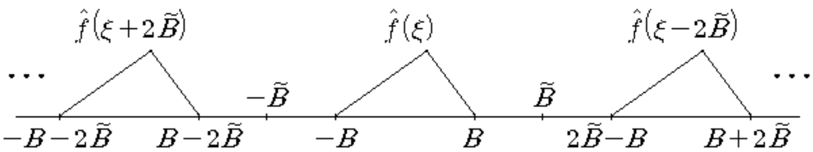

Figure 2: $\tilde{B} \geq B$

Figure 2 illustrates how the summation in (1) behaves when $\tilde{B} \geq B$. Hence

$$\begin{aligned}\hat{f}(\xi) &= \sum_{n\in\mathbb{Z}}\hat{f}\left(\xi+2\tilde{B}n\right)\chi_{[-\tilde{B},\tilde{B}]}(\xi)\\ &= \frac{\pi}{\tilde{B}}\sum_{n\in\mathbb{Z}} f\left(n\frac{\pi}{\tilde{B}}\right)e^{-in\frac{\pi}{\tilde{B}}\xi}\chi_{[-\tilde{B},\tilde{B}]}(\xi)\end{aligned}$$

from which WSKS sampling expansion follows by taking the inverse Fourier transform. Finally, the mode of convergence of the WSKS sampling series follows since PW_B is the so-called 'reproducing kernel Hilbert space' with the bounded reproducing kernel. $\square$

Note that if $0 < \tilde{B} < B$ (see Figure 3), then

$$\sum_{n\in\mathbb{Z}}\hat{f}\left(\xi+2\tilde{B}n\right)\chi_{[-\tilde{B},\tilde{B}]}(\xi) \;\neq\; \hat{f}(\xi),$$

which causes some distortion, called the aliasing.

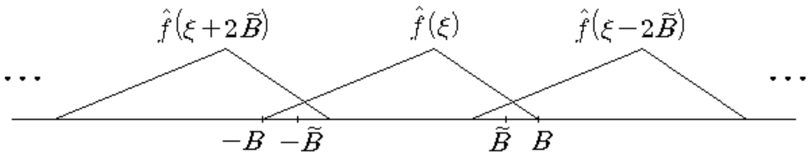

Figure 3: $\tilde{B} < B$

Recall that for any $f(t) \in PW_B$ and any $\tilde{B} \geq B$,

$$f(t) = \sum_{n\in\mathbb{Z}} f\left(n\frac{\pi}{\tilde{B}}\right) \operatorname{sinc}\left(\frac{\tilde{B}}{\pi}t - n\right)$$

if and only if

$$\begin{aligned}\hat{f}(\xi) &= \frac{\pi}{\tilde{B}} \sum_{n\in\mathbb{Z}} f\left(n\frac{\pi}{\tilde{B}}\right) e^{-in\frac{\pi}{\tilde{B}}\xi} \chi_{[-\tilde{B},\tilde{B}]}(\xi) \\ &= \frac{\pi}{\tilde{B}} \sum_{n\in\mathbb{Z}} f\left(n\frac{\pi}{\tilde{B}}\right) e^{-in\frac{\pi}{\tilde{B}}\xi} \chi_{[-B,B]}(\xi).\end{aligned}$$

So, taking its inverse Fourier transform gives

$$f(t) = \frac{B}{\tilde{B}} \sum_{n\in\mathbb{Z}} f\left(n\frac{\pi}{\tilde{B}}\right) \operatorname{sinc}\left(\frac{B}{\pi}t - n\frac{B}{\tilde{B}}\right).$$

Hence for any $f(t) \in PW_B$ and any $\tilde{B} > B$, we have two sampling series:

$$f(t) = \sum_{n\in\mathbb{Z}} f\left(n\frac{\pi}{B}\right) \operatorname{sinc}\left(\frac{B}{\pi}t - n\right)$$

which is an orthonormal basis expansion in the Hilbert space PW_B, and

$$f(t) = \frac{B}{\tilde{B}} \sum_{n\in\mathbb{Z}} f\left(n\frac{\pi}{\tilde{B}}\right) \operatorname{sinc}\left(\frac{B}{\pi}t - n\frac{B}{\tilde{B}}\right)$$

which is an oversampling 'frame' expansion in the Hilbert space PW_B.

By setting $t = k\frac{\pi}{\tilde{B}}$ in the above oversampling expansion with $\tilde{B} > B$, we have

$$\begin{aligned}f\left(k\frac{\pi}{\tilde{B}}\right) &= \frac{B}{\tilde{B}} \sum_{n\in\mathbb{Z}} f\left(n\frac{\pi}{\tilde{B}}\right) \operatorname{sinc}\left(\frac{B}{\tilde{B}}(k-n)\right) \\ &= \frac{B}{\tilde{B}} \left[f\left(k\frac{\pi}{\tilde{B}}\right) + \sum_{n\neq k} f\left(n\frac{\pi}{\tilde{B}}\right) \operatorname{sinc}\left(\frac{B}{\tilde{B}}(k-n)\right)\right]\end{aligned}$$

so that

$$\left(1-\frac{B}{\tilde{B}}\right) f\left(k\frac{\pi}{\tilde{B}}\right) = \frac{B}{\tilde{B}}\sum_{n\neq k} f\left(n\frac{\pi}{\tilde{B}}\right)\operatorname{sinc}\left(\frac{B}{\tilde{B}}(k-n)\right),\ k\in\mathbb{Z}.$$

Hence by oversampling, we can recover any single (in fact, any finitely many) missing sample, say, $f(k\frac{\pi}{B})$ from the other samples $\{f(n\frac{\pi}{B}) : n \neq k\}$.

Even, oversampling can be used to reduce the noise sensitivity or to speed up the convergence rate of the sampling series.

Classical WSKS sampling theorem has been extended to signals, which are band-limited in some generalized sense, e.g. signals in Bernstein space

$$B^p_\sigma = \{f(z) \in E_\sigma : f(t) \in L^p(\mathbb{R})\}\ (1 \leq p \leq \infty,\ \sigma > 0).$$

In fact, any $f(t) \in B^p_\sigma$ is a tempered distribution, of which its Fourier transform $\widehat{f}(\xi)$ is a compactly supported distribution with supp $\widehat{f} \subseteq [-\sigma, \sigma]$.

In order to extend the sampling theorem to signals, which are possibly time-limited (so not band-limited by Heisenberg's uncertainty principle), we need the concept of shift invariant subspaces of $L^2(\mathbb{R})$, which are building blocks of multi-resolution analysis (MRA) and wavelet theory. By Plancherel's theorem, PW_π is unitarily isomorphic to $L^2[-\pi,\pi]$ via $\frac{1}{\sqrt{2\pi}}\mathcal{F}$ so PW_π is a Hilbert subspace of $L^2(\mathbb{R})$ of which $\{\operatorname{sinc}(t-n) : n \in \mathbb{Z}\}$ is an orthonormal basis. Hence we may express PW_π as

$$\begin{aligned} PW_\pi &= \{f \in L^2(\mathbb{R}) : \text{supp } \hat{f}(\xi) \subset [-\pi,\pi]\} \\ &= \overline{\text{span}}\{\operatorname{sinc}(t-n) : n \in \mathbb{Z}\} \\ &= \{\sum_{n\in\mathbb{Z}} c(n)\operatorname{sinc}(t-n) : \mathbf{c} = \{c(n)\}_{n\in\mathbb{Z}} \in l^2\}, \end{aligned}$$

which is a prototype of shift invariant space generated by $\operatorname{sinc} t$. Here, shift invariance means: if $f(t) \in PW_\pi$, then $f(t-n) \in PW_\pi$ for any $n \in \mathbb{Z}$. Moreover

$$\frac{1}{2\pi}\operatorname{sinc}(\cdot - s) \in PW_\pi \text{ for any } s \text{ in } \mathbb{R}$$

and

$$\langle f(t), \frac{1}{2\pi}\operatorname{sinc}(t-s)\rangle_{L^2(\mathbb{R})} = f(s) \text{ for any } f \in PW_\pi.$$

Hence PW_π is a reproducing kernel Hilbert space (RKHS) with the reproducing kernel $q(t,s) = \frac{1}{2\pi}\operatorname{sinc}(t-s)$ in the sense that:

A Hilbert space H consisting of complex valued functions on $\mathbb{R}$ is called a reproducing kernel Hilbert space (RKHS) if there is a function $q(t,s)$ on $\mathbb{R}\times\mathbb{R}$, called the reproducing kernel of H satisfying

- $q(\cdot, s) \in H$ for each s in $\mathbb{R}$;
- $\langle f(t), q(t,s)\rangle = f(s),\ f \in H.$

Then any sequence $\{f_n(t)\}$ converging in an RKHS H converges also uniformly on any subset of $\mathbb{R}$ on which $q(s,s)$ is bounded ([12]).

2 Sampling on Shift Invariant Spaces

For any $\phi(t) \in L^2(\mathbb{R})$, let $V(\phi) := \overline{\text{span}}\{\phi(t-n) : n \in \mathbb{Z}\}$ be the closed subspace of $L^2(\mathbb{R})$, called the shift invariant space generated by $\phi(t)$. Then $\{\phi(t-n) : n \in \mathbb{Z}\}$ is

- an orthonormal basis (ONB) of $V(\phi)$ if

$$\|\sum_{n\in\mathbb{Z}} c(n)\phi(t-n)\|^2 = \|\mathbf{c}\|^2 := \sum_{n\in\mathbb{Z}} |c(n)|^2, \quad \mathbf{c} = \{c(n)\}_{n\in\mathbb{Z}} \in l^2;$$

- a Riesz basis of $V(\phi)$ with Riesz bounds $B \geq A > 0$ if

$$A\|\mathbf{c}\|^2 \leq \|\sum_{n\in\mathbb{Z}} c(n)\phi(t-n)\|^2 \leq B\|\mathbf{c}\|^2, \ \mathbf{c} = \{c(n)\}_{n\in\mathbb{Z}} \in l^2;$$

- a frame of $V(\phi)$ with frame bounds $B \geq A > 0$ if

$$A\|f\|^2 \leq \sum_{n\in\mathbb{Z}} |\langle f, \phi(t-n)\rangle|^2 \leq B\|f\|^2, \ f \in V(\phi).$$

When $\{\phi(t-n) : n \in \mathbb{Z}\}$ is an ONB or a Riesz basis or a frame of $V(\phi)$, we call $\phi(t)$ an orthonormal or a Riesz (or stable) or a frame generator of the shift invariant space $V(\phi)$.

If $\{\phi(t-n) : n \in \mathbb{Z}\}$ is an ONB (resp. a Riesz basis) of $V(\phi)$, then it is a Riesz basis (resp. a frame) of $V(\phi)$ but not conversely in general. If $\{\phi(t-n) : n \in \mathbb{Z}\}$ is a frame of $V(\phi)$, then there is another frame $\{\psi(t-n) : n \in \mathbb{Z}\}$, called a dual frame of $\{\phi(t-n) : n \in \mathbb{Z}\}$, such that

$$f(t) = \sum_{n\in\mathbb{Z}} \langle f(t), \psi(t-n)\rangle \phi(t-n), \ f \in V(\phi),$$

which is called the frame expansion of $f(t)$. Note that members of a frame may not be linearly independent, which is a merit rather than a demerit.

Let $\phi(t) \in L^2(\mathbb{R})$, $G_\phi(\xi) := \sum_{n\in\mathbb{Z}} |\hat{\phi}(\xi + 2n\pi)|^2$ and $B \geq A > 0$. Then ([3]) $\phi(t)$ is

(a) an orthonormal generator if and only if

$$G_\phi(\xi) = 1 \text{ a.e. on } \mathbb{R};$$

(b) a Riesz generator with bounds (A, B) if and only if

$$A \ \leq \ G_\phi(\xi) \ \leq \ B \ \text{ a.e. on } \mathbb{R};$$

(c) a frame generator with bounds (A, B) if and only if

$$A \ \leq \ G_\phi(\xi) \ \leq \ B \ \text{ a.e. on } \operatorname{supp} G_\phi.$$

For any frame generator $\phi(t) \in L^2(\mathbb{R})$, let

$$T(\mathbf{c}) := (\mathbf{c} * \phi)(t) = \sum_{k\in\mathbb{Z}} c(k)\phi(t-k), \quad \mathbf{c} = \{c(k)\}_{k\in\mathbb{Z}} \in l^2$$

be the synthesis operator of the frame $\{\phi(t-n) : n \in \mathbb{Z}\}$. Then T is a bounded linear operator from l^2 onto $V(\phi)$. Hence T is an isomorphism from $N(T)^\perp$ onto $V(\phi)$ so that

$$V(\phi) = \{(\mathbf{c} * \phi)(t) : \mathbf{c} \in l^2\} = \{(\mathbf{c} * \phi)(t) : \mathbf{c} \in N(T)^\perp\},$$

where $N(T) := \left\{\mathbf{c} \in l^2 : T(\mathbf{c}) = 0\right\}$ and $N(T)^\perp$ is the orthogonal complement of $N(T)$ in l^2. If $\phi(t)$ is a Riesz generator, then T is an isomorphism from l^2 onto $V(\phi) = \{(\mathbf{c} * \phi)(t) : \mathbf{c} \in l^2\}$.

If $\phi(t) \in L^2(\mathbb{R})$ is a frame generator satisfying

$$\begin{gathered} \phi(t) \text{ is everywhere well-defined on } \mathbb{R} \\ \text{and} \\ C_\phi(t) := \sum_{n\in\mathbb{Z}} |\phi(t+n)|^2 < \infty,\ t \in \mathbb{R}, \end{gathered} \tag{2}$$

then

$$V(\phi) \ = \ \{\ (\mathbf{c} * \phi)(t)\ :\ \mathbf{c} \in N(T)^\perp\}$$

is an RKHS of which any $(\mathbf{c} * \phi)(t)$ converges both in $L^2(\mathbb{R})$ and absolutely on $\mathbb{R}$ ([17]).

For any $\phi(t) \in L^2(\mathbb{R})$ satisfying (2), let

$$Z_\phi(t,\xi) \ := \ \sum_{n\in\mathbb{Z}} \phi(t+n)e^{-in\xi}$$

be the Zak transform of $\phi(t)$. Then $Z_\phi(t,\xi) \in L^2[0, 2\pi]$ for each t in $\mathbb{R}$.

For any measurable function $f(t)$ on $\mathbb{R}$, let

$$\|f\|_0 := \sup_{|E|=0} \inf_{\mathbb{R}\setminus E} |f(t)| \text{ and } \|f\|_\infty := \inf_{|E|=0} \sup_{\mathbb{R}\setminus E} |f(t)|$$

be the essential infimum and the essential supremum of $|f(t)|$ respectively where $|E|$ is the Lebesgue measure of E.

Theorem 2 (General irregular sampling)([2], [17])**.** *Let $\phi(t)$ be a frame generator satisfying* (2) *so that $V(\phi) = \{(\mathbf{c} * \phi)(t) : \mathbf{c} \in N(T)^\perp\}$ is an RKHS. Then for any sampling points $\{t_n\}_{n\in\mathbb{Z}}$ in $\mathbb{R}$, the followings are all equivalent.*

(a) There is a frame $\{S_n(t) : n \in \mathbb{Z}\}$ of $V(\phi)$ such that

$$f(t) = \sum_{n\in\mathbb{Z}} f(t_n)S_n(t),\ f(t) \in V(\phi) \tag{3}$$

and $\{f(t_n)\}_{n\in\mathbb{Z}}$ *is a moment sequence of a function to* $\{S_n(t) : n \in \mathbb{Z}\}$*, that is,*

$$f(t_n) = \langle g(t), S_n(t)\rangle,\ n \in \mathbb{Z}$$

for some $g(t)$ *in* $V(\phi)$*;*

(b) (sampling inequality) there are constants $\beta \geq \alpha > 0$ such that

$$\alpha\|f\|^2 \leq \sum_{n\in\mathbb{Z}} |f(t_n)|^2 \leq \beta\|f\|^2,\ f \in V(\phi).$$

(c) $\{q(t, t_n) : n \in \mathbb{Z}\}$ is a frame of $V(\phi)$, where $q(t, s)$ is the reproducing kernel of $V(\phi)$.

Furthermore, if any one of the above three equivalent statements holds, then the sampling series (3) converges both in $L^2(\mathbb{R})$ and absolutely and uniformly on any subset of $\mathbb{R}$ on which $C_\phi(t)$ is bounded.

Theorem 3 (Regular shifted sampling)([17])**.** *Let* $\phi(t)$ *be a frame generator satisfying* (2) *so that* $V(\phi) = \left\{(\mathbf{c} * \phi)(t) : \mathbf{c} \in N(T)^\perp\right\}$ *is an RKHS. Then for any* $0 \leq \sigma < 1$*, the followings are all equivalent.*

(a) There is a frame $\{\, S(t-n) \,:\, n \in \mathbb{Z}\}$ *of* $V(\phi)$ *such that*

$$f(t) \;=\; \sum_{n\in\mathbb{Z}} f(\sigma+n)S(t-n), \quad f \in V(\phi); \tag{4}$$

(b) There are constants $\beta \geq \alpha > 0$ *such that*

$$\alpha \;\leq\; |Z_\phi(\sigma,\xi)| \;\leq\; \beta \;\; \textit{a.e. on supp}\, G_\phi;$$

(c) (sampling inequality) there are constants $\beta \geq \alpha > 0$ *such that*

$$\alpha\|f\|^2 \;\leq\; \sum_{n\in\mathbb{Z}} |f(\sigma+n)|^2 \;\leq\; \beta\|f\|^2, \quad f \in V(\phi).$$

Moreover in this case,

$$\hat{S}(\xi) \;=\; \frac{\hat{\phi}(\xi)}{Z_\phi(\sigma,\xi)}\chi_{\mathrm{supp}\,\hat{\phi}}(\xi).$$

In Theorem 3, the sampling series (4) converges both in $L^2(\mathbb{R})$ and absolutely on $\mathbb{R}$. Moreover it converges uniformly on any subset of $\mathbb{R}$ on which $C_\phi(t)$ is bounded. If $\phi(t) \in L^2(\mathbb{R}) \cap C(\mathbb{R})$ is a continuous frame generator satisfying $\sup_{\mathbb{R}} C_\phi(t) < \infty$, then $V(\phi) = \{\, (\mathbf{c} * \phi)(t) \,:\, \mathbf{c} \in l^2\}$ is an RKHS and the sampling series (4) converges uniformly on $\mathbb{R}$.

Example 1 (Cardinal B-splines). *Let $\phi_0(t) = \chi_{[0,1)}(t)$ and*

$$\phi_n(t) = \phi_{n-1}(t) * \phi_0(t) = \int_0^1 \phi_{n-1}(t-s)ds, \ n \geq 1$$

be the cardinal B-spline of degree n. Then $\phi_0(t)$ is an orthonormal generator and $\phi_n(t)$ for $n \geq 1$ is a continuous Riesz generator.
Moreover since $\phi_n(t)$ has compact support, $\sup_{\mathbb{R}} C_{\phi_n}(t) = \sup_{\mathbb{R}} \sum_{k\in\mathbb{Z}} |\phi_n(t+k)|^2 < \infty$ so that $V(\phi_n) = \{(\mathbf{c} * \phi_n)(t) : \mathbf{c} \in l^2\}$ is an RKHS for any $n \geq 0$.

For $\phi_1(t) = t\chi_{[0,1)}(t) + (2-t)\chi_{[1,2)}(t)$ and $0 \leq \sigma < 1$,

$$\phi_1(\sigma) = \sigma, \ \phi_1(\sigma+1) = 1-\sigma, \ \phi_1(\sigma+n) = 0 \text{ for } n \neq 0, 1$$

so that $Z_{\phi_1}(\sigma, \xi) = \sigma + (1-\sigma)e^{-i\xi}$. Then

$$\|Z_{\phi_1}(\sigma,\xi)\|_0 = |2\sigma - 1| \text{ and } \|Z_{\phi_1}(\sigma,\xi)\|_\infty = 1.$$

Hence we have for any σ with $0 \leq \sigma < 1$ and $\sigma \neq \frac{1}{2}$, a Riesz basis expansion

$$f(t) = \sum_{n\in\mathbb{Z}} f(\sigma+n)S(t-n), \ f \in V(\phi_1),$$

which converges in $L^2(\mathbb{R})$ and absolutely and uniformly on $\mathbb{R}$.
For $\phi_2(t) = \frac{1}{2}t^2\chi_{[0,1)}(t) + \frac{1}{2}(6t - 2t^2 - 3)\chi_{[1,2)}(t) + \frac{1}{2}(3-t)^2\chi_{[2,3)}(t)$,

$$\|Z_{\phi_2}(0,\xi)\|_0 = 0 \ \text{ but } \ 0 < \|Z_{\phi_2}(\frac{1}{2},\xi)\|_0 < \|Z_{\phi_2}(\frac{1}{2},\xi)\|_\infty < \infty$$

so that there is a Riesz basis expansion

$$f(t) = \sum_{n\in\mathbb{Z}} f(\frac{1}{2}+n)S(t-n), \ f \in V(\phi_2)$$

which converges in $L^2(\mathbb{R})$ and uniformly on $\mathbb{R}$.

3 Multi-channel Sampling

Reconstructing a signal from samples which are taken from its several channeled (or modulated) signals is called a multi-channel sampling or a generalized sampling. The multi-channel sampling method goes back to the works by Shannon [25] and Fogel [9], where the reconstruction of band-limited signals from samples of the signal and its derivatives was suggested. Later, Papoulis [22] introduced arbitrary multi-channel sampling on Paley-Wiener spaces. Recently using the Fourier duality between $L^2[0, 2\pi]$ and the shift invariant space $V(\phi)$, García and Pérez-Villarón [11] obtained stable generalized sampling in shift invariant spaces. See [10, 18, 28] for related and further extended results.

Let $\{L_j[\cdot]\}_{j=1}^N$ be linear time invariant (LTI) systems with suitable impulse responses $\{l_j(t)\}_{j=1}^N$ so that

$$L_j[f](t) = (f * l_j)(t) = \int_{-\infty}^{\infty} f(s) l_j(t-s) ds, \ 1 \le j \le N,$$

where

(i) $l_j(t) = \delta(t+a), \ a \in \mathbb{R}$ or

(ii) $l_j(t) \in L^2(\mathbb{R})$ or

(iii) $\widehat{l_j}(\xi) \in L^\infty(\mathbb{R})$ when $\sum_{n\in\mathbb{Z}} |\widehat{\phi}(\xi + 2n\pi)| \in L^2[0, 2\pi]$.

Then our goal is to recover any signal f in $V(\phi)$ as

$$f(t) = \sum_{j=1}^{N} \sum_{n\in\mathbb{Z}} L_j[f](\sigma_j + rn) s_{j,n}(t),$$

where

- r is a positive integer;
- $0 \le \sigma_j < r$;
- $\{s_{j,n}(t)\}_{j,n}$ is a frame of $V(\phi)$.

Let $\psi_j = L_j[\phi]$, $g_j(\xi) = \frac{1}{2\pi} Z_{\psi_j}(\sigma_j, \xi)$,

$$G(\xi) = [g_j(\xi + (k-1)\tfrac{2\pi}{r})]_{j=1,}^{N}{}_{k=1}^{r}$$

and

- $\lambda_M(\xi) :=$ the largest eigenvalue of $G(\xi)^* G(\xi)$
- $\lambda_m(\xi) :=$ the smallest eigenvalue of $G(\xi)^* G(\xi)$
- $\beta_G := \|\lambda_M(\xi)\|_\infty$
- $\alpha_G := \|\lambda_m(\xi)\|_0$.

Theorem 4. *(Multi-channel shifted sampling)([11, 15]) Let $\phi(t)$ be a continuous Riesz generator satisfying* (2) *so that $V(\phi) = \{(\mathbf{c} * \phi)(t) : \mathbf{c} \in \ell^2\}$ is an RKHS. Assume that $\beta_G < \infty$, that is, all $g_j(\xi)$'s are in $L^\infty[0, 2\pi]$. The followings are all equivalent.*

(a) There is a frame $\{s_{j,n}(t) : 1 \le j \le N, \ n \in \mathbb{Z}\}$ of $V(\phi)$ for which

$$f(t) = \sum_{j=1}^{N} \sum_{n\in\mathbb{Z}} L_j[f](\sigma_j + rn) s_{j,n}(t), \ f(t) \in V(\phi);$$

(b) There is a frame $\{s_j(t-rn) : 1 \le j \le N,\ n \in \mathbb{Z}\}$ of $V(\phi)$ for which for any $f(t) \in V(\phi)$

$$f(t) = \sum_{j=1}^{N} \sum_{n\in\mathbb{Z}} L_j[f](\sigma_j + rn)s_j(t-rn);$$

(c) $0 < \alpha_G$.

In this case, the sampling series in (a) and (b) converge not only in $L^2(\mathbb{R})$ but also absolutely and uniformly on any subset of $\mathbb{R}$ on which $C_\phi(t)$ is bounded. Moreover, the frames in (a) and (b) are Riesz bases if and only if $r = N$.

Example 2. *Let $\phi(t) = \mathrm{sinc}\, t$ so that $V(\phi) = PW_\pi$, and*

$$\hat{\ell}_1(\xi) = 1,\ \hat{\ell}_2(\xi) = -i\,\mathrm{sgn}\,\xi$$

so that $L_1[f](t) = f(t)$ and $L_2[f](t) = \widetilde{f}(t) = \frac{1}{\pi}\,\text{p.v.} \int_{-\infty}^{\infty} \frac{f(s)}{t-s}\,ds$, the Hilbert transform of $f(t)$, where p.v. stands for the Cauchy principal value. Take $\sigma_1 = \sigma_2 = 0$ and $r_1 = r_2 = 2$. Then

$$f(t) = \sum_{n\in\mathbb{Z}} f(2n)S_1(t-2n) + \sum_{n\in\mathbb{Z}} \widetilde{f}(2n)S_2(t-2n), \qquad f \in PW_\pi,$$

where $S_1(t) = \mathrm{sinc}\, t,\ S_2(t) = \frac{\cos \pi t - 1}{\pi t}$. The series converges absolutely and uniformly on $\mathbb{R}$.

4 Average sampling

In most physical circumstances, acquisition devices do not produce signal values at the exact instances. A common substitute is to integrate the signal over small neighborhoods of the sampling instances. We call this sampling procedure an average sampling.

Then our goal is to find a condition under which there is a frame $\{S_n(t) : n \in \mathbb{Z}\}$ of $V(\phi)$ such that an average sampling expansion

$$f(t) = \sum_{n\in\mathbb{Z}} \langle f, u_n\rangle S_n(t),\ f \in V(\phi)$$

holds. Here $\langle\cdot,\cdot\rangle$ is the inner product in $L^2(\mathbb{R})$ and $\{u_n(t) : n \in \mathbb{Z}\}$ are weight functions satisfying

- $0 \le u_n(t) \in L^2(\mathbb{R})$;
- supp $u_n(t) \subset [n-a, n+b]$ ($a, b \ge 0$ and $a+b > 0$);
- $\int_{-\infty}^{\infty} u_n(t)dt = \int_{n-a}^{n+b} u_n(t)dt = 1,\ n \in \mathbb{Z}$.

Let $\phi(t)$ be a frame generator satisfying

- $\phi(t)$ is locally absolutely continuous on $\mathbb{R}$, and $\phi'(t) \in L^2(\mathbb{R})$;

- $L := \|Z_{\phi'}(t, \xi)\|_\infty < \infty$;
- there are constants $\beta \geq \alpha > 0$ such that

$$\alpha \leq |Z_\phi(0, \xi)| \leq \beta \text{ a.e. on supp } G_\phi. \tag{5}$$

Then $V(\phi)$ is an RKHS, $\sup_{\mathbb{R}} C_\phi(t) < \infty$, and any norm converging sequence in $V(\phi)$ also converges absolutely and uniformly on $\mathbb{R}$ ([16]). Note also that by Theorem 3, the condition (5) holds if and only if there is a frame $\{S(t-n) : n \in \mathbb{Z}\}$ of $V(\phi)$ such that $f(t) = \sum_{n\in\mathbb{Z}} f(n)S(t-n),\ f \in V(\phi)$.

Theorem 5 ([16, 26])**.** *Let $\{u_n(t) : n \in \mathbb{Z}\}$ be any sequence of weight functions with* supp $u_n(t) \subset [n-a, n+b]$ *and $\delta := max\{a, b\}$. If*

$$\sqrt{\delta(a+b)} > \frac{\alpha}{L},$$

then there is a frame $\{S_n(t) : n \in \mathbb{Z}\}$ of $V(\phi)$ such that

$$f(t) = \sum_{n\in\mathbb{Z}} \langle f, u_n\rangle S_n(t),\ f \in V(\phi), \tag{6}$$

which converges in $L^2(\mathbb{R})$ and absolutely and uniformly on $\mathbb{R}$.

If average functions $u_n(t)$ are uniformly bounded in L^∞- or L^2-sense, then we have:

Theorem 6 ([16])**.** *Let $\{u_n(t) : n \in \mathbb{Z}\}$ be any sequence of weight functions with* supp $u_n(t) \subset [n-a, n+b]$ *and $\delta := max\{a, b\}$.*

(a) Assume $M := \sup_{n\in\mathbb{Z}} \|u_n(t)\|_\infty < \infty$. If $\sqrt{\delta}(a+b)^{3/2} < \frac{\alpha}{LM}$ or $\sqrt{\delta}(a+b) > \frac{\alpha}{L\sqrt{M}}$, then (6) *holds on $V(\phi)$.*

(b) Assume $M := \sup_{n\in\mathbb{Z}} \|u_n(t)\|_{L^2(\mathbb{R})} < \infty$. If $\sqrt{\delta(a+b)} < \frac{\alpha}{LM}$, then (6) *holds on $V(\phi)$.*

5 Consistent Sampling

Let $\phi(t) \in L^2(\mathbb{R})$ be a frame generator and $\psi(t)$ its dual generator. Then

$$\widetilde{f}(t) := \sum_{n\in\mathbb{Z}} \langle f(t), \psi(t-n)\rangle \phi(t-n)$$

is the orthogonal projection of $f(t) \in L^2(\mathbb{R})$ onto $V(\phi)$. Note here that the analysis filter $\psi(t)$ and the synthesis filter $\phi(t)$ are not independent but are dual each other, which may fail in other interesting signal processing. Note also that

$$\langle \widetilde{f}(t), \psi(t-n)\rangle = \langle f(t), \psi(t-n)\rangle, \quad n \in \mathbb{Z},$$

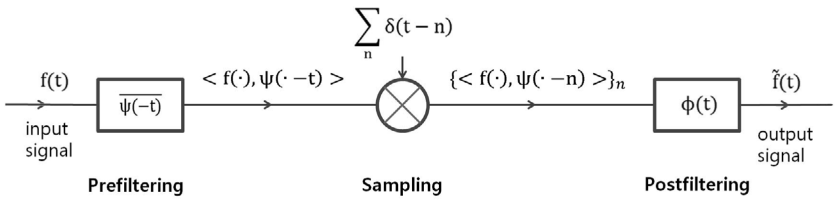

Figure 4: Approximation-sampling procedure

which means that the input signal $f(t)$ and the output signal $\widetilde{f}(t)$ provide the same measurements. This approximation-sampling procedure is illustrated in Figure 4, where means the convolution product.

Let $\mathcal{H}$ be a separable Hilbert space, $\{v_j\}$ countable analysis vectors in $\mathcal{H}$, forming a frame of the sampling space $\mathcal{V} := \overline{\text{span}}\{v_j\}$, and $\{w_k\}$ countable synthesis vectors in $\mathcal{H}$, forming a frame of the reconstruction space $\mathcal{W} := \overline{\text{span}}\{w_k\}$.

Let $S(\mathbf{c}) = \sum\limits_j c(j)v_j$ and $T(\mathbf{d}) = \sum\limits_k d(k)w_k$ ($\mathbf{c},\ \mathbf{d} \in \ell_2$) be the synthesis operators for $\{v_j\}$ and $\{w_k\}$ respectively. Then S^*, the adjoint of S, given by

$$S^*(f) = \{\langle f, v_j\rangle\} \in \ell_2,\ f \in \mathcal{H},$$

is the sampling operator.

We now look for a sampling operator $\widetilde{P}$ on $\mathcal{H}$, which approximates an input f in $\mathcal{H}$ by $\widetilde{f} = \widetilde{P}(f)$ in $\mathcal{W}$ from its generalized measurements $\mathbf{c} = S^*(f)$. We require

(a) (stability) $\widetilde{P} \in L(\mathcal{H}, \mathcal{W})$, i.e., $\widetilde{P}$ is a bounded linear operator from $\mathcal{H}$ into $\mathcal{W}$,

(b) (sampling) $\widetilde{P}(f) = 0$ if $S^*(f) = 0$, i.e., $N(S^*) \subseteq N(\widetilde{P})$,

(c) (consistency) $S^*(\widetilde{P}f) = S^*(f)$, i.e., $\langle f, v_j\rangle = \langle \widetilde{P}(f), v_j\rangle$ for all j.

Consistency means that the input f and the output $\widetilde{P}(f)$ look the same to the observers, who can observe signals only through the acquisition devices, say $\{v_j\}$.

We call $\widetilde{P}$ satisfying (a), (b), (c) a consistent sampling operator. Note ([23]) that $\widetilde{P}$ satisfies (a) and (b) if and only if

$$\widetilde{P} = TQS^* \text{ for some } Q \in L(\ell_2).$$

Let $C(\mathcal{W}, \mathcal{V})$ be the set of all consistent sampling operators.

Theorem 7 ([20]). *The followings are all equivalent.*

(a) $C(\mathcal{W}, \mathcal{V}) \neq \emptyset$;

(b) $\mathcal{H} = \mathcal{W} + \mathcal{V}^\perp$;

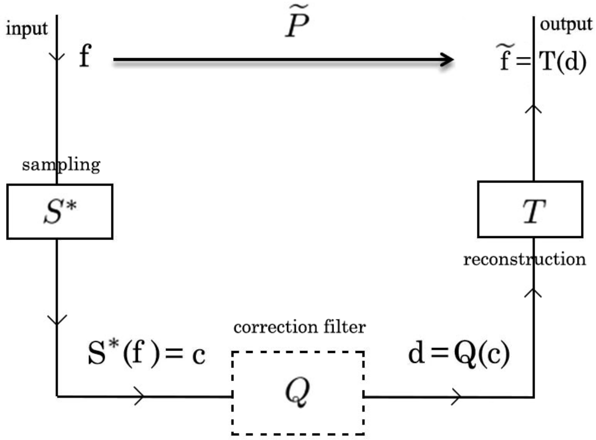

Figure 5: Consistent sampling

(c) $R(S^*T) = R(S^*)$.

In this case, $\mathcal{C}(\mathcal{W}, \mathcal{V}) = \{P_{L,\mathcal{V}^\perp} \mid L \in \mathcal{L}\}$ *where*

$$\mathcal{L} := \{\text{closed complementary subspaces of } \mathcal{W} \cap \mathcal{V}^\perp \text{ in } \mathcal{W}\}$$

and

$$\mathcal{C}(\mathcal{W}, \mathcal{V}) = \{T(S^*T)^\dagger S^* + TP_{N(S^*T)}YS^* \mid Y \in L(\ell_2)\}.$$

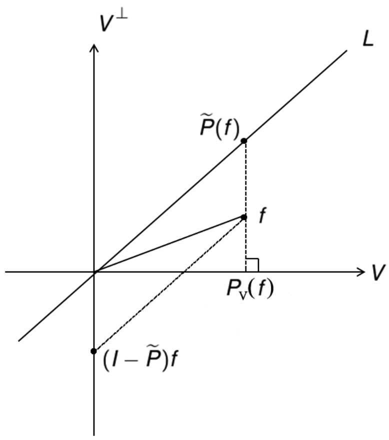

Figure 6: Consistent approximation

In particular, there is a unique consistent sampling operator $\widetilde{P}$ if and only if $\mathcal{H} = \mathcal{W} \oplus \mathcal{V}^\perp$. In this case, $\widetilde{P} = P_{\mathcal{W},\mathcal{V}^\perp} = T(S^*T)^\dagger S^*$.

Note that $S^*(f) = S^*(\widetilde{P}(f))$ if and only if $P_\mathcal{V}(f) = P_\mathcal{V}(\widetilde{P}(f))$ since $N(S^*) = \mathcal{V}^\perp$. Hence for any f in $\mathcal{H}$, $P_\mathcal{V}(f)$ can be visualized as in the Figure 6.

The next theorem provides us a practical method of calculating (or rather approximating) $\widetilde{P}(f)$ of any f in $\mathcal{H}$ through the iteration process.

Theorem 8 ([20])**.** *Assume $\mathcal{H} = \mathcal{W} + \mathcal{V}^\perp$ and $\widetilde{P} = P_{L,\mathcal{V}^\perp}$, where $L \in \mathcal{L}$. Then*

$$\widetilde{P}(f) = \lim_{n\to\infty} f_n, \quad f \in \mathcal{H}$$

and

$$\|P_\mathcal{V}(f - f_n)\| \le \|\widetilde{P}(f) - f_n\| \le \frac{\alpha^{2n-1}}{1-\alpha}\|P_\mathcal{V}(f)\|$$

where $\alpha = \|P_{\mathcal{V}^\perp} P_L\|$ and

$$\begin{cases} f_1 := P_L P_\mathcal{V}(f) \\ f_n := f_1 + P_L P_{\mathcal{V}^\perp}(f_{n-1}) \quad \text{for } n \ge 2. \end{cases}$$

We now give concrete expressions of frame expansions of consistent approximation using the notion of oblique dual frames introduced in [4, 7].

Let A and B be two closed subspaces of $\mathcal{H}$. Given a frame $\{a_n\}_{n\in I}$ of A, a *dual frame* of $\{a_n\}_{n\in I}$ is a frame $\{\tilde{a}_n\}_{n\in I}$ of A satisfying

$$f = \sum_{n\in I} \langle f, \tilde{a}_n\rangle\, a_n,\ f \in A.$$

When $\mathcal{H} = \mathcal{A} \oplus \mathcal{B}^\perp$, a frame $\{b_n\}_{n\in I}$ of B is called an *oblique dual frame* of $\{a_n\}_{n\in I}$ on B if

$$f = \sum_{n\in I} \langle f, b_n\rangle\, a_n,\ f \in A, \tag{7}$$

or equivalently,

$$f = \sum_{n\in I} \langle f, a_n\rangle\, b_n,\ f \in B.$$

Theorem 9 ([6, 8])**.** *Assume $\mathcal{H} = \mathcal{W} + \mathcal{V}^\perp$ and let $L \in \mathcal{L}$ and $\{u_i |\ i \in I\}$ a frame of L with pre-frame operator U. Then $P_{L,\mathcal{V}^\perp} = U(S^*U)^\dagger S^*$ and*

(a) $\{\tilde{v}_i := S(U^*S)^\dagger(e_i^I) |\ i \in I\}$ is an oblique dual frame of $\{u_i\}_{i\in I}$ on $\mathcal{V}$ (with pre-frame operator $S(U^*S)^\dagger$);

(b) $\{\tilde{u}_j := U(S^*U)^\dagger(e_j^J) |\ j \in J\}$ is an oblique dual frame of $\{v_j\}_{j\in J}$ on L (with pre-frame operator $U(S^*U)^\dagger$);

(c) For any $f \in \mathcal{H}$,

$$P_{L,\mathcal{V}^\perp}(f) = \sum_{i\in I} \langle f, \tilde{v}_i\rangle\, u_i = \sum_{j\in J} \langle f, v_j\rangle\, \tilde{u}_j$$

where $\mathbf{b} = \{\langle f, \tilde{v}_i\rangle\}_{i\in I}$ and $\mathbf{c} = S^*(f) = \{\langle f, v_j\rangle\}_{j\in I}$ have the minimum norm properties:
$\|\mathbf{b}\| \le \|\tilde{\mathbf{b}}\|$ for any $\tilde{\mathbf{b}} = \{\tilde{b}(i)\}_{i\in I}$ satisfying $f = \sum_{i\in I} \tilde{b}(i)\, u_i$,
$\|\mathbf{c}\| \le \|\tilde{\mathbf{c}}\|$ for any $\tilde{\mathbf{c}} = \{\tilde{c}(j)\}_{j\in J}$ satisfying $f = \sum_{j\in I} \tilde{c}(j)\, \tilde{u}_j$.

Although consistency is very natural in considering the acquisition process of samples, we are interested in its relative performance compared to the best least square approximation, i.e., the corresponding orthogonal projection. Assume $\mathcal{H} = \mathcal{W} + \mathcal{V}^{\perp}$ and let for any fixed L in $\mathcal{L} = \{L | L \oplus (\mathcal{W} \cap \mathcal{V}^{\perp}) = \mathcal{W}\}$

$$\tilde{P} = P_{L,\mathcal{V}^{\perp}} : \mathcal{H} \longrightarrow L$$

be the unique consistent sampling operator valued in L.

The question is how good the approximation $\tilde{P}f$ of $f \in \mathcal{H} \backslash L$ is, compared to orthogonal projection $P_L f$ of f onto L?

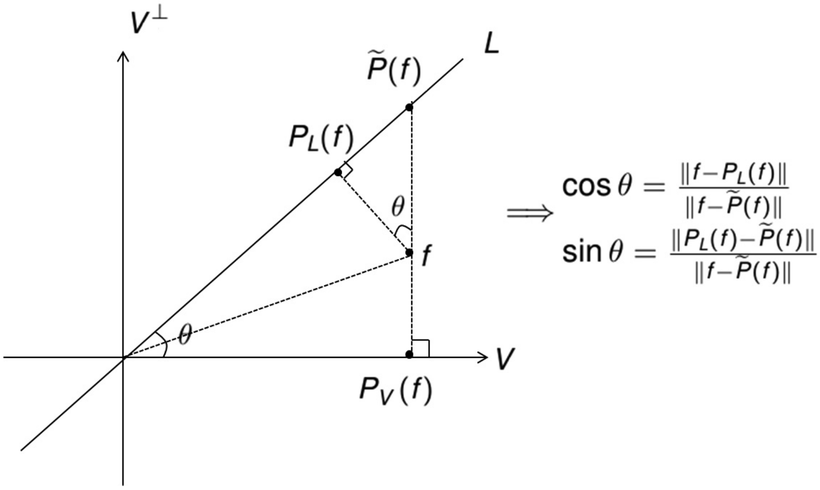

Figure 7: Performance analysis

Figure 7 provides a pictorial motivation for the necessity of the concept ‘angle’ between two closed subspaces of a Hilbert space. For any two non-trivial closed subspaces A and B of a Hilbert space $\mathcal{H}$, let

$$R(A, B) = \cos \Theta^{R}(A, B) = \inf_{\substack{v \in A \\ \|v\|=1}} \|P_B v\| \; (= R(B^{\perp}, A^{\perp}))$$

and

$$S(A, B) = \cos \Theta^{S}(A, B) = \sup_{\substack{v \in A \\ \|v\|=1}} \|P_B v\| \; (= S(B, A)),$$

where P_B is the orthogonal projection onto B. $R(A, B)$ and $S(A, B)$ are the worst and the best estimate of the relative length reduction when vectors in A are projected onto B. The angle $\Theta^{S}(A, B)$ is called the Dixmier angle between A and B ([5, 27]).

Theorem 10 ([13, 20, 29])**.** *Assume $\mathcal{H} = \mathcal{W} + \mathcal{V}^{\perp}$ and let $\widetilde{P} = P_{L,\mathcal{V}^{\perp}}$ for $L \in \mathcal{L}$. Then for all $f \in \mathcal{H} \backslash L$,* *(a)* $0 < R(L, \mathcal{V}) \le \dfrac{\|f - P_L(f)\|}{\|f - \tilde{P}(f)\|} \le S(L^\perp, \mathcal{V}^\perp) \le 1$;

(b) $0 \le R(\mathcal{V}^\perp, L) \le \dfrac{\|P_L(f) - \tilde{P}(f)\|}{\|f - \tilde{P}(f)\|} \le S(L, \mathcal{V}^\perp) < 1.$

6 Oversampling

Let $\phi(t)$ be a Riesz generator satisfying (2). Then Theorem 3 claims that the followings are all equivalent on the shift invariant space $V(\phi)$:

(a) There is a Riesz basis $\{S(t-n) : n \in \mathbb{Z}\}$ of $V(\phi)$ such that

$$f(t) = \sum_{n \in \mathbb{Z}} f(n) S_n(t),\ f \in V(\phi);$$

(b) $0 < \|Z_\phi(0, \xi)\|_0 \le \|Z_\phi(0, \xi)\|_\infty < \infty$;

(c) (sampling inequality) There are constants $\beta \ge \alpha > 0$ such that

$$\alpha \|f\|^2 \le \sum_{n \in \mathbb{Z}} |f(n)|^2 \le \beta \|f\|^2,\ f \in V(\phi).$$

Moreover, in this case

$$S(t) = \mathcal{F}^{-1}\left(\frac{\hat{\phi}(\xi)}{\hat{\phi}^*(\xi)}\right)$$

and $S(t)$ is cardinal, i.e., $S(n) = \delta_{0,n},\ n \in \mathbb{Z}$.

Above regular sampling expansion theorem has been studied and extended further by many authors([1, 14, 30]) under varied conditions on the regularity and/or decaying property of the generator $\phi(t)$.

What can we say on the sampling expansion of signals in $V(\phi)$ when the condition (b) above does not hold?

One way to overcome the difficulty is to raise the sampling rate, that is, to use the oversampling method, for which we need, a priori, a scale of shift invariant spaces of $L^2(\mathbb{R})$.

Let $\{V_j\}_{j \in \mathbb{Z}}$ be an MRA with a stable scaling function $\phi(t)$, that is,

- $\cdots \subset V_{-1} \subset V_0 \subset V_1 \cdots$ are closed subspaces of $L^2(\mathbb{R})$;
- $\cap_j V_j = \{0\}$ and $\overline{\cup_j V_j} = L^2(\mathbb{R})$;

- $f(t) \in V_j$ if and only if $f(2t) \in V_{j+1}$;
- $V_0 = V(\phi)$ where $\phi(t)$ is a Riesz generator.

Assume further that

- $\hat{\phi}(\xi) \in L^2(\mathbb{R}) \cap L^1(\mathbb{R})$ so $\phi(t) \in L^2(\mathbb{R}) \cap C(\mathbb{R})$;
- $C_\phi(t) = \sum_{n\in\mathbb{Z}} |\phi(t+n)|^2 < \infty$ for any t in $\mathbb{R}$.

Then each $V_j = \{\sum_{n\in\mathbb{Z}} c(n)\phi(2^j t - n) : \mathbf{c} \in l^2\}$ becomes an RKHS.

Let $\phi(t) = \sum_{n\in\mathbb{Z}} p(n)\phi(2t-n)$ with $\{p(n)\}_{n\in\mathbb{Z}} \in l^2$ or equivalently,

$$\hat{\phi}(\xi) \;=\; m_\phi\left(\frac{\xi}{2}\right)\hat{\phi}\left(\frac{\xi}{2}\right)$$

be the two-scale relation of $\phi(t)$, where

$$m_\phi(\xi) := \frac{1}{2}\sum_{n\in\mathbb{Z}} p(n)e^{-in\xi} \in L^\infty[0, 2\pi].$$

Iterating the two-scale relation $N(\geq 0)$ times, we obtain

$$\hat{\phi}\left(2^N\xi\right) \;=\; R_N(\xi)\hat{\phi}(\xi),$$

where $R_0(\xi) := 1$ and $R_N(\xi) := \prod_{k=0}^{N-1} m_\phi\left(2^k\xi\right) \in L^\infty[0, 2\pi]$ $(N \geq 1)$. Let $E_N :=$ supp $R_N(\xi)$. Then $E_0 = \mathbb{R}$ and $E_N = \bigcap_{k=0}^{N-1} 2^{-k}\text{supp}\, m_\phi(\xi)$ for $N \geq 1$ so that $E_N \supset E_{N+1}$ for $N \geq 0$.

Theorem 11 (Oversampling)([19])**.** *Let $N \geq 1$ be an integer. Then there is a frame sequence $\{S(t-n) : n \in \mathbb{Z}\}$ in V_0 for which the oversampling expansion holds:*

$$f(t) \;=\; \sum_{n\in\mathbb{Z}} f\left(\frac{n}{2^N}\right) S\left(2^N t - n\right), \quad f \in V_0 \tag{8}$$

if and only if there are constants $\beta \geq \alpha > 0$ such that

$$\alpha \;\leq\; \left|\hat{\phi}^*(\xi)\right| \;\leq\; \beta \quad \text{a.e. on } E_N.$$

Moreover in this case, we may take $S(t)$ to be such that

$$\hat{S}(\xi) \;=\; \frac{\hat{\phi}(\xi)}{\hat{\phi}^*(\xi)}\chi_{E_N}(\xi) \quad \text{on } \mathbb{R}$$

and the oversampling series (8) converges both in $L^2(\mathbb{R})$ and absolutely and uniformly on $\mathbb{R}$.

Theorem 12 (Oversampling property)([19])**.** *Let $N \geq 0$ be an integer. Then $\phi(t)$ has the oversampling property with rate N, i.e.,*

$$f(t) = \sum_{n \in \mathbb{Z}} f\left(\frac{n}{2^N}\right) \phi\left(2^N t - n\right), \ f \in V_0 \tag{9}$$

if and only if

$$\hat{\phi}^*(\xi) = 1 \quad \text{a.e. on } E_N.$$

In this case, the oversampling expansion (9) converges both in $L^2(\mathbb{R})$ and absolutely and uniformly on $\mathbb{R}$.

Theorem 13 (Oversampling property)([19])**.** *Assume that $\hat{\phi}(\xi) \in L^2(\mathbb{R}) \cap L^1(\mathbb{R})$. Then for any integer $N \geq 0$, the followings are all equivalent:*

(a) *$\phi(t)$ has the oversampling property with rate N, i.e.,*

$$f(t) = \sum_{n \in \mathbb{Z}} f\left(\frac{n}{2^N}\right) \phi\left(2^N t - n\right), \ f \in V_0;$$

(b) $\hat{\phi}(\xi) = \hat{\phi}\left(\frac{\xi}{2^N}\right) \sum_{n \in \mathbb{Z}} \hat{\phi}\left(\xi + 2^{N+1} n\pi\right)$ *a.e. on* $\mathbb{R}$;

(c) $Z_\phi(0, \xi) = 1$ *a.e. on* $E_N = \operatorname{supp} R_N$;

(d) $\displaystyle\sum_{n \in \mathbb{Z}} \hat{\phi}(\xi + 2n\pi) = 1$ *a.e. on* $E_N = \operatorname{supp} R_N$.

In particular, if $\phi(t)$ has the oversampling property with rate N, then $\phi(t)$ has the oversampling property with rate $\tilde{N}$ for any $\tilde{N} \geq N$.

Acknowledgements

The second author KHK appreciates deeply the warm and lavish hospitality from the organizers Prof. T. Takiguchi and Prof H. Fujiwara. The first author is partially supported by National Institute for Mathematical Sciences funded by the Ministry of Science, ICT & Future Planning of Korea (B21501), and the second and third authors are partially supported by the National Research Foundation of Korea (NRF) (2012R1A1A2038650).

References

[1] W. Chen and S. Itoh, *A sampling theorem for shift-invariant subspace*, IEEE Trans. Signal Processing, vol. 46, 2822-2824, 1998.

[2] W. Chen, S. Itoh and J. Shiki, *On sampling in shift invariant spaces*, IEEE Trans. Inform. Theory, vol. 48, 2802-2810, 2002.

[3] O. Christensen, *An introduction to frames and Riesz bases*, Birkhäuser, Boston, 2003.

[4] O. Christensen and Y. C. Eldar, *Oblique dual frames and shift invariant spaces*, Appl. Comput. Harmon. Anal., vol. 17, no. 1, 48-68, 2004.

[5] F. Deutsch, *The angle between subspaces of a Hilbert space*, Approximation Theory, Wavelets and Applications, NATO Science Series vol. 454, 107-130, 1995.

[6] Y. C. Eldar, *Sampling without input constraints: consistent reconstruction in arbitrary spaces*, in: A. Zayed and J. Benedetto (Eds.), Sampling, Wavelets and Tomography, Birkhäuser, Boston, 33-60, 2004.

[7] Y. C. Eldar and C. Christensen, *Characterization of oblique dual frame pairs*, EURASIP J. Appl. Signal Process., vol. 2006, 1-11, 2006.

[8] Y. C. Eldar and T. Werther, *Generalized framework for consistent sampling in Hilbert spaces*, Int. J. Wavelets Multiresolut. Inf. Process., vol. 3, no. 3, 347-359, 2005.

[9] L. J. Fogel, *A note on the sampling theorem*, IRE Trans. Inf. Theory, vol. 1, 47-48, 1955.

[10] A. G. García, J. M. Kim, K. H. Kwon, and G. J. Yoon, *Multi-channel sampling on shift-invariant spaces with frame generators*, Int. J. Wavelets Multiresolut. Inf. Process., vol. 10, no. 1, 1250003 (20 pp), 2012.

[11] A. G. García and G. Pérez-Villarón, *Dual frames in $L^2(0,1)$ connected with generalized sampling in shift-invariant spaces*, Appl. Comput. Harmon. Anal., vol. 20, 422-433, 2006.

[12] J. R. Higgins, *Sampling theory in Fourier and signal analysis: Foundations*, Oxford Univ. Press, Oxford, 1996.

[13] A. Hirabayashi, K. H. Kwon and J. Lee, *Consistent sampling with multi-, pre- and post-filterings*, Int. J. Wavelets Multiresolut. Inf. Process., vol. 11, no. 1, 1350008 (16 pp), 2013.

[14] A. J. E. M. Janssen, *The Zak-transform and sampling theorem for savelet subspaces*, IEEE Trans. Signal Processing, vol. 41, 3360-3364, Dec. 1993.

[15] S. Kang, J. M. Kim, and K. H. Kwon, *Asymmetric multi-channel sampling in shift invariant spaces*, J. Math. Anal. Appl., vol. 367, 20-28, 2010.

[16] S. Kang and K.H. Kwon, *Generalized average sampling in shift invarinat spaces*, J. Math. Anal. Appl., vol. 377, 70-78, 2011.

[17] J. M. Kim and K. H. Kwon, *Sampling expansion in shift invariant spaces*, Int. J. Wavelets Multiresolut. Inf. Process., vol. 6, 223-248, 2008.

[18] J. M. Kim and K. H. Kwon, *Vector sampling expansion in Riesz bases setting and its aliasing error*, Appl. Comput. Harmon. Anal., vol. 25, 315-334, 2008.

[19] K. H. Kwon and D. G. Lee, *Oversampling expansion in wavelet subspaces*, IEICE Trans. Fundamentals, vol. E94-A, no. 5, 1184-1193, 2011.

[20] K. H. Kwon and D. G. Lee, *Generalized consistent sampling in abstract Hilbert spaces*, submitted for publication.

[21] H. Nyquist, *Certain topics in telegraph transmission theory*, AIEE Trans., vol. 47, 617-644, 1928.

[22] A. Papoulis, *Generalized sampling expansion*, IEEE Trans. Circuits Syst., vol. 24, no. 11, 652-654, 1977.

[23] W. Rudin, *Functional Analysis*, 2nd ed., International Series in Pure and Applied Mathematics, McGraw-Hill, NY, 1991.

[24] C. E. Shannon, *A mathematical theory of communications*, Bell Lab. Tech. J., vol. 27, 379-423, 1948.

[25] C. E. Shannon, *Communications in the presence of noise*, Proc. IRE, vol. 37, 10-21, 1949.

[26] W. Sun and X. Zhou, *Average sampling in shift invariant subspaces with symmetric averaging functions*, J. Math. Anal. Appl., vol. 287, 279-295, 2003.

[27] W. Tang, *Oblique projections, biorthogonal Riesz bases and multiwavelets in Hilbert spaces*, Proc. Amer. Math. Soc., vol. 128, no. 2, 463-473, 1999.

[28] M. Unser, *Sampling-50 years after Shannon*, Proc. IEEE, vol. 88, no. 4, 569-587, 2000.

[29] M. Unser and A. Aldroubi, *A general sampling theory for nonideal acquisition devices*, IEEE Trans. Signal Process., vol. 42, no. 11, 2915-2925, 1994.

[30] G. G. Walter, *A sampling theorem for wavelet subspaces*, IEEE Trans. on Information Theory, vol. 38, pp. 881-884, 1992.

[1]
Division of Mathematics and Informational Statistics, Wonkwang University
Iksan 570-749, S. Korea
e-mail:skang@wku.ac.kr

[2]
Department of Mathematical Sciences, KAIST
Daejeon 305-701, S. Korea
e-mail: khkwon@kaist.edu, daegwan@kaist.ac.kr

Beyond Shannon: Generalized Sampling

K. H. Kwon

Department of Mathematical Sciences
KAIST

Fukuoka 2014. 12. 16 – 12. 19

Contents

Introduction

Think analog. But act digital.

In signal processing, "sampling" is the reduction of a continuous-time signal (analog signal) $f(t)$ into a discrete-time signal $\{\, f(t_n)\}_{n\in\mathbb{Z}}$ (digital signal).

Goal : Recover $f(t)$ by $\{\, f(t_n)\}_{n\in\mathbb{Z}}$ as $f(t) = \sum_n f(t_n)\, S_n(t)$ or $f(t) = \sum_j \sum_n \mathcal{L}_j(f)(t_{j,n})\, S_{j,n}(t)$.

Fundamental questions : What class of analog signals admits such sampling series?
How to take sample points $\{t_n\}$ and reconstruction functions $\{S_n(t)\}$?

Extreme examples :
any straight line

$$f(t) = at + b = f(0)(1-t) + f(1)t$$

and
any entire analytic function

$$f(z) = \sum_{n=0}^{\infty} \frac{1}{n!} f^{(n)}(0) z^n.$$

H. Nyquist, Certain topics in telegraph transmission theory, AIEE Trans., 47 (1928), 617-644.

C. E. Shannon, A mathematical theory of communications, Bell Lab. Tech. J., 1948

A signal $f(t)$ of finite energy, i.e., $f(t) \in L^2(\mathbb{R})$ is band-limited if its Fourier transform (frequency spectrum) $\hat{f}(\xi) = \int_{-\infty}^{\infty} f(t)e^{-it\xi}dt$ has the compact support.

For any $B > 0$, Paley-Wiener space

$$PW_B := \{f(t) \in L^2(\mathbb{R}) : \mathrm{supp}\ \hat{f}(\xi) \subseteq [-B, B]\}$$

$$= \{f(z) \in E_B : f(t) \in L^2(\mathbb{R})\}$$

where, E_B is the space of entire analytic functions of exponential type $\leq B$.

WSKS (Whittaker-Shannon-Kotel'nikov-Someya) sampling theorem

Any signal $f(t) \in PW_B$ can be reconstructed by its uniform sample values $\{f\left(n\frac{\pi}{\tilde{B}}\right)\}$ as a cardinal series :

$$f(t) = \sum_{n\in\mathbb{Z}} f\left(n\frac{\pi}{\tilde{B}}\right) \operatorname{sinc}\left(\frac{\tilde{B}}{\pi}t - n\right), \quad \text{for any } \tilde{B} \geq B$$

which converges both in $L^2(\mathbb{R})$ and absolutely and uniformly on $\mathbb{R}$. Here $\operatorname{sinc} t = \frac{\sin \pi t}{\pi t}$ is the cardinal sine function and $\frac{\tilde{B}}{\pi}$ (samples/sec) is the sampling rate and $\frac{B}{\pi}$ is the Nyquist rate, the smallest possible sampling rate.

Proof.

For simplicity, assume $\tilde{B} = B = \pi$ so that $f(t) \in PW_\pi$.
Then $\hat{f}(\xi) \in L^2(\mathbb{R})$ and $\hat{f}(\xi) = 0$ a.e. for $|\xi| > \pi$ so that

$$\hat{f}(\xi) = \frac{1}{2\pi} \sum_{n\in\mathbb{Z}} \langle \hat{f}(\xi), e^{-in\xi} \rangle_{L^2[-\pi,\pi]} e^{-in\xi} = \sum_{n\in\mathbb{Z}} f(n) e^{-in\xi} \text{ in } L^2[-\pi,\pi]$$

and so

$$\hat{f}(\xi) \; = \; \sum_{n\in\mathbb{Z}} f(n) e^{-in\xi} \chi_{[-\pi,\pi]}(\xi).$$

Taking the inverse Fourier transform gives

$$f(t) = \sum_{n\in\mathbb{Z}} f(n) \frac{\sin \pi(t-n)}{\pi(t-n)} = \sum_{n\in\mathbb{Z}} f(n) \operatorname{sinc}(t-n). \quad \square$$

Classical WSKS-sampling theorem has been extended to signals, which are band-limited in some generalized sense, e.g. signals in Bernstein space

$$B_\sigma^p = \{f(z) \in E_\sigma : f(t) \in L^p(\mathbb{R})\} \ (1 \le p \le \infty, \ \sigma > 0).$$

In order to extend sampling theorem to signals, which are possibly time-limited (so not band-limited by Heisenberg's uncertainty principle), we need the concept of shift invariant subspaces of $L^2(\mathbb{R})$, which are building blocks of MRA and wavelet theory.

By Plancherel's theorem, $\frac{1}{\sqrt{2\pi}}\mathcal{F} : PW_\pi \cong L^2[-\pi, \pi]$ so PW_π is a Hilbert subspace of $L^2(\mathbb{R})$ of which $\{\mathrm{sinc}(t-n) : n \in \mathbb{Z}\}$ is an ONB. Hence we may express PW_π as

$$\begin{aligned} PW_\pi &= \{f \in L^2(\mathbb{R}) : \mathrm{supp}\ \hat{f}(\xi) \subset [-\pi, \pi]\} \\ &= \overline{\mathrm{span}}\{\mathrm{sinc}(t-n) : n \in \mathbb{Z}\} \\ &= \{\sum_{n\in\mathbb{Z}} c(n)\mathrm{sinc}(t-n) : \mathbf{c} = \{c(n)\} \in l^2\}, \end{aligned}$$

which is a shift invariant space generated by $\mathrm{sinc}\ t$. That is, if $f(t) \in PW_\pi$, then $f(t-n) \in PW_\pi$ for any $n \in \mathbb{Z}$.

Moreover

$$\frac{1}{2\pi}\operatorname{sinc}(\cdot - s) \in PW_\pi \text{ for any } s \text{ in } \mathbb{R}$$

and

$$\langle f(t), \frac{1}{2\pi}\operatorname{sinc}(t-s)\rangle_{L^2(\mathbb{R})} = f(s) \text{ for any } f \in PW_\pi.$$

Hence PW_π is a reproducing kernel Hilbert space (RKHS) with reproducing kernel $q(t,s) = \frac{1}{2\pi}\operatorname{sinc}(t-s)$ in the sense that:

A Hilbert space H consisting of complex valued functions on $\mathbb{R}$ is called a reproducing kernel Hilbert space (RKHS) if there is a function $q(t,s)$ on $\mathbb{R}\times\mathbb{R}$, called the reproducing kernel of H satisfying

- $q(\cdot, s) \in H$ for each s in $\mathbb{R}$;
- $\langle f(t), q(t,s)\rangle = f(s),\ f \in H.$

Then any sequence $\{f_n(t)\}$ converging in an RKHS H converges also uniformly on any set in $\mathbb{R}$ on which $q(s,s)$ is bounded.

Sampling on Shift Invariant Spaces

For any $\phi(t) \in L^2(\mathbb{R})$, let $V(\phi) := \overline{\mathrm{span}}\{\phi(t-n) : n \in \mathbb{Z}\}$ be the closed subspace of $L^2(\mathbb{R})$, called the shift invariant space generated by $\phi(t)$. Then $\{\phi(t-n) : n \in \mathbb{Z}\}$ is

- an ONB of $V(\phi)$ if

$$\|\sum_{n\in\mathbb{Z}} c(n)\phi(t-n)\|^2 = \|\mathbf{c}\|^2 := \sum_{n\in\mathbb{Z}} |c(n)|^2, \ \mathbf{c} = \{c(n)\}_{n\in\mathbb{Z}} \in l^2;$$

- a Riesz basis of $V(\phi)$ with Riesz bounds $B \geq A > 0$ if

$$A\|\mathbf{c}\|^2 \leq \|\sum_{n\in\mathbb{Z}} c(n)\phi(t-n)\|^2 \leq B\|\mathbf{c}\|^2, \ \mathbf{c} = \{c(n)\}_{n\in\mathbb{Z}} \in l^2;$$

- a frame of $V(\phi)$ with frame bounds $B \geq A > 0$ if

$$A\|f\|^2 \leq \sum_{n\in\mathbb{Z}} |\langle f, \phi(t-n)\rangle|^2 \leq B\|f\|^2, \ f \in V(\phi).$$

When $\{\phi(t-n) : n \in \mathbb{Z}\}$ is an ONB or a Riesz basis or a frame of $V(\phi)$, we call $\phi(t)$ an orthonormal or a Riesz (or stable) or a frame generator of the shift invariant space $V(\phi)$.

Then $\{\phi(t-n) : n \in \mathbb{Z}\}$ is
an ONB of $V(\phi) \Longrightarrow$ a Riesz basis of $V(\phi) \Longrightarrow$ a frame of $V(\phi)$ $\Longrightarrow \exists$ a dual frame $\{\psi(t-n) : n \in \mathbb{Z}\}$ of $V(\phi)$ (not necessarily unique) such that

$$f(t) = \sum_{n\in\mathbb{Z}} \langle f(t), \psi(t-n)\rangle \phi(t-n),\ f \in V(\phi),$$

which is called the frame expansion of $f(t)$. Members of a frame may not be linearly independent, which is a merit rather than a demerit.

Proposition 1.
Let $\phi(t) \in L^2(\mathbb{R})$, $G_\phi(\xi) := \sum_{n\in\mathbb{Z}} |\hat{\phi}(\xi + 2n\pi)|^2$ and $B \geq A > 0$.
Then $\phi(t)$ is

(a) an orthonormal generator iff

$$G_\phi(\xi) = 1 \text{ a.e. on } \mathbb{R};$$

(b) a Riesz generator with bounds (A, B) iff

$$A \ \leq\ G_\phi(\xi)\ \leq\ B \text{ a.e. on } \mathbb{R};$$

(c) a frame generator with bounds (A, B) iff

$$A \ \leq\ G_\phi(\xi)\ \leq\ B \text{ a.e. on } \operatorname{supp} G_\phi.$$

For any frame generator $\phi(t) \in L^2(\mathbb{R})$, let

$$T(\mathbf{c}) := (\mathbf{c} * \phi)(t) = \sum_{k\in\mathbb{Z}} c(k)\phi(t-k), \quad \mathbf{c} = \{\, c(k)\}_{k\in\mathbb{Z}} \in l^2$$

be the synthesis operator of the frame $\{\phi(t-n) : n \in \mathbb{Z}\}$.
Then T is a bounded linear operator from l^2 onto $V(\phi)$.
Hence T is an isomorphism from $N(T)^{\perp}$ onto $V(\phi)$ so that

$$V(\phi) = \{(\mathbf{c} * \phi)(t) : \mathbf{c} \in l^2\} = \{(\mathbf{c} * \phi)(t) : \mathbf{c} \in N(T)^{\perp}\},$$

where $N(T) := \big\{\mathbf{c} \in l^2 : T(\mathbf{c}) = 0\big\}$ and $l^2 = N(T) \oplus N(T)^{\perp}$.
If $\phi(t)$ is a Riesz generator, then T is an isomorphism from l^2 onto $V(\phi) = \{(\mathbf{c} * \phi)(t) : \mathbf{c} \in l^2\}$.

If $\phi(t) \in L^2(\mathbb{R})$ is a frame generator satisfying

($*$) $\phi(t)$ is everywhere well defined on $\mathbb{R}$ and $C_\phi(t) := \sum_{n\in\mathbb{Z}} |\phi(t+n)|^2 < \infty$, $t \in \mathbb{R}$,

then

$$V(\phi) \;=\; \{\,(\mathbf{c} * \phi)(t) \,:\, \mathbf{c} \in N(T)^{\perp}\}$$

is an RKHS of which any $(\mathbf{c} * \phi)(t)$ converges both in $L^2(\mathbb{R})$ and absolutely on $\mathbb{R}$.

For any $\phi(t) \in L^2(\mathbb{R})$ satisfying $(*)$, let

$$Z_\phi(t,\xi) \ := \ \sum_{n\in\mathbb{Z}} \phi(t+n)e^{-in\xi} \ \in \ L^2[0,2\pi] \quad \text{for each } t \text{ in } \mathbb{R}$$

be the Zak transform of $\phi(t)$.

For any measurable function $f(t)$ on $\mathbb{R}$, let

$$\|f\|_0 := \sup_{|E|=0} \inf_{R\setminus E} |f(t)| \text{ and } \|f\|_\infty := \inf_{|E|=0} \sup_{R\setminus E} |f(t)|$$

be the essential infimum and the essential supremum of $|f(t)|$ respectively where $|E|$ is the Lebesgue measure of E.

Theorem 2. (General irregular sampling)(CIS, KK)
Let $\phi(t)$ be a frame generator satisfying $(*)$ so $V(\phi) = \{(\mathbf{c} * \phi)(t) : \mathbf{c} \in N(T)^\perp\}$ is an RKHS. Then for any sampling points $\{t_n\}_{n\in\mathbb{Z}}$ in $\mathbb{R}$, the followings are all equivalent.

(a) There is a frame $\{S_n(t) : n \in \mathbb{Z}\}$ of $V(\phi)$ such that

$$f(t) = \sum_{n\in\mathbb{Z}} f(t_n)S_n(t), \ f(t) \in V(\phi)$$

and $\{f(t_n)\}_{n\in\mathbb{Z}}$ is a moment sequence of a function to $\{S_n(t) : n \in \mathbb{Z}\}$, that is,

$$f(t_n) = \langle g(t), S_n(t)\rangle, \ n \in \mathbb{Z}$$

for some $g(t)$ in $V(\phi)$.

(b) (sampling inequality) $\exists \beta \geq \alpha > 0$ such that

$$\alpha \|f\|^2 \leq \sum_{n \in \mathbb{Z}} |f(t_n)|^2 \leq \beta \|f\|^2, \ f \in V(\phi).$$

(c) $\{q(t, t_n) : n \in \mathbb{Z}\}$ is a frame of $V(\phi)$, where $q(t, s)$ is the reproducing kernel of $V(\phi)$.

Furthermore, if any one of the above three equivalent statements holds, then the sampling series converges both in $L^2(\mathbb{R})$ and absolutely and uniformly on any subset E of $\mathbb{R}$ on which $C_\phi(t)$ is bounded.

Theorem 3. (Regular shifted sampling)(KK)
Let $\phi(t)$ be a frame generator satisfying $(*)$ so $V(\phi) = \left\{(\mathbf{c} * \phi)(t) : \mathbf{c} \in N(T)^{\perp}\right\}$ is an RKHS. Then for any $0 \leq \sigma < 1$, the followings are equivalent.

(a) There is a frame $\{\, S(t-n) \,:\, n \in \mathbb{Z}\}$ of $V(\phi)$ such that

$$f(t) \;=\; \sum_{n \in \mathbb{Z}} f(\sigma + n) S(t-n), \quad f \in V(\phi).$$

(b) There are constants $\beta \geq \alpha > 0$ such that

$$\alpha \;\leq\; |Z_\phi(\sigma,\xi)| \;\leq\; \beta \ \text{ a.e. on } \operatorname{supp} G_\phi.$$

(c) (sampling inequality) $\exists \beta \geq \alpha > 0$ such that

$$\alpha \|f\|^2 \;\leq\; \sum_{n\in\mathbb{Z}} |f(\sigma+n)|^2 \;\leq\; \beta \|f\|^2, \quad f \in V(\phi).$$

Moreover in this case,

$$\hat{S}(\xi) \;=\; \frac{\hat{\phi}(\xi)}{Z_\phi(\sigma,\xi)} \chi_{\operatorname{supp}\hat{\phi}}(\xi).$$

In Theorem 3, all sampling series converge both in $L^2(\mathbb{R})$ and absolutely on $\mathbb{R}$. Moreover they converge uniformly on any subset of $\mathbb{R}$ on which $C_\phi(t) = \sum_{n\in\mathbb{Z}} |\phi(t+n)|^2$ is bounded.

If $\phi(t) \in L^2(\mathbb{R}) \cap C(\mathbb{R})$ is a continuous frame generator satisfying $\sup_{\mathbb{R}} C_\phi(t) < \infty$, then $V(\phi) = \{\, (\mathbf{c} * \phi)(t) \,:\, \mathbf{c} \in l^2\}$ is an RKHS and the sampling series converges uniformly on $\mathbb{R}$.

Examples

Cardinal B-splines
Let $\phi_0(t) = \chi_{[0,1)}(t)$ and

$$\phi_n(t) = \phi_{n-1}(t) * \phi_0(t) = \int_0^1 \phi_{n-1}(t-s)ds,\ n \geq 1$$

be the cardinal B-spline of degree n. Then $\phi_0(t)$ is an orthonormal generator and $\phi_n(t)$ for $n \geq 1$ is a continuous Riesz generator.
Moreover since $\phi_n(t)$ has compact support, $\sup\limits_{\mathbb{R}} C_{\phi_n}(t) = \sup\limits_{\mathbb{R}} \sum\limits_{k\in\mathbb{Z}} |\phi_n(t+k)|^2 < \infty$ so that $V(\phi_n) = \{(\mathbf{c} * \phi_n)(t) : \mathbf{c} \in l^2\}$ is an RKHS for any $n \geq 0$.

For $\phi_1(t) = t\chi_{[0,1)}(t) + (2-t)\chi_{[1,2)}(t)$ and $0 \leq \sigma < 1$,

$$\phi_1(\sigma) = \sigma,\ \phi_1(\sigma+1) = 1-\sigma,\ \phi_1(\sigma+n) = 0 \text{ for } n \neq 0, 1$$

so that $Z_{\phi_1}(\sigma, \xi) = \sigma + (1-\sigma)e^{-i\xi}$. Then

$$\|Z_{\phi_1}(\sigma,\xi)\|_0 = |2\sigma - 1| \text{ and } \|Z_{\phi_1}(\sigma,\xi)\|_\infty = 1.$$

Hence we have for any σ with $0 \leq \sigma < 1$ and $\sigma \neq \frac{1}{2}$, a Riesz basis expansion

$$f(t) = \sum_{n\in\mathbb{Z}} f(\sigma+n)S(t-n),\ f \in V(\phi_1),$$

which converges in $L^2(\mathbb{R})$ and uniformly on $\mathbb{R}$.

For
$\phi_2(t) = \frac{1}{2}t^2\chi_{[0,1)}(t) + \frac{1}{2}(6t-2t^2-3)\chi_{[1,2)}(t) + \frac{1}{2}(3-t)^2\chi_{[2,3)}(t)$,

$$\|Z_{\phi_2}(0,\xi)\|_0 = 0 \text{ but } 0 < \|Z_{\phi_2}(\frac{1}{2},\xi)\|_0 < \|Z_{\phi_2}(\frac{1}{2},\xi)\|_\infty < \infty$$

so that there is a Riesz basis expansion

$$f(t) = \sum_{n\in\mathbb{Z}} f(\frac{1}{2}+n)S(t-n), \ f \in V(\phi_2)$$

which converges in $L^2(\mathbb{R})$ and uniformly on $\mathbb{R}$.

Multi-channel Sampling

Let $\{L_j[\cdot]\}_{j=1}^N$ be LTI systems with suitable impulse responses $\{l_j(t)\}_{j=1}^N$ so that

$$L_j[f](t) = (f * l_j)(t) = \int_{-\infty}^{\infty} f(s)l_j(t-s)ds, \ 1 \le j \le N.$$

Goal: Recover any signal f in $V(\phi)$ as

$$f(t) = \sum_{j=1}^{N}\sum_{n\in\mathbb{Z}} L_j[f](\sigma_j + rn)s_{j,n}(t),$$

where

- r is a positive integer;
- $0 \le \sigma_j < r$;
- $\{s_{j,n}(t)\}_{j,n}$ is a frame of $V(\phi)$.

Let $\psi_j = L_j[\phi]$, $g_j(\xi) = \frac{1}{2\pi} Z_{\psi_j}(\sigma_j, \xi)$,

$$G(\xi) = [g_j(\xi + (k-1)\tfrac{2\pi}{r})]_{j=1,}^{N}{}_{k=1}^{r}$$

and

- $\lambda_M(\xi) :=$ the largest eigenvalue of $G(\xi)^* G(\xi)$
- $\lambda_m(\xi) :=$ the smallest eigenvalue of $G(\xi)^* G(\xi)$
- $\beta_G := \|\lambda_M(\xi)\|_\infty$
- $\alpha_G := \|\lambda_m(\xi)\|_0$.

Theorem 4.
Assume that $\beta_G < \infty$, that is, all $g_j(\xi)$ are in $L^\infty[0, 2\pi]$. TFAE.

- There is a frame $\{s_{j,n}(t) : 1 \le j \le N,\ n \in \mathbb{Z}\}$ of $V(\phi)$ for which

$$f(t) = \sum_{j=1}^{N} \sum_{n\in\mathbb{Z}} L_j[f](\sigma_j + rn) s_{j,n}(t),\ f(t) \in V(\phi);$$

- there is a frame $\{s_j(t - rn) : 1 \le j \le N,\ n \in \mathbb{Z}\}$ of $V(\phi)$ for which for any $f(t) \in V(\phi)$

$$f(t) = \sum_{j=1}^{N} \sum_{n\in\mathbb{Z}} L_j[f](\sigma_j + rn) s_j(t - rn);$$

- $0 < \alpha_G$.
- It is a Riesz basis expansion iff $r = N$.

Example
Let $\phi(t) = \operatorname{sinc} t$ *so that* $V(\phi) = PW_\pi$ *and*

$$\hat{\ell}_1(\xi) = 1,\ \hat{\ell}_2(\xi) = -i \operatorname{sgn} \xi$$

so that $L_1[f](t) = f(t)$ *and* $L_2[f](t) = \widetilde{f}(t)$, *the Hilbert transform of* $f(t)$. *Take* $\sigma_1 = \sigma_2 = 0$ *and* $r_1 = r_2 = 2$. *Then*

$$f(t) = \sum_{n\in\mathbb{Z}} f(2n) S_1(t-2n) + \sum_{n\in\mathbb{Z}} \widetilde{f}(2n) S_2(t-2n), \qquad f \in PW_\pi,$$

where $S_1(t) = \operatorname{sinc} t,\ S_2(t) = \frac{\cos \pi t - 1}{\pi t}$.
The series converges absolutely and uniformly on $\mathbb{R}$.

Consistent Sampling

Let $\phi(t) \in L^2(\mathbb{R})$ be a frame generator and $\psi(t)$ its dual generator. Then

$$\widetilde{f}(t) := \sum_{n\in\mathbb{Z}} \langle f(t), \psi(t-n)\rangle \phi(t-n)$$

is the orthogonal projection of $f(t) \in L^2(\mathbb{R})$ onto $V(\phi)$. Note here that the analysis filter $\psi(t)$ and the synthesis filter $\phi(t)$ are not independent but are dual each other, which may fail in other interesting signal processing. Note also that

$$\langle \widetilde{f}(t), \psi(t-n)\rangle = \langle f(t), \psi(t-n)\rangle, \quad n \in \mathbb{Z}.$$

We call

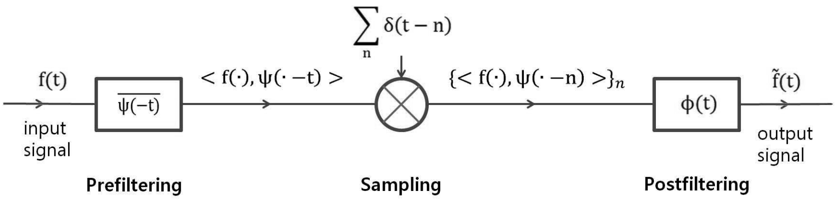

the approximation-sampling procedure, where $\boxed{\quad}$ means the convolution product.

Let $\mathcal{H}$ be a separable Hilbert space
$\{v_j\}$ analysis vectors, forming a frame of sampling space $\mathcal{V} := \overline{\mathrm{span}}\{v_j\}$;
$\{w_k\}$ synthesis vectors, forming a frame of reconstruction space $\mathcal{W} := \overline{\mathrm{span}}\{w_k\}$.

Let $S(\mathbf{c}) = \sum_j c(j) v_j$ and $T(\mathbf{d}) = \sum_k d(k) w_k$ ($\mathbf{c},\ \mathbf{d} \in \ell_2$) be the synthesis operators for $\{v_j\}$ and $\{w_k\}$. Then

$$S^* : \mathcal{H} \ni f \ \longmapsto \ S^*(f) = \{\langle f, v_j \rangle\} \in \ell_2$$

is the sampling operator.

Problem: Look for a sampling operator $\widetilde{P}$ on $\mathcal{H}$, which approximates an input f in $\mathcal{H}$ by $\widetilde{f} = \widetilde{P}(f)$ from its measurements $\mathbf{c} = S^*(f)$.

We require

(a) (stability) $\widetilde{P} \in L(\mathcal{H}, \mathcal{W})$,

(b) (sampling) $\widetilde{P}(f) = 0 \text{ if } S^*(f) = 0, \quad \text{i.e., } N(S^*) \subseteq N(\widetilde{P})$,

(c) (consistency)
$S^*(\widetilde{P}f) = S^*(f), \quad \text{i.e., } \langle f, v_j \rangle = \langle \widetilde{P}(f), v_j \rangle, \forall j.$

Consistency means that the input f and the output $\widetilde{P}(f)$ look the same to the observers.

Call $\widetilde{P}$ satisfying (a), (b), (c) a consistent sampling operator. Note that $\widetilde{P}$ satisfies (a) and (b) iff

$$\widetilde{P} = TQS^* \text{ for some } Q \in L(\ell_2)$$

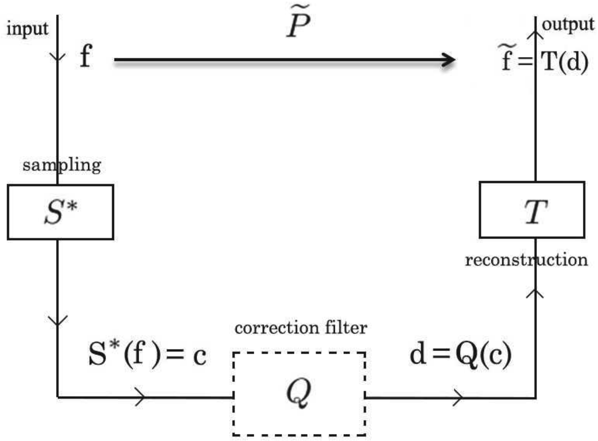

Let $C(\mathcal{W},\mathcal{V})$ be the set of all consistent sampling operators.

Theorem 5. (Lee, KK)
The followings are all equivalent.
(a) $C(\mathcal{W},\mathcal{V}) \neq \emptyset$;
(b) $\mathcal{H} = \mathcal{W} + \mathcal{V}^{\perp}$;
(c) $R(S^*T) = R(S^*)$.
In this case, $\mathcal{C}(\mathcal{W},\mathcal{V}) = \{P_{L,\mathcal{V}^{\perp}} \mid L \in \mathcal{L}\}$ where

$$\mathcal{L} := \{\text{closed complementary subspaces of } \mathcal{W}\cap\mathcal{V}^{\perp} \text{ in } \mathcal{W}\}$$

and

$$\mathcal{C}(\mathcal{W},\mathcal{V}) = \{T(S^*T)^{\dagger}S^* + TP_{N(S^*T)}YS^* \mid Y \in L(\ell_2)\}.$$

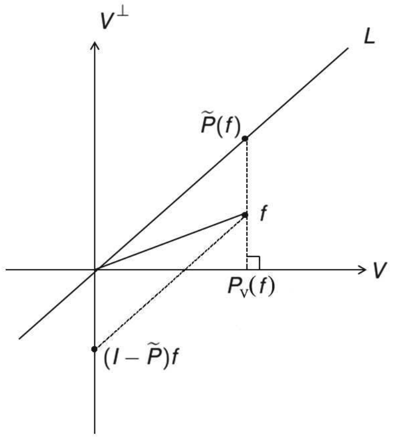

$$S^*(f) = S^*(\widetilde{P}(f)) \;\Leftrightarrow\; P_{\mathcal{V}}(f) = P_{\mathcal{V}}(\widetilde{P}(f)).$$

In particular, there is a unique consistent sampling operator $\widetilde{P}$ iff $\mathcal{H} = \mathcal{W}\oplus\mathcal{V}^{\perp}$. In this case, $\widetilde{P} = P_{\mathcal{W},\mathcal{V}^{\perp}} = T(S^*T)^{\dagger}S^*$.

Theorem 6. (Lee, KK)
Assume $\mathcal{H} = \mathcal{W} + \mathcal{V}^{\perp}$ and $\widetilde{P} = P_{L,\mathcal{V}^{\perp}}$, where $L \in \mathcal{L}$. Then

$$\widetilde{P}(f) = \lim_{n\to\infty} f_n, \quad f \in \mathcal{H}$$

and

$$\|P_{\mathcal{V}}(f - f_n)\| \le \|\widetilde{P}(f) - f_n\| \le \frac{\alpha^{2n-1}}{1-\alpha}\|P_{\mathcal{V}}(f)\|$$

where $\alpha = \|P_{\mathcal{V}^{\perp}} P_L\|$ and

$$\begin{cases} f_1 := P_L P_{\mathcal{V}}(f) \\ f_n := f_1 + P_L P_{\mathcal{V}^{\perp}}(f_{n-1}) \quad \text{for } n \ge 2. \end{cases}$$

Performance Analysis

Assume $\mathcal{H} = \mathcal{W} + \mathcal{V}^{\perp}$ and let for each L in
$\mathcal{L} = \{L | L \oplus (\mathcal{W} \cap \mathcal{V}^{\perp}) = \mathcal{W}\}$

$$\tilde{P} = P_{L,\mathcal{V}^{\perp}} : \mathcal{H} \longrightarrow L$$

be the unique consistent approximate operator valued in L.

Question: How good is the approximation $\tilde{P}f$ of $f \in \mathcal{H} \backslash L$ compared to orthogonal projection $P_L f$ of f onto L?

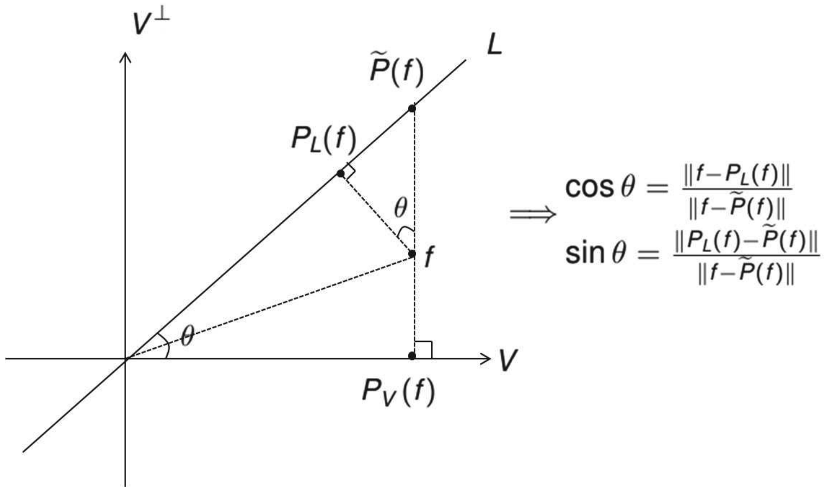

For any two non-trivial closed subspaces A and B of a Hilbert space $\mathcal{H}$, let

$$R(A,B) = \cos\Theta^R(A,B) = \inf_{\substack{v\in A\\ \|v\|=1}} \|P_B v\| \ (= R(B^\perp, A^\perp))$$

and

$$S(A,B) = \cos\Theta^S(A,B) = \sup_{\substack{v\in A\\ \|v\|=1}} \|P_B v\| \ (= S(B,A)),$$

where P_B is the orthogonal projection onto B. $R(A,B)$ and $S(A,B)$ are the worst and the best estimate of the relative length reduction when vectors in A are projected onto B.

Theorem 7. (Unser, Aldroubi; KK, Lee)
Assume $\mathcal{H} = \mathcal{W} + \mathcal{V}^\perp$ and let $\widetilde{P} = P_{L,\mathcal{V}^\perp}$ for $L \in \mathcal{L}$. Then for all $f \in \mathcal{H}\backslash L$,

(a) $0 < R(L, \mathcal{V}) \leq \dfrac{\|f - P_L(f)\|}{\|f - \tilde{P}(f)\|} \leq S(L^\perp, \mathcal{V}^\perp) \leq 1;$

(b) $0 \leq R(\mathcal{V}^\perp, L) \leq \dfrac{\|P_L(f) - \tilde{P}(f)\|}{\|f - \tilde{P}(f)\|} \leq S(L, \mathcal{V}^\perp) < 1.$

Thanks for your attention.

Evaluation of Crack Tip Fields and Role of Fracture Mechanics

Cheng Hua
Department of Mechanics and Engineering Science, Fudan University, Shanghai, China

Abstract: Fracture Mechanics has been accepted as an effective engineering methodology to evaluate the behavior of a crack tip fields and it seems to be considered as an almost established method. However, its system widely accepted at present contains some substantial problems that still remain to be solved. For instance, although the energy release rate is positioned as an important parameter in linear fracture mechanics, it cannot be extended inelastic fracture problems and, moreover, the crack parameters used in fracture mechanics such as stress intensity factor K, J-integral and C* parameter are defined just under special constitutive equation. As the results, the scope of the application of fracture mechanics is compelled to be limited without due cause. In this lecture, the outline of fracture mechanics is introduced first, then, what the basic issues are in the role of fracture mechanics is made clear.

Keywords: crack; fracture mechanics; stress intensity factor; path-independent integral

Introduction:

Fracture mechanics is mechanics of solids containing displacement discontinuities (cracks) with special attention to their growth. Fracture mechanics is a theory that determines material failure by fracture criteria. Linear Elastic Fracture Mechanics (LEFM) is the basic theory of fracture that deals with sharp cracks in elastic bodies. It is applicable to any materials as long as the material is elastic except in a vanishingly small region at the crack tip (assumption of small scale yielding). Elastic-Plastic Fracture Mechanics (EPFM) is the theory of ductile fracture, usually characterized by stable crack growth (ductile metals). The fracture process is accompanied by formation of large plastic zone at the crack tip.

(1) Basic forms of cracks propagating:

- Crack Ⅰ (opening mode): By normal stress σ, the cracks propagating direction is vertical to the direction of loading stress;
- Crack Ⅱ (slipping mode): By shear stress τ, the cracks propagating direction is parallel to the direction of loading stress;
- Crack Ⅲ (tearing mode): By shear stress τ, the cracks line is parallel to the direction of loading stress.

(2) Stress field at the crack tip

for crack mode I:

$$\begin{cases} \sigma_x = \dfrac{K_\mathrm{I}}{\sqrt{2\pi r}}\cos\dfrac{\theta}{2}\left(1-\sin\dfrac{\theta}{2}\sin\dfrac{3\theta}{2}\right) \\ \sigma_y = \dfrac{K_\mathrm{I}}{\sqrt{2\pi r}}\cos\dfrac{\theta}{2}\left(1+\sin\dfrac{\theta}{2}\sin\dfrac{3\theta}{2}\right) \\ \tau_{xy} = \dfrac{K_\mathrm{I}}{\sqrt{2\pi r}}\cos\dfrac{\theta}{2}\sin\dfrac{\theta}{2}\cos\dfrac{3\theta}{2} \end{cases}$$

while $K_\mathrm{I} = \sigma\sqrt{\pi a}$ is Stress Intensity Factor (SIF).

Generally, the stresses at the crack tip can by expressed as:

$$\sigma_{ij} = K_p f(r,\theta) \qquad (i, j = x, y, z) \quad (p= \text{I}, \text{II}, \text{III})$$

Stress Intensity Factors

$$\left.\begin{aligned} K_I &= \sigma\sqrt{\pi a} \\ K_{II} &= \tau\sqrt{\pi a} \\ K_{III} &= \tau\sqrt{\pi a} \end{aligned}\right\}$$

Discussion:

- ①*Ki (i= I, II,III)* are independent of co-ordinate. They are parameters to describe the intensity of the stress field around the crack tips;
- ②*Ki (i= I, II,III)* are close-related with the form, the size and the direction of the cracks;
- ③*Ki (i= I, II,III)* are correlated with the value of the loading and the loading form;
- ④*Ki (i= I, II,III)* are interrelated with the properties of the loaded material;
- The physical meaning of *Ki (i= I, II,III)* : They are mechanical parameters which are artificially introduced to describe the intensity of the stress field around the crack tips;
- By using these factors, the problem of solving the stress fields and displacements is simplified as just seeking for *Ki (i= I, II,III)*;
- Unit: *Ki (i= I, II,III)* ——[force]×[length]$^{-3/2}$ =[N]×[m]$^{-3/2}$

(3) Fracture criterion

$$K_i \geq K_{ic} \qquad (i = \text{I,II,III})$$

K_{IC} ——fracture tenacity/toughness, describing the resistance of crack propagating, determined by test（plane stress crack and plane strain crack）.

- When the thickness of the sample is small enough, the crack tip will be in a state of plane stress. When the crack line moves, its plastic area is relatively big enough to enhance K_{ic};
- When the thickness of the sample is big enough, the crack tip will be in a state of plane strain. When the crack line moves, its plastic area is relatively small enough to decrease $K_{ic} \to K_{Ic}$.

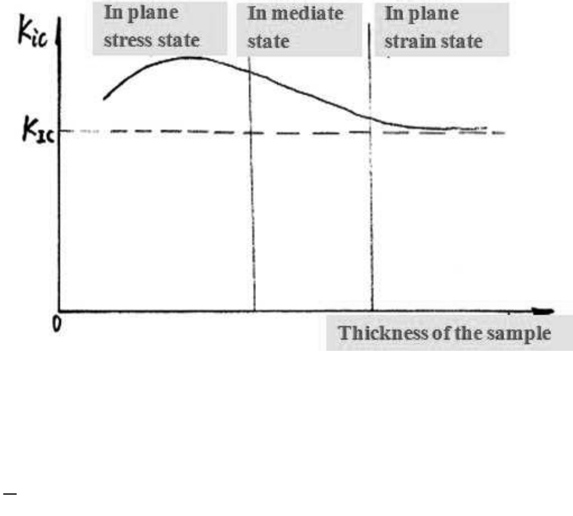

K_{IC}—— plane strain fracture toughness
$K_I = K_{IC}$ (fracture criterion for crack Ⅰ)

K_{IC} is a material constant, independent of the geometry of the testing sample. The thickness of the sample should be large enough to guarantee that the crack tip is in a state of plane strain.

(4) J-integral definition

The *J*-integral can be defined as a path-independent contour integral that measures the strength of the singular stresses and strains near a crack tip. Its value should be approximate constant far-field as well as near-crack field. However, *J*-integral constancy may be questionable after crack initiation. Also, dominance of the *J*-integral becomes more debatable if the structure composition is heterogeneous. The following equation shows an expression for *J* in its 2-D form, where crack lies in the XY plane with *x*-axis parallel to the crack (the following Figure):

$$J = \int_{\Gamma} \left[\left(W - \sigma_x \frac{\partial u}{\partial x} - \tau_{xy} \frac{\partial v}{\partial x} \right) dy + \left(\tau_{yx} \frac{\partial u}{\partial x} + \sigma_y \frac{\partial v}{\partial x} \right) dx \right]$$

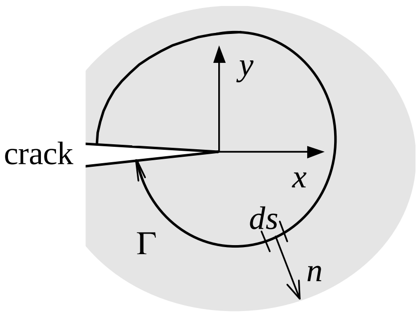

$$dy = n_x ds$$
$$dx = -n_y ds$$

Fig. Definition of contour for J-integral evaluation

In the above equation, Γ means any path surrounding the crack tip, W is strain energy density, σ_{ij} is component stress and u_i is displacement vector.

1. Stress field near the Crack Tip

The first step is to consider

Stress distribution around circular hole and elliptical hole:

Inglis (1913) analyzed for the flat plate with an elliptical hole with major axis 2a and minor axis 2b, subjected to far end stress

The linear elastic solution of the stress at the tip of the major axis is given by :

$$\sigma_{\max} = \sigma_0\left[1+2\left(\frac{a}{b}\right)\right]$$

The Inglis solution

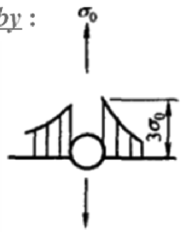

circular hole

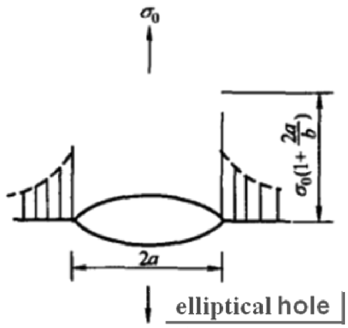

elliptical hole

For circular hole (b=a) :

$$\sigma_{\max} = 3\sigma_0$$

The paper looks like:
(Inglis, 1913)

The Mathematical Method (Linear Elastic Mechanics)

Inglis solution

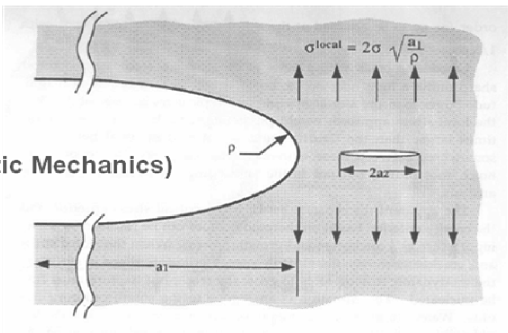

STRESSES IN A PLATE DUE TO THE PRESENCE OF CRACKS AND SHARP CORNERS.

By C. E. INGLIS, Esq., M.A., Fellow of King's College, Cambridge.

[Read at the Spring Meetings of the Fifty-fourth Session of the Institution of Naval Architects, March 14, 1913; Professor J. H. BILES, LL.D., D.Sc., Vice-President, in the Chair.]

PART I.

THE methods of investigation employed for this problem are mathematical rather than

Linear elasticity *solution* of an elliptic hole in a large plate (*Inglis solution*)

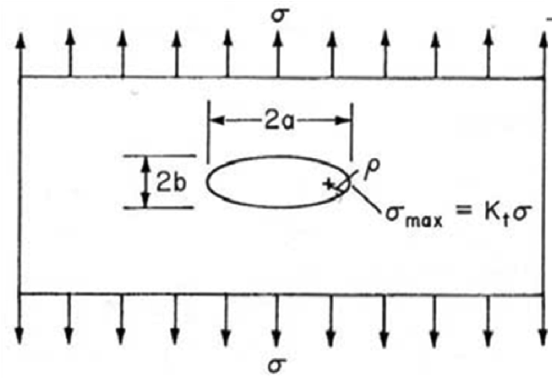

Stress Concentration Factor (SCF)

$$K_T = \frac{\sigma_{\max}}{\sigma} = 1 + \frac{2a}{b}$$

$$\rho = \frac{b^2}{a}$$

$$\sigma_{\max} \cong 2\sigma\sqrt{\frac{a}{\rho}} \quad (\rho << a)$$

- σ_0 → applied stress
- σ_{max} → stress at crack tip
- ρ → crack tip radius

$$\sqrt{\frac{a}{\rho}} \to \infty \, (\rho \to 0)$$

SCF

$$K_t \to \infty$$

Stress concentration and Stress singularity :

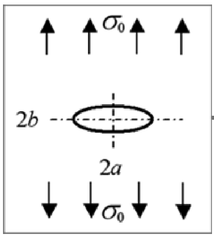

b=*a*, circular hole

$$\sigma_{\max} = 3\sigma_0$$

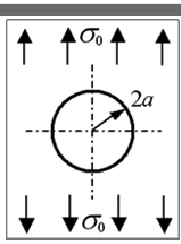

Stress Concentration:

$$K_t = \frac{\sigma_{\max}}{\sigma_0} = 3$$

Stress Concentration Factor (SCF)

b→0, Crack

$$\sigma_{\max} \to \infty$$

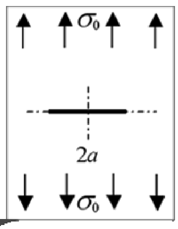

Stress Singularity:

$$K_t = \frac{\sigma_{\max}}{\sigma_0} = ?$$

How To Quantify? Lead to "Stress Intensity Factor (SIF)"

$$\sigma_{\max} = \sigma_0\left[1 + 2\left(\frac{a}{b}\right)\right] \approx 2\sigma_0\sqrt{\frac{a}{\rho}}$$

Cracks have a sharp tip and lead to stress singularity

The second to study **Stress singularity :**

Linear Elastic Mechanics

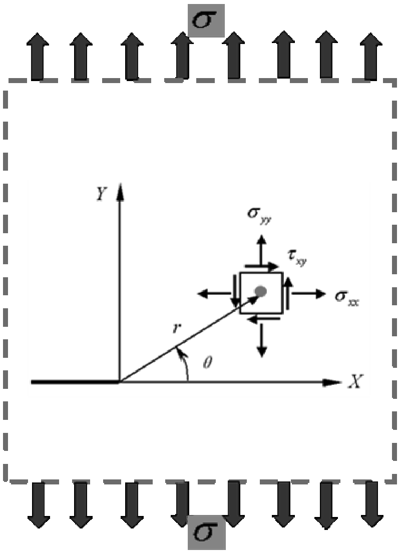

Crack length:2a

Stress near the crack tip

$$\begin{cases}\sigma_{xx} = \sigma\sqrt{\dfrac{a}{2r}}\cos\left(\dfrac{\theta}{2}\right)\left[1-\sin\left(\dfrac{\theta}{2}\right)\sin\left(\dfrac{3\theta}{2}\right)\right]+\cdots \\ \sigma_{yy} = \sigma\sqrt{\dfrac{a}{2r}}\cos\left(\dfrac{\theta}{2}\right)\left[1+\sin\left(\dfrac{\theta}{2}\right)\sin\left(\dfrac{3\theta}{2}\right)\right]+\cdots \\ \tau_{xy} = \sigma\sqrt{\dfrac{a}{2r}}\sin\left(\dfrac{\theta}{2}\right)\cos\left(\dfrac{\theta}{2}\right)\cos\left(\dfrac{3\theta}{2}\right)+\cdots\end{cases}$$

$$\boxed{\sigma_{ij}(r,\theta) \propto \frac{1}{\sqrt{r}} \quad (r \to 0)}$$

This feature is called Stress Singularity

2. Stress Intensity Factor-SIF

Irwin (1957) proposed a new physical quantity --- Stress Intensity Factor (SIF)

$$K = \lim_{r\to 0}\sqrt{2\pi r}\,\sigma_{yy}(r,0) = \sigma\sqrt{\pi a}$$

K is called the "Stress Intensity Factor"

Stress Field Near the Crack Tip

$$\sigma_x = \frac{K}{\sqrt{2\pi r}}\cos\frac{\theta}{2}\left(1-\sin\frac{\theta}{2}\sin\frac{3\theta}{2}\right)$$

$$\sigma_y = \frac{K}{\sqrt{2\pi r}}\cos\frac{\theta}{2}\left(1+\sin\frac{\theta}{2}\sin\frac{3\theta}{2}\right)$$

$$\tau_{xy} = \frac{K}{\sqrt{2\pi r}}\cos\frac{\theta}{2}\sin\frac{\theta}{2}\cos\frac{3\theta}{2}$$

$$\boxed{\sigma_{ij}(r,\theta) \propto \frac{1}{\sqrt{r}} \quad (r \to 0)}$$

Dr George R. Irwin
(1907-1998)

Why K? → The legend: Irwin chose the letter *K after J.A. Kies, one of his co-workers*

Solution to an Infinite Cracked Panel:

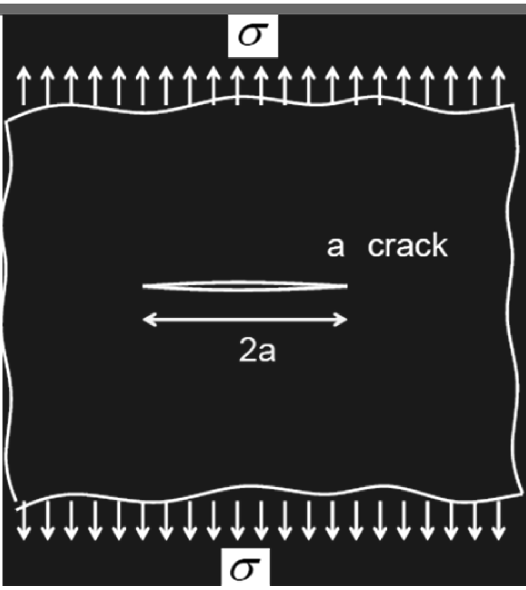

A Through Thickness Crack In an Infinite Plate subject to Uniform Tensile Stress

$$K = \sigma\sqrt{\pi a}$$

Solution to a Finite Size Cracked Panel :

Isida

$$K = Y\sigma\sqrt{a}$$

Westergaard
Irwin(1958)
Koiter(1959)

$$K = \sigma\sqrt{\pi a}\sqrt{\frac{W}{\pi a}\tan\frac{\pi a}{W}}$$

Fedderson:

$$K = \sigma\sqrt{\pi a}\sqrt{\sec\frac{\pi a}{W}}$$

More Exact

$$K = \sigma\sqrt{\pi a}\sqrt{\sec\frac{\pi a}{W}}\left\{1-.1\left(\frac{a}{W}\right)^2+0.96\left(\frac{a}{W}\right)^4\right\}$$

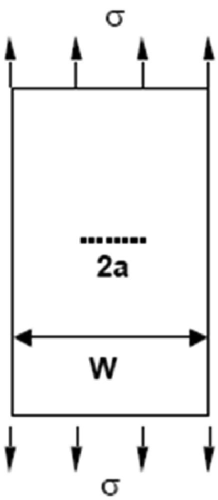

1. Rooke DP and Cartwright DJ (1976). Compendium of Stress Intensity Factors. Procurement Executive, Ministry of Defence. H.M.S.O.
2. Tada H, Paris PC, and Irwin GR (1985). The Stress Intensity Factor Handbook. Hellertown, Philadelphia: Del Research Corporation
3. Murakami Y (1987). Stress Intensity Factors Handbook. New York: Pergamon.

Solution to a Finite Size Cracked Panel :

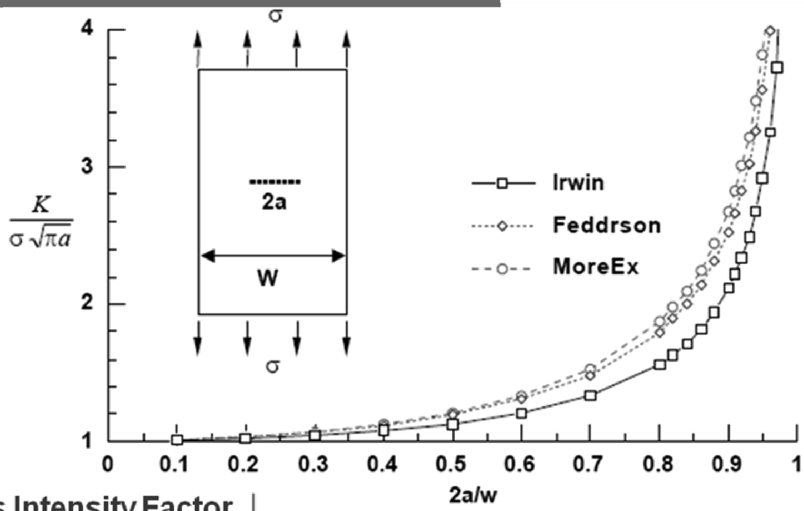

K: Stress Intensity Factor

K Factor defines the stress field around the crack tip, taking into account *crack length, applied stress and shape factor* (which accounts for finite size of the component and local geometric features)

Solution to a Finite Size Cracked Panel :

The Applied Stress
The Crack Shape and Size
The Structural Configuration

⬇ Affect

The Value of The Stress Intensity Factor, K

$$K = \sigma\sqrt{\pi a}\cdot F$$

F : Correction factor

In the 1950s Irwin and coworkers introduced the concept of Stress Intensity Factor, which defines the stress field around the crack tip, taking into account crack length, applied stress and shape factor (which accounts for finite size of the component and local geometric features).

Dr George R. Irwin
(1907-1998)

After having received the A.B. in English and Physics from Knox College and the M.A. and Ph. D in Physics from the University of Illinois, **George Irwin began his career in 1937. at the U.S. Naval Research Lab (NRL) where he developed several new ballistics research techniques.** As a result, the NRL Ballistics Branch, which was headed by Irwin, was able to develop non-metallic armors for fragment protection. These armors received trial use in World War II and extensive use during the Korean and Vietnam Wars. **The early years of this work led to an interest in brittle fracture and provided a basis for Irwin's pioneering work in fracture mechanics.** **The basic concepts established by Irwin and his team from 1946 to 1960 are now used world wide for fracture control in aircraft, nuclear reactor vessels and other fracture- critical applications.**

His numerous awards include ASTM Honorary Member, Timoshenko Medal of ASME, Gold Medal of ASM, The Grand Medal of the French Metallurgical Society, Tetmajer Medal o the Technical University of Vienna, member of the National Academy of Engineering and foreign membership in the Royal Society of London. He was appointed to Boeing University Professor at Lehigh University in 1967. He later joined the University of Maryland's Department of Engineering where he has been and active researcher and advisor of graduate students since 1972.

3. Elementary Fracture Mechanics

Modes of Fracture (the three modes of crack surface displacement):

- **Mode I** - ***Opening mode*** **or tensile mode**
- **Mode II** - ***Sliding mode*** **or in-plane shear mode**
- **Mode III** - ***Tearing mode*** **or anti-plane shear mode**

***Stress Intensity Factor*:**

- K_I for Mode I
- K_{II} for Mode II
- K_{III} for Mode III

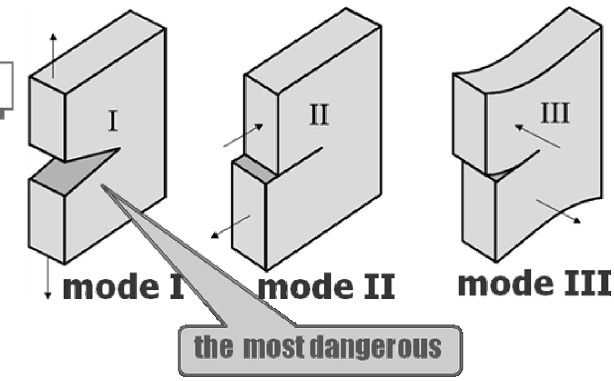

Similar to Mode I

K_{II} for Mode II and K_{III} for Mode III:

Stress near the crack tip

$$\sigma_{ij}(r,\theta) = \frac{K_{II}}{\sqrt{2\pi r}} f_{ij}^{II}(\theta)$$

$$K_{II} = \lim_{r\to 0} \sqrt{2\pi r}\,\tau_{xy}(r,0)$$

$$\sigma_{ij}(r,\theta) = \frac{K_{III}}{\sqrt{2\pi r}} f_{ij}^{III}(\theta)$$

$$K_{III} = \lim_{r\to 0} \sqrt{2\pi r}\,\tau_{yz}(r,0)$$

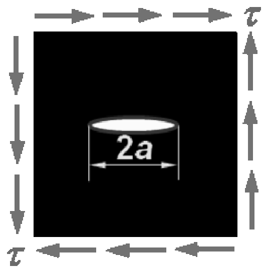

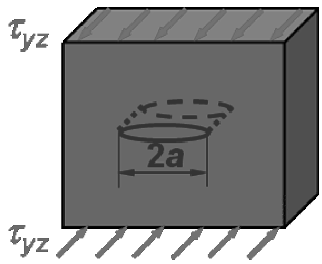

Mode I + Mode II + Mode III

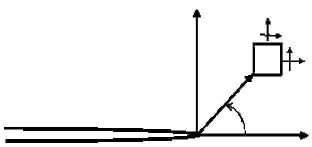

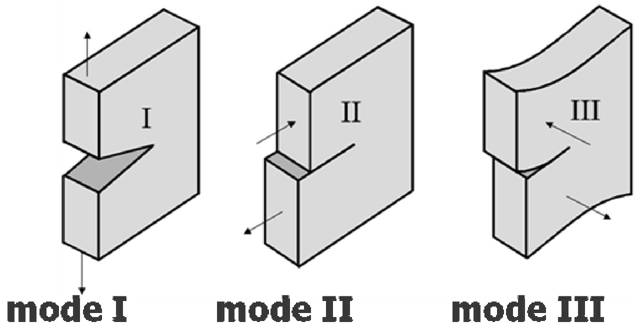

$$\sigma_{ij} = \sum_{m=I}^{III} \frac{K_m}{\sqrt{2\pi r}} f_{ij}^{(m)}(\theta) + O(1)$$

m = I, II, III

i, j=1, 2, 3

Basic types of fracture:
(according to whether the material has obvious plastic deformation before fracture)

- **Brittle Fracture**
- **Ductile Fracture**

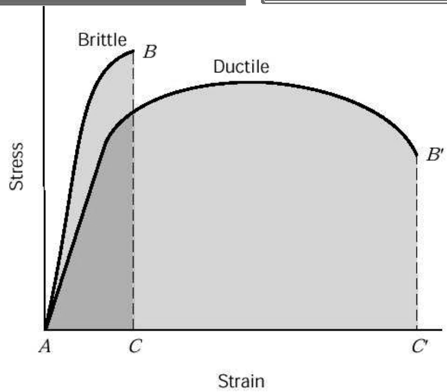

Brittle fracture - is more catastrophic and has been intensively studied

- Brittle fracture →
  - cracks are sharp & no crack tip blunting
  - No energy spent in plastic deformation at the crack tip

Ductile fracture - involves a large amount of plastic deformation

- Ductile fracture →
  - Crack tip blunting by plastic deformation at tip
  - Energy spent in plastic deformation at the crack tip

Related Subjects

- ***Linear Elastic*** **Fracture Mechanics (LEFM)**
- ***Elastic-Plastic*** **Fracture Mechanics (EPFM)**

Linear Elastic **Fracture Mechanics (LEFM) :**

- **Refer to Brittle material**
- **The structure obeys Hooke's law and global behavior is linear and if any local small scale crack tip plasticity is ignored**
- **Central to LEFM is the concept of *K* introduced by Irwin**

Elastic-Plastic **Fracture Mechanics (EPFM) :**

- **Refer to Ductile material**
- **The structure obeys an elastic-plastic constitutive**
- **Central to EPFM is the concept of *J-integral* introduced by James R. Rice**

The Previous Conditions:

Suppose a structure with an interior crack (existing crack)

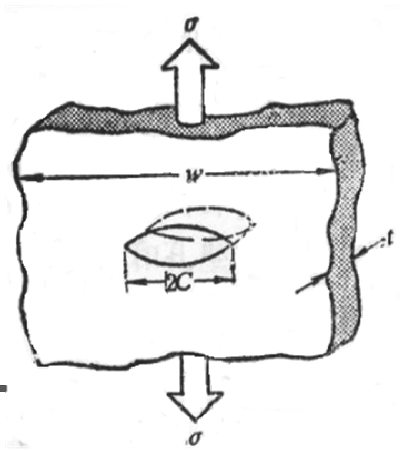

Two different points of view

- **Energy balance Griffith theory** (1921, Griffith, UK) — **Energy based**
- **The crack tip stress intensity** (1957, Irwin, USA) — **Stress based**

4. Griffith's Energy Balance Approach

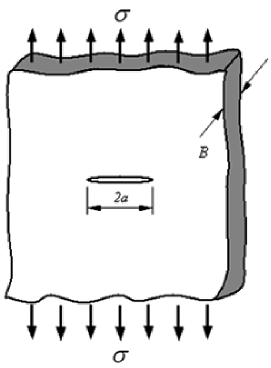

$A = 2aB$

$dA = 2Bda$

Griffith Proposed:

$$-\left(\frac{\partial W}{\partial A}\right) \geq \frac{G_c}{2}$$

Where,

A: Surface area of specimen
G_c: Amount of energy required to tear through a unit area of the material
Factor 2: Two newly formed surfaces

Dr Alan A. Griffith (1893-1963)

Griffith's Theory :

A crack would propagate in a stressed material only when, by doing so, it brought about a reduction in elastically stored energy W more than sufficient to meet the free energy requirements of newly formed fracture surfaces

Griffith AA, The phenomena of rupture and flow in solids, Philosophical Transactions, Series A, 1920(221): 163-198.

The core idea of Griffith theory

Crack extension force
= crack growth resistance

or named "Crack driving force", The release of potential energy Such as elastic energy

or named "Material resistance", The new surface energy formed on the crack surface

Strain energy release rate is introduced by Irwin

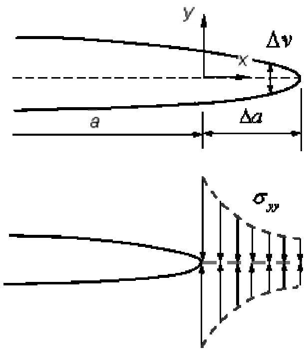

$$\boxed{G = \lim_{\Delta a \to 0} \frac{1}{\Delta A} \int_0^{\Delta A} \left(\sigma_{yy} \Delta v + \tau_{xy} \Delta u\right) dA}$$

For the infinite plate There are

$$\Delta v = \frac{8\sigma}{E} \sqrt{\frac{(a+\Delta a)(\Delta a - x)}{2}} \quad \text{(plane stress)}$$

$$\sigma_{yy} = \sigma \sqrt{\frac{a}{2x}}$$

$$\int_0^{\Delta A} \sigma_{yy} \Delta v dA = \frac{4\sigma^2}{E} \sqrt{a(a+\Delta a)} \int_0^{\Delta a} \sqrt{\frac{\Delta a - x}{x}} B dx$$

$$= \frac{4\sigma^2 B}{E} \sqrt{a(a+\Delta a)} \int_0^{\Delta a} \sqrt{\frac{\Delta a - x}{x}} dx$$

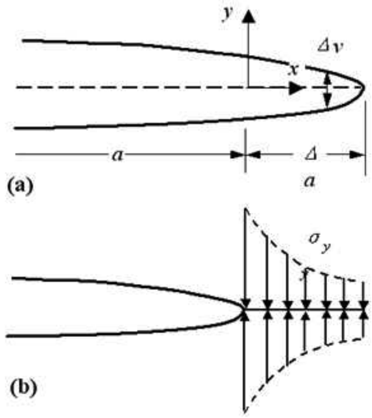

$$\int_0^{\Delta A} \sigma_{yy}\Delta v dA = \frac{4\sigma^2}{E}\sqrt{a(a+\Delta a)}\int_0^{\Delta a}\sqrt{\frac{\Delta a - x}{x}}B dx$$

$$= \frac{4\sigma^2 B}{E}\sqrt{a(a+\Delta a)}\int_0^{\Delta a}\sqrt{\frac{\Delta a - x}{x}}dx$$

$$\int_0^{\Delta a}\sqrt{\frac{\Delta a - x}{x}}dx = \frac{\pi}{2}\Delta a$$

$$\int_0^{\Delta A} \sigma_{yy}\Delta v dA = \frac{2\pi\sigma^2 B\Delta a}{E}\sqrt{a(a+\Delta a)}$$

$$G = \lim_{\Delta A\to 0}\frac{1}{\Delta A}\int_0^{\Delta A}\sigma_{yy}\Delta v dA$$

$$= \lim_{\Delta a\to 0}\frac{1}{2B\Delta a}\frac{2\pi\sigma^2 B\Delta a}{E}\sqrt{a(a+\Delta a)}$$

$$= \frac{\pi\sigma^2 a}{E}$$

The relationship between G and K

$$\sigma_c = \left(\frac{2E\gamma}{\pi a_c}\right)^{1/2} \qquad \sigma_c = \left(\frac{2E\gamma}{\pi(1-\nu^2)a_c}\right)^{1/2}$$

$$\sigma\sqrt{\pi a} = \sqrt{EG} \qquad \sigma\sqrt{\pi a} = \sqrt{EG/(1-\nu)}$$

$$G_I = \frac{K_I^2}{E'},\ E' = \begin{cases} E & \text{plane stress} \\ E/(1-\nu^2) & \text{plane strain} \end{cases}$$

$$G_T = G_I + G_{II} + G_{III}$$

5. J-integral

By idealizing elastic-plastic deformation as non-linear elastic, Rice (1968) proposed *J*-integral, for egions beyond LEFM

The Previous Conditions:

- In loading path elastic-plastic can be modeled as non-linear elastic but not in unloading part.
- Also *J*-integral uses deformation plasticity. It states that the stress state can be determined knowing the initial and final configuration. The plastic strain is in proportional load, i.e. $\frac{d\sigma_1}{\sigma_1} = \frac{d\sigma_2}{\sigma_2} = \frac{d\sigma_3}{\sigma_3} = \frac{d\sigma_4}{\sigma_4} = \frac{d\sigma_5}{\sigma_5} = \frac{d\sigma_6}{\sigma_6} = k$

- Under the above conditions, *J*-integral characterizes the crack tip stress and crack tip strain and energy release rate uniquely.
- *J*-integral is numerically equivalent to G for linear elastic material. It is a path-independent integral.
- When the above conditions are not satisfied, *J* becomes path dependent and does not relates to any physical quantities.

$$J = \int_{\Gamma} \left(W n_1 - T_i \frac{\partial u_i}{\partial x_1} \right) ds$$

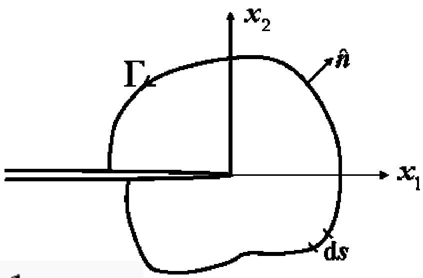

Strain energy density $W = \frac{1}{2}\sigma_{ij}\varepsilon_{ij}$

Traction force $T_i = \sigma_{ij} n_j$

***J* is a path-independent integral**

HRR Field (1968, Rice, Rosengren, Hutchinson):

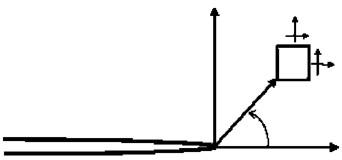

$$\begin{cases} \sigma_{ij}(r,\theta) = \alpha\left(\dfrac{J}{\alpha I_n r}\right)^{\frac{1}{n+1}} f_{ij}(\theta,n) \\ \varepsilon_{ij}(r,\theta) = \left(\dfrac{J}{\alpha I_n r}\right)^{\frac{n}{n+1}} g_{ij}(\theta,n) \\ u_i(r,\theta) = \alpha\left(\dfrac{J}{\alpha I_n}\right)^{\frac{1}{n+1}} r^{\frac{1}{1+n}} h_i(\theta,n) \end{cases}$$

Evaluation of *J*-Integral:

--*J* integral provides a unique measure of the strength of the singular fields in nonlinear fracture. However there are a few important Limitations, (Hutchinson, 1993)

1. Deformation theory of plasticity should be valid with small strain behavior with monotonic loading.

2. If finite strain effects dominate and microscopic failures occur, then this region should be much smaller compared to J dominated region, again based on the HRR singularity.

$$\sigma_{ij} = \sigma_y\left(\frac{J}{\alpha\sigma_y\sigma_y I_n r}\right)^{\frac{1}{n+1}} \sigma^I{}_{ij}(\theta,n)$$

6. Fracture Toughness and Fracture Criterion

Fracture toughness:

The resistance of a material to failure in the presence of a crack.

Fracture criterion: $K_i \le K_{ic} \quad (i = \mathrm{I,II,III})$

K_{ic} required for a crack to propagate describing the resistance of crack propagating, determined by test（plane stress crack and plane strain crack）

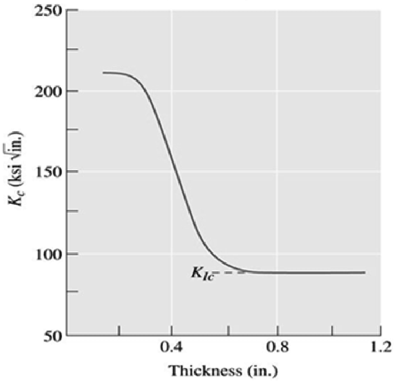

The fracture toughness K_{ic} of a high yield strength steel decreases with increasing thickness, eventually leveling off at the *plane strain fracture toughness, K_{ic}*

Effect of plate thickness on fracture toughness

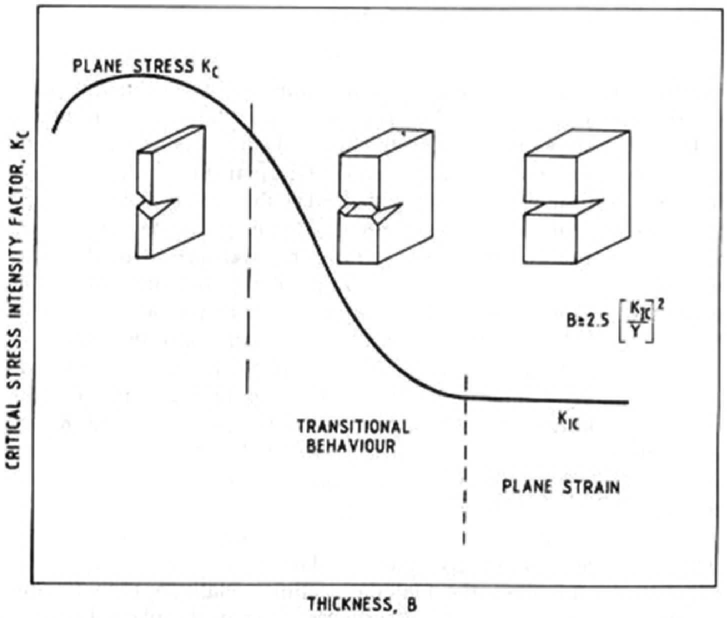

Material test standard :

Designation: E 399 – 90 (Reapproved 1997)

Standard Test Method for
Plane-Strain Fracture Toughness of Metallic Materials[1]

This standard is issued under the fixed designation E 399; the number immediately following the designation indicates the year of original adoption or, in the case of revision, the year of last revision. A number in parentheses indicates the year of last reapproval. A superscript epsilon (ϵ) indicates an editorial change since the last revision or reapproval.

This standard has been approved for use by agencies of the Department of Defense.

Designation: E 1820 – 01

Standard Test Method for
Measurement of Fracture Toughness[1]

This standard is issued under the fixed designation E 1820; the number immediately following the designation indicates the year of original adoption or, in the case of revision, the year of last revision. A number in parentheses indicates the year of last reapproval. A superscript epsilon (ϵ) indicates an editorial change since the last revision or reapproval.

Material or structure fracture control is the following three main factors:

Crack size and shape

Applied Stress

Fracture toughness of material

Fracture mechanics analysis

Material testing

K_I fracture criterion K_{IC}

The Importance of Fracture Mechanics:

The fracture mechanics approach allows us to design and select materials while taking into account the inevitable presence of cracks. There are three variables to consider:

- The property of the material (K_c or K_{Ic})
- The stress σ that the material must withstand
- The size of the crack

↓

If we know two of these variables, the third can be determined.

$$K = f\left(\frac{a}{W}, \cdots\right)\sigma\sqrt{\pi a} \le K_{1c}$$

Applied Stress σ	Crack size a	Fracture toughness K_{IC}
Known	Known	Choose materials satisfy the K_{ic} value fracture criterion promised not to break
Determine the working stress to allow to use	Known	Known
Known	Determine the allowable crack siz	Known

Fracture mechanics identifies three primary factors :

- **Material Fracture Toughness** Material fracture toughness may be defined as the ability to carry loads or deform plastically in the presence of a notch. It may be described in terms of the critical stress intensity factor, *KIc*, under a variety of conditions. (These terms and conditions are fully discussed in the following chapters.)
- **Crack Size** Fractures initiate from discontinuities that can vary from extremely small cracks to much larger weld or fatigue cracks. Furthermore, although good fabrication practice and inspection can minimize the size and number of cracks, most complex mechanical components cannot be fabricated without discontinuities of one type or another.
- **Stress Level** For the most part, tensile stresses are necessary for brittle fracture to occur. These stresses are determined by a stress analysis of the particular component.
- Other factors such as temperature, loading rate, stress concentrations, residual stresses, etc., influence these three primary factors.

7. Role of Fracture Mechanics

7.1 Mechanics of Materials and Fracture Mechanics

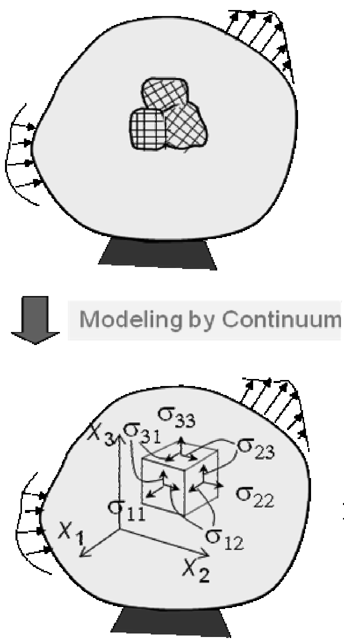

Mechanics of Materials

Equilibrium equation

$$\frac{\partial \sigma_{11}}{\partial x_1}+\frac{\partial \sigma_{12}}{\partial x_2}+\frac{\partial \sigma_{13}}{\partial x_3}=0$$

:

$$\sigma_{12}=\sigma_{21}\quad , \quad \cdots$$

Relation between Displacement and strain

$$\varepsilon_{11}=\frac{\partial u_1}{\partial x_1}\quad , \quad \cdots$$

$$\varepsilon_{12}=\frac{1}{2}\left(\frac{\partial u_1}{\partial x_2}+\frac{\partial u_2}{\partial x_1}\right)$$

:

Stress-strain relation

Boundary condition $T_i=\overline{T}_i$ on S_σ

$u_i=\overline{u}_i$ on S_u

(i=1,2,3)

Continuum mechanics under small displacement

$\downarrow$

Mechanics of Materials

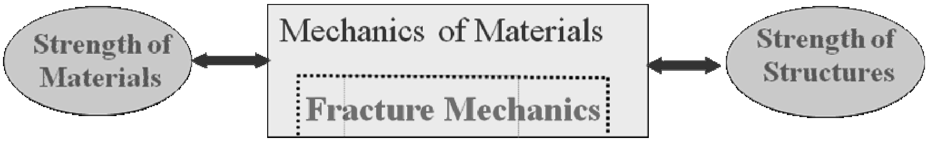

Mechanics of Materials and Fracture Mechanics

Crack Problem（Fracture Mechanics）

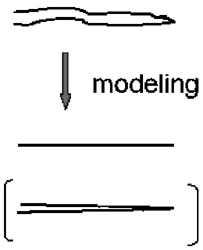

Stress, Strain, Strain energy density $\rightarrow \infty$

other parameters are necessary

Fracture Mechanics

Stress around a crack tip

Linear Elasticity

$$\sigma_{ij} = \frac{A_1}{\sqrt{r}} f_{ij}^{(1)}(\theta) + A_2 f_{ij}^{(2)}(\theta) + A_3 \sqrt{r} f_{ij}^{(3)}(\theta) + \cdots$$

$K = \sqrt{2\pi}\, A_1$ ： Stress Intensity Factor

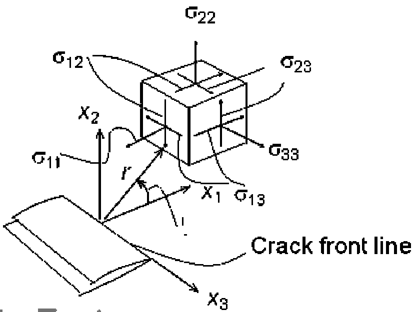

Deformation mode around a crack tip

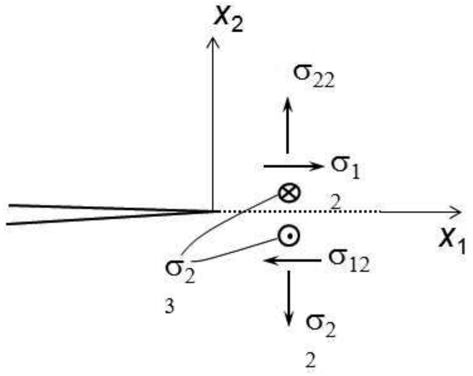

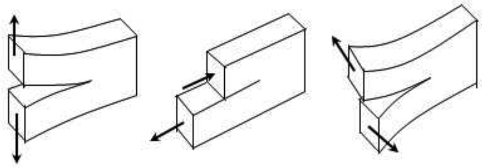

Mode Ⅰ   Mode Ⅱ   Mode Ⅲ

Mode I

$$\begin{Bmatrix}\sigma_{11}\\ \sigma_{22}\\ \sigma_{12}\end{Bmatrix} = \frac{K_{\mathrm{I}}}{\sqrt{2\pi r}}\cos\frac{\theta}{2}\begin{Bmatrix}1-\sin\frac{\theta}{2}\sin\frac{3\theta}{2}\\ 1+\sin\frac{\theta}{2}\sin\frac{3\theta}{2}\\ \sin\frac{\theta}{2}\cos\frac{3\theta}{2}\end{Bmatrix}$$

$$\begin{Bmatrix}u_1\\ u_2\end{Bmatrix} = \frac{K_{\mathrm{I}}}{2G}\sqrt{\frac{r}{2\pi}}\begin{Bmatrix}\cos\frac{\theta}{2}\left(\kappa-1+2\sin^2\frac{\theta}{2}\right)\\ \sin\frac{\theta}{2}\left(\kappa+1-2\cos^2\frac{\theta}{2}\right)\end{Bmatrix}$$

Mode II

$$\begin{Bmatrix}\sigma_{11}\\ \sigma_{22}\\ \sigma_{12}\end{Bmatrix} = \frac{K_{\mathrm{II}}}{\sqrt{2\pi r}}\begin{Bmatrix}\sin\frac{\theta}{2}\left(2+\cos\frac{\theta}{2}\cos\frac{3\theta}{2}\right)\\ \sin\frac{\theta}{2}\cos\frac{\theta}{2}\cos\frac{3\theta}{2}\\ \cos\frac{\theta}{2}\left(1-\sin\frac{\theta}{2}\sin\frac{3\theta}{2}\right)\end{Bmatrix}$$

$$\begin{Bmatrix}u_1\\ u_2\end{Bmatrix} = \frac{K_{\mathrm{II}}}{2G}\sqrt{\frac{r}{2\pi}}\begin{Bmatrix}\sin\frac{\theta}{2}\left(\kappa+1+2\cos^2\frac{\theta}{2}\right)\\ -\cos\frac{\theta}{2}\left(\kappa-1-2\sin^2\frac{\theta}{2}\right)\end{Bmatrix}$$

Mode III

$$\begin{Bmatrix}\sigma_{13}\\ \sigma_{23}\end{Bmatrix} = \frac{K_{\mathrm{III}}}{\sqrt{2\pi r}}\begin{Bmatrix}-\sin\frac{\theta}{2}\\ \cos\frac{\theta}{2}\end{Bmatrix}$$

$$u_3 = \frac{2K_{\mathrm{III}}}{G}\sqrt{\frac{r}{2\pi}}\sin\frac{\theta}{2}$$

$$\begin{cases}\text{plane strain} & \kappa = 3-4\nu\\ \text{plane stress} & \kappa = (3-\nu)/(1+\nu)\end{cases}$$

- **7.2 Summary of Fracture Parameters**

Energy Release Rate

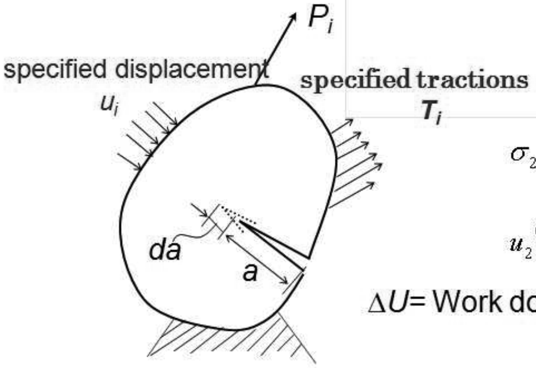

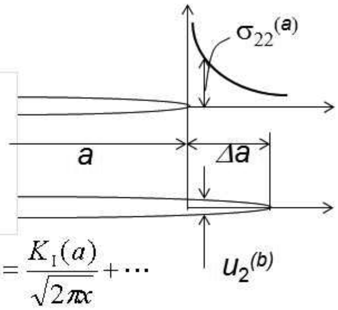

$$\sigma_{22}^{(a)} = \frac{K_{\mathrm{I}}(a)}{\sqrt{2\pi x}} + \cdots$$

$$u_2^{(b)} = \frac{\kappa+1}{2G}K_{\mathrm{I}}(a+\Delta a)\sqrt{\frac{\Delta a - x_1}{\pi}} + \cdots$$

ΔU= Work done by external force ΔL

$$-2\int_0^{\Delta a}\frac{1}{2}\sigma_{22}^{(a)}Bu_2^{(b)}dx_1$$

$$\mathcal{G} = \frac{dL}{dA} - \frac{dU}{dA}$$

$$dA = Bda$$

$$\mathcal{G} = \lim_{\Delta a\to 0}\frac{2}{B\Delta a}\int_0^{\Delta a}\frac{1}{2}\sigma_{22}^{(a)}Bu_2^{(b)}dx_1$$

$$= \frac{\kappa+1}{8G}(K_{\mathrm{I}}^2 + K_{\mathrm{II}}^2) + \frac{K_{\mathrm{III}}^2}{2G}$$

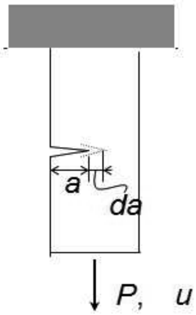

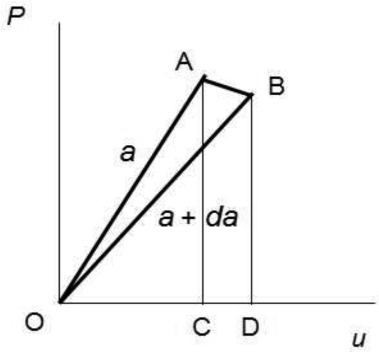

$$\mathcal{G}=\frac{dL}{dA}-\frac{dU}{dA}=\frac{1}{2}P^2\frac{d\lambda}{Bda}=\frac{\kappa+1}{8G}(K_{\mathrm{I}}{}^2+K_{\mathrm{II}}{}^2)+\frac{K_{\mathrm{III}}{}^2}{2G}$$

$u=\lambda P$ λ: Compliance

$$U=\frac{1}{2}Pu$$

Elastoplastic Body

n power law (deformation theory):

$$\left(\frac{\bar{\varepsilon}}{\varepsilon_0}\right)=\left(\frac{\bar{\sigma}}{\sigma_0}\right)^n \qquad (\ n \geqq 1\ )$$

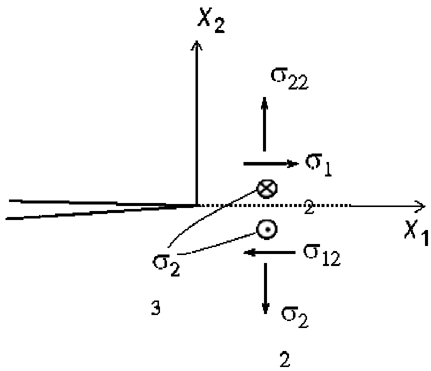

$$\sigma_{ij}=K_\sigma r^{-1/(n+1)}\tilde{\sigma}_{ij}(\theta,n)+\cdots$$

$$\varepsilon_{ij}=K_\varepsilon r^{-n/(n+1)}\tilde{\varepsilon}_{ij}(\theta,n)+\cdots$$

: HRR singularity

K_σ : Plastic stress intensity factor

K_ε : Plastic strain intensity factor

$$\frac{K_\varepsilon}{\varepsilon_0}=\left(\frac{K_\sigma}{\sigma_0}\right)^n$$

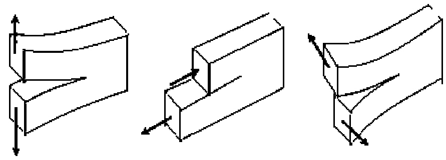

mode I mode II mode III

J integral

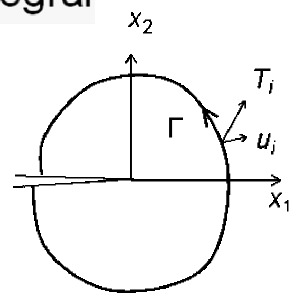

$$\sigma_{ij} = \frac{\partial W}{\partial \varepsilon_{ij}} = f_{ij}(\varepsilon_{11}, \varepsilon_{22}, \cdots, \varepsilon_{31})$$

W : Strain Energy Density

(deformation theory)

Path Independent Integral

$$J = \int_{\Gamma} \left(W dx_2 - T_i u_{i,1} d\Gamma \right)$$

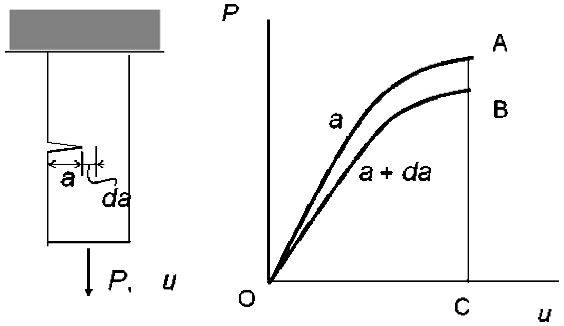

Load-Displacement Curves

Elastic Body → Energy Release Rate

Linear Elastic Body

$$J = \mathcal{G} = \frac{\kappa+1}{8G}(K_{\mathrm{I}}{}^2 + K_{\mathrm{II}}{}^2) + \frac{K_{\mathrm{III}}{}^2}{2G} = \frac{1}{2}P^2 \frac{d\lambda}{Bda}$$

Elastoplastic Body (deformation theory)

n power law → **Meaning is not clear**

$$J = \frac{I_n \varepsilon_0 K_\sigma{}^{n+1}}{\sigma_0{}^n} = I_n K_\sigma K_\varepsilon = \frac{I_n \sigma_0 K_\varepsilon{}^{(n+1)/n}}{\varepsilon_0{}^{1/n}}$$

$$\sigma_{ij} = K_\sigma r^{-1/(n+1)} \tilde{\sigma}_{ij}(\theta, n) + \cdots$$

$$K_\sigma = \sigma_0 \left(\frac{J}{I_n \varepsilon_0 \sigma_0} \right)^{1/(n+1)}$$

Evaluation of Creep Behavior:

Creep- **a time dependent, permanent deformation at high temperature, occurring at constant load or constant stress.**

Creep rate - The rate at which a material deforms when a stress is applied at a high temperature.

During the creep test, strain or elongation is measured as a function of time and plotted to give the creep curve.

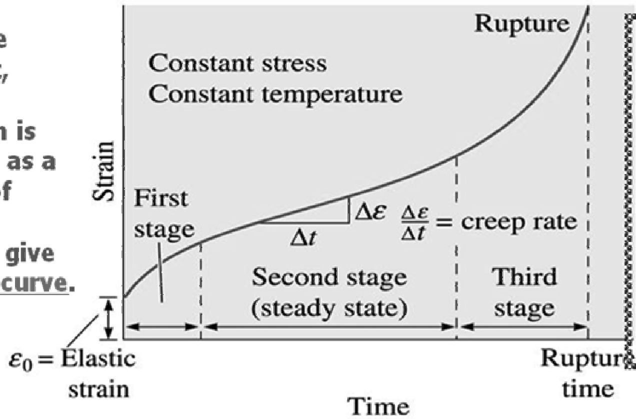

The resulting curve shows three stages. During the first stage, dislocations climb and break free from whatever was pinning them. The second stage of creep is characterized by a steady rate of strain. In the third stage, necking and failure occur.

Creep Crack (C^* parameter)

Analogy to Elastoplastic Problem under Deformation Theory

Elastoplastic	Stationary Creep $(\dot{\varepsilon}^e_{ij} = \dot{\varepsilon}^p_{ij} = 0)$
$\sigma_{ij,j} = 0$	$\sigma_{ij,j} = 0$
$\varepsilon_{ij} = \frac{1}{2}(u_{i,j} + u_{j,i})$	$\dot{\varepsilon}^{cr}_{ij} = \frac{1}{2}(\dot{u}_{i,j} + \dot{u}_{j,i})$
$\sigma_{ij} = \frac{\partial W}{\partial \varepsilon_{ij}}$	$\sigma_{ij} = \frac{\partial W'}{\partial \dot{\varepsilon}^{cr}_{ij}}$
$J = \int_\Gamma \left(W dx_2 - T_i u_{i,1} d\Gamma\right)$	$C^* = \int_\Gamma \left(W' dx_2 - T_i \dot{u}_{i,1} d\Gamma\right)$
n power law $\left(\frac{\varepsilon}{\varepsilon_0}\right) = \left(\frac{\sigma}{\sigma_0}\right)^n$	Norton's rule
$\sigma_{ij} = \sigma_0 \left(\frac{J}{I_n \varepsilon_0 \sigma_0}\right)^{1/(n+1)} r^{-1/(n+1)} \tilde{\sigma}_{ij}(\theta, n) + \cdots$	$\sigma_{ij} = \sigma_0 \left(\frac{C^*}{I_n A}\right)^{1/(n+1)} r^{-1/(n+1)} \tilde{\sigma}_{ij}(\theta, n) + \cdots$

Actual Deformation around a Crack Tip

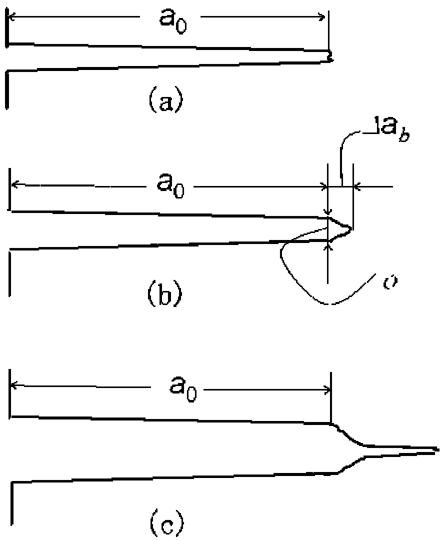

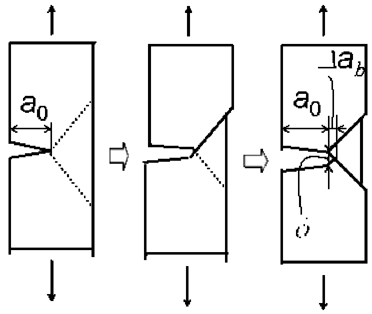

ϕ : COD
(or CTOD)

$\phi =$

COD: Crack Opening Displacement

➢ 7.3 Fracture Parameters and their Availabilities

Stress Intensity Factor
Energy Release Rate

} **Linear Fracture Mechanics**

Plastic Stress Intensity Factor
(Plastic Strain Intensity Factor)
J integral
COD

} **Nonlinear Fracture Mechanics**
(Elastoplastic Fracture Mechanics)

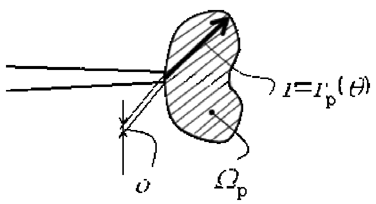

Small Scale Yielding
$r \ll a$

⟹ Linear Fracture Mechanics

Large Scale Yielding
$r \sim a$

⟹ Nonlinear Fracture Mechanics

Stress Intensity Factor

Plastic Stress（Strain）Intensity Factor

$$\begin{Bmatrix}\sigma_{11}\\ \sigma_{22}\\ \sigma_{12}\end{Bmatrix}=\frac{K_I}{\sqrt{2\pi r}}\cos\frac{\theta}{2}\begin{Bmatrix}1-\sin\frac{\theta}{2}\sin\frac{3\theta}{2}\\ 1+\sin\frac{\theta}{2}\sin\frac{3\theta}{2}\\ \sin\frac{\theta}{2}\cos\frac{3\theta}{2}\end{Bmatrix}$$

$$\sigma_{ij}=K_\sigma r^{-1/(n+1)}\tilde{\sigma}_{ij}(\theta,n)+\cdots$$
$$\varepsilon_{ij}=K_\varepsilon r^{-n/(n+1)}\tilde{\varepsilon}_{ij}(\theta,n)+\cdots$$

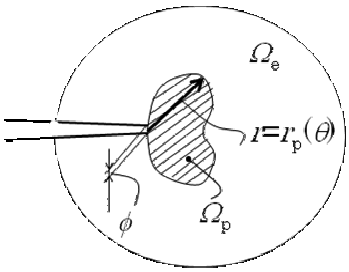

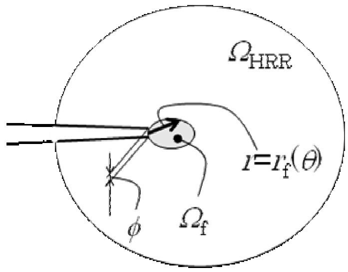

- **7.4 Applications to Fracture Phenomena**

Brittle Fracture (no plasticity)

$$K_I = K_{IC}$$ (also for a stably growing crack)

or

$$\mathcal{G}=\mathcal{G}_{IC}=\frac{\kappa+1}{8G}K_{IC}^2(=2\gamma,\ \text{Griffith})$$

Quasi-brittle Fracture (small scale yielding)

$$K_I = K_{IC}$$ (also for a stably growing crack)

or

$$\mathcal{G}=\mathcal{G}_{IC}=\frac{\kappa+1}{8G}K_{IC}^2(=2\gamma,\ \text{Griffith - Orowan})$$

Ductile Fracture (large scale yielding)

$$J = J_{IC}$$ (? for a stably growing crack)

Brittle or Quasi-brittle Fracture

Stable

$$\frac{dK_{\mathrm{I}}}{da} < 0 \left(= \frac{dK_{\mathrm{IC}}}{da}\right)$$

Unstable

$$\frac{dK_{\mathrm{I}}}{da} \geq 0 \left(= \frac{dK_{\mathrm{IC}}}{da}\right)$$

Ductile Fracture

Stable

$$\frac{dJ}{da} < \frac{dR}{da}$$

Unstable

$$\frac{dJ}{da} \geq \frac{dR}{da}$$

Mixed Mode Fracture

Brittle or quasi-brittle fracture

criterion

Ductile fracture

?

Fatigue Crack

$$\frac{da}{dN} = f(\Delta K)$$

Creep Crack

$$\frac{da}{dt} = f(C^*) \quad \text{for stationary creep}$$

➢ 7.5 Problems in Conventional Fracture Mechanics

1. The concept of energy release rate was considered successfully applied to elastoplastic fracture under small scale yielding. But, it failed to explain elastoplastic fracture under large scale yielding.

2. There exists no crack parameter that can be defined without depending on constitutive equation. Elastoplastic crack parameter J is defined just under deformation theory. It loses its meaning when unloading occurs and it is applicable just before the onset of crack growth. There is no way to deal with a growing elastoplastic crack.

3. There is no parameter for mixed mode elastoplastic crack.

4. Depending on phenomena, different parameters are required depending on phenomena.

References

J.R. Rice, *A path independent integral and the approximate analysis of strain concentration by notches and cracks*. J. Appl. Mechanics, Trans. ASME E35, 1968, pp. 379-386.

J.R. Rice, *Mathematical analysis in the mechanics of fracture*. H. Liebowitz, Editor, Treatise on fracture vol. 2, Academic Press, New York (1968).

H. Tada, P.C. Paris and G.R. Irwin, *The Stress Analysis of Cracks Handbook* (1973, 1985, 2000).

J. W. Hutchinson, *Notes on Nonlinear Fracture Mechanics* (http://imechanica.org/node/755).

Alan Zehnder, *Lecture Notes on Fracture Mechanics* (http://hdl.handle.net/1813/3075).

Evaluation of Crack Tip Fields and Role of Fracture Mechanics

Cheng Hua
Department of Mechanics and Engineering Science, Fudan University, Shanghai, China

FUDAN UNIVERSITY 1905-2005

Collaboration between theory and practice in inverse problems
Fukuoka, Japan, December 16-19, 2014

OUTLINE

1. Stress field near the Crack Tip
2. Stress Intensity Factor-SIF
3. Elementary Fracture Mechanics
4. Griffith's Energy Balance Approach
5. J-integral
6. Fracture Toughness and Fracture Criterion

Collaboration between theory and practice in inverse problems
Fukuoka, Japan, December 16-19, 2014

1. Stress field at the crack tip

The first step is to consider

Stress distribution around circular hole and elliptical hole:

Inglis (1913) analyzed for the flat plate with an elliptical hole with major axis 2a and minor axis 2b, subjected to far end stress

The linear elastic solution of the stress at the tip of the major axis is given by :

$$\sigma_{\max} = \sigma_0\left[1 + 2\left(\frac{a}{b}\right)\right]$$

The Inglis solution

For circular hole (b=a) :

$$\sigma_{\max} = 3\sigma_0$$

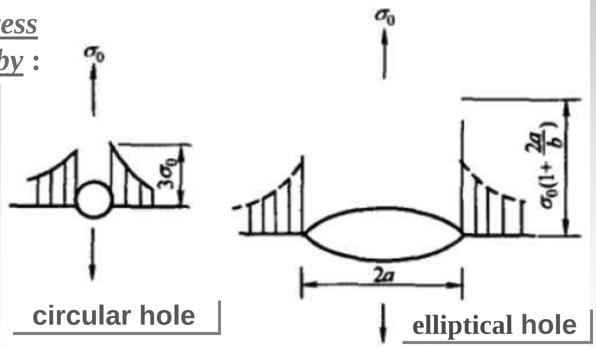

circular hole

elliptical hole

1. Stress field at the crack tip

The paper looks like:
(Inglis, 1913)

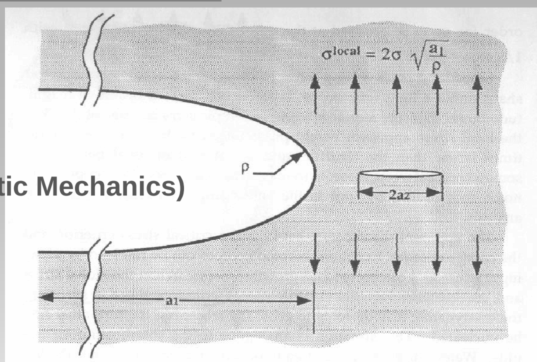

The Mathematical Method (Linear Elastic Mechanics)

Inglis solution

STRESSES IN A PLATE DUE TO THE PRESENCE OF CRACKS AND SHARP CORNERS.

By C. E. INGLIS, Esq., M.A., Fellow of King's College, Cambridge.

[Read at the Spring Meetings of the Fifty-fourth Session of the Institution of Naval Architects, March 14, 1913; Professor J. H. BILES, LL.D., D.Sc., Vice-President, in the Chair.]

PART I.

THE methods of investigation employed for this problem are mathematical rather than

1. Stress field at the crack tip

Linear elasticity *solution* of an elliptic hole in a large plate (*Inglis solution*)

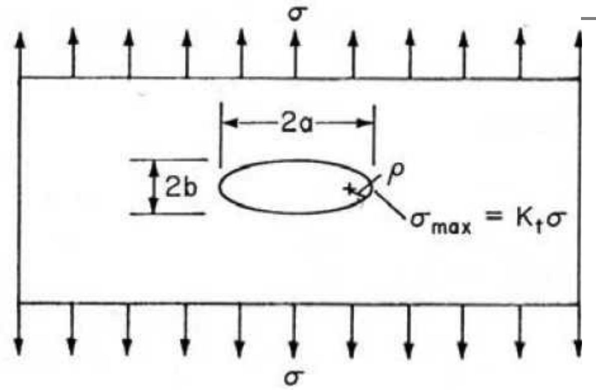

Stress Concentration Factor (SCF)

$$K_T = \frac{\sigma_{\max}}{\sigma} = 1 + \frac{2a}{b}$$

$$\rho = \frac{b^2}{a}$$

$$\sigma_{\max} \cong 2\sigma\sqrt{\frac{a}{\rho}} \quad (\rho << a)$$

- σ_0 → applied stress
- σ_{max} → stress at crack tip
- ρ → crack tip radius

$$\sqrt{\frac{a}{\rho}} \to \infty\,(\rho \to 0) \to$$

SCF

$$K_t \to \infty$$

1. Stress field at the crack tip

Stress concentration and Stress singularity :

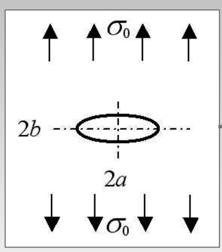

b=a, **circular hole**

$$\sigma_{\max} = 3\sigma_0$$

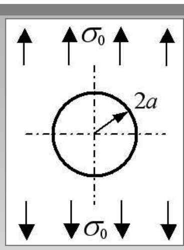

Stress Concentration:

$$K_t = \frac{\sigma_{\max}}{\sigma_0} = 3$$

Stress Concentration Factor (SCF)

$b \to 0$, **Crack**

$$\sigma_{\max} \to \infty$$

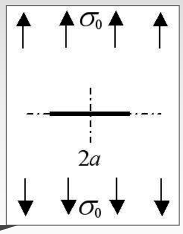

Stress Singularity:

$$K_t = \frac{\sigma_{\max}}{\sigma_0} = ?$$

How To Quantify?
Lead to "Stress Intensity Factor (SIF)"

$$\sigma_{\max} = \sigma_0\left[1 + 2\left(\frac{a}{b}\right)\right] \approx 2\sigma_0\sqrt{\frac{a}{\rho}}$$

Cracks have a sharp tip and lead to stress singularity

1. Stress field at the crack tip

The second to study **Stress singularity :**

Linear Elastic Mechanics

σ

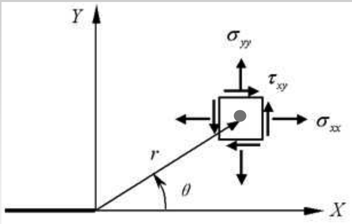

σ

Crack length:2a

Stress near the crack tip

$$\begin{cases} \sigma_{xx} = \sigma\sqrt{\dfrac{a}{2r}}\cos\left(\dfrac{\theta}{2}\right)\left[1-\sin\left(\dfrac{\theta}{2}\right)\sin\left(\dfrac{3\theta}{2}\right)\right]+\cdots \\ \sigma_{yy} = \sigma\sqrt{\dfrac{a}{2r}}\cos\left(\dfrac{\theta}{2}\right)\left[1+\sin\left(\dfrac{\theta}{2}\right)\sin\left(\dfrac{3\theta}{2}\right)\right]+\cdots \\ \tau_{xy} = \sigma\sqrt{\dfrac{a}{2r}}\sin\left(\dfrac{\theta}{2}\right)\cos\left(\dfrac{\theta}{2}\right)\cos\left(\dfrac{3\theta}{2}\right)+\cdots \end{cases}$$

$$\boxed{\sigma_{ij}(r,\theta) \propto \frac{1}{\sqrt{r}} \quad (r \to 0)}$$

This feature is called
Stress Singularity

OUTLINE

Collaboration between theory and practice in inverse problems
Fukuoka, Japan, December 16-19, 2014

2. Stress Intensity Factor (SIF)

Irwin (1957) proposed a new physical quantity --- Stress Intensity Factor (SIF)

$$K = \lim_{r \to 0} \sqrt{2\pi r}\,\sigma_{yy}(r,0) = \sigma\sqrt{\pi a}$$

K is called the "Stress Intensity Factor"

Stress Field Near the Crack Tip

$$\sigma_x = \frac{K}{\sqrt{2\pi r}}\cos\frac{\theta}{2}\left(1-\sin\frac{\theta}{2}\sin\frac{3\theta}{2}\right)$$

$$\sigma_y = \frac{K}{\sqrt{2\pi r}}\cos\frac{\theta}{2}\left(1+\sin\frac{\theta}{2}\sin\frac{3\theta}{2}\right)$$

$$\tau_{xy} = \frac{K}{\sqrt{2\pi r}}\cos\frac{\theta}{2}\sin\frac{\theta}{2}\cos\frac{3\theta}{2}$$

$$\boxed{\sigma_{ij}(r,\theta) \propto \frac{1}{\sqrt{r}} \quad (r \to 0)}$$

Dr George R. Irwin
(1907-1998)

Why K?

The legend: Irwin chose the letter *K* *after J.A. Kies, one of his co-workers*

Collaboration between theory and practice in inverse problems
Fukuoka, Japan, December 16-19, 2014

2. Stress Intensity Factor (SIF)

Solution to an Infinite Cracked Panel:

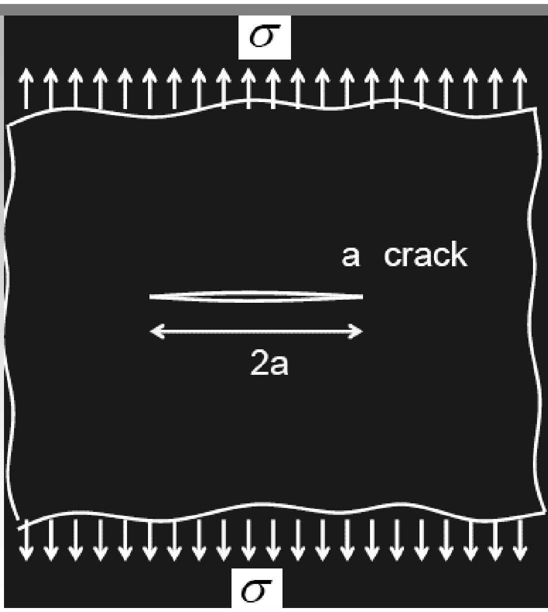

A Through Thickness Crack
In an Infinite Plate subject
to Uniform Tensile Stress

$$K = \sigma\sqrt{\pi a}$$

Collaboration between theory and practice in inverse problems
Fukuoka, Japan, December 16-19, 2014

2. Stress Intensity Factor (SIF)

Solution to a Finite Size Cracked Panel :

Isida

$$K = Y\sigma\sqrt{a}$$

Fedderson:

$$K = \sigma\sqrt{\pi a}\sqrt{\sec\frac{\pi a}{W}}$$

More Exact

$$K = \sigma\sqrt{\pi a}\sqrt{\sec\frac{\pi a}{W}}\left\{1-.1\left(\frac{a}{W}\right)^2+0.96\left(\frac{a}{W}\right)^4\right\}$$

Westergaard
Irwin(1958)
Koiter(1959)

$$K = \sigma\sqrt{\pi a}\sqrt{\frac{W}{\pi a}\tan\frac{\pi a}{W}}$$

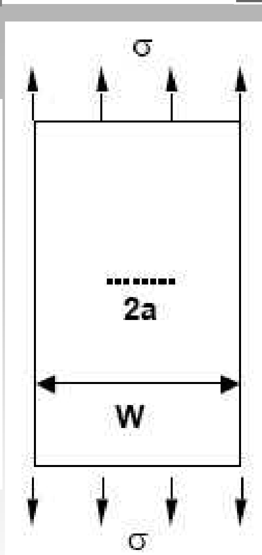

1. Rooke DP and Cartwright DJ (1976). Compendium of Stress Intensity Factors. Procurement Executive, Ministry of Defence. H.M.S.O.
2. Tada H, Paris PC, and Irwin GR (1985). The Stress Intensity Factor Handbook. Hellertown, Philadelphia: Del Research Corporation
3. Murakami Y (1987). Stress Intensity Factors Handbook. New York: Pergamon.

2. Stress Intensity Factor (SIF)

Solution to a Finite Size Cracked Panel :

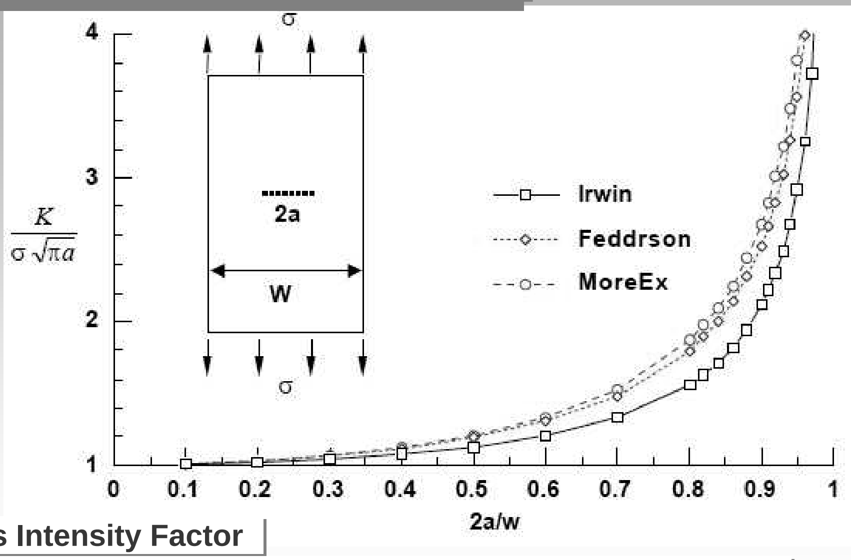

***K*: Stress Intensity Factor**

***K* Factor defines the stress field around the crack tip, taking into account *crack length, applied stress and shape factor* (which accounts for finite size of the component and local geometric features)**

2. Stress Intensity Factor (SIF)

Solution to a Finite Size Cracked Panel :

The Applied Stress
The Crack Shape and Size
The Structural Configuration

⬇ Affect

The Value of The Stress Intensity Factor, K

$$K = \sigma\sqrt{\pi a} \cdot F$$

F : Correction factor

Collaboration between theory and practice in inverse problems
Fukuoka, Japan, December 16-19, 2014

Father of Modern Fracture Mechanics

In the 1950s Irwin and coworkers introduced the concept of Stress Intensity Factor, which defines the stress field around the crack tip, taking into account crack length, applied stress and shape factor (which accounts for finite size of the component and local geometric features).

Dr George R. Irwin
(1907-1998)

After having received the A.B. in English and Physics from Knox College and the M.A. and Ph. D in Physics from the University of Illinois, **George Irwin began his career in 1937, at the U.S. Naval Research Lab (NRL) where he developed several new ballistics research techniques.** As a result, the NRL Ballistics Branch, which was headed by Irwin, was able to develop non-metallic armors for fragment protection. These armors received trial use in World War II and extensive use during the Korean and Vietnam Wars. **The early years of this work led to an interest in brittle fracture and provided a basis for Irwin's pioneering work in fracture mechanics. The basic concepts established by Irwin and his team from 1946 to 1960 are now used world wide for fracture control in aircraft, nuclear reactor vessels and other fracture- critical applications.**

His numerous awards include ASTM Honorary Member, Timoshenko Medal of ASME, Gold Medal of ASM, The Grand Medal of the French Metallurgical Society, Tetmajer Medal o the Technical University of Vienna, **member of the National Academy of Engineering** and foreign membership in the Royal Society of London. He was appointed to Boeing University Professor at Lehigh University in 1967. He later joined the University of Maryland's Department of Engineering where he has been and active researcher and advisor of graduate students since 1972.

Collaboration between theory and practice in inverse problems
Fukuoka, Japan, December 16-19, 2014

OUTLINE

1. Stress field near the Crack Tip
2. Stress Intensity Factor-SIF
3. Elementary Fracture Mechanics
4. Griffith's Energy Balance Approach
5. J-integral
6. Fracture Toughness and Fracture Criterion

3. Elementary Fracture Mechanics

Modes of Fracture (the three modes of crack surface displacement):

- **Mode I** - ***Opening mode*** **or tensile mode**
- **Mode II** - ***Sliding mode*** **or in-plane shear mode**
- **Mode III** - ***Tearing mode*** **or anti-plane shear mode**

Stress Intensity Factor :

- K_I for Mode I
- K_{II} for Mode II
- K_{III} for Mode III

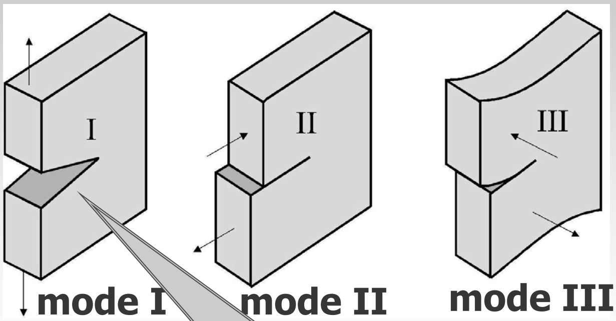

the most dangerous

3. Elementary Fracture Mechanics

Similar to Mode I

K_{II} **for Mode II** **and** K_{III} **for Mode III:**

Stress near the crack tip

$$\sigma_{ij}(r,\theta) = \frac{K_{II}}{\sqrt{2\pi r}} f_{ij}^{II}(\theta)$$

$$K_{II} = \lim_{r\to 0} \sqrt{2\pi r}\,\tau_{xy}(r,0)$$

$$\sigma_{ij}(r,\theta) = \frac{K_{III}}{\sqrt{2\pi r}} f_{ij}^{III}(\theta)$$

$$K_{III} = \lim_{r\to 0} \sqrt{2\pi r}\,\tau_{yz}(r,0)$$

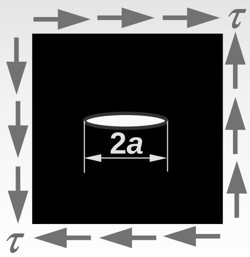

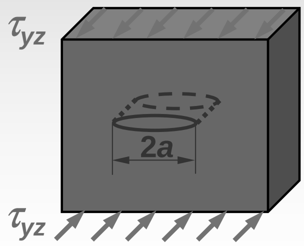

Collaboration between theory and practice in inverse problems
Fukuoka, Japan, December 16-19, 2014

3. Elementary Fracture Mechanics

Mode I + Mode II + Mode III

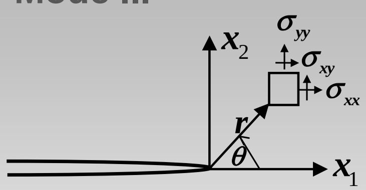

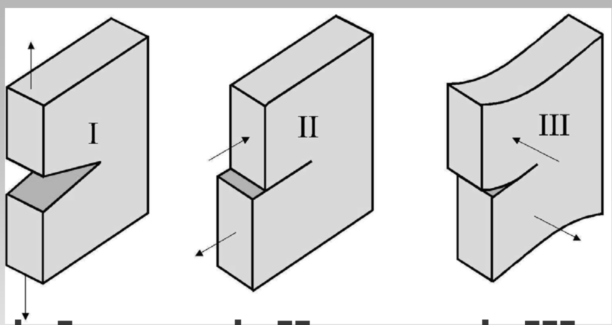

mode I K_I **mode II** K_{II} **mode III** K_{III}

$$\sigma_{ij} = \sum_{m=I}^{III} \frac{K_m}{\sqrt{2\pi r}} f_{ij}^{(m)}(\theta) + O(1)$$

m = I, II, III

i, j=1, 2, 3

Collaboration between theory and practice in inverse problems
Fukuoka, Japan, December 16-19, 2014

3. Elementary Fracture Mechanics

Basic types of fracture:
(according to whether the material has obvious plastic deformation before fracture)

- **Brittle Fracture**
- **Ductile Fracture**

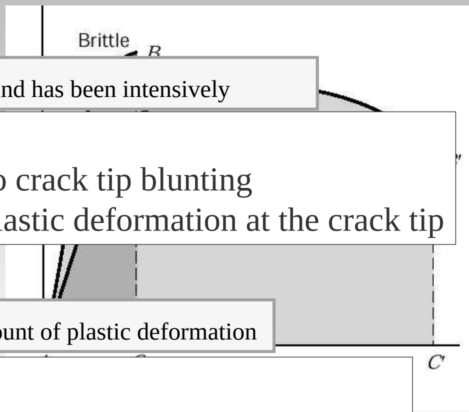

Brittle fracture - is more catastrophic and has been intensively studied

- Brittle fracture →
  - ▶ cracks are sharp & no crack tip blunting
  - ▶ No energy spent in plastic deformation at the crack tip

Ductile fracture - involves a large amount of plastic deformation

- Ductile fracture →
  - ▶ Crack tip blunting by plastic deformation at tip
  - ▶ Energy spent in plastic deformation at the crack tip

Collaboration between theory and practice in inverse problems
Fukuoka, Japan, December 16-19, 2014

3. Elementary Fracture Mechanics

Related Subjects

- ***Linear Elastic* Fracture Mechanics (LEFM)**
- ***Elastic-Plastic* Fracture Mechanics (EPFM)**

Linear Elastic Fracture Mechanics (LEFM) :

- **Refer to Brittle material**
- **The structure obeys Hooke's law and global behavior is linear and if any local small scale crack tip plasticity is ignored**
- **Central to LEFM is the concept of *K* introduced by Irwin**

Elastic-Plastic Fracture Mechanics (EPFM) :

- **Refer to Ductile material**
- **The structure obeys an elastic-plastic constitutive**
- **Central to EPFM is the concept of *J-integral* introduced by James R. Rice**

Collaboration between theory and practice in inverse problems
Fukuoka, Japan, December 16-19, 2014

3. Elementary Fracture Mechanics

The Previous Conditions:

Suppose a structure with an interior crack (existing crack)

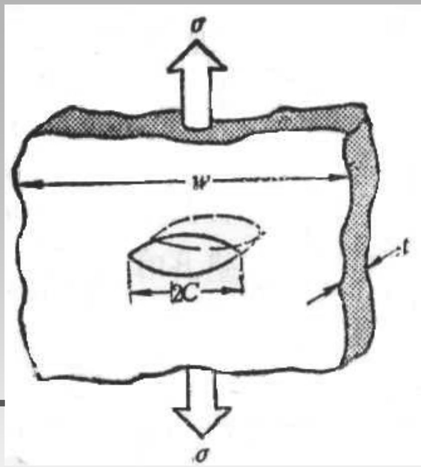

Two different points of view

- **Energy balance Griffith theory** (1921, Griffith, UK) — **Energy based**
- **The crack tip stress intensity** (1957, Irwin, USA) — **Stress based**

OUTLINE

4. Griffith's Energy Balance Approach

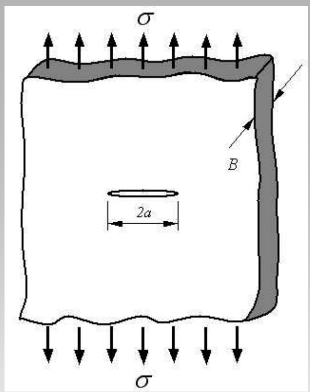

$A = 2aB$

$dA = 2Bda$

Griffith Proposed:

$$-\left(\frac{\partial W}{\partial A}\right) \geq \frac{G_c}{2}$$

Where,

A: Surface area of specimen
G_c: Amount of energy required to tear through a unit area of the material
Factor 2: Two newly formed surfaces

Dr Alan A. Griffith
(1893-1963)

Griffith's Theory :

A crack would propagate in a stressed material only when, by doing so, it brought about a reduction in elastically stored energy W more than sufficient to meet the free energy requirements of newly formed fracture surfaces

Griffith AA, The phenomena of rupture and flow in solids, Philosophical Transactions, Series A, 1920(221): 163-198.

4. Griffith's Energy Balance Approach

The core idea of Griffith theory

Crack extension force
＝ crack growth resistance

or named "Crack driving force", The release of potential energy Such as elastic energy

or named "Material resistance", The new surface energy formed on the crack surface

Collaboration between theory and practice in inverse problems
Fukuoka, Japan, December 16-19, 2014

4. Griffith's Energy Balance Approach

Strain energy release rate is introduced by Irwin

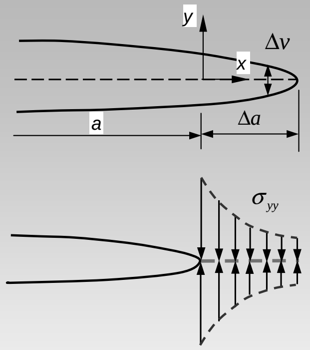

$$G = \lim_{\Delta a \to 0} \frac{1}{\Delta A} \int_0^{\Delta A} \left(\sigma_{yy} \Delta v + \tau_{xy} \Delta u \right) dA$$

For the infinite plate There are

$$\Delta v = \frac{8\sigma}{E} \sqrt{\frac{(a+\Delta a)(\Delta a - x)}{2}} \quad \textbf{(plane stress)}$$

$$\sigma_{yy} = \sigma \sqrt{\frac{a}{2x}}$$

$$\int_0^{\Delta A} \sigma_{yy} \Delta v dA = \frac{4\sigma^2}{E} \sqrt{a(a+\Delta a)} \int_0^{\Delta a} \sqrt{\frac{\Delta a - x}{x}} B dx$$

$$= \frac{4\sigma^2 B}{E} \sqrt{a(a+\Delta a)} \int_0^{\Delta a} \sqrt{\frac{\Delta a - x}{x}} dx$$

4. Griffith's Energy Balance Approach

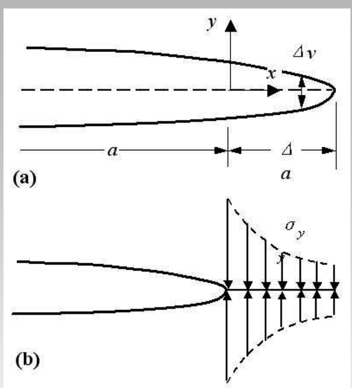

$$\int_0^{\Delta A} \sigma_{yy} \Delta v dA = \frac{4\sigma^2}{E} \sqrt{a(a+\Delta a)} \int_0^{\Delta a} \sqrt{\frac{\Delta a - x}{x}} B dx$$

$$= \frac{4\sigma^2 B}{E} \sqrt{a(a+\Delta a)} \int_0^{\Delta a} \sqrt{\frac{\Delta a - x}{x}} dx$$

$$\int_0^{\Delta a} \sqrt{\frac{\Delta a - x}{x}} dx = \frac{\pi}{2} \Delta a$$

$$\int_0^{\Delta A} \sigma_{yy} \Delta v dA = \frac{2\pi\sigma^2 B \Delta a}{E} \sqrt{a(a+\Delta a)}$$

$$G = \lim_{\Delta A \to 0} \frac{1}{\Delta A} \int_0^{\Delta A} \sigma_{yy} \Delta v dA$$

$$= \lim_{\Delta a \to 0} \frac{1}{2B\Delta a} \frac{2\pi\sigma^2 B \Delta a}{E} \sqrt{a(a+\Delta a)}$$

$$= \frac{\pi\sigma^2 a}{E}$$

Collaboration between theory and practice in inverse problems
Fukuoka, Japan, December 16-19, 2014

4. Griffith's Energy Balance Approach

The relationship between G and K

$$\sigma_c = \left(\frac{2E\gamma}{\pi a_c}\right)^{1/2} \qquad \sigma_c = \left(\frac{2E\gamma}{\pi(1-\nu^2)a_c}\right)^{1/2}$$

$$\sigma\sqrt{\pi a} = \sqrt{EG} \qquad \sigma\sqrt{\pi a} = \sqrt{EG/(1-\nu)}$$

$$G_I = \frac{K_I^2}{E'}, E' = \begin{cases} E & \text{plane stress} \\ E/(1-\nu^2) & \text{plane strain} \end{cases}$$

$$G_T = G_I + G_{II} + G_{III}$$

OUTLINE

1. Stress field near the Crack Tip
2. Stress Intensity Factor-SIF
3. Elementary Fracture Mechanics
4. Griffith's Energy Balance Approach
5. J-integral
6. Fracture Toughness and Fracture Criterion

Collaboration between theory and practice in inverse problems
Fukuoka, Japan, December 16-19, 2014

5. The *J* - integral

By idealizing elastic-plastic deformation as non-linear elastic, Rice (1968) proposed *J*-integral, for egions beyond LEFM

The Previous Conditions:

- **In loading path elastic-plastic can be modeled as non-linear elastic but not in unloading part.**
- **Also *J*-integral uses deformation plasticity. It states that the stress state can be determined knowing the initial and final configuration. The plastic strain is in proportional load, i.e.** $\frac{d\sigma_1}{\sigma_1} = \frac{d\sigma_2}{\sigma_2} = \frac{d\sigma_3}{\sigma_3} = \frac{d\sigma_4}{\sigma_4} = \frac{d\sigma_5}{\sigma_5} = \frac{d\sigma_6}{\sigma_6} = k$

- **Under the above conditions, *J*-integral characterizes the crack tip stress and crack tip strain and energy release rate uniquely.**
- ***J*-integral is numerically equivalent to G for linear elastic material. <u>It is a path-independent integral.</u>**
- **When the above conditions are not satisfied, *J* becomes path dependent and does not relates to any physical quantities.**

5. The *J* - integral

$$J = \int_{\Gamma} \left(W n_1 - T_i \frac{\partial u_i}{\partial x_1} \right) ds$$

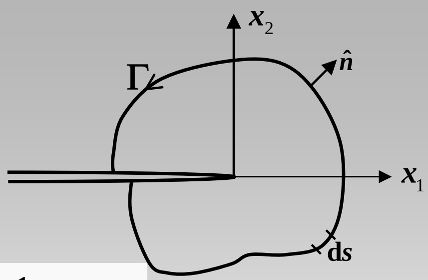

Strain energy density $W = \frac{1}{2}\sigma_{ij}\varepsilon_{ij}$

Traction force $T_i = \sigma_{ij} n_j$

***J* is a path-independent integral**

5. The *J* - integral

HRR Field (1968, Rice, Rosengren, Hutchinson):

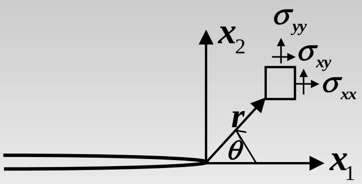

$$\begin{cases} \sigma_{ij}(r,\theta) = \alpha\left(\dfrac{J}{\alpha I_n r}\right)^{\frac{1}{n+1}} f_{ij}(\theta,n) \\[2ex] \varepsilon_{ij}(r,\theta) = \left(\dfrac{J}{\alpha I_n r}\right)^{\frac{n}{n+1}} g_{ij}(\theta,n) \\[2ex] u_i(r,\theta) = \alpha\left(\dfrac{J}{\alpha I_n}\right)^{\frac{1}{n+1}} r^{\frac{1}{1+n}} h_i(\theta,n) \end{cases}$$

5. The *J* - integral

Evaluation of *J*-Integral:

--*J* integral provides a unique measure of the strength of the singular fields in nonlinear fracture. However there are a few important Limitations, (Hutchinson, 1993)

1. Deformation theory of plasticity should be valid with small strain behavior with monotonic loading.

2. If finite strain effects dominate and microscopic failures occur, then this region should be much smaller compared to J dominated region, again based on the HRR singularity.

$$\sigma_{ij} = \sigma_y\left(\frac{J}{\alpha\sigma_y\sigma_y I_n r}\right)^{\frac{1}{n+1}} \sigma^{I}{}_{ij}(\theta,n)$$

Collaboration between theory and practice in inverse problems
Fukuoka, Japan, December 16-19, 2014

OUTLINE

1. Stress field near the Crack Tip
2. Stress Intensity Factor-SIF
3. Elementary Fracture Mechanics
4. Griffith's Energy Balance Approach
5. J-integral
6. Fracture Toughness and Fracture Criterion

Collaboration between theory and practice in inverse problems
Fukuoka, Japan, December 16-19, 2014

6. Fracture Toughness and Fracture Criterion

Fracture toughness:

The resistance of a material to failure in the presence of a crack.

Fracture criterion: $K_i \le K_{ic} \qquad (i = \mathrm{I,II,III})$

K_{ic} required for a crack to propagate describing the resistance of crack propagating, determined by test（plane stress crack and plane strain crack）

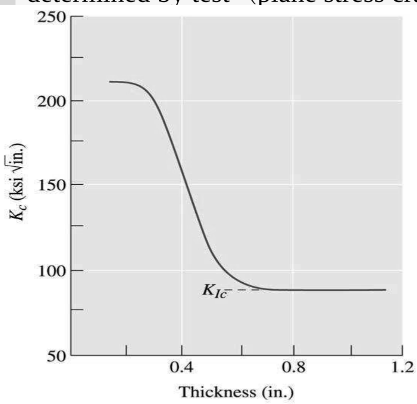

The fracture toughness K_{ic} of a high yield strength steel decreases with increasing thickness, eventually leveling off at the *plane strain fracture toughness*, K_{Ic}

Collaboration between theory and practice in inverse problems
Fukuoka, Japan, December 16-19, 2014

6. Fracture Toughness and Fracture Criterion

Effect of plate thickness on fracture toughness

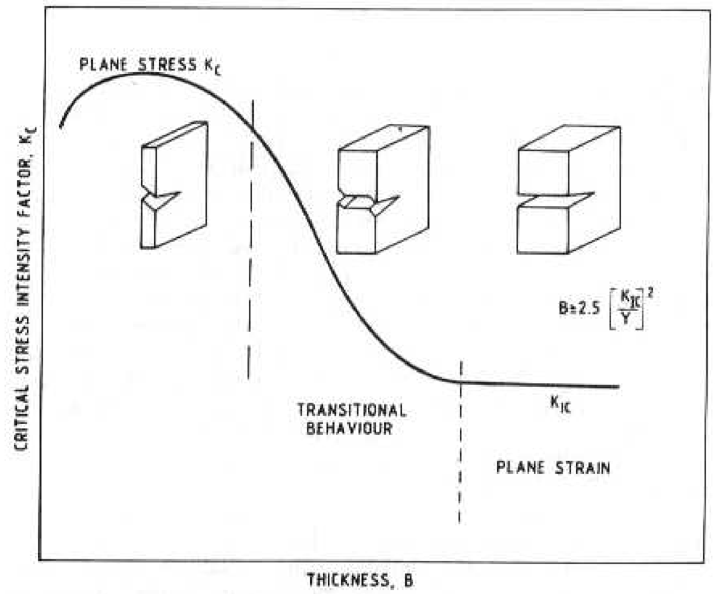

6. Fracture Toughness and Fracture Criterion

Material test standard :

Designation: E 399 – 90 (Reapproved 1997)

INTERNATIONAL

Standard Test Method for
Plane-Strain Fracture Toughness of Metallic Materials[1]

This standard is issued under the fixed designation E 399; the number immediately following the designation indicates the year of original adoption or, in the case of revision, the year of last revision. A number in parentheses indicates the year of last reapproval. A superscript epsilon (ϵ) indicates an editorial change since the last revision or reapproval.

This standard has been approved for use by agencies of the Department of Defense.

Designation: E 1820 – 01

INTERNATIONAL

Standard Test Method for
Measurement of Fracture Toughness[1]

This standard is issued under the fixed designation E 1820; the number immediately following the designation indicates the year of original adoption or, in the case of revision, the year of last revision. A number in parentheses indicates the year of last reapproval. A superscript epsilon (ϵ) indicates an editorial change since the last revision or reapproval.

6. Fracture Toughness and Fracture Criterion

Material or structure fracture control is the following three main factors:

Crack size and shape

Applied Stress

Fracture toughness of material

Fracture mechanics analysis

Material testing

K_I fracture criterion K_{IC}

Collaboration between theory and practice in inverse problems
Fukuoka, Japan, December 16-19, 2014

6. Fracture Toughness and Fracture Criterion

The Importance of Fracture Mechanics:

The fracture mechanics approach allows us to design and select materials while taking into account the inevitable presence of cracks. There are three variables to consider:

- The property of the material (K_c or K_{Ic})
- The stress σ that the material must withstand
- The size of the crack

If we know two of these variables, the third can be determined.

Collaboration between theory and practice in inverse problems
Fukuoka, Japan, December 16-19, 2014

6. Fracture Toughness and Fracture Criterion

$$K = f(\frac{a}{W}, \cdots)\sigma\sqrt{\pi a} \le K_{1c}$$

Applied Stress σ	Crack size a	Fracture toughness K_{IC}
Known	Known	Choose materials satisfy the K_{ic} value fracture criterion promised not to break
Determine the working stress to allow to use	Known	Known
Known	Determine the allowable crack siz	Known

6. Fracture Toughness and Fracture Criterion

Fracture mechanics identifies three primary factors :

- **Material Fracture Toughness** Material fracture toughness may be defined as the ability to carry loads or deform plastically in the presence of a notch. It may be described in terms of the critical stress intensity factor, *KIc*, under a variety of conditions. (These terms and conditions are fully discussed in the following chapters.)
- **Crack Size** Fractures initiate from discontinuities that can vary from extremely small cracks to much larger weld or fatigue cracks. Furthermore, although good fabrication practice and inspection can minimize the size and number of cracks, most complex mechanical components cannot be fabricated without discontinuities of one type or another.
- **Stress Level** For the most part, tensile stresses are necessary for brittle fracture to occur. These stresses are determined by a stress analysis of the particular component.
- Other factors such as temperature, loading rate, stress concentrations, residual stresses, etc., influence these three primary factors.

Role of Fracture Mechanics

- **Mechanics of Materials and Fracture Mechanics**
- **Summary of Fracture Parameters**
- **Fracture Parameters and their Availabilities**
- **Applications to Fracture Phenomena**
- **Problems in Conventional Fracture Mechanics**

Collaboration between theory and practice in inverse problems
Fukuoka, Japan, December 16-19, 2014

Mechanics of Materials and Fracture Mechanics

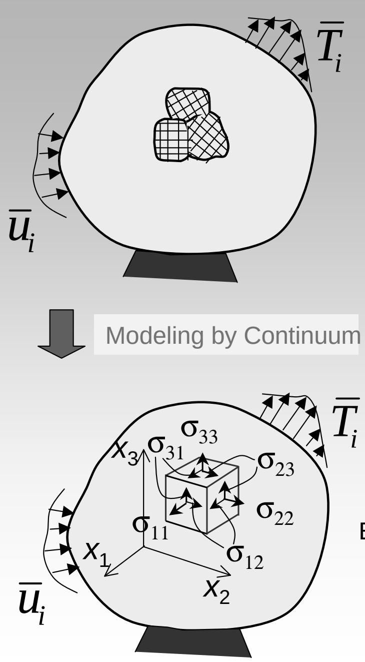

Mechanics of Materials

Equilibrium equation

$$\frac{\partial \sigma_{11}}{\partial x_1} + \frac{\partial \sigma_{12}}{\partial x_2} + \frac{\partial \sigma_{13}}{\partial x_3} = 0$$

:

$$\sigma_{12} = \sigma_{21} \quad , \quad \ldots$$

Relation between Displacement and strain

$$\varepsilon_{11} = \frac{\partial u_1}{\partial x_1} \quad , \quad \ldots$$

$$\varepsilon_{12} = \frac{1}{2}\left(\frac{\partial u_1}{\partial x_2} + \frac{\partial u_2}{\partial x_1}\right)$$

:

Stress-strain relation

Boundary condition $T_i = \overline{T}_i$ on S_σ

$u_i = \overline{u}_i$ on S_u

(i=1,2,3)

Continuum mechanics under small displacement

↓

Mechanics of Materials

Collaboration between theory and practice in inverse problems
Fukuoka, Japan, December 16-19, 2014

➢Mechanics of Materials and Fracture Mechanics

Strength of Materials ⟷ Mechanics of Materials [Fracture Mechanics] ⟷ Strength of Structures

Mechanics of Materials and **Fracture Mechanics**

Collaboration between theory and practice in inverse problems
Fukuoka, Japan, December 16-19, 2014

Crack Problem （Fracture Mechanics）

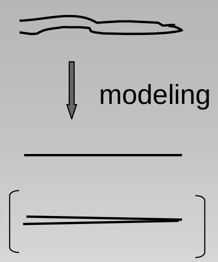

Stress, Strain, Strain energy density $\longrightarrow \infty$

↓

other parameters are necessary

↓

Fracture Mechanics

Stress around a crack tip

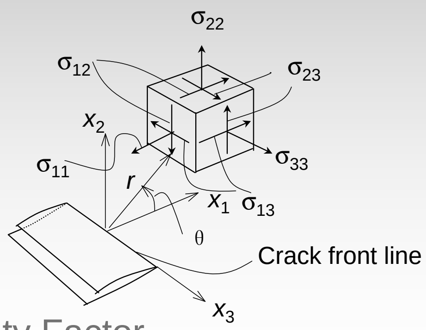

Linear Elasticity

$$\sigma_{ij} = \frac{A_1}{\sqrt{r}} f_{ij}^{(1)}(\theta) + A_2 f_{ij}^{(2)}(\theta) + A_3 \sqrt{r} f_{ij}^{(3)}(\theta) + \cdots$$

$K = \sqrt{2\pi} A_1$ ： Stress Intensity Factor

Collaboration between theory and practice in inverse problems
Fukuoka, Japan, December 16-19, 2014

Deformation mode around a crack tip

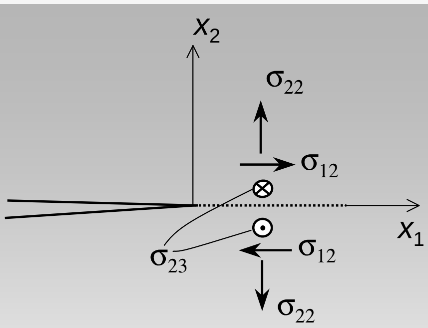

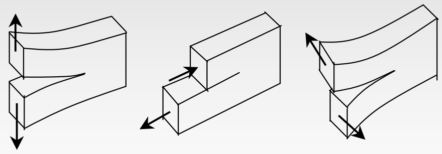

Mode Ⅰ **Mode Ⅱ** **Mode Ⅲ**

Mode I

$$\begin{Bmatrix}\sigma_{11}\\ \sigma_{22}\\ \sigma_{12}\end{Bmatrix}=\frac{K_{\mathrm{I}}}{\sqrt{2\pi r}}\cos\frac{\theta}{2}\begin{Bmatrix}1-\sin\frac{\theta}{2}\sin\frac{3\theta}{2}\\ 1+\sin\frac{\theta}{2}\sin\frac{3\theta}{2}\\ \sin\frac{\theta}{2}\cos\frac{3\theta}{2}\end{Bmatrix}$$

$$\begin{Bmatrix}u_1\\ u_2\end{Bmatrix}=\frac{K_{\mathrm{I}}}{2G}\sqrt{\frac{r}{2\pi}}\begin{Bmatrix}\cos\frac{\theta}{2}\left(\kappa-1+2\sin^2\frac{\theta}{2}\right)\\ \sin\frac{\theta}{2}\left(\kappa+1-2\cos^2\frac{\theta}{2}\right)\end{Bmatrix}$$

Mode II

$$\begin{Bmatrix}\sigma_{11}\\ \sigma_{22}\\ \sigma_{12}\end{Bmatrix}=\frac{K_{\mathrm{II}}}{\sqrt{2\pi r}}\begin{Bmatrix}\sin\frac{\theta}{2}\left(2+\cos\frac{\theta}{2}\cos\frac{3\theta}{2}\right)\\ \sin\frac{\theta}{2}\cos\frac{\theta}{2}\cos\frac{3\theta}{2}\\ \cos\frac{\theta}{2}\left(1-\sin\frac{\theta}{2}\sin\frac{3\theta}{2}\right)\end{Bmatrix}$$

$$\begin{Bmatrix}u_1\\ u_2\end{Bmatrix}=\frac{K_{\mathrm{II}}}{2G}\sqrt{\frac{r}{2\pi}}\begin{Bmatrix}\sin\frac{\theta}{2}\left(\kappa+1+2\cos^2\frac{\theta}{2}\right)\\ -\cos\frac{\theta}{2}\left(\kappa-1-2\sin^2\frac{\theta}{2}\right)\end{Bmatrix}$$

Mode III

$$\begin{Bmatrix}\sigma_{13}\\ \sigma_{23}\end{Bmatrix}=\frac{K_{\mathrm{III}}}{\sqrt{2\pi r}}\begin{Bmatrix}-\sin\frac{\theta}{2}\\ \cos\frac{\theta}{2}\end{Bmatrix}$$

$$u_3=\frac{2K_{\mathrm{III}}}{G}\sqrt{\frac{r}{2\pi}}\sin\frac{\theta}{2}$$

plane strain
$\kappa=3-4\nu$
plane stress
$\kappa=(3-\nu)/(1+\nu)$

Collaboration between theory and practice in inverse problems
Fukuoka, Japan, December 16-19, 2014

➢Summary of Fracture Parameters

Energy Release Rate

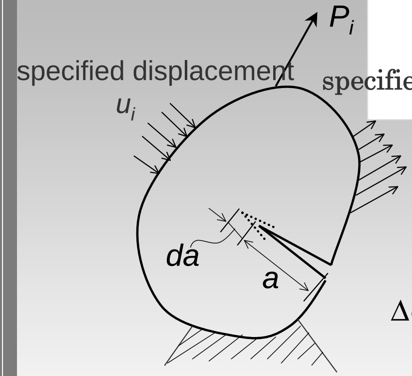

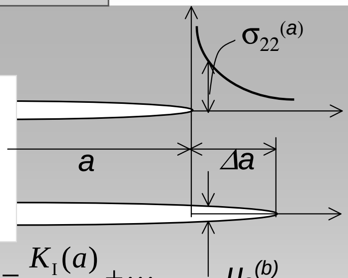

$$\sigma_{22}{}^{(a)}=\frac{K_{\mathrm{I}}(a)}{\sqrt{2\pi x}}+\cdots$$

$$u_2{}^{(b)}=\frac{\kappa+1}{2G}K_{\mathrm{I}}(a+\Delta a)\sqrt{\frac{\Delta a-x_1}{\pi}}+\cdots$$

ΔU= Work done by external force ΔL

$$2\int_0^{\Delta a}\frac{1}{2}\sigma_{22}{}^{(a)}Bu_2{}^{(b)}dx_1$$

$$\mathcal{G}=\frac{dL}{dA}-\frac{dU}{dA}$$

$$dA=Bda$$

$$\mathcal{G}=\lim_{\Delta a\to 0}\frac{2}{B\Delta a}\int_0^{\Delta a}\frac{1}{2}\sigma_{22}{}^{(a)}Bu_2{}^{(b)}dx_1$$

$$=\frac{\kappa+1}{8G}(K_{\mathrm{I}}{}^2+K_{\mathrm{II}}{}^2)+\frac{K_{\mathrm{III}}{}^2}{2G}$$

Collaboration between theory and practice in inverse problems
Fukuoka, Japan, December 16-19, 2014

➢Summary of Fracture Parameters

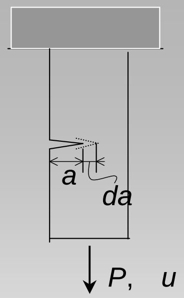

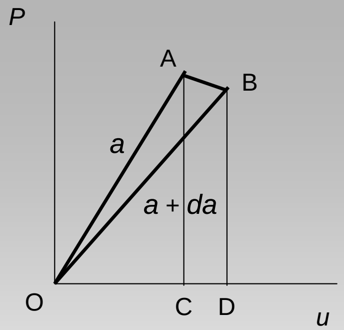

$$\mathcal{G} = \frac{dL}{dA} - \frac{dU}{dA} = \frac{1}{2}P^2\frac{d\lambda}{Bda} = \frac{\kappa+1}{8G}(K_{\mathrm{I}}{}^2 + K_{\mathrm{II}}{}^2) + \frac{K_{\mathrm{III}}{}^2}{2G}$$

$$u = \lambda P$$ λ： Compliance

$$U = \frac{1}{2}Pu$$

Collaboration between theory and practice in inverse problems
Fukuoka, Japan, December 16-19, 2014

➢Summary of Fracture Parameters

Elastoplastic Body

***n* power law (deformation theory) :**

$$\left(\frac{\bar{\varepsilon}}{\varepsilon_0}\right) = \left(\frac{\bar{\sigma}}{\sigma_0}\right)^n \qquad (\ n \geqq 1\ )$$

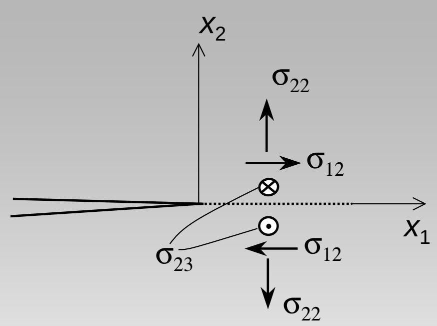

$$\sigma_{ij} = K_\sigma r^{-1/(n+1)}\tilde{\sigma}_{ij}(\theta, n) + \cdots$$

$$\varepsilon_{ij} = K_\varepsilon r^{-n/(n+1)}\tilde{\varepsilon}_{ij}(\theta, n) + \cdots$$

： HRR singularity

K_σ ： Plastic stress intensity factor

K_ε ： Plastic strain intensity factor

$$\frac{K_\varepsilon}{\varepsilon_0} = \left(\frac{K_\sigma}{\sigma_0}\right)^n$$

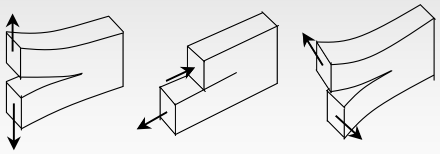

mode I mode II mode III

Collaboration between theory and practice in inverse problems
Fukuoka, Japan, December 16-19, 2014

➢Summary of Fracture Parameters

J integral

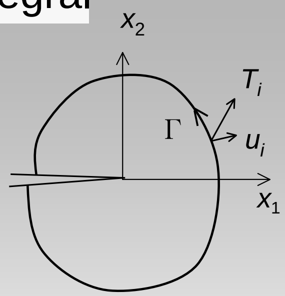

$$\sigma_{ij} = \frac{\partial W}{\partial \varepsilon_{ij}} = f_{ij}(\varepsilon_{11}, \varepsilon_{22}, \cdots, \varepsilon_{31})$$

W : Strain Energy Density

(deformation theory)

Path Independent Integral

$$J = \int_\Gamma \left(W dx_2 - T_i u_{i,1} d\Gamma \right)$$

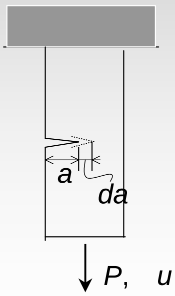

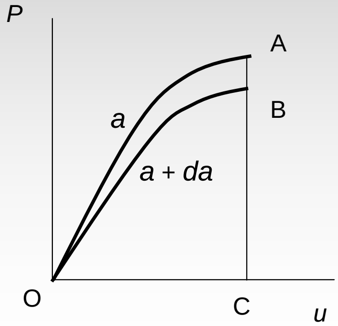

Load-Displacement Curves

$$J = -\frac{dU}{Bda} \quad , \quad U = \int_0^u P du$$

➢Summary of Fracture Parameters

Elastic Body ⟹ Energy Release Rate

Linear Elastic Body

$$J = \mathcal{G} = \frac{\kappa + 1}{8G}\left(K_{\mathrm{I}}^{2} + K_{\mathrm{II}}^{2}\right) + \frac{K_{\mathrm{III}}^{2}}{2G} = \frac{1}{2} P^2 \frac{d\lambda}{Bda}$$

Elastoplastic Body (deformation theory)

n power law ⟹ **Meaning is not clear**

$$J = \frac{I_n \varepsilon_0 K_\sigma^{\,n+1}}{\sigma_0^{\,n}} = I_n K_\sigma K_\varepsilon = \frac{I_n \sigma_0 K_\varepsilon^{\,(n+1)/n}}{\varepsilon_0^{\,1/n}}$$

$$\sigma_{ij} = K_\sigma r^{-1/(n+1)} \tilde{\sigma}_{ij}(\theta, n) + \cdots$$

$$K_\sigma = \sigma_0 \left(\frac{J}{I_n \varepsilon_0 \sigma_0} \right)^{1/(n+1)}$$

➢Summary of Fracture Parameters

Evaluation of Creep Behavior:

Creep- a time dependent, permanent deformation at high temperature, occurring at constant load or constant stress.

Creep rate - The rate at which a material deforms when a stress is applied at a high temperature.

During the creep test, strain or elongation is measured as a function of time and plotted to give the creep curve.

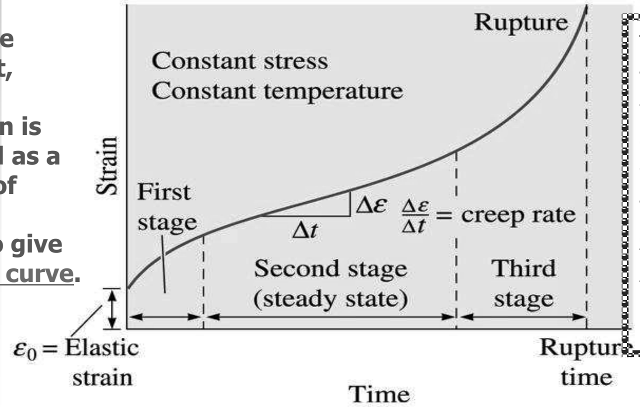

The resulting curve shows three stages. During the first stage, dislocations climb and break free from whatever was pinning them. The second stage of creep is characterized by a steady rate of strain. In the third stage, necking and failure occur.

➢Summary of Fracture Parameters

Creep Crack (*C** parameter)

Analogy to Elastoplastic Problem under Deformation Theory

Elastoplastic

$$\sigma_{ij,j} = 0$$

$$\varepsilon_{ij} = \frac{1}{2}(u_{i,j} + u_{j.i})$$

$$\sigma_{ij} = \frac{\partial W}{\partial \varepsilon_{ij}}$$

$$\Downarrow$$

$$J = \int_\Gamma \left(W dx_2 - T_i u_{i,1} d\Gamma \right)$$

n power law $\left(\frac{\varepsilon}{\varepsilon_0}\right) = \left(\frac{\sigma}{\sigma_0}\right)^n$

$$\sigma_{ij} = \sigma_0 \left(\frac{J}{I_n \varepsilon_0 \sigma_0} \right)^{1/(n+1)} r^{-1/(n+1)} \tilde{\sigma}_{ij}(\theta, n) + \cdots$$

Stationary Creep $(\dot{\varepsilon}_{ij}^e = \dot{\varepsilon}_{ij}^p = 0)$

$$\sigma_{ij,j} = 0$$

$$\dot{\varepsilon}_{ij}^{cr} = \frac{1}{2}(\dot{u}_{i,j} + \dot{u}_{j.i})$$

$$\sigma_{ij} = \frac{\partial W'}{\partial \dot{\varepsilon}_{ij}^{cr}}$$

$$\Downarrow$$

$$C^* = \int_\Gamma \left(W' dx_2 - T_i \dot{u}_{i,1} d\Gamma \right)$$

Norton's rule $\dot{\varepsilon}^{cr} = A\sigma^n$

$$\sigma_{ij} = \sigma_0 \left(\frac{C^*}{I_n A} \right)^{1/(n+1)} r^{-1/(n+1)} \tilde{\sigma}_{ij}(\theta, n) + \cdots$$

➢Summary of Fracture Parameters

Actual Deformation around a Crack Tip

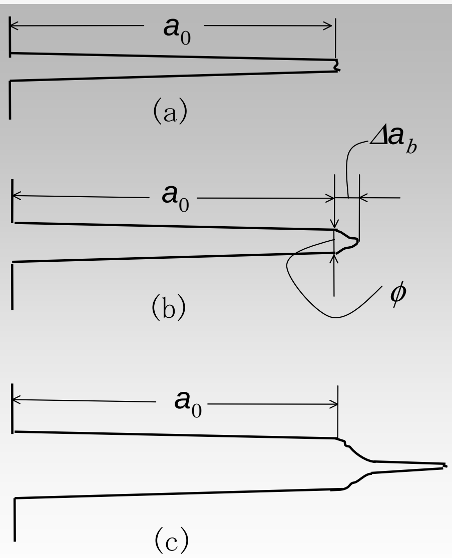

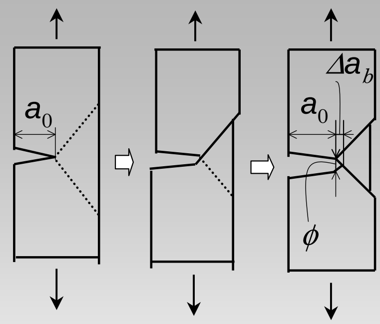

ϕ : COD
(**or** CTOD)

$$\phi = \frac{J}{\lambda \sigma_f}$$

COD: Crack Opening Displacement

Collaboration between theory and practice in inverse problems
Fukuoka, Japan, December 16-19, 2014

➢Fracture Parameters and their Availabilities

Stress Intensity Factor
Energy Release Rate

Linear Fracture Mechanics

Plastic Stress Intensity Factor
(Plastic Strain Intensity Factor)
J integral
COD

Nonlinear Fracture Mechanics
(Elastoplastic Fracture Mechanics)

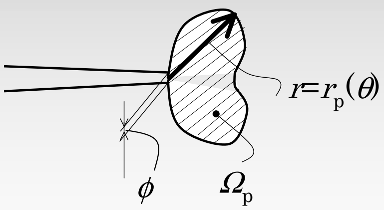

Small Scale Yielding
$r \ll a$

⟹ Linear Fracture Mechanics

Large Scale Yielding
$r \sim a$

⟹ Nonlinear Fracture Mechanics

Collaboration between theory and practice in inverse problems
Fukuoka, Japan, December 16-19, 2014

➢Fracture Parameters and their Availabilities

Stress Intensity Factor

Plastic Stress（Strain）Intensity Factor

$$\begin{Bmatrix} \sigma_{11} \\ \sigma_{22} \\ \sigma_{12} \end{Bmatrix} = \frac{K_{\mathrm{I}}}{\sqrt{2\pi r}} \cos\frac{\theta}{2} \begin{Bmatrix} 1-\sin\frac{\theta}{2}\sin\frac{3\theta}{2} \\ 1+\sin\frac{\theta}{2}\sin\frac{3\theta}{2} \\ \sin\frac{\theta}{2}\cos\frac{3\theta}{2} \end{Bmatrix}$$

$$\sigma_{ij} = K_{\sigma} r^{-1/(n+1)} \tilde{\sigma}_{ij}(\theta, n) + \cdots$$

$$\varepsilon_{ij} = K_{\varepsilon} r^{-n/(n+1)} \tilde{\varepsilon}_{ij}(\theta, n) + \cdots$$

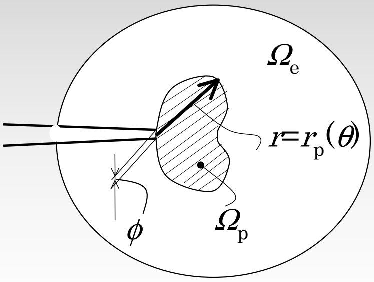

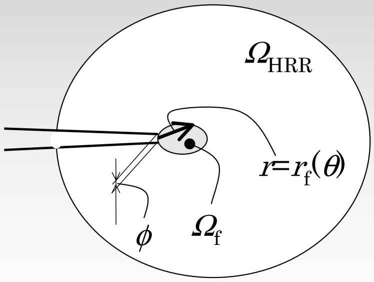

➢Applications to Fracture Phenomena

Brittle Fracture (no plasticity)

$K_{\mathrm{I}} = K_{\mathrm{IC}}$ (also for a stably growing crack)

or

$$\mathcal{G} = \mathcal{G}_{\mathrm{IC}} = \frac{\kappa+1}{8G} K_{\mathrm{IC}}^2 (= 2\gamma, \text{Griffith})$$

Quasi-brittle Fracture (small scale yielding)

$K_{\mathrm{I}} = K_{\mathrm{IC}}$ (also for a stably growing crack)

or

$$\mathcal{G} = \mathcal{G}_{\mathrm{IC}} = \frac{\kappa+1}{8G} K_{\mathrm{IC}}^2 (= 2\gamma, \text{Griffith - Orowan})$$

Ductile Fracture (large scale yielding)

$J = J_{\mathrm{IC}}$ (? for a stably growing crack)

➢Applications to Fracture Phenomena

Brittle or Quasi-brittle Fracture

Stable

$$\frac{dK_{\mathrm{I}}}{da} < 0 \left(= \frac{dK_{\mathrm{IC}}}{da}\right)$$

Unstable

$$\frac{dK_{\mathrm{I}}}{da} \geq 0 \left(= \frac{dK_{\mathrm{IC}}}{da}\right)$$

Ductile Fracture

Stable

$$\frac{dJ}{da} < \frac{dR}{da}$$

Unstable

$$\frac{dJ}{da} \geq \frac{dR}{da}$$

➢Applications to Fracture Phenomena

Mixed Mode Fracture

Brittle or quasi-brittle fracture

$\sigma_{\theta \max}$ criterion

Ductile fracture

?

Fatigue Crack

$$\frac{da}{dN} = f(\Delta K)$$

Creep Crack

$$\frac{da}{dt} = f(C^*)$$ for stationary creep

➢Problems in Conventional Fracture Mechanics

1. The concept of energy release rate was considered successfully applied to elastoplastic fracture under small scale yielding. But, it failed to explain elastoplastic fracture under large scale yielding.

2. There exists no crack parameter that can be defined without depending on constitutive equation. Elastoplastic crack parameter *J* is defined just under deformation theory. It loses its meaning when unloading occurs and it is applicable just before the onset of crack growth. There is no way to deal with a growing elastoplastic crack.

3. There is no parameter for mixed mode elastoplastic crack.

4. Depending on phenomena, different parameters are required depending on phenomena.

Basic properties of concrete and its non destructive testing

Noriyuki MITA* and Takashi TAKIGUCHI†

Abstract

In this article, we first review the basic theory of concrete from the viewpoint of the building material. It is our goal is to establish a determinate non-destructive testing method for concrete structures by application of acoustic tomography. In order to accomplish our purpose, we propose a problem of integral geometry based on our experiments on the concrete structures. We also discuss how important our problems is and introduce several examples in practical applications to which the researches on our problem should be applied.

Keywords: non-destructive testing of concrete structures, inverse problems, acoustic tomography, integral geometry

1 Introduction

In this article, we first review the outline of concrete theory, with which most of the readers may not be familiar. For the general theory of concrete, confer [1]. We also recommend [3] for Japanese readers. It is one of our main purposes to establish a determinate non-destructive testing method for concrete structures, which has not been developed yet for the time being. For this purpose, we propose a problem for the development of a new non-destructive testing method for concrete structures applying acoustic tomography. For the development of the acoustic CT for our purpose, we studied how the ultrasonic waves and the electromagnetic acoustic pulses propagate in the cement paste, the mortar and the concrete by experiments. By the results of our experiments, we study the propagation of the ultrasonic waves and the electromagnetic acoustic pulses in the cement paste, the mortar and the concrete, which yields an inverse problem of the acoustic tomography applied to the determinate non-destructive testing method for concrete structures we are trying to establish. We shall also discuss its importance in view of both practice and theory. Especially, we shall claim that theoretical aspect of this problem has strong connection with the integral geometry.

*Faculty of Human Resources Development, Polytechnic University of Japan, 2-32-1, OgawaNishi-machi, Kodaira, Tokyo, 187-0035, JAPAN. email: mitanori@uitec.ac.jp

†Supported in part by JSPS Grant-in-Aid for Scientific Research (C) 26400184.
Department of Mathematics, National Defense Academy of Japan, 1-10-20, Hashirimizu, Yokosuka, Kanagawa, 239-8686, JAPAN. email: takashi@nda.ac.jp

This article consists of the following sections.

§1. Introduction

§2. Basic properties of concrete

§3. Damage by salt on the expressway bridges

§4. Propagation of the ultrasonic waves and the electromagnetic acoustic pulses

§5. An inverse problem of the acoustic tomography

§6. Conclusion

In this section, as the introduction of this article, we introduce the outline of our article. In the next section, we shall review basic properties of concrete, where we also discuss how we understand the concrete in this paper. In the third section, we shall introduce the motivation of our research. The motivation of this research occured from the problem of the damage by salt on the expressway bridges. In the fourth section, we study how the ultrasonic waves and the electromagnetic acoustic pulses propagate in the cement paste, the mortar and the concrete by the experiments, which is a key to discuss our main purpose, to study how to establish a determinate non-destructive testing method for concrete structures, in Section 5. We first introduce our experiments to study the propagation the ultrasonic waves and the electromagnetic acoustic pulses in the cement paste, the mortar and the concrete. By examining the results of our experiments, we conclude that we can treat the ultrasonic waves and the electromagnetic acoustic pulses as linear elastic waves for our purpose. Section 5 is devoted for the main purpose of this article. We shall pose an inverse problem for establishment of a determinate non-destructive testing method for concrete structures, for which we shall apply the results of our experiments and their examination discussed in Section 4. The problem posed in this section is also interesting in view of pure mathematics, especially, in view of integral geometry. In the final section, we shall summarize our conclusions.

The authors are grateful to Professors Hisashi Yamasaki and Ryusei Yamashita for their devoted help for our experiments.

2 Basic properties of concrete

In this section, we shall review basic properties of concrete. Before reviewing the definition and some basic properties of concrete, the authors claim that

Claim 2.1. *The concrete materials are artificial* (*gigantic*) *stones or megaliths.*

Let us first discuss why the authors claim Claim 2.1. Take Valley Temple, Egypt (BC2500?) and Parthenon, Athens (BC447-432), for example, which are made of megaliths. At that period around those areas, there were plenty of megaliths available, therefore they made Valley Temple and Parthenon of megaliths which are very suitable for edifices. On the other hand, let us turn to Colosseum, Rome (AD70-80). Its bailey or external wall being made of megaliths, its interior structure is infilled with stones bricks and sand, which we take as an origin of the concrete. It may be because of the shortage of the megaliths in Rome about 2000 years ago. Note that the structure of Colosseum safely exists more than 2000 years after its foundation. Hence we can say that the primitive concrete materials applied to the interior infillment of Colosseum have played their important role as the substitute for the megaliths very well for a long time, which is one of the reasons why the authors claim Claim 2.1. Though we still have many other reasons, we would not mention them in detail, since they directly have little to do with our main purpose in this article.

Let us define what the concrete is.

Definition 2.1. The concrete is the mixture of the four materials, the cement (C), the water (W), the sand (fine aggregate：S) and the gravel (coarse aggregate: G). Sometimes, if necessary, we add some admixture to the above mixture of the four materials to make harder concrete.

Remark 2.1.

(i) The mixture of the cement and the water is called the cement paste.

(ii) The mixture of the cement, the water, and the sand (the cement paste and the sand) is called the mortar.

(iii) The concrete can be understood as the mixture of the mortar and the gravel.

(iv) It being usually said that the concrete is the mixture of the four materials, the cement, the water, the sand and the gravel as mentioned above, it is very important to add the air as the fifth component of the concrete, especially for the main purpose in this article. Since concrete is a porous medium, as is well known, it is very important to study how the air is included in a concrete structure for its non-destructive testing.

Let us introduce the merits of the concrete.

Property 2.1 (Merits of the concrete)**.**
The merits of the concrete as a building material are as follows.

(a) *Excellent durability against the weather, the chemical materials and the mechanical force.*

(b) *High fire-resistance and water-resistance.*

(c) *High compressive strength.*

(d) *High corrosion resistance for steel.*

(e) *The coefficients of thermal expansion* (*CTE*) *of the concrete and the steel are exactly the same.*

(f) *Easily made and shaped in any form because of its fluidity before it gets hard.*

(g) *Its cost is very cheap* (*about 120 dollars/m^3*).

Let us give some remarks on Property 2.1. The first three properties are very close to the ones of the stones and the megaliths, which is one of the reasons why the authors claimed Claim 2.1. The properties (d) and (e) are essentially important for the reinforced concrete (RC) structures. The property (d) is by the chemical property of the cement. Very roughly speaking, the main component of the cement is calcium oxide (CaO), whose combination with the water yields

$$CaO + H_2O \to Ca(OH)_2, \tag{1}$$

which is known as the hydration reaction of the cement. It is well known that calcium hydroxide ($Ca(OH)_2$) shows strong alkalinity, which prevents the steel from getting oxidized. We claim that this property is much better than "being artificial stones or megaliths", especially as the material of the RC structures. If the CTE of the concrete and the steel are different, the RC structures easily have some cracks in their interior by the change of the temperature. By the properties (d) and (e), the RC was called as "the miracle and the permanent material" at its initial stage of application to the buildings. It turned out, however, that it was neither miracle nor permanent. The concrete gets neutralized by the carbon dioxide (CO_2) in the air a few decades after its placing, whose chemical reaction is represented by

$$Ca(OH)_2 + CO_2 \to CaCO_3 + H_2O. \tag{2}$$

After the neutralization of the concrete, a part of the steel inside the RC structure gets corroded by the water contained in its interior. The corroded steel intumesces very much, which would make cracks or ruin the structure. Therefore the life span of the RC structure is referred about a half century, these days. In spite of it, it is true that the reinforced concrete is very cheap, durable and easily treated material for the buildings before the steel in its interior gets corroded. By these facts, it is very important to study how to find the defects in the concrete structures and how to repair and maintain them. We also note that the properties (f) and (g) are very good, important and superior to the megaliths as the building material.

Of course, there are demerits of the concrete.

Property 2.2 (Demerits of the concrete)**.**
The demerits of the concrete as a building material are as follows.

(α) *Low tensile strength.*

(β) *It easily gets cracks in and on itself.*

(γ) *It is very heavy in the RC structures.*

Let us give some remarks on Property 2.2. As for (α), the tensile strength of the concrete is about $1/10$ of its compressive one. It is very weak compared with its bending strength which is about a third of its compressive one. From this problem, there arises the necessity to reinforce the concrete. The demerit (β) causes problems in the load bearing ability and durability. It also causes the water leakage. The RC structures are generally said to be weak to the damage by the earthquake because of the demerit (γ). The demerits (α) and (β) are inferior to the megaliths as the building material. The demerit (γ) is the same one as the megaliths.

3 Damage by salt on the expressway bridges

It is our main purpose in this article to study how to establish a determinate non-destructive testing method for concrete structures, which shall be discussed in the fifth section. In this section, we shall introduce a problem of the damage by salt on the expressway bridges over the sea, which motived our study to establish a determinate non-destructive testing method for concrete structures. By the wind or a tide, sea water blows up and pour over the expressway bridges. As a result, the salt soaks into the interior of the bridges. In the interior of an expressway bridge, there are a number of steel wires inbedded for the reinforcement. By the soaked salt, the steel wires would be corroded by chloridation. In this process, the corrosion of the steel wires is much faster than the corrosion by oxidization, since chloridation cannot be helped by the alkalinity of the cement. This damage by the salt is one of the severest problems on the maintenance of the expressway bridges over the sea. For the time being, they check the damage of the expressway bridges by salt by application of a destructive test. They first pull out some pieces of concrete from the brides. By checking whether they contain the salt or not, they determine the parts of the bridge damaged by salt. This is a typical example of the destructive test and costs much time and labor costs. For development of the better testing methods, we pose the following problem.

Problem 3.1. *Establish a good non-destructive testing method for the bridges, which also works well to cut off the testing time and the labor costs for the test.*

Remark 3.1. Note that if we solve Problem 3.1 then we could cut off the the testing time and the labor costs for the test as well as the damage to the bridge by the test.

For simplicity, assume that the bridge is a rectangular parallelepiped. Its damage by salt must be detected before it soaks into the interior of the bridges longer than $1m$ from each edge surface, otherwise the steel wire inside the bridge might be got corroded by the damage by salt.

Therefore, we pose our problem concretely in the following way.

Problem 3.2. *Establish a good non-destructive testing method to determine the place damaged by salt inside the bridge within the distance less than* $1m$ *from each edge surface.*

In order to solve this problem, we shall apply an acoustic tomography. In the next section, we shall study the propagation of the ultrasonic waves and the electromagnetic acoustic pulses in concrete structures within the length of $1m$ by experiments, which shall be applied to pose a problem for establishment of non-destructive testing method for concrete structures by acoustic tomography.

4 Propagation of the ultrasonic waves and the electromagnetic acoustic pulses

As we have mentioned at the end of the last section, we shall apply the properties of the sound as a tool of the non-destructive testing for concrete structures. In this section, as a preparation for the next section, we study how the ultrasonic waves and the electromagnetic acoustic pulses propagate in the cement paste, the mortar and the concrete by the experiments. We first introduce our experiments to study the propagation the ultrasonic waves and the electromagnetic acoustic pulses propagate in the cement paste, the mortar and the concrete. By the examining the results of our experiments, we shall study the propagation of the ultrasonic waves and the electromagnetic acoustic pulses in concrete structures of the length about $1m$ or less.

Let us introduce the outline of our experiments.

Outline of our experiments

- Velocity of the sound;
  - Velocity of the ultrasonic wave is denoted by V_u (m/s).
  - Velocity of the electromagnetic acoustic pulse is denoted by V_e (m/s).
- Length of test pieces;
  We prepared test pieces of the length 100, 200, 300, 400, 800 and $1200mm$ in order to check
  - the decay of the acoustic velocity
  - the propagation of the sound
- Inclusions;
  We prepared two types of test pieces.
  - Normal test pieces
  - Test pieces with styrofoam of the length 200 or 300 mm included in their inside

  These test pieces are made use of to determine the propagation of the sound.

We first made the test pieces of cement paste and mortar as shown in Figure 1.

Table 1 : Mix Proportion of Cement Paste

	Water	Cement	Air	Total
Weight(kg)	553	1382	–	1935
Volume(ℓ)	553	437	10	1000

※W/C=40% , Air=1%

Table 2 : Mix Proportion of Cement Mortar

	Water	Cement	Sand	Air	Total
Weight(kg)	331	828	1035	–	2195
Volume(ℓ)	331	262	397	10	1000

※W/C=40% , S/C=1 .25 , Air=1%

Figure 1: Components of the test pieces

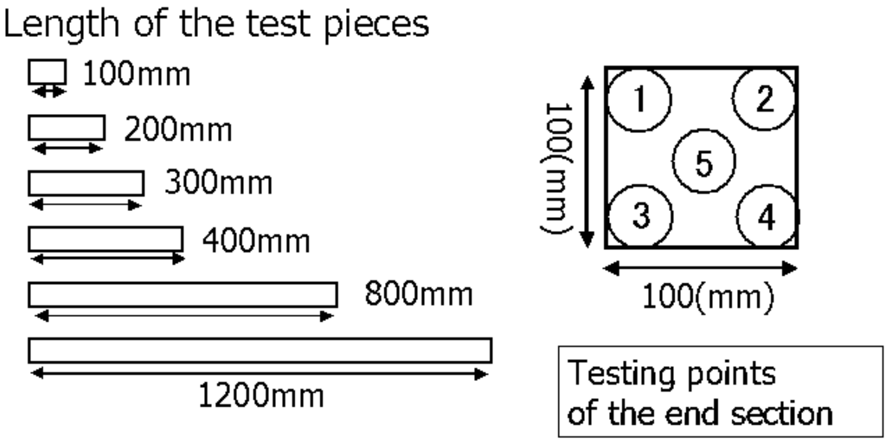

Figure 2: Length of the test pieces and testing points

Experiment 1.

We first experimented on the normal test pieces. We projected the ultrasonic waves and the electromagnetic acoustic pulses from the testing points numbered ①, $\cdots$, ⑤ on one end square of the test pieces (see figure 2). We name them as 'source points'. We received them at the same-numbered testing points on the other end square. We name them as 'observation points'. We have measured the time for the sound to travel between the source and the observation points. The results of these experiments are summed up in Figures 3 and 4, where we mean that the age of the test pieces is x weeks by the term 'xW'.

Remark that the average of the results on the point ① and ② are treated as 'upper points', the average of the results on the point ③ and ④ are treated as 'lower points'and the point ⑤ is denoted by the center point.

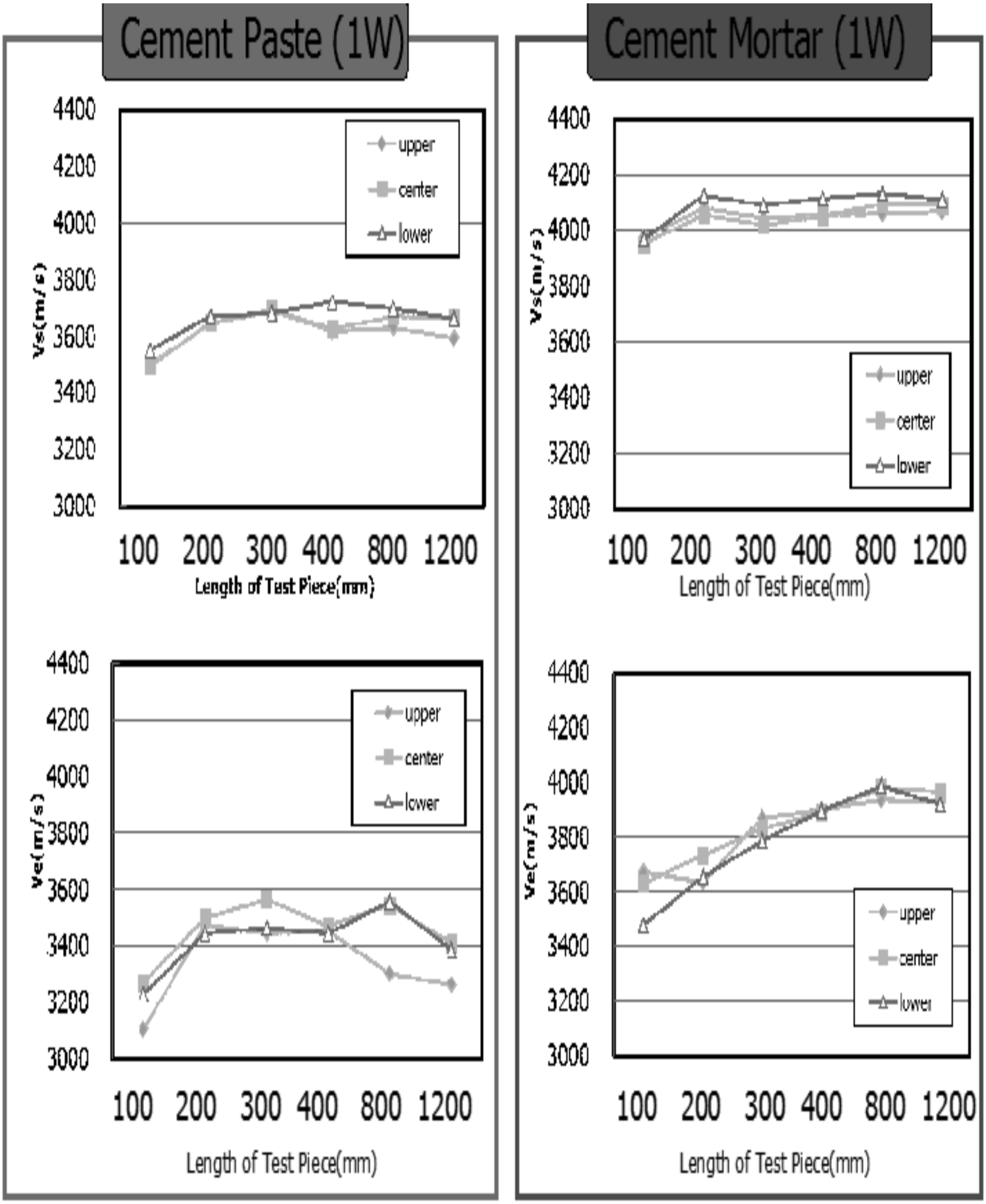

Figure 3: Normal test pieces (age of a week)

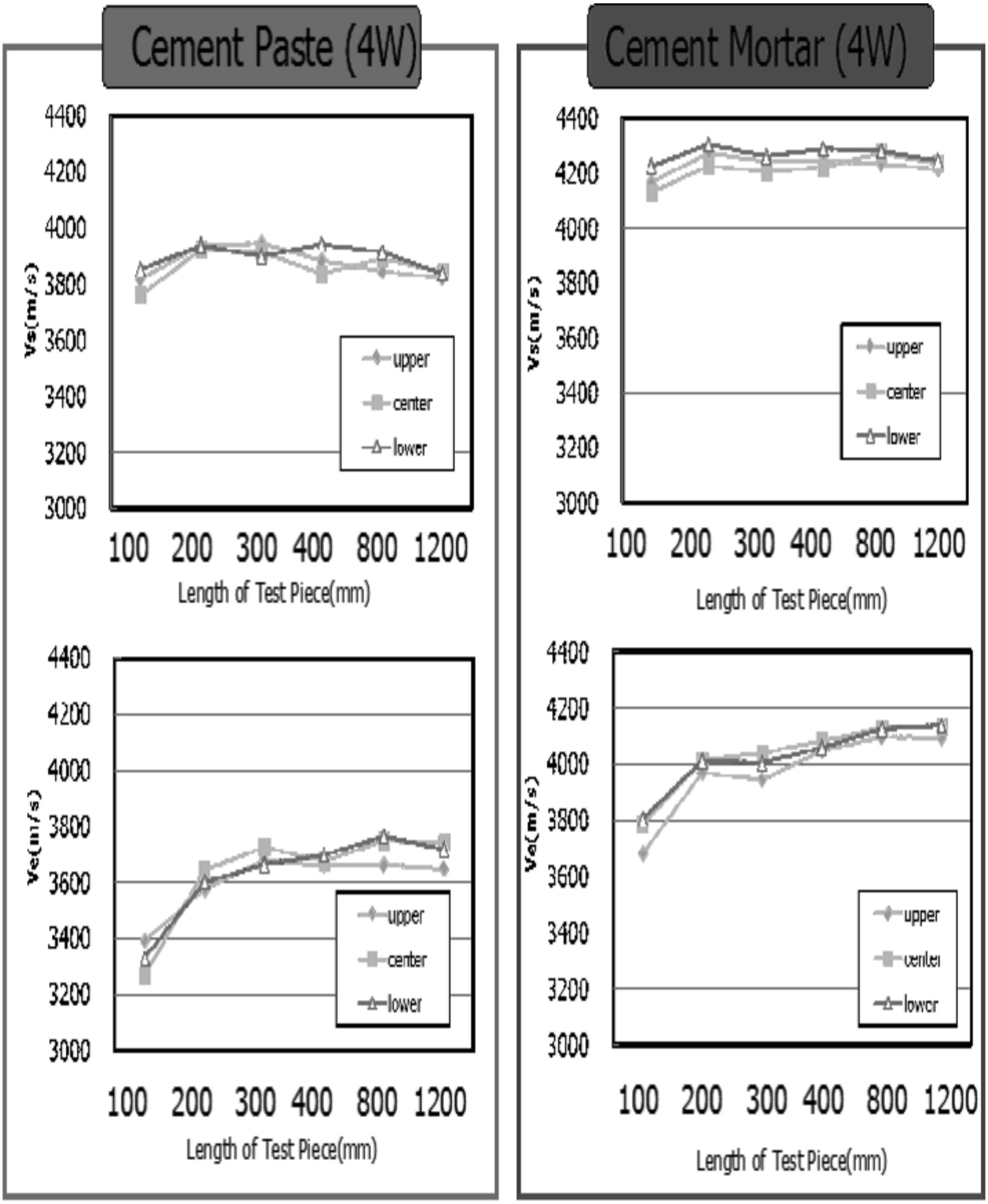

Figure 4: Normal test pieces (age of 4 weeks)

By reviewexamining the results by Experiment 1, we obtain the following properties.

Property 4.1.

- *We have rediscovered the well known basic property of concrete; the more time goes by, the harder the test pieces are, which is caused by the reaction of hydration of concrete.*
- *We also have rediscovered the well known basic property, the gravity settling of cement, in terms of the acoustic velocity; the lower the testing points are, the faster the acoustic velocity is, which is because of the fact that the lower the points are, the larger their density is, causeb by the gravity settling of cement.*
- *We can conclude that for the test pieces of the length less than* $1200mm$, *there is no decay of the acoustic velocity from the viewpoint of its first arriving time.*

The last property is essentially important for our study.

Experiment 2.

We simultaneously made the test pieces of the length $400mm$ ($100mm \times 100mm \times 400mm$) with styrofoam of the length 200 and $300mm$ included in their inside (confer Figure 5). We performed the same experiments as Experiment 1, whose results are reviewexamined in the following .

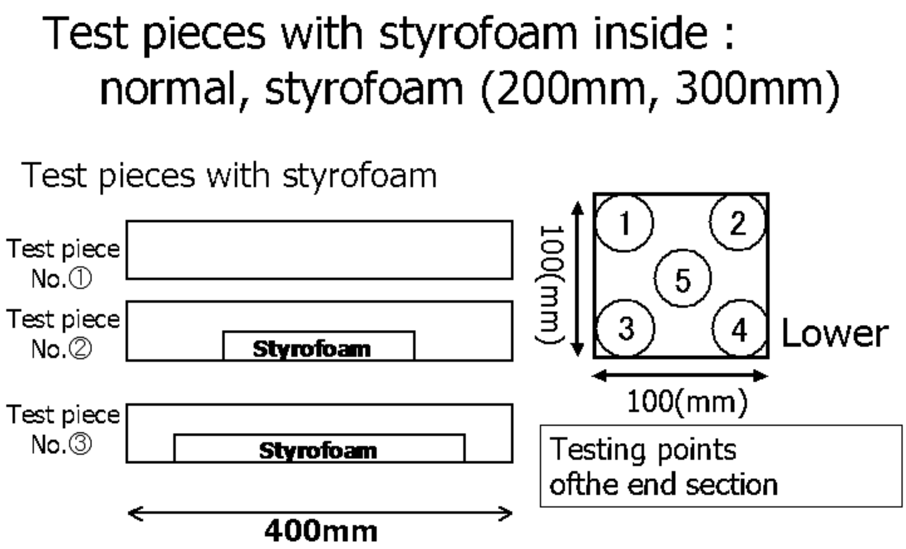

Figure 5: Test pieces with styrofoam

In Experiment 2, the (formal) velocity, which is calculated by

$$\frac{\text{length of the test piece } (meters)}{\text{arriving time } (sconds)}, \tag{3}$$

in the lower points is smaller than the that of upper points, applying which we studied the propagation of the sound in the test pieces. We hypothesized that the propagation of the sound in the test pieces is as the following Hypothesis which is also shown in Figure 6.

Hypothesis 4.1. The first arrival wave of the ultrasonic one and the electromagnetic acoustic pulse takes the fastest route in the test pieces of the cement paste, the mortar and the concrete.

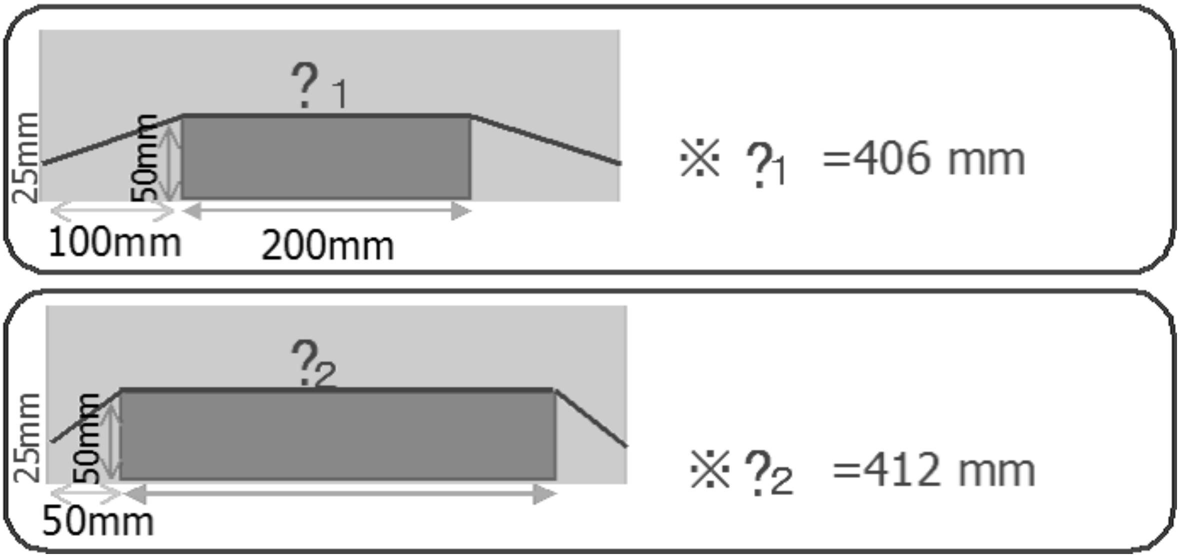

Figure 6: Propagation of the sound

Applying Hypothesis 4.1, we have modified the length of the orbit along which the sound propagates, that is, V_s' and V_e' are given by

$$\frac{0.00406 \ (meters)}{\text{arriving time } (seconds)} \tag{4}$$

for the lower points in the test pieces with styrofoam of the length 200mm and by

$$\frac{0.00412 \ (meters)}{\text{arriving time } (seconds)} \tag{5}$$

for the lower points in the test pieces with styrofoam of the length 300mm. Confer Figure 6 for the image of these modifications. The results of Experiment 2 with the modification of the velocities are summarized in Figures 7, 8 and 9.

Table 3 : Modified Data of Cement Paste

Test Piece	Testing Point	Vs(m/s)	Vs'(m/s)	Ve(m/s)	Ve'(m/s)
No-Styrofoam	Upper	3777	–	3506	–
	Center	3788	–	3626	–
	Lower	3808	–	3648	–
Styrofoam 200mm	Upper	3800	–	3508	–
	Center	3824	–	3663	–
	Lower	3701	3831	3540	3595
Styrofoam 300mm	Upper	3867	–	3664	–
	Center	3873	–	3695	–
	Lower	3731	3866	3496	3686

Table 4 : Modified Data of Cement Mortar

Test Piece	Testing Point	Vs(m/s)	Vs'(m/s)	Ve(m/s)	Ve'(m/s)
No-Styrofoam	Upper	4223	–	3952	–
	Center	4203	–	4022	–
	Lower	4229	–	4021	–
Styrofoam 200mm	Upper	4207	–	3968	–
	Center	4160	–	3999	–
	Lower	4079	4186	3918	4009
Styrofoam 300mm	Upper	4222	–	3983	–
	Center	4191	–	4034	–
	Lower	4035	4239	3893	4085

※Vs', Ve' : **Modified** Data

Figure 7: Tables of modification of the velocity

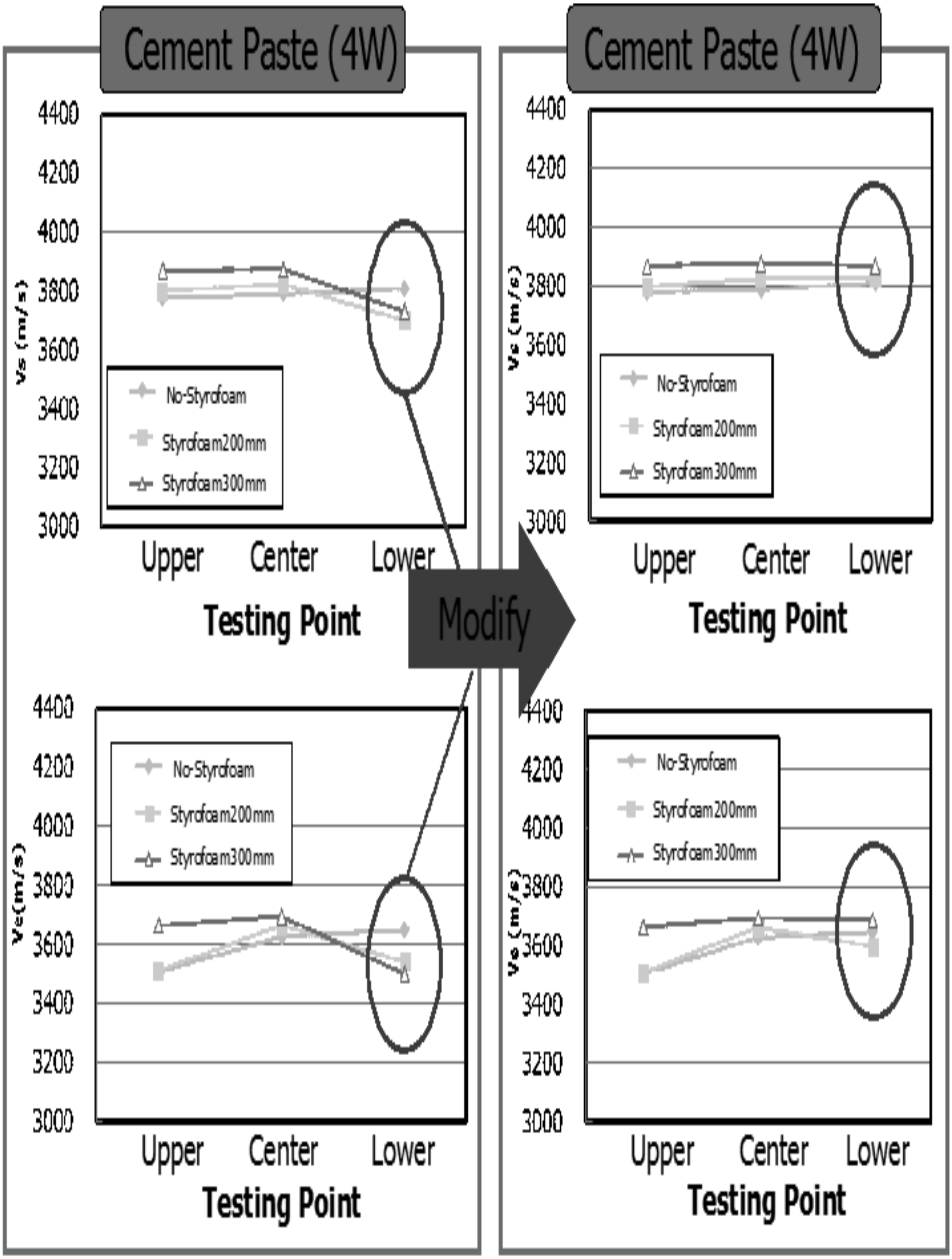

Figure 8: Test pieces of cement paste with styrofoam (age of 4 weeks)

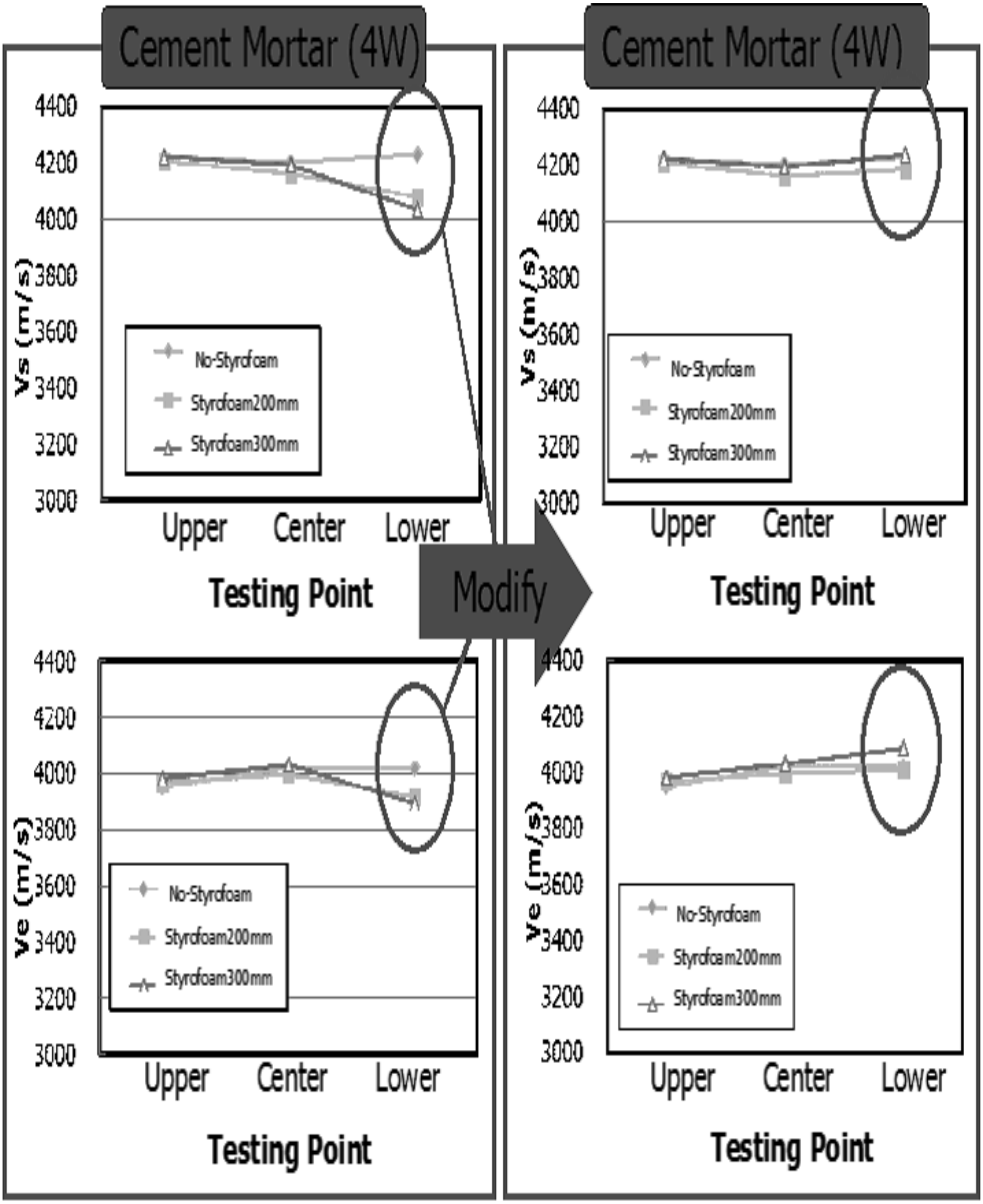

Figure 9: Test pieces of mortar with styrofoam (age of 4 weeks)

Let us summarize the conclusions of Experiments 1 and 2.

Conclusion 4.1 (Conclusion of Experiments 1 and 2)**.**

- *The first arrival wave of the ultrasonic one and the electromagetic acoustic pulse takes the fastest route in the test pieces of the cement paste, the mortar and the concrete.*

- *In the test pieces of the length less than 1200mm, there is no decay of the speed of the ultrasonic waves and the electromagetic acoustic pulses with respect to the length of the test pieces.*

Remark 4.1. For the time being, there does not exist determinate non-destructive testing method for concrete structures. It is our newer idea than the existing ones [2, 4] to focus on the first arrival time of the sound and pose a problem for the development of the acoustic CT, which may yield a determinate non-destructive testing method. We shall discuss this problem in the nest section.

The first conclusion in Conclusion 4.1 is so important for our main purpose that we summarized it as an important property.

Property 4.2. *The first arrival wave of the ultrasonic one and the electromagnetic acoustic pulse takes the fastest route in the test pieces of the cement paste, the mortar and the concrete.*

Property 4.2 plays an important role to pose a problem for establishment of a determinate non-destructive testing method in the next section.

Remark 4.2. Having introduced the results of our experiments mainly on the data of ultrasonic waves, we have almost the same results on electromagnetic acoustic pulses, which shall be introduced in our forthcoming paper.

5 An inverse problem of the acoustic tomography

As was studied in the previous section, we know that the the first arrival wave of the ultrasonic one and the electromagnetic acoustic pulse takes the fastest route in the concrete structures of the length less than $1.2m$ and there is no decay in the velocity of the sound within the length of $1{:}2m$, which is what Conclusion 4.1 claims. In view these properties, we pose the following problem in order to establish a determinate non-destructive testing method for concrete structures, which is the main purpose in this article.

Problem 5.1 (Problem for non-destructive testing for concrete structure)**.**
Let $\Omega \subset \mathbb{R}^3$ be a domain and $f(x)$, $(x \in \Omega)$ be the propagation speed of the sound. For $\alpha, \beta \in \partial\Omega$, we denote by $\gamma_{\alpha,\beta}$ a route from α to β through Ω. Reconstruct $f(x)$ $(x \in \Omega)$ out of the data

$$\min_{\gamma_{\alpha,\beta}} \int_{\gamma_{\alpha,\beta}} 1/f(x) d\gamma, \tag{6}$$

for $\forall \alpha, \beta \in \partial\Omega$.

By Problem 5.1 we mean the problem "Reconstruct the acoustic velocity $f(x)$ at the all points $x \in \Omega$ out of the data of the acoustic arrival time between the all pairs of the points on the boudary."Study of Problem 5.1 is very important not only for solution of Problem 3.2, but to establish a determinate non-destructing testing method for general concrete structures including RC ones. Let us give some remarks on Problem 5.1.

Remark 5.1 (Remarks on Problem 5.1)**.**

- It is impossible to reconstruct the information of some points x's where $f(x)$'s are very small. For example, we cannot reconstruct the acoustic velocity of the styrofoam if it is included near the center of the test piece since no acoustic wave would go through it because of Property 4.2. However, it does not matter very much, since what we focus on in Problem 3.2 is the part damage by salt where the density (accordingly the acoustic velocity) is relatively large.
- It is an interesting problem to determine the optimal subset of reconstructible by the acoustic CT established by the application of Problem 5.1.

As an application of the study of Problem 5.1, we of course have Problem 3.2 in mind. In Problem 3.2, we have to detect detect the $2 \sim 3kg$ of salt included in the $1m^3$ of concrete in order to detect the damaged parts of the expressway bridges by salt, which yields the following problem.

Problem 5.2 (Another problem to solve Problem 3.2)**.**
Is it possible to detect the $2 \sim 3kg$ of salt included in the $1m^3$ of concrete, by the acoustic tomography as an application of Problem 5.1?

In order to solve this problem, we shall conduct other experiments.

As another application of the study of Problem 5.1, we take non-destructive testing of RC structures, for which we have to study the propagation of the sound in the longer concrete structures.

Problem 5.3 (Another problem for non-destructive testing).
Study the propagation of the ultrasonic wave and the electromagnetic acoustic pulse in the longer concrete structures and pose a mathematical problem for longer concrete structures.

The study of this problem can be very helpful for non-destructive testing for more general concrete structures, especially to detect the corroded steel in RC structures.

Remark 5.2. It is very important to develop the study of Problems 3.2 and 5.3, especially in view of redevelopment of infrastructures.

As we have discussed above, study of Problem 5.1 is very important in view of practice, especially in view of redevelopment of infrastructures. It is also important in view of both pure and applied mathematics, especially in integral geometry. Let us mention how important the study of Problem 5.1 is in view of pure and applied mathematics.

Remark 5.3 (Importance of Problem 5.1 in mathematics).

- It is a very interesting problem to establish an reconstruction formula for Problem 5.1 in view of integral geometry.
- It is another interesting problem in Problem 5.1 to determine the subset of Ω where the reconstruction is impossible because it has no intersection with any γ giving (6). This problem is also interesting in view of integral geometry.
- In practice, we have to study various incomplete data problems of Problems 5.1 by the restriction arisen from various reasons, which is interesting in view of pure mathematics, especially in view of integral geometry, which is also very important in applied mathematics.

6 Conclusion

In this section, we summarize our conclusions in the article.

Conclusion 6.1 (Conclusion of this paper)**.**

- *For development of the acoustic CT, we studied how the first arrival wave propagates in the cement paste and the mortar.*
- *Applying the property of the first arriving wave, we have posed a problem for the development of the acoustic CT.*
- *The acoustic CT for concrete structure may be the first determinate non-destructive testing method for concrete structures.*
- *The problems posed in this study are interesting in view of the study of mathematics.*

We still have too many unsolved problems for the study of Problem 5.1 to be applied to both practice and mathematics, some of which have already been discussed throughout this paper. Therefore we would not dare to summarize open problems to be solved for further development at the end of this article.

References

[1] Dunham C. W. : *The theory and practice of reinforced concrete* (*third edition*), McGrow-Hill, New York, (1953).

[2] Jones R. and Facaoaru I. : *Materials and Structures,* Research and Testing, **2**, (1969) p. 275.

[3] 國府勝郎, 辻幸和, 下山善秀: 『コンクリート工学 (I) 施工 (新訂第七版)』, 彰国社 (2010).

[4] Motooka S. and Okujima M. : *Study on Detection of Buried Steel Bar in Concrete with Electromagnetic Impact Driving Method,* Proceedings of 2nd Symposium on Ultrasonics Electronics, (1981) pp.144-146.

Noriyuki MITA
Faculty of Human Resources Development,
Polytechnic University of Japan,
2-32-1, OgawaNishimachi, Kodaira,
Tokyo, 187-0035, JAPAN
e-mail: mitanori@uitec.ac.jp

Takashi TAKIGUCHI
Department of Mathematics,
National Defense Academy of Japan,
1-10-20, Hashirimizu, Yokosuka,
Kanagawa, 239-8686, JAPAN
e-mail: takashi@nda.ac.jp

Basic Properties of Concrete and its Non Destructive Testing

Polytechnic University of Japan
Noriyuki MITA
National Defense Academy of Japan
Takashi Takiguchi

Parthenon, Athens (BC447-432)

Made of Gigantic Stone

Valley Temple, Egypt (BC2500?)

Treasury of Atreus, Mycenae (BC1400)

Lintel Stone

Colosseum, Rome (AD70-80)

Made of (Roman) Concrete

Concrete of Colosseum

Form : Made of Stone and Blick, Infill the Concrete

Concrete

Concrete is an Artificial Stone.

Made of : Cement(C),
Water(S),
Sand(Fine Aggregate : S),
Gravel(Coarse Aggregate : G)
Admixture etc.

Cement Paste	: Cement + Water
Mortar	: Cement Paste + Sand
Concrete	: Mortar + Gravel

Materials of Concrete ($1m^3$)

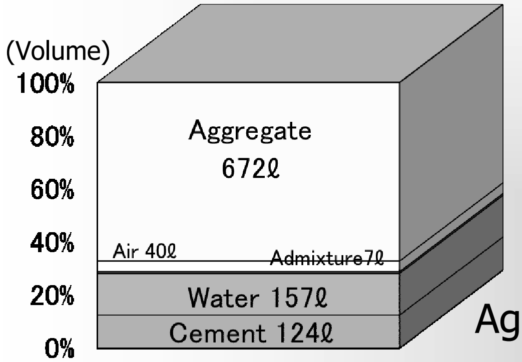

Materials of Concrete $1m^3$
(**Water / Cement ratio** 40%,
Aggregate / Cement ratio 4．0)

Concrete $1m^3$:

- Cement : 100 ℓ
- Water : 200 ℓ
- Sand : 300 ℓ
- Gravel : 400 ℓ

Aggregate(Sand+Gravel) : 70%

Void of Aggregate
→ Filling with Cement Paste

General Characteristics of Concrete

Merit :

- Excellent Durability
  (Weather,Chemical,Mechanical, Highly Fire-Resistance, Water Resistance)
- High Compressive Strength
- High Corrosion Resistance for Steel
- How to make is simple
- Cheap → 15000yen/m^3

General Characteristics of Concrete

Demerit :

- Low Tensile Strength
  (1/10 of Compressive Strength)
  cf. Bending Strength－1/3 of Compressive Strength
  → Necessity of Reinforcement
- Easily Cracked
  → Problems for Load Bearing Ability, Durability, Water Leakage
- Large Mass
  → Damage at Earthquake Time

Compressive Strength and Workability

Water Cement ratio theory :

Compressive Strength of Concrete is determined by the Weight ratio of Water / Cement (W/C).

W/C : High ⇨
- Compressive Strength : Low
- Workability : High

W/C : Low ⇨
- Compressive Strength : High
- Workability : Low

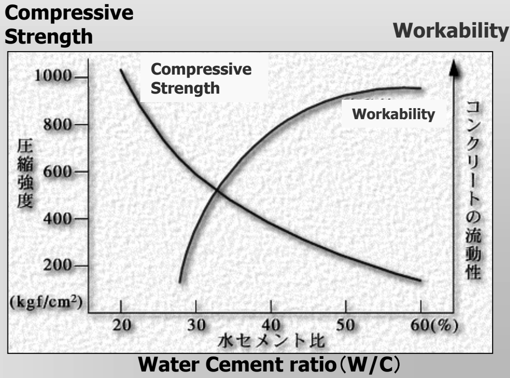

Reinforced Concrete(RC) Construction Site

Reinforcement

Concrete Form

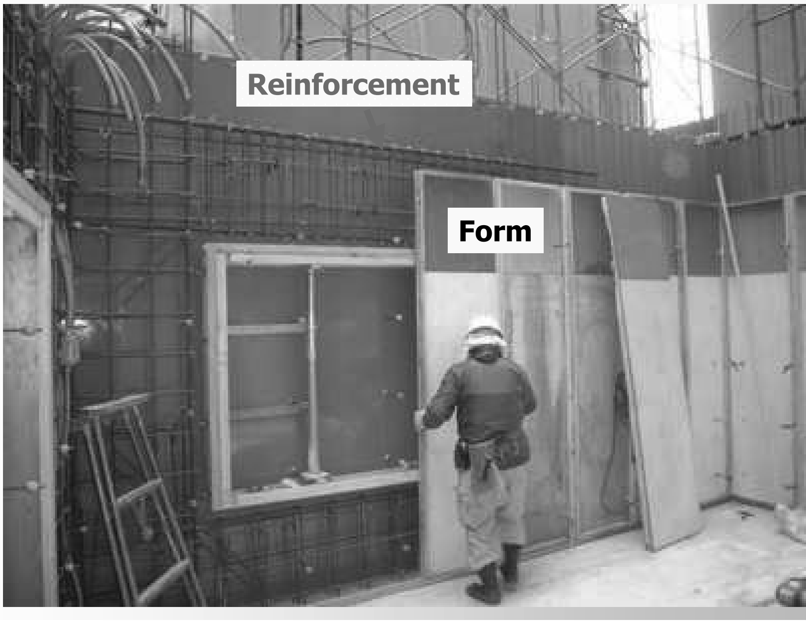

Placing of Concrete

Defect of Concrete Placing

Compressive Strength Test of Concrete

In case of Existing Building

Collecting for Test Piece

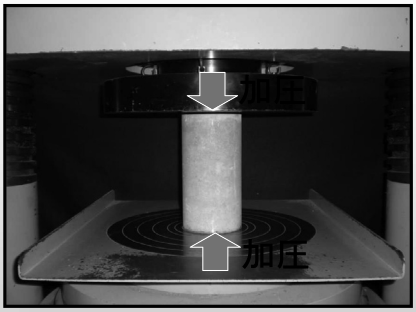

Compressive Strength Test

Problems :
- Damage of the Skeleton
- Damage of the Reinforcement
- Collecting for Test Piece at the Narrow Space

→ Necessity of Nondestructive Testing Method

Standard Nondestructive Testing Method of Concrete

Rebound Hammer Method

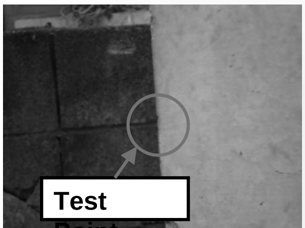

Before

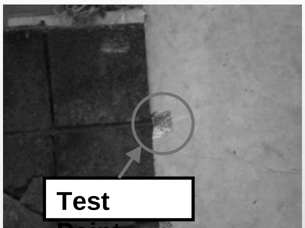

After

Problems :
- **Estimation from Surface Hardness**
- **Destruction at the Test**

Supersonic Waves Method

Testing Machine

Problems :
- **Small Input Energy**
  (Electric Power：1W)
  → High Attenuation
- **Big Sensor**
  (φ50mm)

Supersonic Waves Method
Sound Velocity : Ve

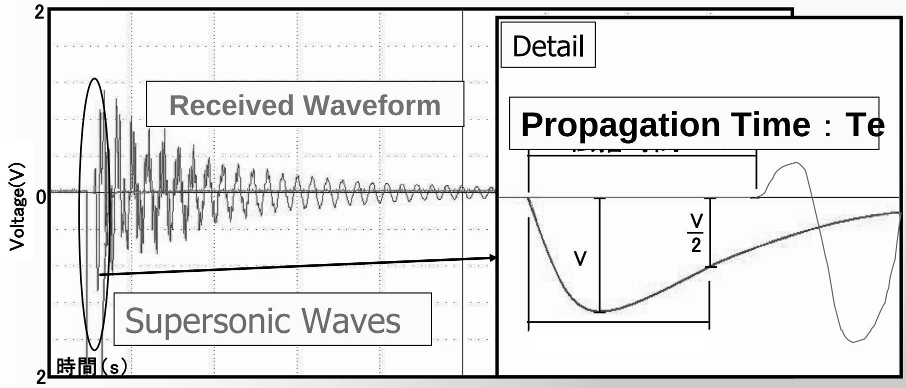

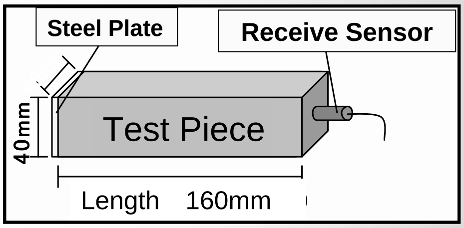

Sound Velocity : Vs

Vs＝L /Te (km/s)

L : Length

Te : Propagation Time

Pulsed Electromagnetic Force Acoustic Method

Characteristics
- Large Input Energy (Electric Power : 700kW)
- Small Sensor (ϕ 11mm)

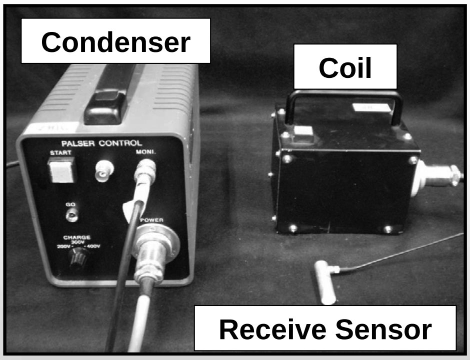

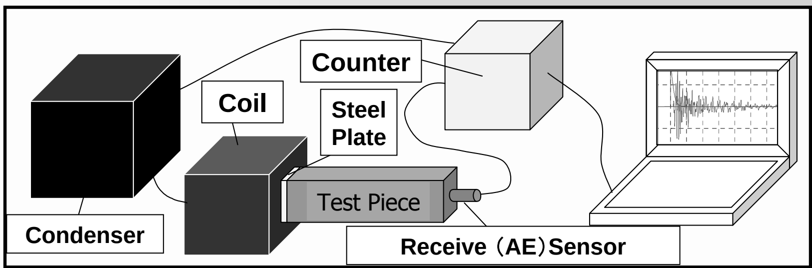

Pulsed Electromagnetic Force Acoustic Method

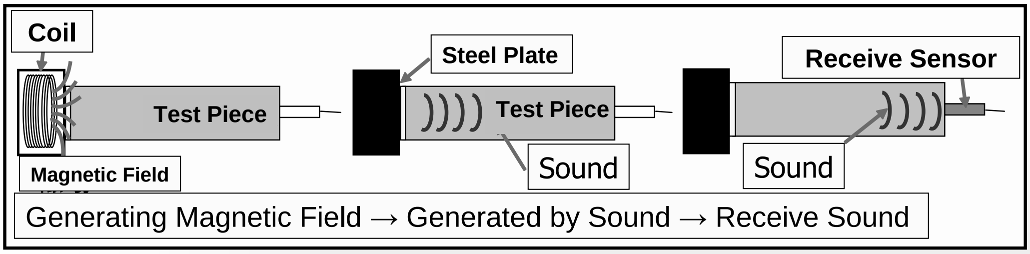

Principle of Pulsed Electromagnetic Force Acoustic Method

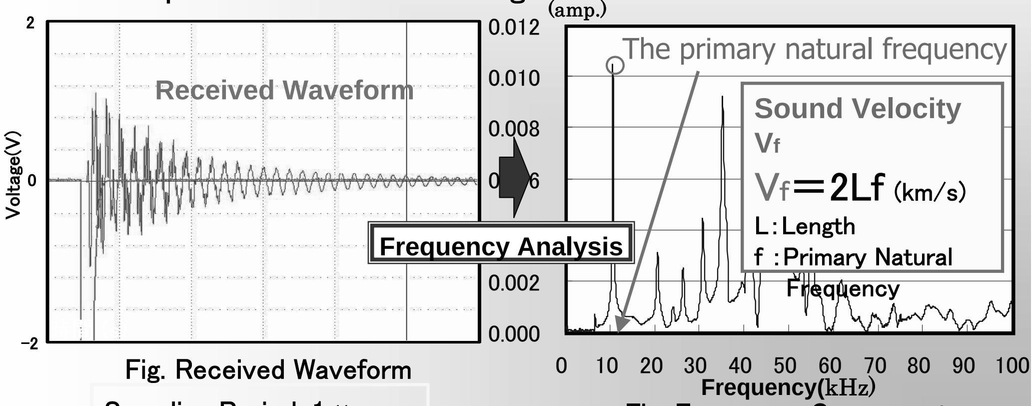

Fig. Received Waveform

Sampling Period : 1 μs
Number of data : 10,000

Fig. Frequency Component

Outline of Test

Materials of Cement Paste and Mortar

Cement(C)	Ordinary Portland Cement	Density : $3.16 g/cm^3$ Specific Surface Area : 3340cm2/g Compressive Strength for 4weeks : $63.5 N/mm^2$
Sand(S)	Silica Sand No.6	Surface-dry Density : $2.62 g/cm^3$ Water Absorption : 0.69% Unit Weight : 1.37kg/ℓ Fineness Modulus : 1.40

Mix Proportion Factor of Mortar

- Sand / Cement ratio(S/C) : 3 levels 1.0, 2.0, 3.0
- Water / Cement ratio(W/C) : 5 levels 20%～60% every10%

Mix Proportion Factor of Cement Paste

- Water / Cement ratio(W/C) : 5 levels 20%～60% every10%

Test Piece : Size 40×40×160(mm), 3 pieces for every condition
Curing : Standard (20℃ in the water)
Measuring Items : Sound Velocity, Compressive Strength

Relations between Sound Velocity Vf and Compressive Strength

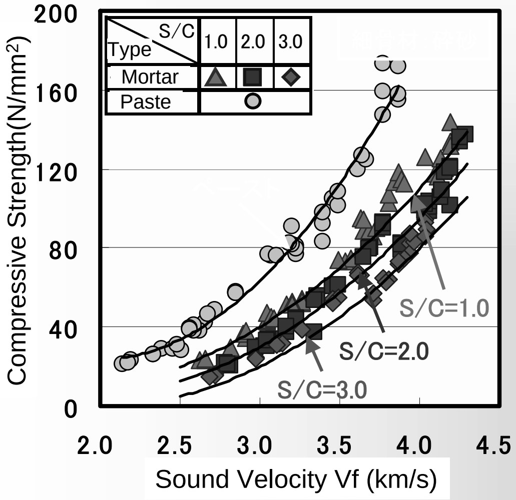

Fig. Sound Velocity – Compressive Strength

Sound Velocity : Vf of Pulsed Electromagnetic Force Acoustic Method ⇨ Fast

Compressive Strength ⇨ High

Relations between Sound Velocity Vf and Compressive Strength

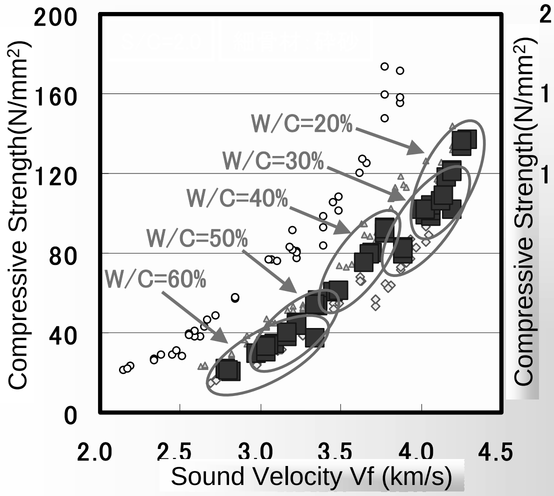

Fig. Effect of W/C

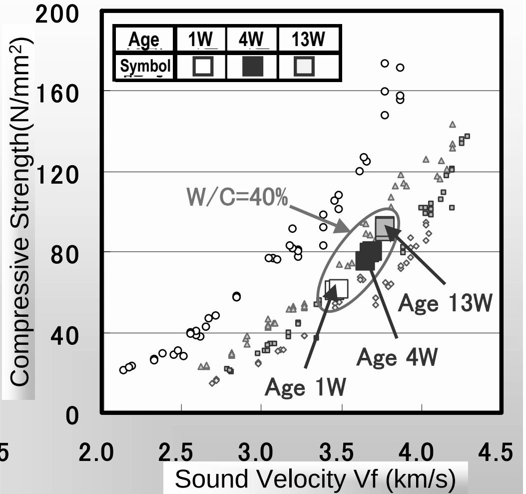

Fig. Effect of Age

W/C and Age : Low ⇨ High

Sound Velocity Vf and Compressive Strength : Low ⇨ High

and Sweep the same line on the each S/C.

Pulsed Electromagnetic Force Acoustic Sound Velocity and Supersonic Sound Velocity

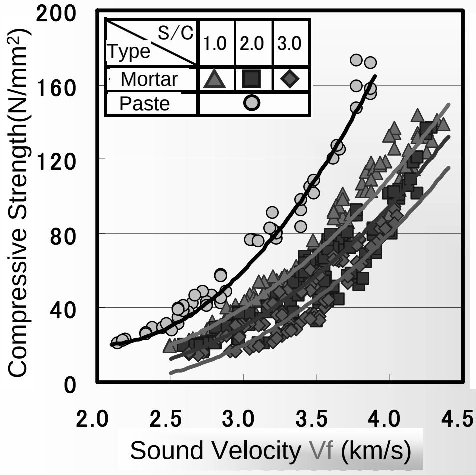

Fig. Pulsed Electromagnetic Force Acoustic Method

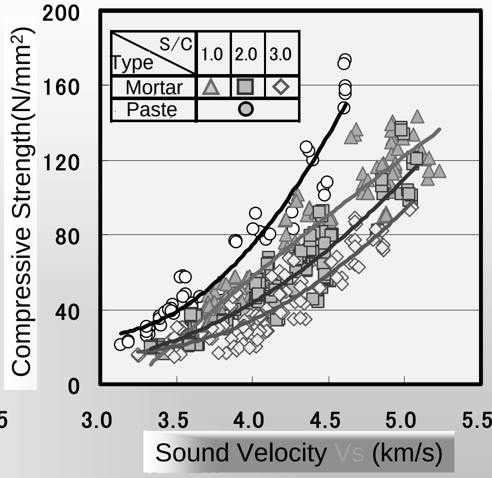

Fig. Supersonic Waves Method

Pulsed Electromagnetic Force Acoustic Sound Velocity Vf	<	Supersonic Sound Velocity Vs

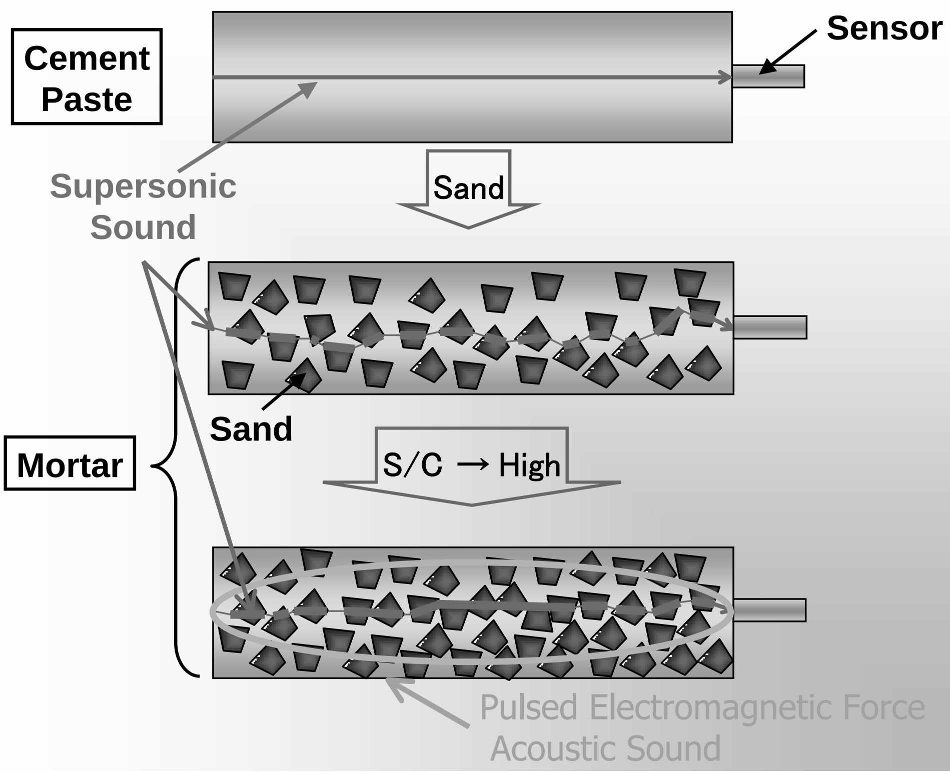

Propagation of Sound in Cement Paste and Mortar

Velocity of Sound :
Velocity of Supersonic : Vs(m/s)
Velocity of Pulsed Electromagnetic Acoustic Sound : Ve (m/s)

- Changing Length of Test Pieces :
  100, 200, 300, 400, 800, 1200 mm
  ➡ Attenuation of Sonic Wave

- Test Pieces with Pores inside :
  Normal, Styrofoam(200mm, 300mm)
  ➡ Propagation of Sonic Wave

Table 1 : Mix Proportion of Cement Paste

	Water	Cement	Air	Total
Weight(kg)	553	1382	–	1935
Volume(ℓ)	553	437	10	1000

※W/C=40% , Air=1%

Table 2 : Mix Proportion of Cement Mortar

	Water	Cement	Sand	Air	Total
Weight(kg)	331	828	1035	–	2195
Volume(ℓ)	331	262	397	10	1000

※W/C=40% , S/C=1 .25 , Air=1%

Attenuation of Sonic Wave

Changing Length of Test Pieces :
100, 200, 300, 400, 800, 1200 mm

Length of Test Piece

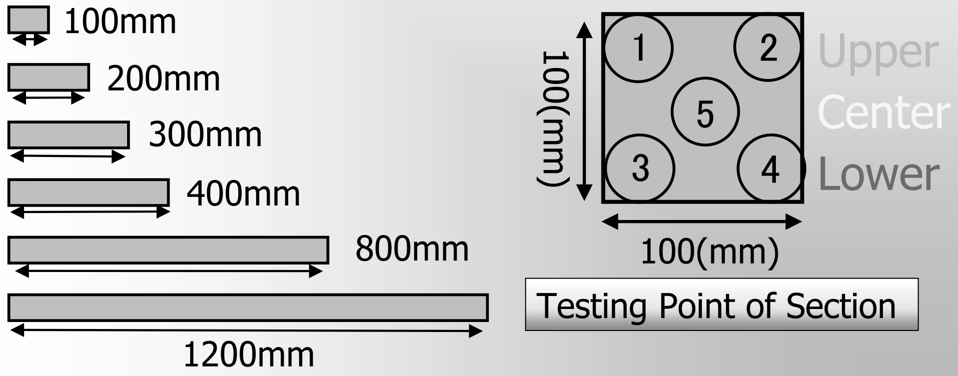

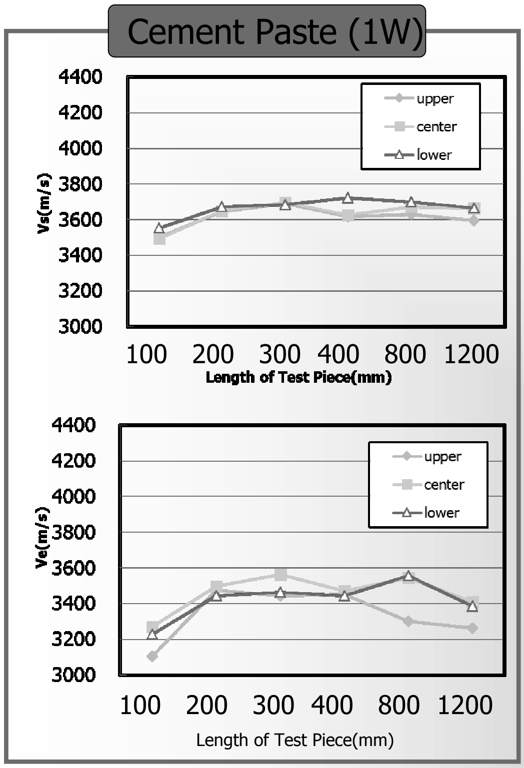

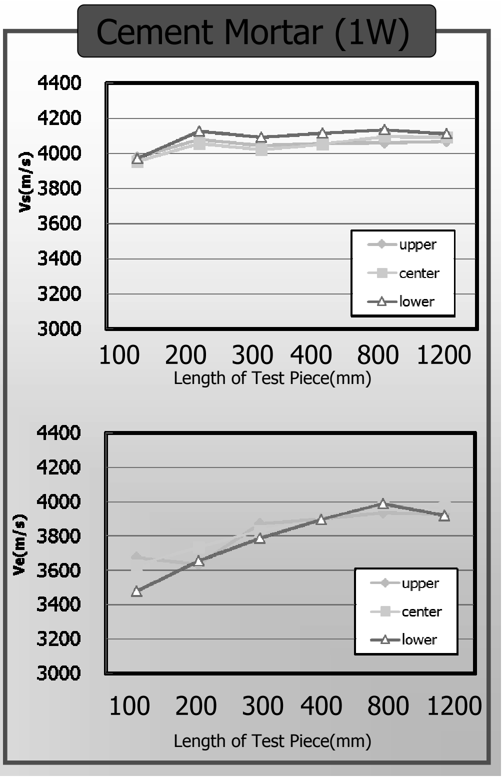

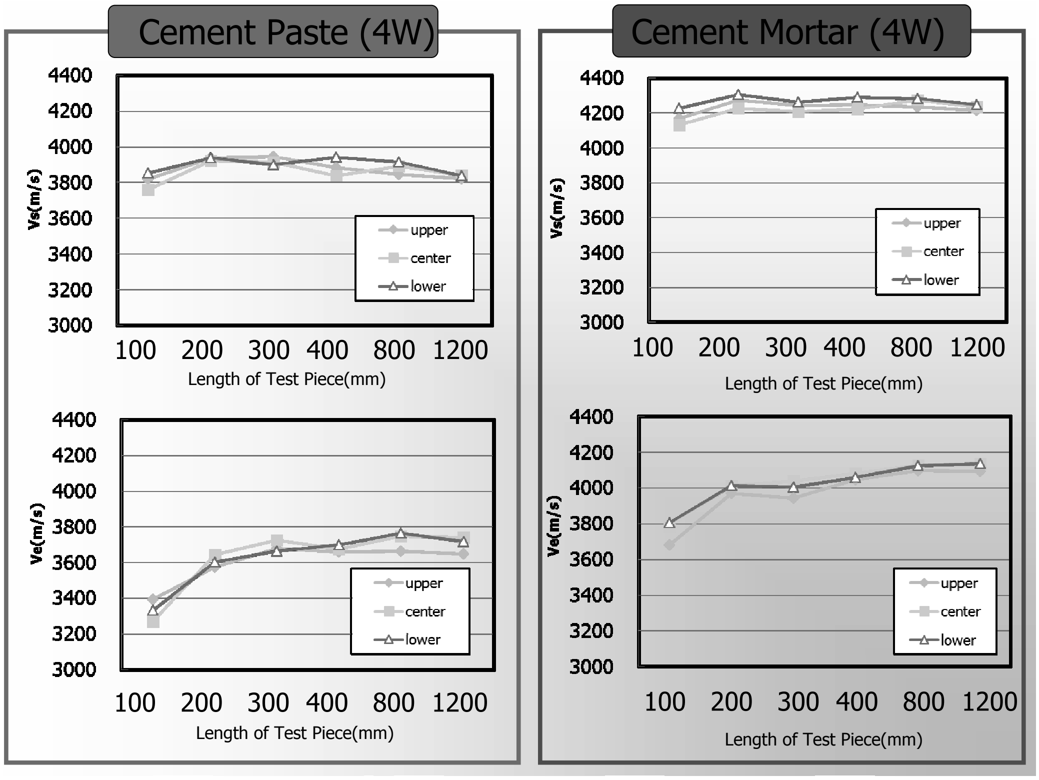

Propagation of Sonic Wave

Test Pieces with Pores inside :
Normal, Styrofoam(200mm, 300mm)

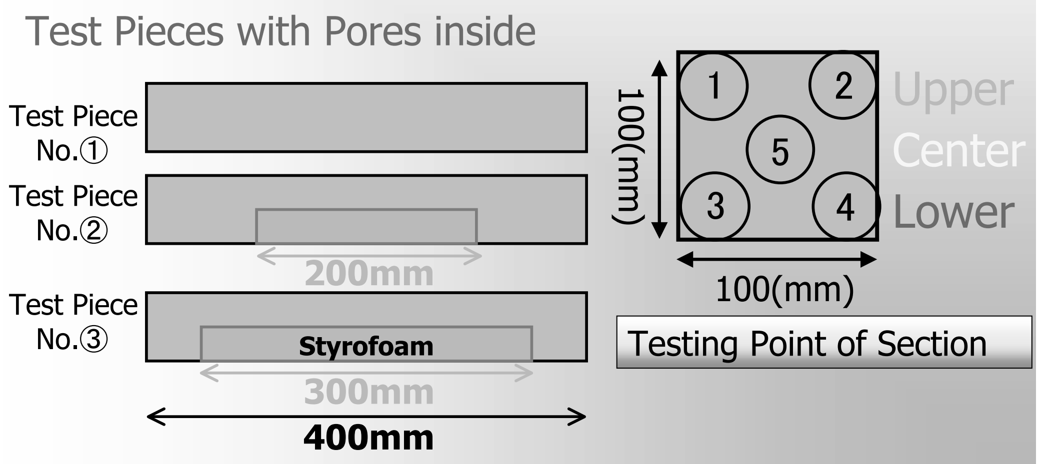

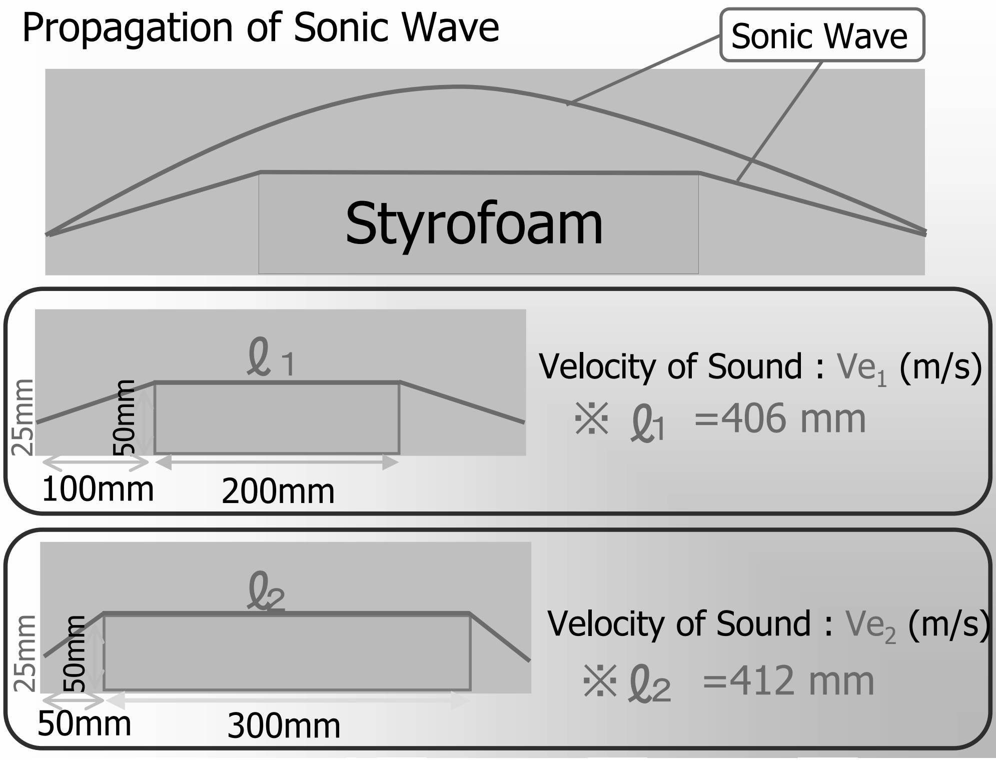

Table 3 : Modified Data of Cement Paste

Test Piece	Testing Point	Vs(m/s)	Vs'(m/s)	Ve(m/s)	Ve'(m/s)
No-Styrofoam	Upper	3777	—	3506	—
	Center	3788	—	3626	—
	Lower	3808	—	3648	—
Styrofoam 200mm	Upper	3800	—	3508	—
	Center	3824	—	3663	—
	Lower	3701	3831	3540	3595
Styrofoam 300mm	Upper	3867	—	3664	—
	Center	3873	—	3695	—
	Lower	3731	3866	3496	3686

Table 4 : Modified Data of Cement Mortar

Test Piece	Testing Point	Vs(m/s)	Vs'(m/s)	Ve(m/s)	Ve'(m/s)
No-Styrofoam	Upper	4223	—	3952	—
	Center	4203	—	4022	—
	Lower	4229	—	4021	—
Styrofoam 200mm	Upper	4207	—	3968	—
	Center	4160	—	3999	—
	Lower	4079	4186	3918	4009
Styrofoam 300mm	Upper	4222	—	3983	—
	Center	4191	—	4034	—
	Lower	4035	4239	3893	4085

※Vs', Ve' : Modified Data

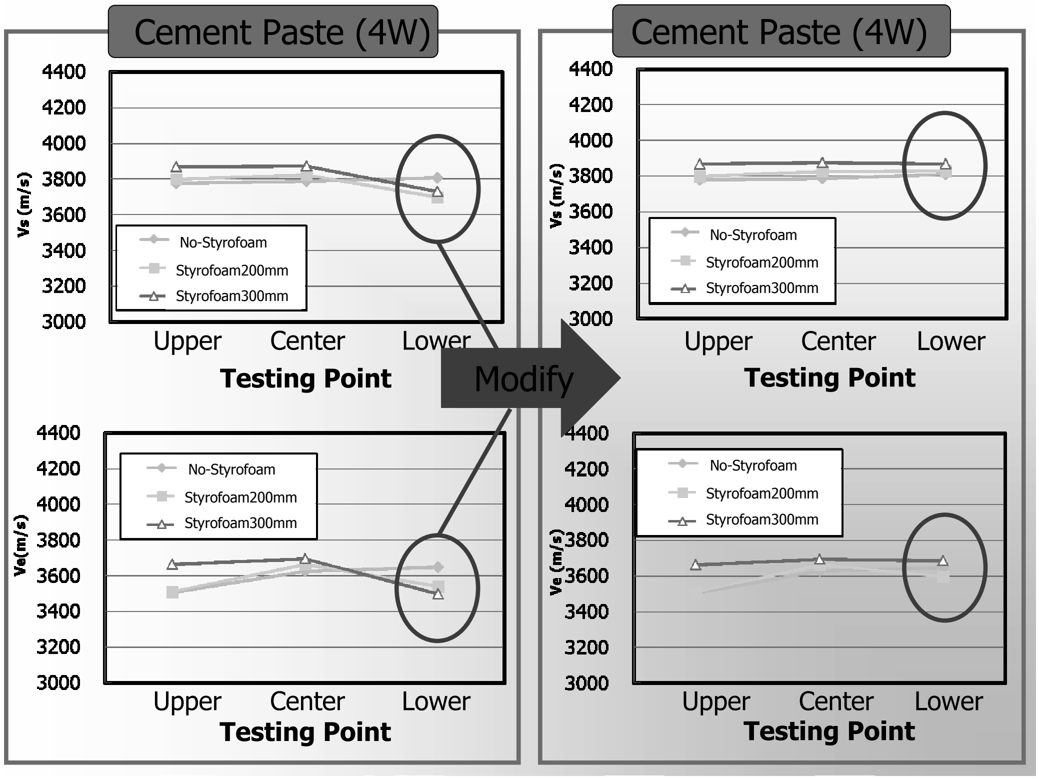
Cement Paste (4W)
Cement Paste (4W)
Modify
Vs (m/s)
Ve(m/s)
Ve (m/s)
4400
4200
4000
3800
3600
3400
3200
3000
No-Styrofoam
Styrofoam200mm
Styrofoam300mm
Upper
Center
Lower
Testing Point

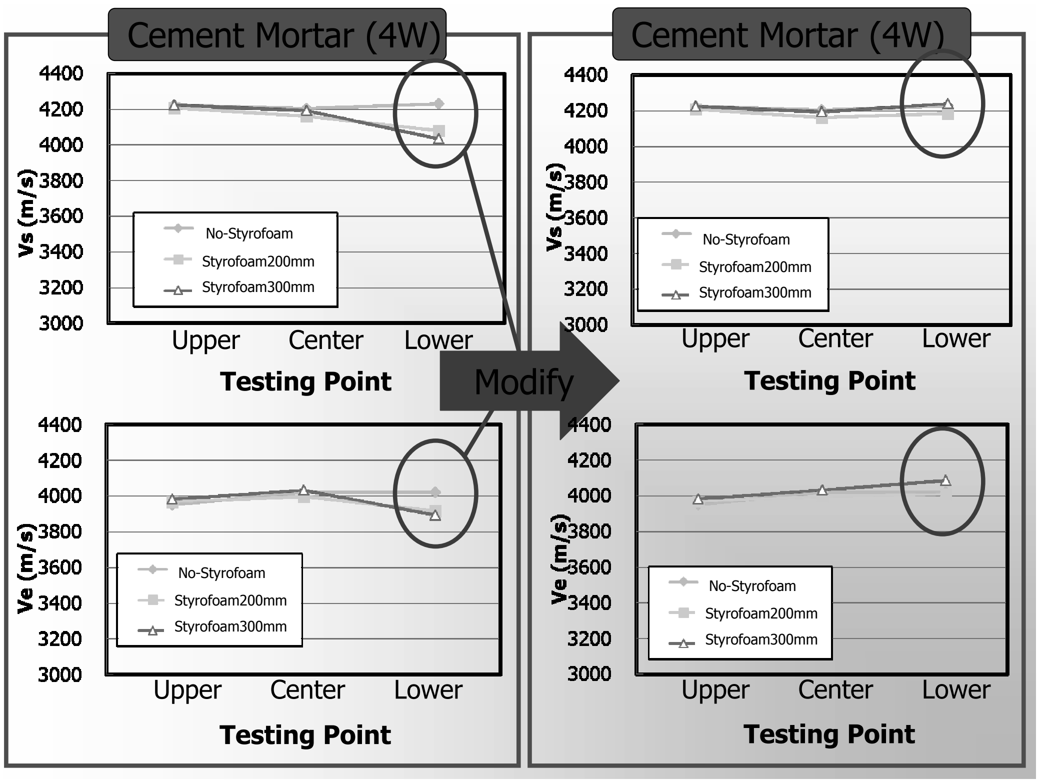
Cement Mortar (4W)
Cement Mortar (4W)
Modify
Vs (m/s)
Ve (m/s)
4400
4200
4000
3800
3600
3400
3200
3000
No-Styrofoam
Styrofoam200mm
Styrofoam300mm
Upper
Center
Lower
Testing Point

Conclucion of the experiments

- The first arrival wave of the ultrasonic one and the electromagetic acoustic pulse one takes the fastest route in the test pieces of the cement paste, the mortar and the concrete.
- In the length less than 1200mm, there is no decay of the speed of the ultrasonic waves nor the electromagetic acoustic pulse ones with respect to the length of test pieces.

Remark 1

For the time being, there does not exist deteminate non-destructive testing method for concrete structures.

It is our new idea to focus on the first arrivel wave and pose a problem for the development of the acoustic CT, which may yield a determinate non-destructive testing method.

Remark 2

It is very important and useful for the development of the acoustic CT that the first arrivel wave would not decay in the test pieces of the length less than 1200 mm.

Problem for the acoustic CT

Problem

Let $\Omega \subset \mathbb{R}^3$ be a domain and $f(x)$, $(x \in \Omega)$ be the propagation speed of the sound. For $\alpha, \beta \in \partial\Omega$, we denote by $\gamma_{\alpha,\beta}$ a route from α to β through Ω. Reconstruct $f(x)$ $(x \in \Omega)$ out of the data $\min_{\gamma_{\alpha,\beta}} \int_{\gamma_{\alpha,\beta}} 1/f(x)d\gamma$, for $\forall \alpha, \beta \in \partial\Omega$.

Some Problems

- It is impossible to reconstruct the information of some points x's where f(x)'s are very small.

  → It does not matter very much.

- It is an interesting problem to determine the optimal subset of reconstructible by the acoustic CT.

Application 1

- Non-destructive testing of the expressway bridges over the oceans.

  → We have to detect the 2 to 3 kg of salt included in the 1 m^3 of concrete.

Our homework

It is our homework to study whether it is possible to detect the 2 to 3 kg of salt in the 1 m^3 of concrete,

for which we shall conduct other experiments.

Application 2

- Non-destructive testing of RC structures.

  → It may be possible to detect the corroded steel in RC structures.

Remark

It is very important to develop the study of the Applications 1 and 2, especially in view of redevelopment of infrastructures.

Conclusion

- For development of the acoustic CT, we studied how the first arrival wave propagates in the cement paste and the mortar.
- Applying the property of the first arriving wave, we have posed a problem for the development of the acoustic CT.

Conclusion (continued)

- The acoustic CT for concrete structure may be the first determinate non-destructive testing method for concrete structures.
- The problems posed in this study are interesting in view of the study of mathematics.

Modeling of atmospheric- and underground migration of radionuclides in the 100 km vicinity of Fukushima

Hiroyuki Ichige*, Inryo Kou*, Yuko Hatano*, University of Tsukuba

Abstract

In the field of nuclear engineering, there are a lot of problems with regard to environmental pollution. After the Fukushima accident, long-term behavior of the air- and soil concentration of radionuclides are of social interest. The problem is that we have limited tools for predicting the their behavior over a long period of time. In the present paper, we explain some of the tools currently available.

1 Introduction

In major nuclear power plant accidents, such as Chernobyl or Fukushima, a huge amount of radionuclides have been released into the atmosphere. In such accidents, long-lived radionuclides, ceasium-137 and strontium-90, for example, pose a serious problem. Radionuclides carried in the initial plume were deposited on the ground, and they keep imposing a risk to the public health for a long period of time. Therefore, it is very important to understand and predict the long-term behavior of radionuclides both in the atmosphere and underground. The problem is that, tools that we can use to cope with the long-term problem are limited. Indeed, we do have a major model for assessment, called as the box model or the compartment model; they are consisted with connected modules indicating the pathways of radionuclides in the environment. The transport from one module to another is described by a rate constant and we have to measure all the values of these constants which consume us a lot of time and trouble. Any mathematical approach, if available, would be very helpful for this problem. In this paper, we describe the problems of radionuclides (a) in the atmosphere and (b) in the soil, then explain our approach.

2 Atmospheric Radionuclides

Radionuclides in the air pose a risk of inner exposure of radiation[1], because inhalation of radionuclides leads to deposition on the lungs and they may cause lung cancer. The seriousness of health damage of inner exposure is usually much higher than that of external exposure[2] under the same amount of exposure, thereby the aerosol concentration of radionuclides is an important issue of the society. The "resuspension[3]" process is believed

*1-1-1 Tennodai, Tsukuba, Ibaraki 305-8573, hatano@risk.tsukuba.ac.jp

[1]「内部被曝」 体内に放射性物質を摂取することによる

[2]「外部被曝」 体の外側から放射線を浴びることによる

[3]「再浮遊」

the most significant source of the long-term aerosol risk. Resuspension is re-floating of particles from the ground surface due to the wind. Once an dust particle (with ceasium attached) is uplifted by wind from the ground, it stays in the air for a while, and is deposited on the ground again due to rainfall or the gravity or downward winds. Such a cycle of resuspension-deposition keeps the air concentration high. Indeed, in the Chernobyl case, it is shown that the resuspension-deposition cycle contributes significantly to the airborne concentration of radionuclides (Klug et al.,1992; Ishikawa, 1995; Nicholson, 1998; Ould-Dada and Baghini, 1992) and health effects on the humans, such as leukemia and genetic abnormalities have been confirmed (IAEA, 2006; Arkhipov et al., 1994; Lazjukd et al., 1997; Romanenko et al., 2008).

In our studies (Hatano and Hatano, 1997; Hatano et al., 1998; Hatano and Hatano, 2003; Ichige et al., 2015), we used a stochastic differential equation for the atmospheric concentration of nuclides as follows. For the atmospheric part,

$$\frac{\partial}{\partial t}\int_{0[m]}^{1000[m]} C_1(t,x,y,\hat{z})d\hat{z} = -v(x,y)\frac{\partial}{\partial \mathbf{x}}\int_{0[m]}^{1000[m]} C_1(t,x,y,\hat{z})d\hat{z}$$

$$-\lambda_{down}\int_{0[m]}^{1000[m]} C_1(t,x,y,\hat{z})d\hat{z} + \lambda_{up}(t)\int_{0[cm]}^{0.5[cm]} C_2(t,x,y,z)dz. \qquad (1)$$

Here C_1 is the atmospheric concentration of a specific nuclide [Bq/m^3]. The horizontal direction is denoted as x, y and the vertical direction as $\hat{z}$. The north-south is y-direction, and east-west is x direction. Since the concentration in the stratosphere is little enough that we assume the 1000 meters of the height to consider. Explanation of other variables are in the following.

For the ground-surface exchange part,

$$\frac{\partial}{\partial t}\int_{0[cm]}^{0.5[cm]} C_2(t,x,y,z)dz = \lambda_{down}\int_{0[m]}^{1000[m]} C_1(t,x,y,\hat{z})d\hat{z}$$

$$-\lambda_{up}(t)\int_{0[cm]}^{0.5[cm]} C_2(t,x,y,z)dz. \qquad (2)$$

The soil part is as follows.

$$\frac{\partial C_2(t,x,y,z)}{\partial t} = k\frac{\partial^2 C_2(t,x,y,z)}{\partial z^2} - w\frac{\partial C_2(t,x,y,z)}{\partial z}. \qquad (3)$$

$$C_2(0,x,y,z) = \exp(-\frac{z}{h}). \qquad (4)$$

$$k\frac{\partial C_2(t,x,y,0)}{\partial z} + wC_2(t,x,y,0) = 0. \qquad (5)$$

Equation (2) is a model of the surface migration of nuclide and C_2 is the surface concentration [Bq/kg-soil], λ_{down} is the deposition rate from the air to the ground, λ_{up} is the resuspension rate. In this model, we assume that the resuspended particles should

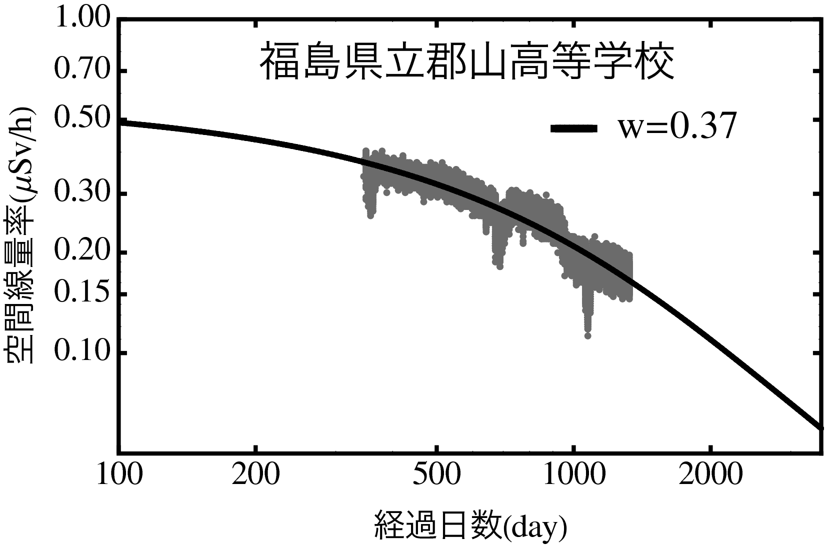

Figure 1: Dose rate at Kouriyama High School.

be within the depth of 0.5cm from the surface. The wind velocity v governs the advection of nuclides. Equation (3) is a model for the migration in the soil. When the nuclides migrates into deep in the soil, the covering soil decrease the radiation, hence the process needs consideration. The constant w is the velocity of infiltration into the soil depending on the conditions of each site, and k is the diffusion coefficient, and h is also a site-specific constant. Equations (4) and (5) are the initial condition and the boundary condition, respectively.

Estimating parameters k, h, v and $\lambda_{up,down}$ in these equations from available data, we obtain the numerical solution of the above equations. We compare the results with the Fukushima data. Only the constant w is determined through the fitting of the actual dose rate. In Fukushima, many sites measure only the dose rate (μSv/hour). Very small number of site has the data in the unit of Becquerel. Therefore, we had to convert the data in Becquerel into the air dose rate, following the method of IAEA-TECDOC-1162. Figures 1$\sim$18 show the results. The significant dropped parts in the dose rate are the days of snowfall or rainfall. Due to the shielding effect of snow coverage (or water coverage), the air dose rate becomes lower. At the sites of low dose areas (the initial dose is less than 1 μSv/hr), the fitting might not so good, but overall results are, we think so far, satisfactory. However, these are "point data". Measured sites are treated as "points" in this research. It is a future problem how we can extrapolate the results to "area"s.

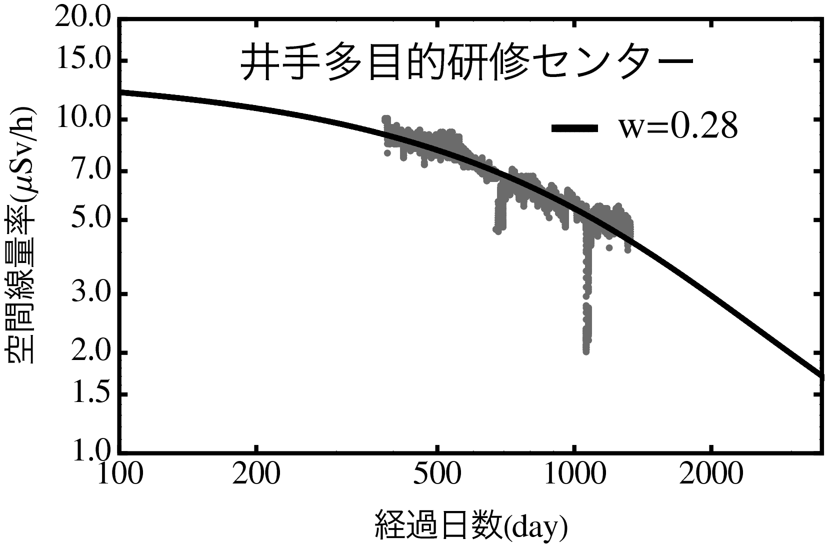

Figure 2: Dose rate at Ide Community Center

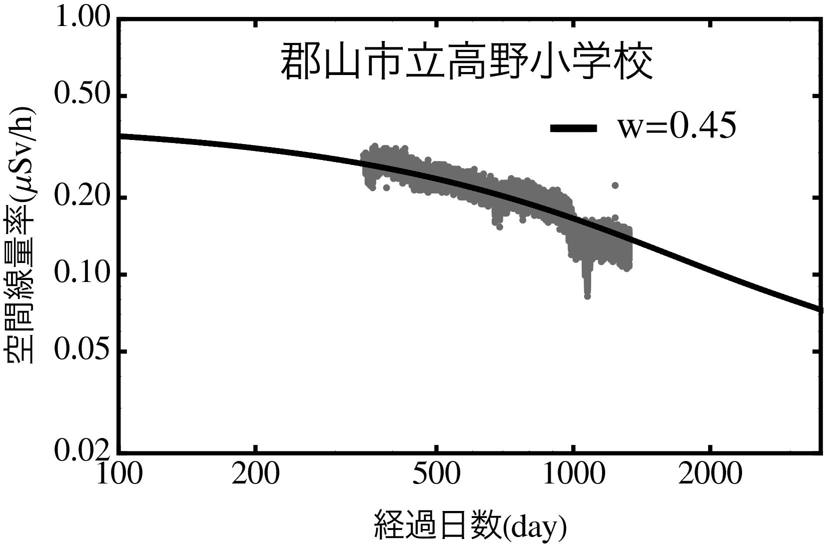

Figure 3: Dose rate at Takano Elementary School.

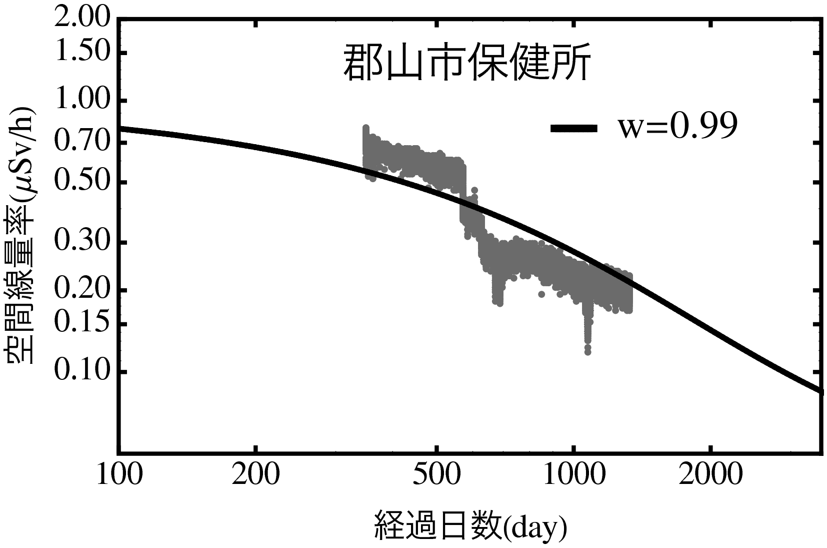

Figure 4: Dose rate at Kouriyama City Health Center.

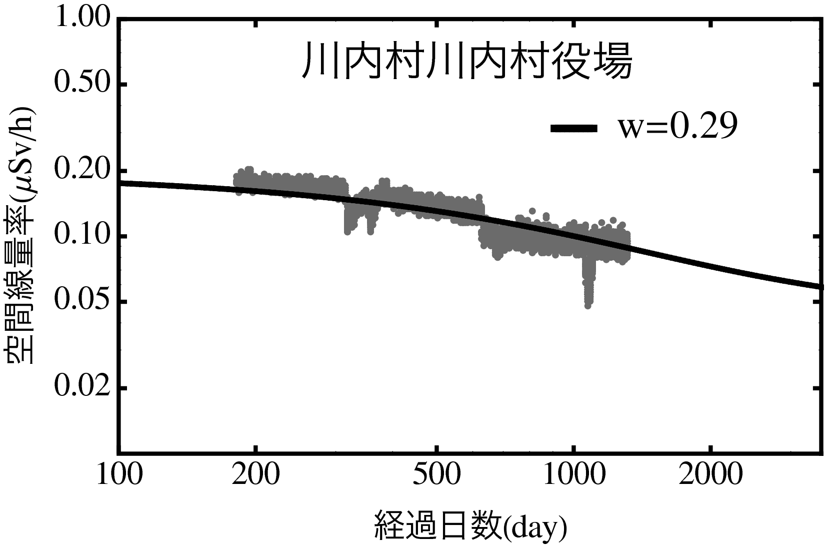

Figure 5: Dose rate at Kawauchi Village Hall.

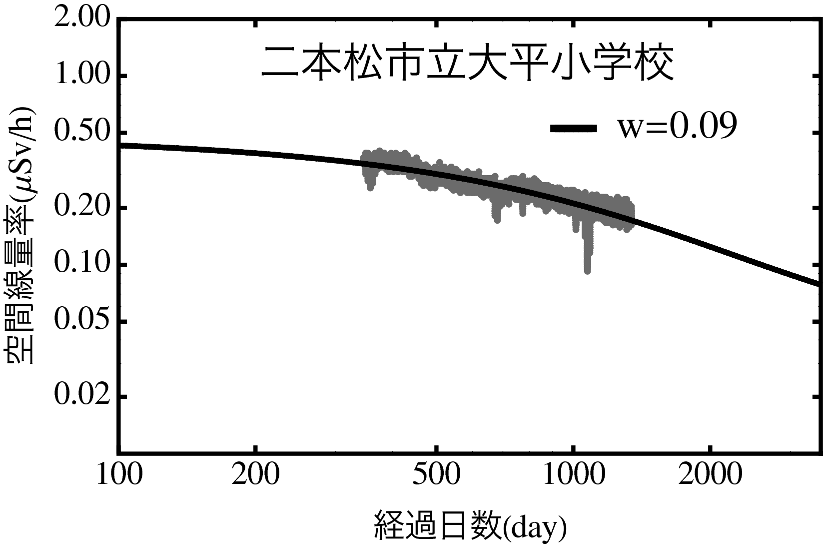

Figure 6: Dose rate at Oodaira Elementary School, Nihonmatsu City.

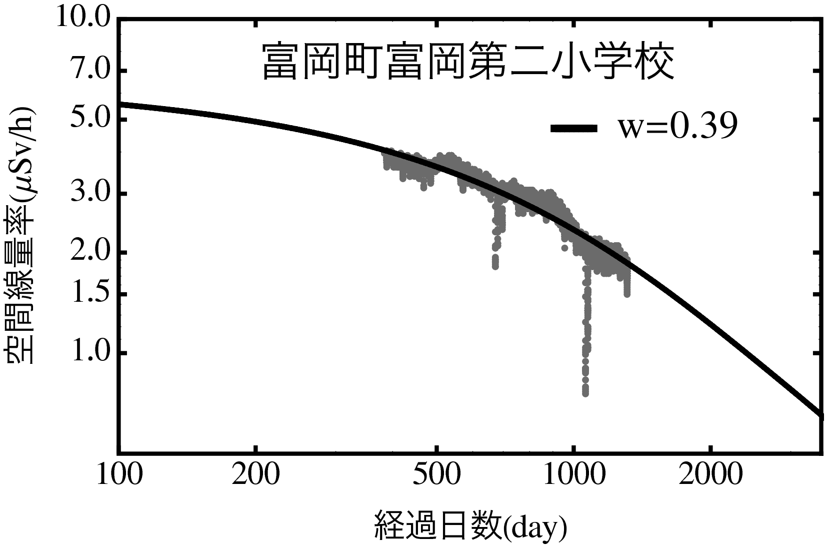

Figure 7: Dose rate at Tomioka 2nd Elementary School.

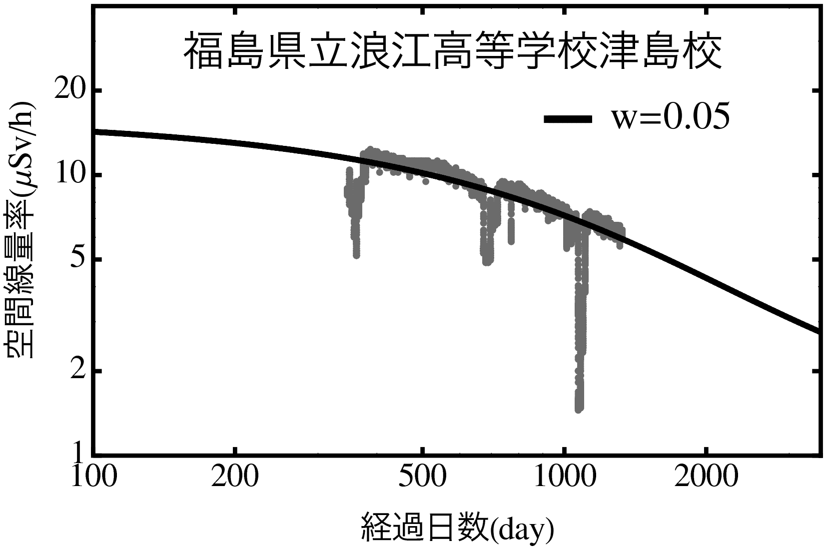

Figure 8: Dose rate at Namie High School, Tsushima part.

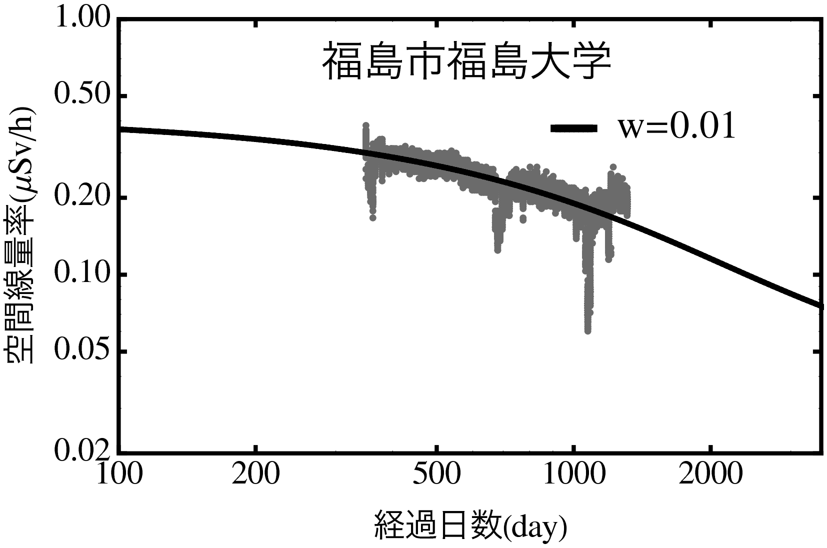

Figure 9: Dose rate at Fukushima University.

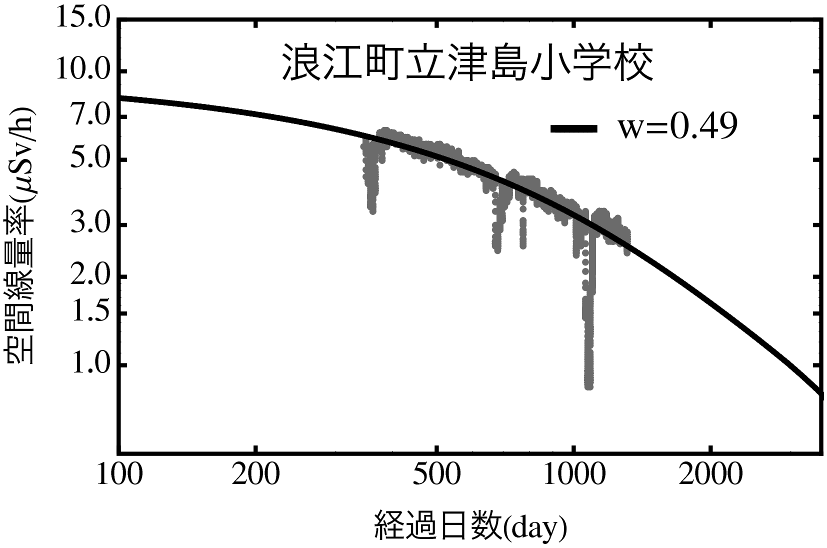

Figure 10: Dose rate at Tsushima Elementary School, Namie Town.

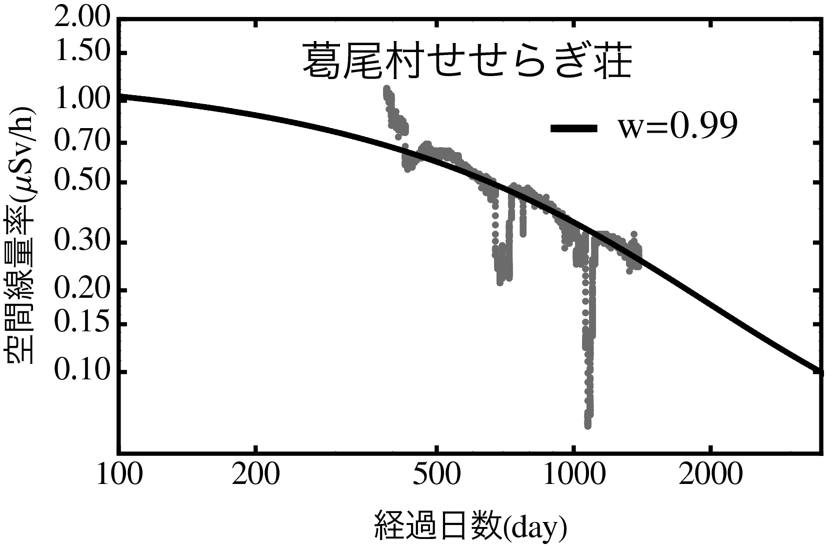

Figure 11: Dose rate at Seseragi House, Katsurao Village.

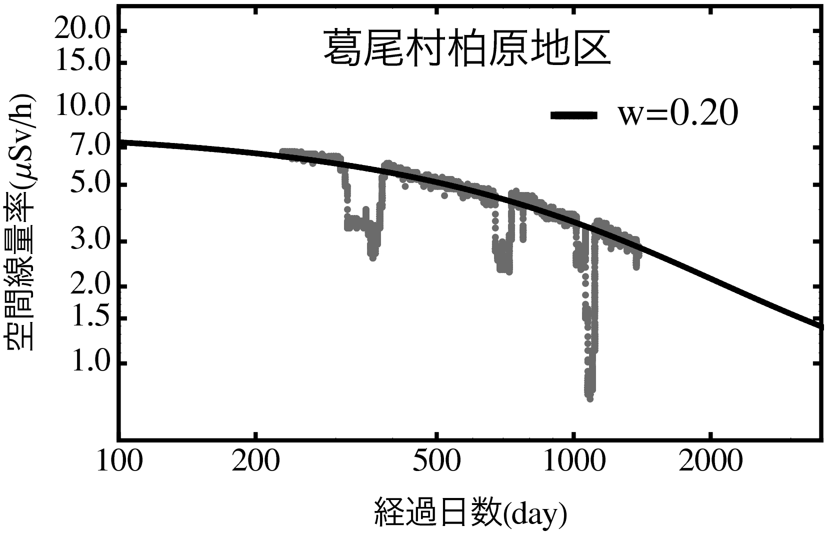

Figure 12: Dose rate at Kashiwabara, Katsurao Village.

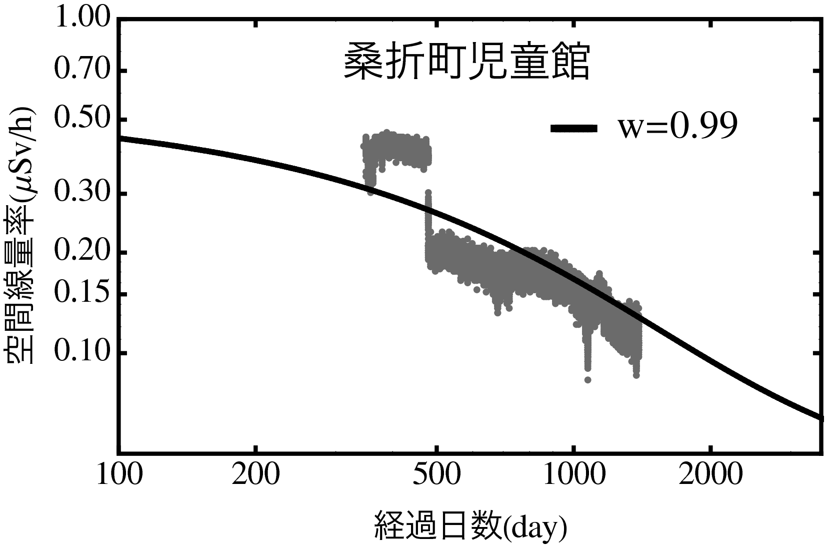

Figure 13: Dose rate at Children's House, Koori Town.

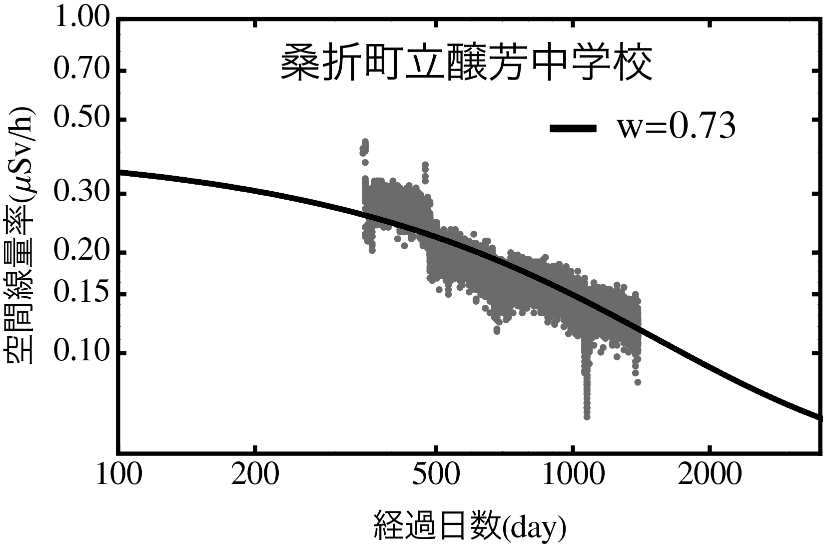

Figure 14: Dose rate at Joho Junior High School, Koori Town.

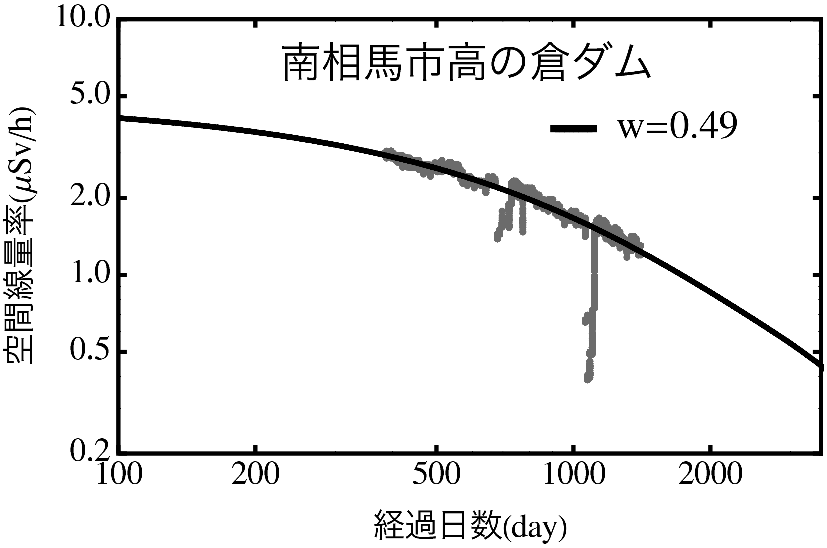

Figure 15: Dose rate at Kura Dum, Minami-Soma.

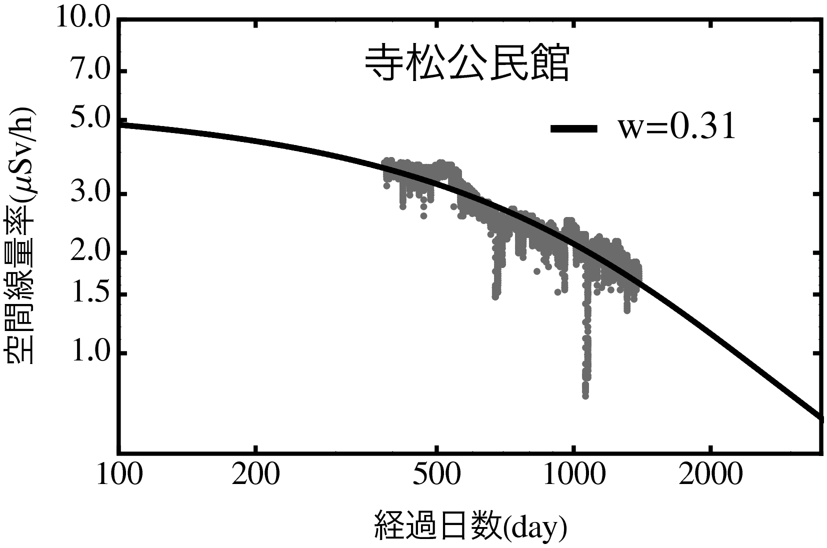

Figure 16: Dose rate at Teramatsu Community Center.

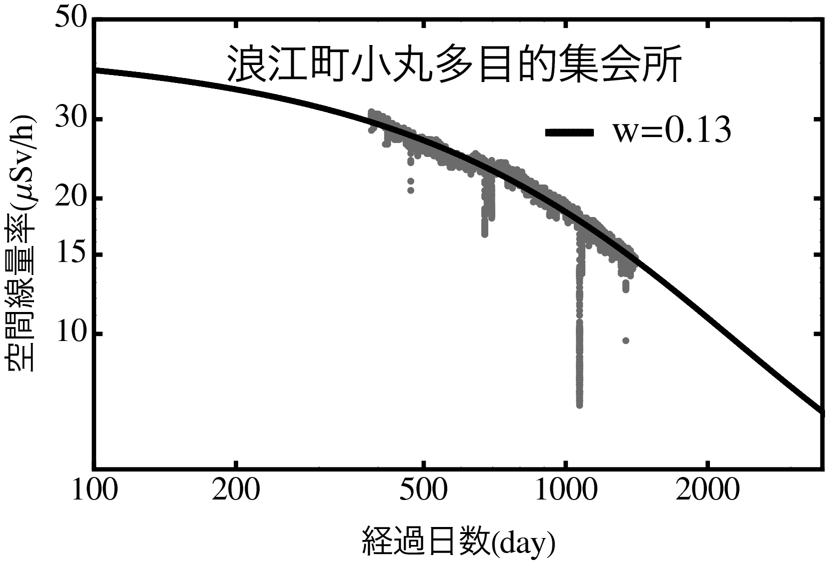

Figure 17: Komaru Community Center, NamieTown.

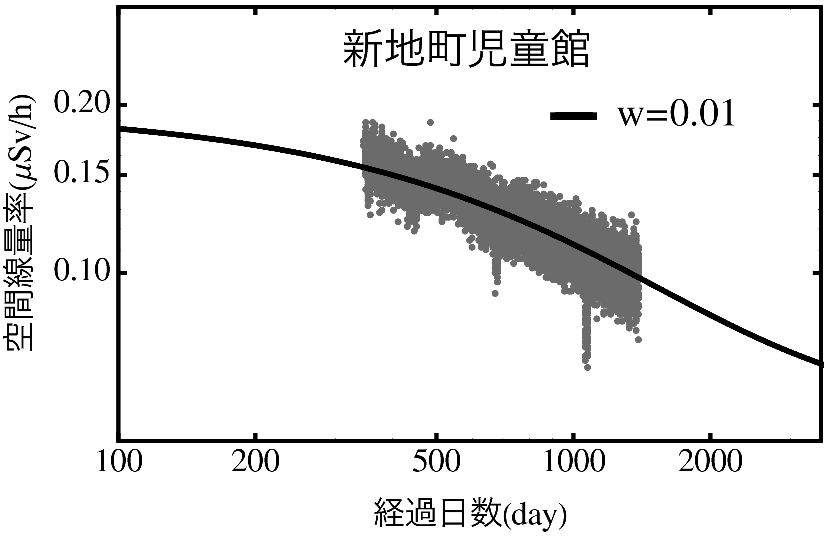

Figure 18: Dose rate at Children's House, Shinchi Town.

3 Radionulides in the soil and their model in porous media

In the previous section, we explained how the atmospheric concentration of radionuclides lingers for a long time, even a decade. In the case of soil contamination, it is worse. Even after 50 years of nuclear tests in the US and the former Soviet Union, we can measure the evidence, traces of radionuclides of fission products, in rivers and streams in Japan. As such, migration in underground is a very long-term problem.

In the problem of transport in porous media, a model called as the Continuous-Time Random Walk (CTRW) has been developed. The original motivation to introduce this model is that the real experimental data does not fit the classical Advection-Dispersion Equation (ADE; the heat equation with the convection term) and searched for a new model to find CTRW. It was developed in order to describe electron transport in a semi-conductor and is a kind of random-walk model with the distribution of waiting time between jumps. Many experiments, both in laboratory scale and field scale, have been shown to follow the CTRW model (Berkowitz and Scher, 1995; Hatano and Hatano, 1998; Bijeljic et al., 2011). When an asymptotically power law is chosen as the waiting-time distribution, the significance of CTRW emerges, and the experimental results (that have not been reproduced by ADE) agree very well with CTRW. We expect that the model may be useful in long-term predictions, because of the power-law characteristics of CTRW. When a power law function, for example, $K(t) = t^{-4/3}$ is plotted against t with the unit of day, the graph is exactly the same shape as when plotted with the t unit of month or year. That is the reason for our interest in the CTRW model.

Up until today, CTRW seems successful. However, there is a big issue in the model: values of parameters in the model cannot be determined a priori. Namely, the values of model parameters cannot be determined until actual measurement data are available. This means that a "pure" prediction is not possible yet. Of course, ADE has the same problem, but we find it interesting (and useful) to connect the values of those model parameters with the characteristics of flows in porous media.

In the present paper, we explain our trial seeking the value of α. It is the index of the waiting time distribution $\psi(t) \sim t^{-\alpha}$ of the CTRW model. It defines the distribution of the waiting time before a random walker takes each jump. We actually measure the velocity in the pores of porous media and thereby obtain the waiting-time distribution. We developed a new technique LAT-PTV method. We use a new method LAT-PTV, the Particle Tracking Velocimetry (PTV) combined with the Laser-Aided Tomography (LAT), originally developed by Matsushima Group (Konagai et al., 1992; Saomoto et al., 2007).

3.1 Experimental Method

We show in Fig. 19 the experimental setup of LAT-PTV. The acrylic container is 135 mm x 135 mm x 450 mm and the illumination beam is created by the laser (Melles Griot 58-GS-305, Nd:UVO 4). The images are taken by CCD camera (Canon EOS-40D) with the frame rate 1 per second. The microparticles for tracking is shown in Fig. 20 (Thermo Scientific, Fluoro-Max green fluorescent polymer microspheres). The PTV computer program is of the ICCRM method (Brevis et al., 2011). Two types of silicon oils (Shin-Estu Kagaku, HIVAC F-4 and KF-56) is mixed in order to match the reflection index of the glass 1.514. The peristatic pump (EYELA, MP-1000) is used for the circulation of the fluids. The acrylic container is filled with spheres (Fig. 21) or irregular-shaped particles (Fig. 22). The image of sphere particles immersed in silicon oil is shown in Fig. 23. Other experimental condition is given in Table 1.

Table 1: Experimental conditions of LAT-PTV.

	Run A	Run B	Run C	Run D	Run E	Run F
Shape	Sphere	Sphere	Sphere	Irregular	Irregular	Irregular
Size	7mmϕ	7mmϕ	7mmϕ	$5 \sim 7$ mm	$5 \sim 7$ mm	$5 \sim 7$ mm
Porosity	0.53	0.58	0.53	0.62	0.62	0.62
Flow rate(ml/h)	445	1358	1920	373	918	2571
mean v_z (mm/s, PTV)	0.011	0.014	0.014	0.011	0.014	0.030
mean v_z (mm/s, Pump)	0.013	0.035	0.055	0.009	0.023	0.063

3.2 Experimental Results

We measured the velocity of the silicon oil by tracking the polymer particles and found that the velocity in the pore distributed as Fig. 24. The velocity in sphere-particles media (Run A, B, C) has rather compact distribution compared with irregular-particles media (Run D, E, F). In Run A, B, and C, when we increase the flow rate, the distribution, on the whole, rather shifts to the right. In contrast, in Run D, E, and F, the shape of the distribution seems to change; in high flow-rate case, high-speed components are append to the profile of the low flow-rate case. This may be due to the variations of pore size. In Run D, E, and F, the pore shapes likely have more variation than Run A, B, and C. Silicon oil may have made itself through in wider pores of the media.

Figures 25, 26 and 27 are our preliminary results of estimating the waiting time $\psi(t)$ and its comparison with probability distributions. For simplicity, we assume that the waiting time is proportional to the inverse of the velocity at a specific time. We made the histogram of Fig. 24 divided into much smaller bins (every 0.0001 mm/s) and disregard the velocities less than 0.0001 mm/s. They are considered to be staying still on the glass surfaces. We tried the normal distribution, the exponential distribution, and the gamma distribution as the candidate for our fit (Figs. 26, 27). The gamma function, as follows, seems most successful.

$$f(t) = \frac{1}{\Gamma(\alpha+1)\theta^{\alpha+1}} t^{\alpha} e^{-t/\theta}, \tag{6}$$

for $\alpha > -1, t > 0$. The values of α are approximately from 5 to 7. The sphere cases, Run A, B, and C have $\alpha = 5.3$, 5.2 and 4.8, respectively. On the other hand, the irregular cases, Run D, E, and F, it was 7.2, 7.2, and 5.2. The irregular cases apparently have larger value of α. The values of θ are around 300 for all the cases. An interesting fact is that some researchers (Berkowitz-Scher group) have been proposing the waiting time function of CTRW to be of the form of the gamma function (but the range of α is different in our case from theirs). We think that it needs more considerations in converting the velocity into the waiting time.

3.3 Summary

In the present paper, we explained the problems of radionuclides due to the Fukushima accident and explain the methods we are currently developing. It seems that our model is satisfactory in reproducing the air dose rate in Fukushima. However, further research should be done for more confident predictions. In the research of soil pollution, we are still struggling in fixing the values of the model parameter. Further research is needed until the CTRW model becomes applicable to real problems.

Aids from the field of inverse problems

For the pollution due to the Fukushima accident, what we want to do is as follows:
(1) Estimating the values of parameter from existing data
(2) Making predictions, or evaluation of the degree of decontamination[4], using (1).
Therefore, precise estimation of those parameters is very important. Also, discussions on the scientific soundness of our model would be appreciated from the point of view of mathematicians.

References

Arkhipov, N.P., Kuchma, N.D., Askbrant, S., Pasternak, P.S., Musica, V.V.: Acute and long-term effects of irradiation on pine (Pinus silvestris) stands post- Chernobyl. Sci. Total Environ. 157, 383-386, 1994.

Bijeljic, Branko, P. Mostaghimi, and M. J. Blunt: Signature of Non-Fickian Solute Transport in Complex Heterogeneous Porous Media, PRL 107, 204502, 2011.

IAEA, ENVIRONMENTAL CONSEQUENCES OF THE CHERNOBYL ACCIDENT AND THEIR REMEDIATION: TWENTY YEARS OF EXPERIENCE, Report of the Chernobyl Fo- rum Expert Group ‘ Environment ’, 2006.

Klug, W., Graziani, G., Grippa, G., Pierce, D., Tassone, C.: Evaluation of Long Range Atmospheric Transport Models Using Environmental Radioactivity Data from the Chernobyl Accident. Technische Hochschule Darmstadt, Darmstadt, Germany, 1992.

Konagai, K., Tamura, C., Rangelow, P. and Matsushima, T.: Laser-Aided Tomography: A Tool for Visualization of Changes in the Fabric of Granular Assemblage, Structural Engineering/ Earthquake Engineering, Vol.9, No.3, pp.193s-201s, JSCE, 1992.

Ichige, H., Fukuchi, S., Hatano,Y., Stochastic model for the fluctuations of the atmospheric concentration of radionuclides and its application to uncertainty evaluation, Atmospheric Environment, 103, 156-162, 2015.

Ishikawa, H., Evaluation of the Effect of Horizontal Diffusion on the Long-Range Atmospheric Transport Simulation with Chelnobyl Data, journal of Applied Meteorology, 34, 1653- 1665, 1995.

[4]「除染」

Hatano, Y., Hatano, N., Ueno, T., Amano, H., Sukhorchkin, A.K., Kazakov, S.V., Aerosol migration near Chernobyl: long-term data and modeling, Atmospheric Environment, 32, 2587- 2594, 1998.

Lazjukd, G.I., Nikokaevi, D.L., Novikova, I.V.: Changes in registered congenital anomaliesin the republic of belarus after the chernobyl accident. Stem Cells 15, 255e260. http://dx.doi.org/10.1002/stem.5530150734, 1997.

Nicholson, K. W., A review of particle resuspension Atmospheric Environment, 22, 2639-2651, 1988.

Ould-Dada, Z., Baghini, Nasser M.: Resuspension of small particles from tree surfaces. Atmos. Environ. 35, 3799-3809, 2001.

Romanenko, A.Y., Finch, S.C., Hatch, M., Lubin, J.H., Bebeshko, V.G., Bazyka, D.A., Gudzenko, N., Dyagil, I.S., Reiss, R.F., Bouville, A., Chumak, V.V., Trotsiuk, N.K., Babkina, N.G., Belyayev, Y., Masnyk, I., Ron, E., Howe, G.R., Zablotska, L.B.: The Ukrainian-American study of leukemia and related disorders among Chornobyl cleanup workers from Ukraine: III. Radiation risks. Radiat. Res. 170, 691e697. http://dx.doi.org/10.1667/RR1403.1, 2008.

Rosner G., R. Winkler, Long-term variation (1986-1998) of post-Chernobyl 90 Sr, 137 Cs, 238 Pu and 239,240 Pu concentrations in air, depositions to ground, resuspension factors and resuspen- sion rates in south Germany, The Science of the Total Environment, 273, 11-25, 2001.

Saomoto, H, Matsushima, T., Yamada, Y.: Development of LAT-PIV visualization technique for particle-fluid system, Structural Eng./Earthquake Eng., JSCE, 24,2, 123s-130s, 2007.

Acknowledgement

The authors are thankful to Dr. Takashi Takiguchi for helpful discussions during the IMI conference.

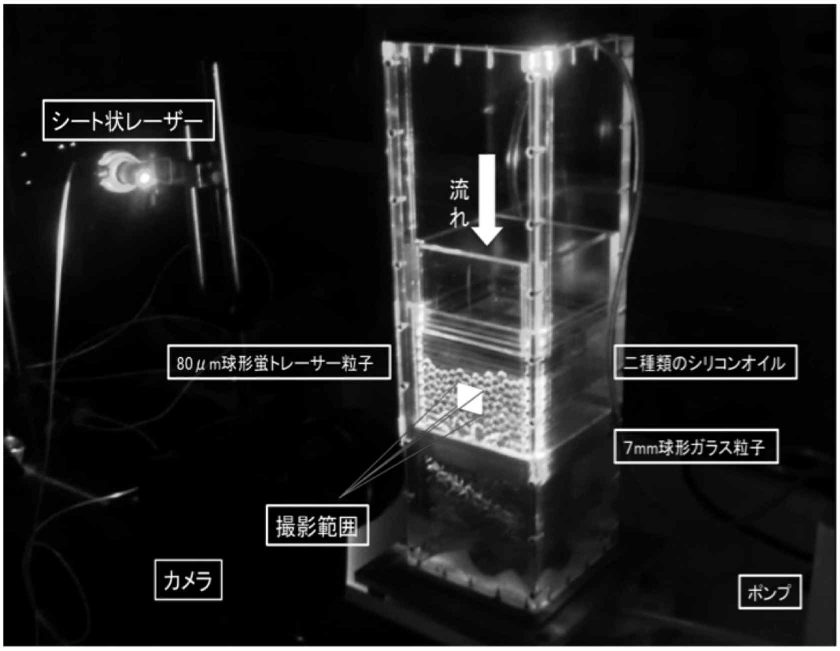

Figure 19: Experimental setup of LAT-PTV method.

Figure 20: PTV particles. 80 μm diameter fluorescent polymer microspheres.

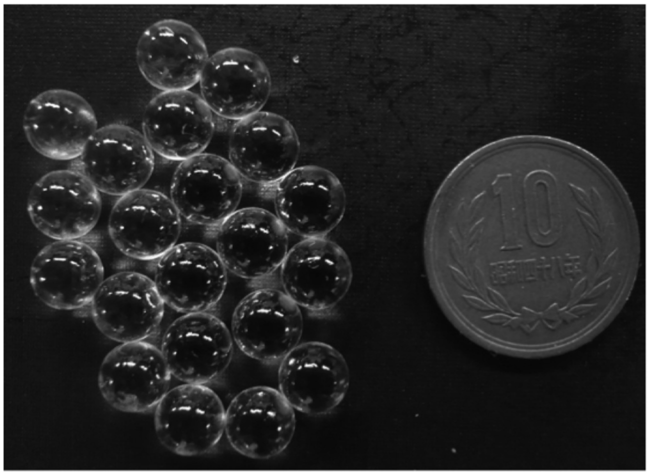

Figure 21: Filling material, sphere particles made of BK-7 glass.

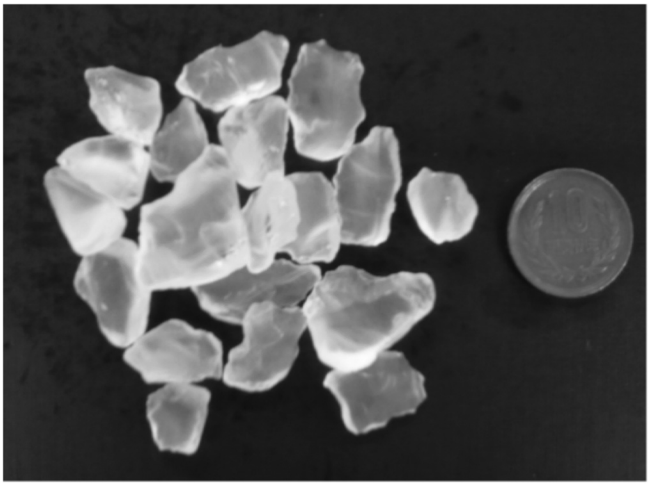

Figure 22: Filling material, irregular-shaped glass.

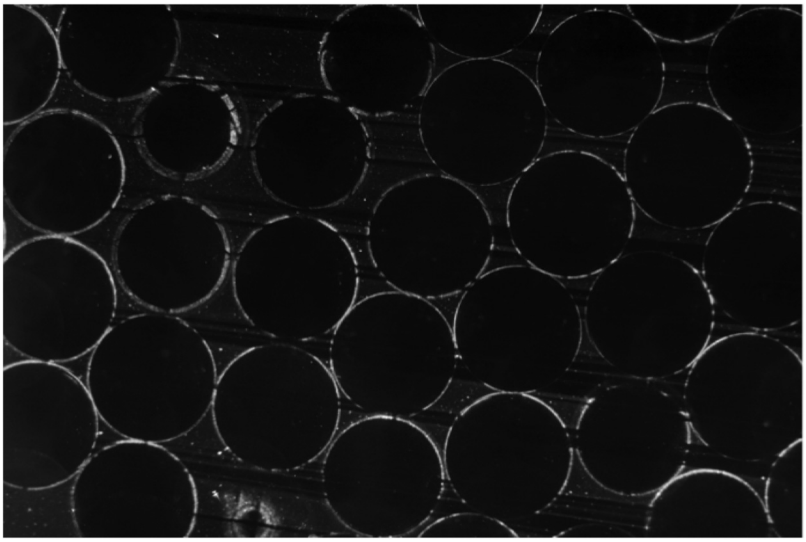

Figure 23: A sample image from LAT-PTV. Sphere particles are immersed in silicon oil, showing their outlines by the green laser light.

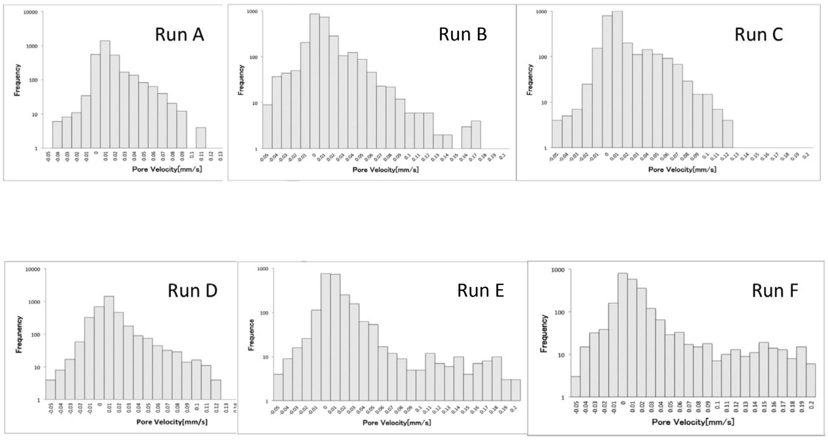

Figure 24: Histograms of the z-direction velocities.

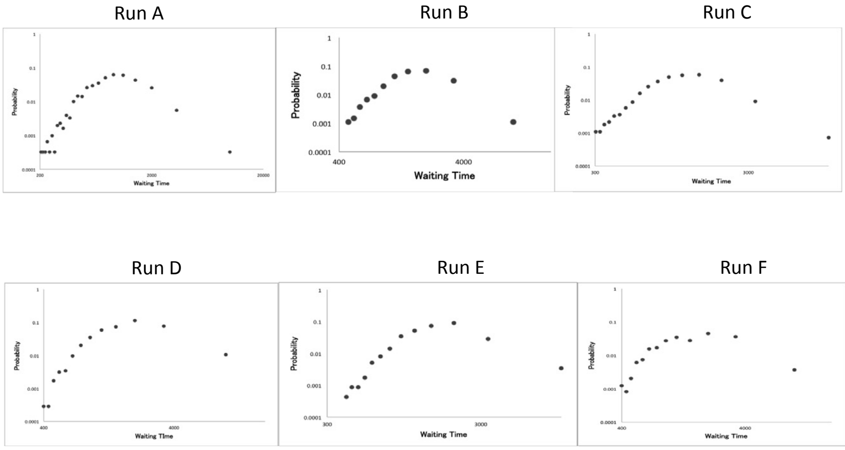

Figure 25: Preliminary result of the waiting time distribution.

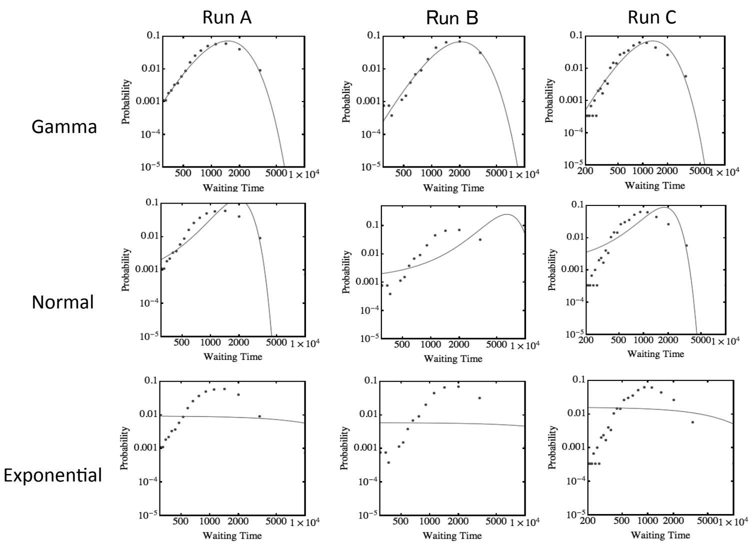

Figure 26: Comparison of the waiting time distribution with the Gamma-, Normal- and Exponential distributions for the sphere particles.

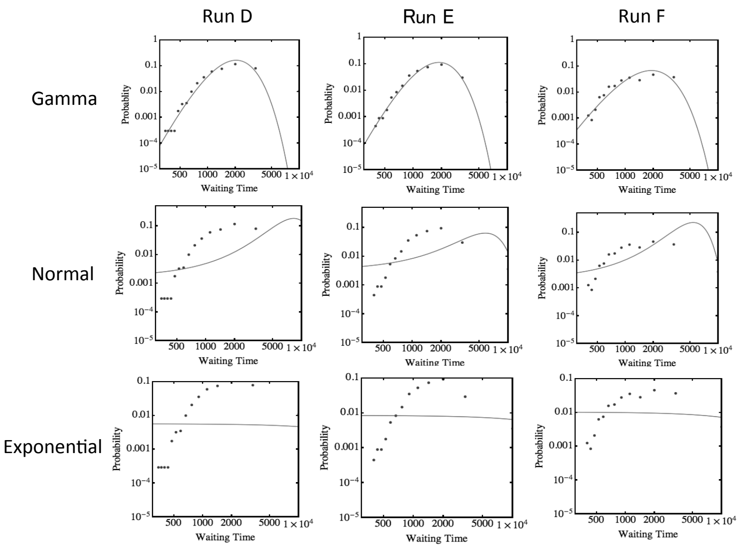

Figure 27: Comparison of the waiting time distribution with the Gamma-, Normal- and Exponential distributions for the irregular-shaped particles.

2014.12.18
逆問題における理論と実用の協働
九州大学IMI

Modeling of Atmospheric and Underground Migration of Radionuclide in the 100 km vicinity of Fukushima

システム情報工学研究科リスク工学専攻
羽田野祐子
University of Tsukuba, Yuko Hatano

PROBLEMS

- Practical problems
  - ■When the refugee can go home？
  - ■How radionuclides do migrate？
  - ■Compensation of Farmland and Fishery

短期(狭い場所)を計測することにより
長期(広い場所)を予測する手法
Short-time measurement -> Long-term prediction

Chernobyl and Fukushima Accident

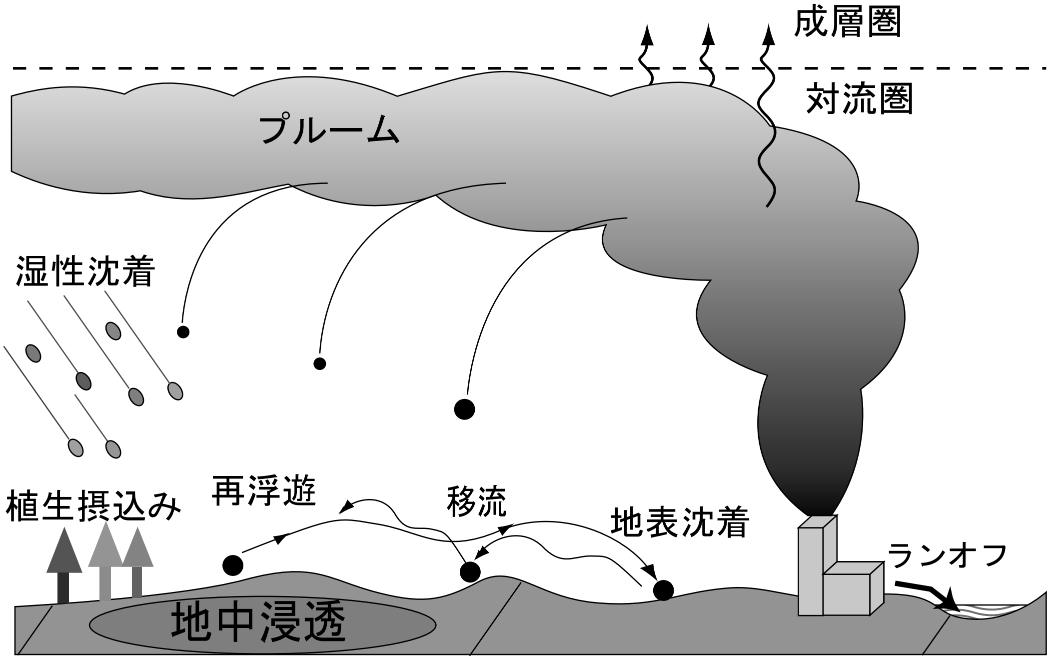

PROBLEM of LONG-TERM PREDICTION

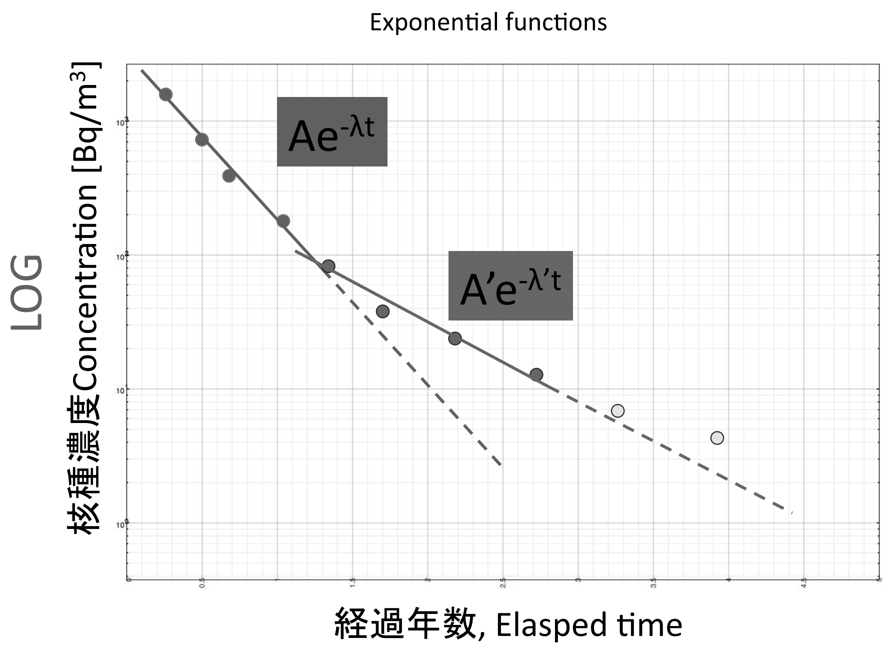

Nevada, U.S.   Nuclear Test Site

最初の10年間は1／tで減っていく
その後は一定

Initial 10 years decrease as 1/t, after that, C(t) is constant.

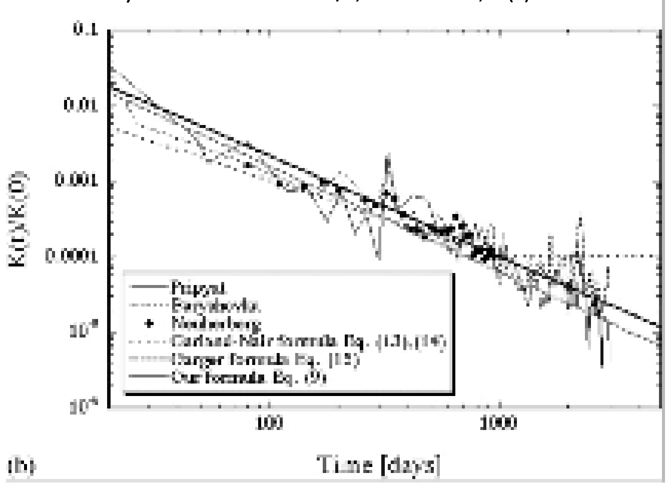

最初の減衰は早いが　次第にそれほど減らなくなってくる

Initial decrease is rapid, but it slows down.

フラクタル図形

一部をとって拡大しても元と同じ形になる

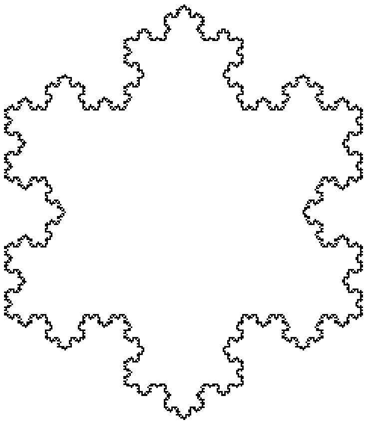

コッホ曲線

シルピンスキー
・ギャスケット

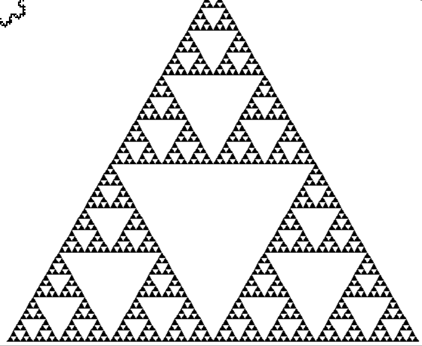

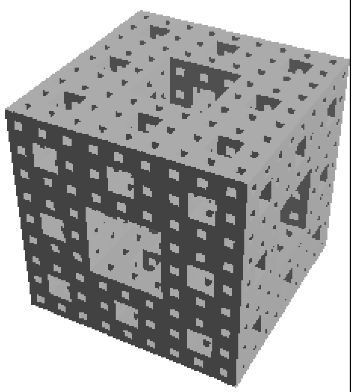

メンガーの
スポンジ

Fractal and Power function

$$K(t) = t^{-4/3}$$

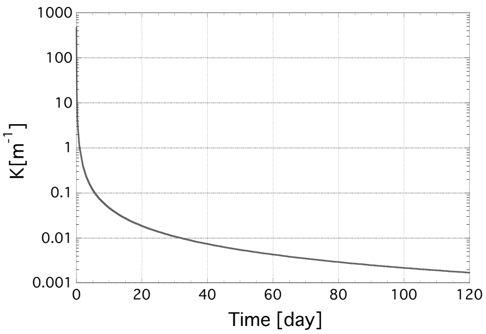

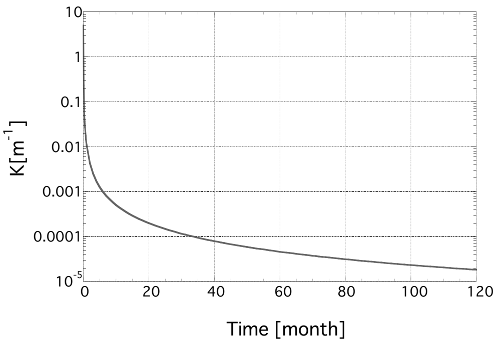

日単位の減衰
Unit in Day

月単位の減衰
Unit in Month

大気中の核種濃度の長期的推移式
ATMOSPHERIC CONCENTRATION OF RADIONUCLIDES

$$C(t) \cong A \exp(-\lambda_{decay} t) t^{-\alpha}$$

$$\boxed{\frac{\partial C}{\partial t} + v_i \frac{\partial C}{\partial x_i} + \lambda_{env}(t) C + \lambda_{decay} C + \lambda_{new}(t) C = \delta(x_1)\delta(x_2)\delta(t)}$$

C : 核種の大気中濃度, Concentration of radionuclides in the air

$v_i(t)$: i方向の風による移流速度, fractal Wind Velocity

λ_{env}: 土壌や川への流出, 植物の取り込み(=a/t), Environemental Effect

λ_{decay} =6.32×10^{-5} : ^{137}Cs 崩壊定数, Decay Constant

λ_{new} : 減衰率自体が指数減衰する効果

Decay rate decrease as Exponential Function(= B exp(-βt))

$$C(t) \cong A \exp(B \exp(-\beta t) - \lambda_{decay} t) t^{-\alpha}$$

福島事故への適用に際し Chernobylからのパラメータ推定

$$C(t) \cong A \exp(B \exp(-\beta t) - \lambda_{decay}\, t)\, t^{-\alpha}$$

- パラメータAとαに対して最小二乗法でフィッティング
- パラメータBとβは関数近似結果の値で固定
- データは汚染源から40km圏内7地点での^{137}Cs観測データ

  （日本原子力研究所発行）
- データ期間は3000日から5000日(1987年−1999年)
- ^{137}Csの観測値は観測1年目を半年平均、以降を3ヶ月平均としてフィッティング

合わせるべきパラメーターは A とαのみ

point70.3 実測値とのフィッティング

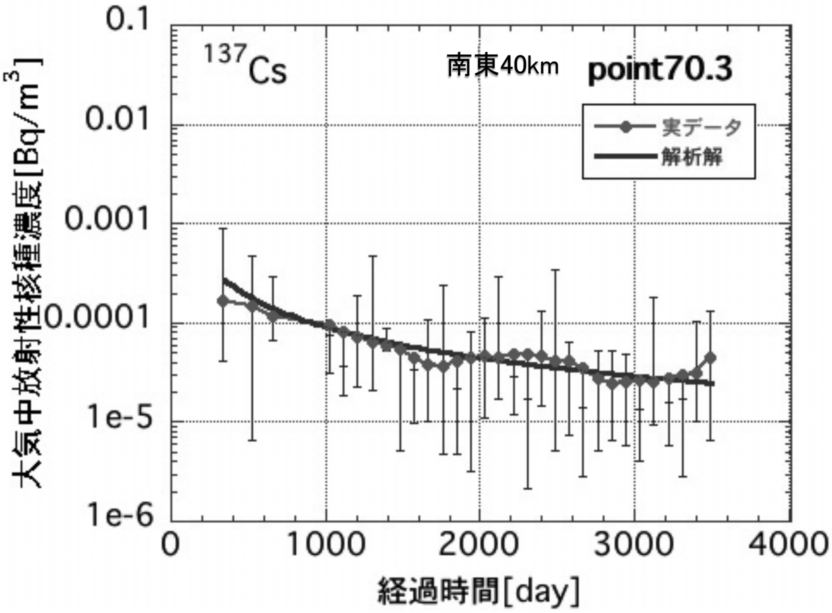

フィッティングパラメータの距離依存性

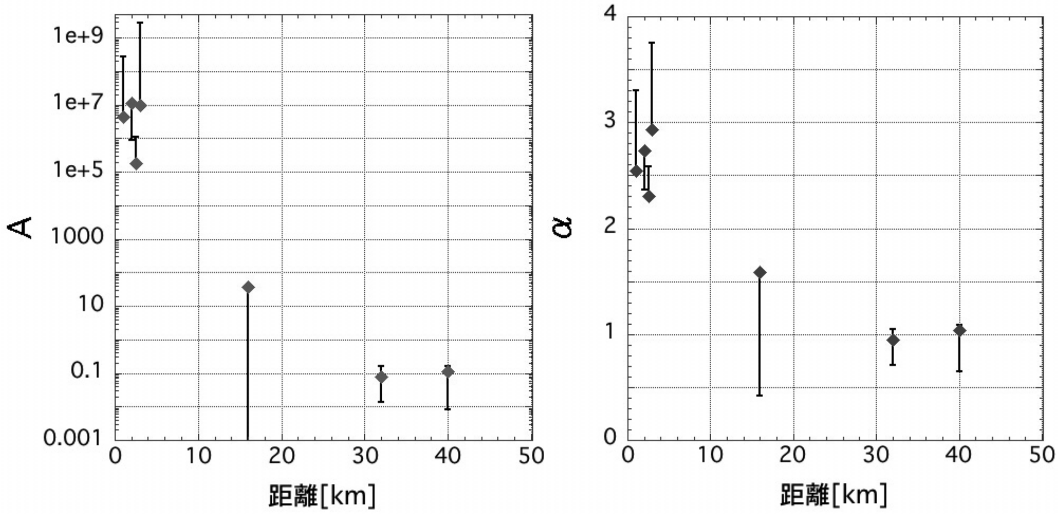

11

パラメータ収束性が改善
IMPROVED PARAMETER CONVERSIONS

OLD MODEL

$$C(t) \cong A\exp(-\lambda_{phy}t)t^{-\alpha}$$

CURRENT MODEL

$$C(t) \cong A\exp(B\exp(-\beta t) - \lambda_{decay}t)t^{-\alpha}$$

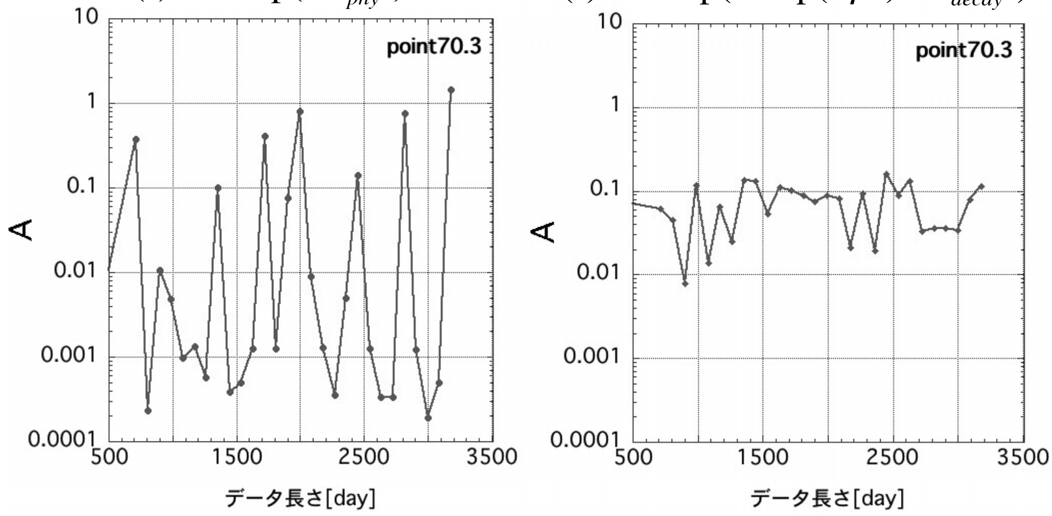

12

旧モデル

$$C(t) \cong A\exp(-\lambda_{phy}t)t^{-\alpha}$$

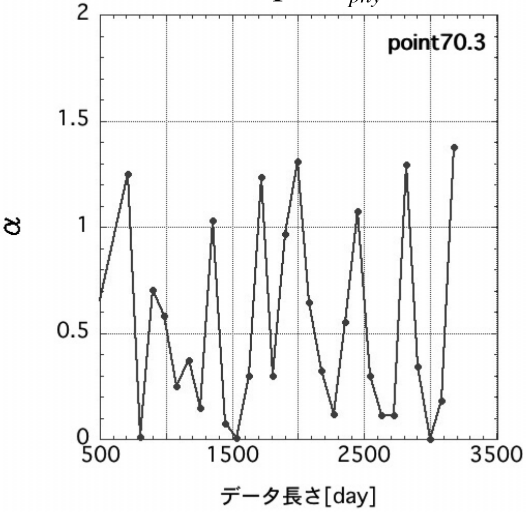

改善後

$$C(t) \cong A\exp(B\exp(-\beta t) - \lambda_{decay}t)t^{-\alpha}$$

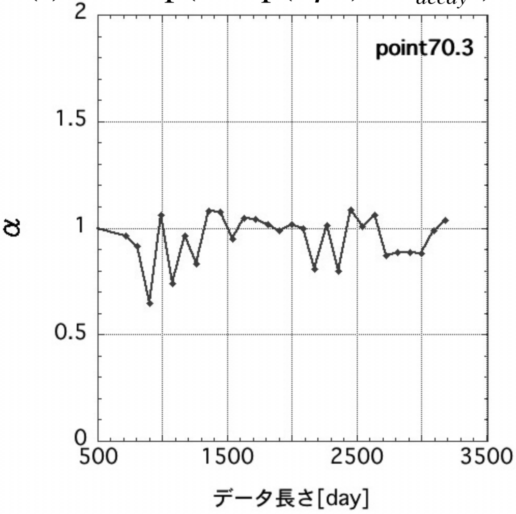

13

Max. and Min. Concentrations

$$C(t) \cong A\exp(B\exp(-\beta t) - \lambda_{decay}\ t)t^{-\alpha}$$

- パラメータAとαの3年以降の最大値・最小値
- パラメータBとβは関数近似結果の値で固定
- データは汚染源から40km圏内6地点での^{137}Cs観測データ
  (日本原子力研究所発行)
- データ期間は3000日から5000日(1987年−1999年)

[South 32km]

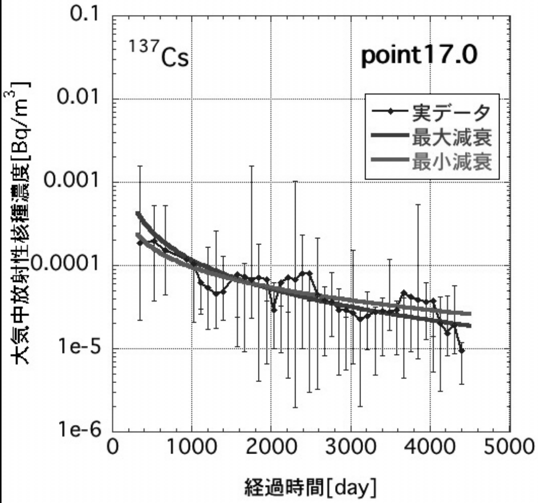

[South 1km]

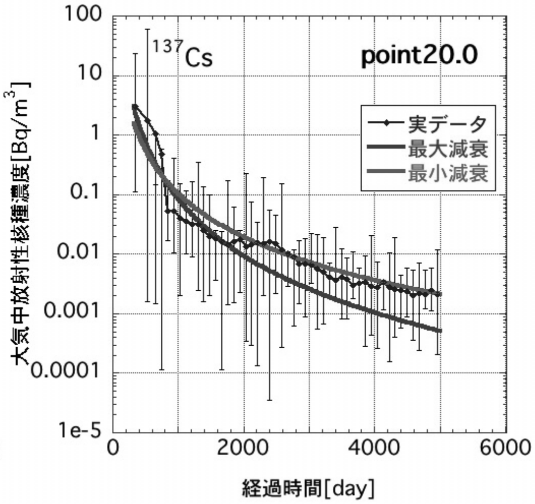

[North West 2km]

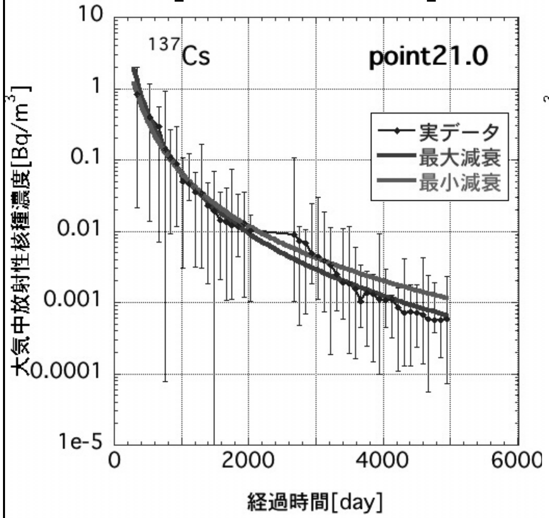

[East 2.6km]

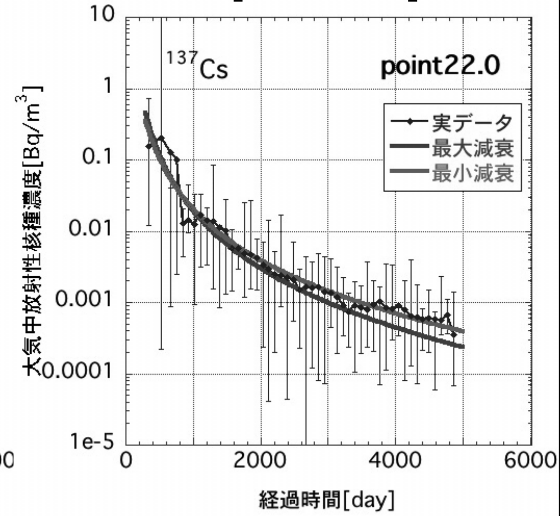

16

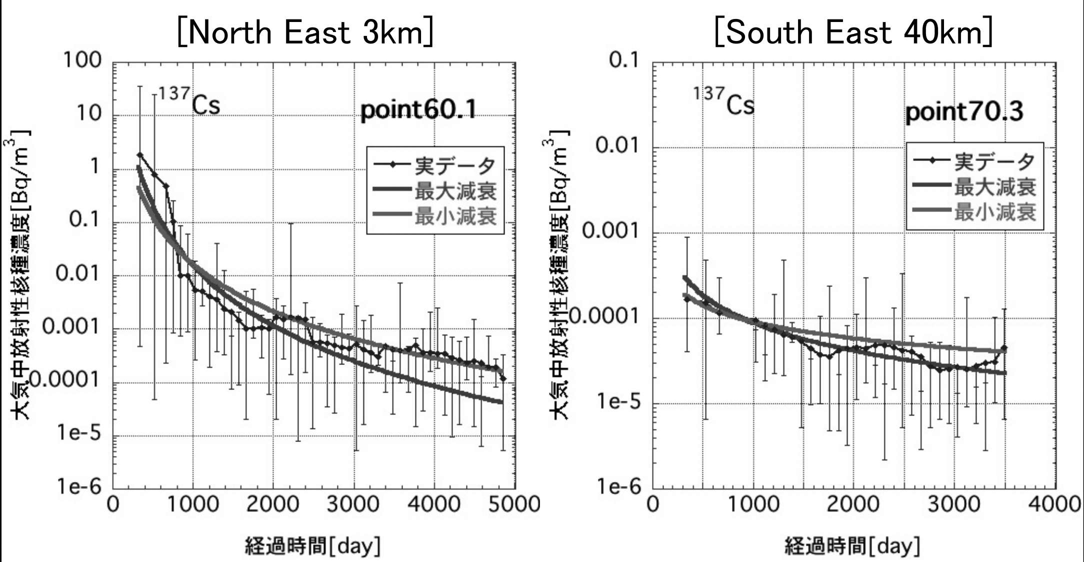

Application to Fukushima

$$C(t) \cong A \exp(B \exp(-\beta t) - \lambda_{decay} t) t^{-\alpha}$$

- Estimating α from Chernobyl case
- B and β : fixed
- Assuming C(50 days) = 1Bq/m^3
- ^{137}Cs Concentration

Our Predictions(initial concentration = 1, 10 yrs after)

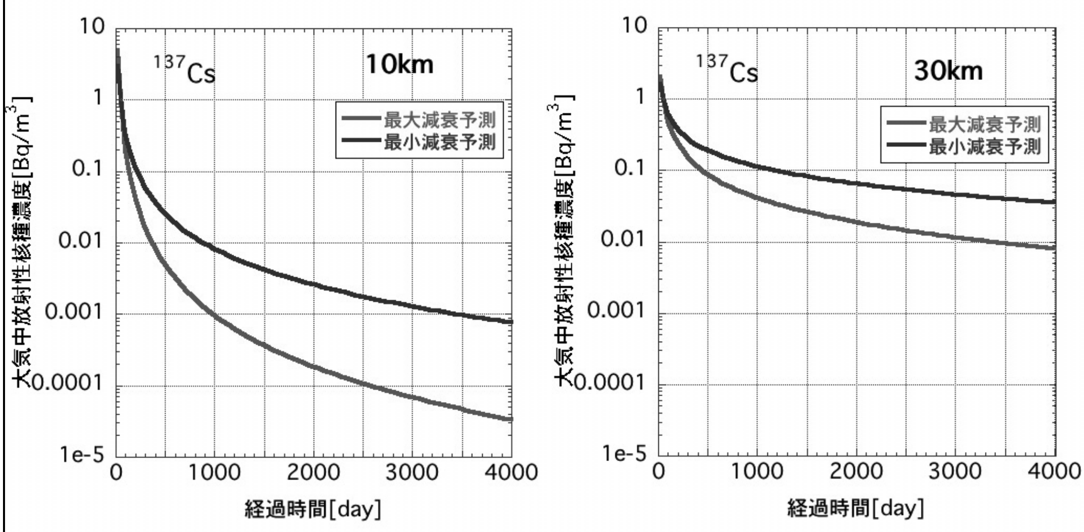

朝日新聞web論座, 2011Nov26

セシウム大気中濃度(つくば市)
Cs-137 Conc. in the air (Tsukuba)

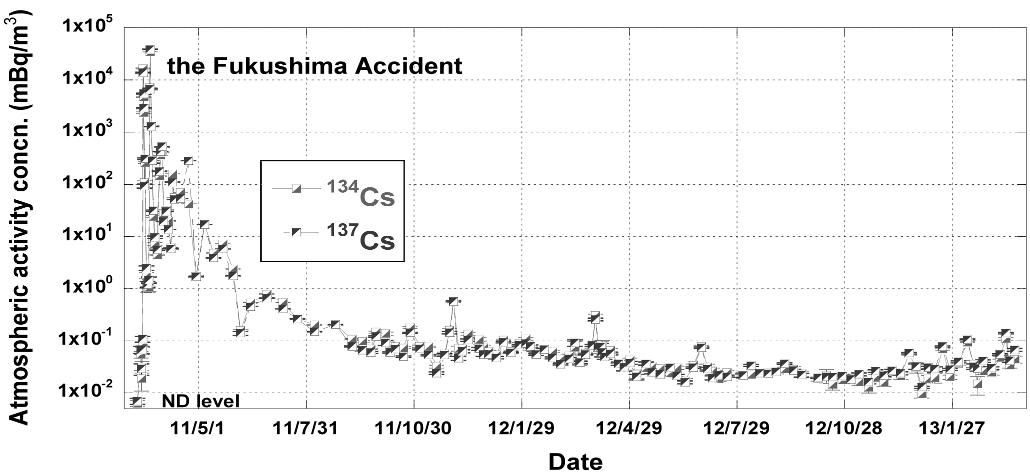

作成:気象研究所

20

モデルとの比較, Comparison with model

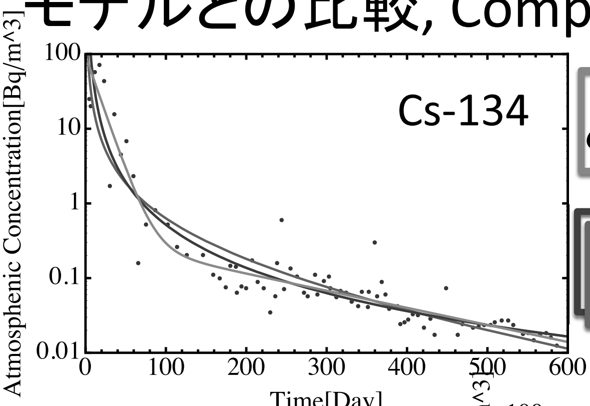

指数関数の和

$$C(t) = 85e^{-0.076t} + 12e^{-0.05t} + 0.33e^{-0.005t}$$

開発モデルその1、その2

$$C(t) = e^{-\lambda t} t^{-\alpha}$$

■つくば市のような低線量地域では
モデルによる差はあまりない

■半減期が長いCs-137については
10年後にモデル間で差が生じ
従来のモデルとの差は1桁程度

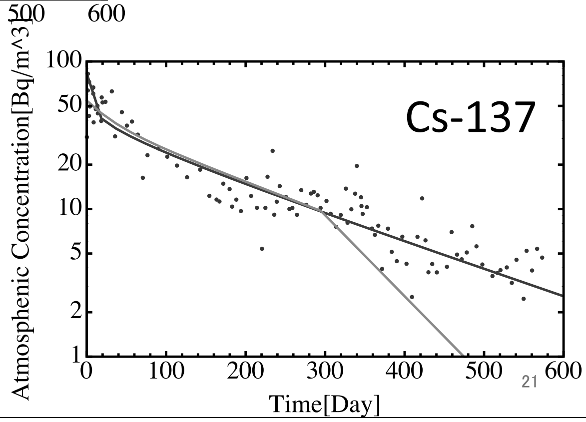

21

まとめ SUMMARY

(1) 長期予測のために、自然界のフラクタルな性質を利用した予測モデルを作成した

(2) 大気中核種濃度に関し、本研究室で開発したモデルとつくば市内大気中核種濃度との比較を行った

(3) チェルノブイリのデータをもとに福島事故10年後の予測を行った

Porous Media Experiments

Yuko Hatano
University of Tsukuba

- sandbox experiment 1,2
  - 86cm × 45cm × 10cm

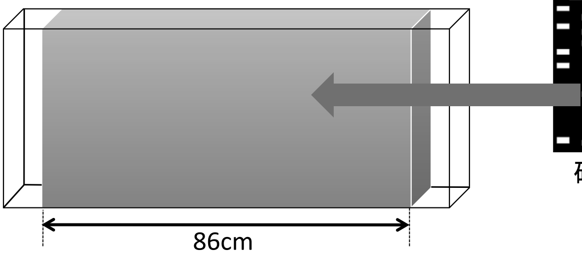

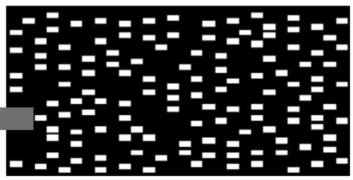

砂は上図に従い、ランダムに充填
■ sand1 □sand3

- sandbox experiment 3
  - 213cm × 65cm × 10cm

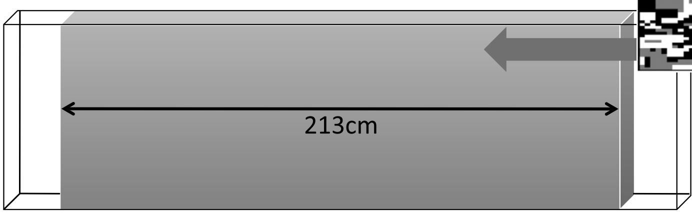

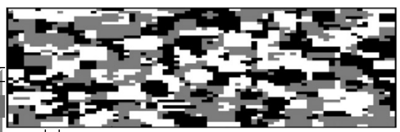

砂は上図に従って充填
■ sand1
■ sand1
□ sand3

- 長水路実験　LONG CHANNEL
  - W260mm × H300mm × L7600mm
  - 東北硅砂6号（平均粒径0.34mm）

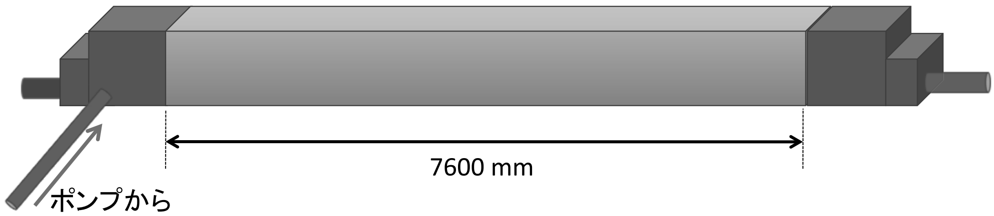

- カラム実験 COLUMN
  - Φ31mm × 107 mm
  - 標準豊浦砂

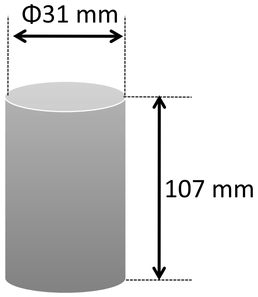

- A field tracer experiment in a fractured till (Siddle 1998)

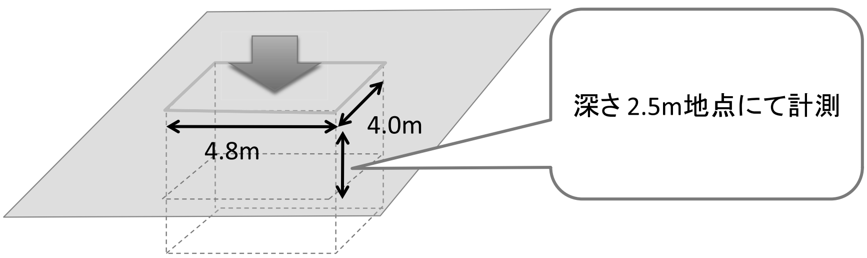

year	scale[m]	α	Q[ml/min]	medium	tracer	experiment	detail
2001	2.13	1.87		containing a uniformly heterogeneous packing of sand	chloride	Silliman and Simpson(1987)	Berkowitz et al (2000)
2001	2.5	1.61		a field tracer experiment in a fractured till	chloride	Sidle et al. 1998	Kosakowski et al. (2001)
2000	0.91	1.87		electrode column		Silman and Simpson(1987)	Berkowitz et al (2000)
2000	1.37	1.87		"			
2000	1.83	1.87		"			
1998	100	1.5		a filed tracer experiment in a heterogeneous alluvial aquifer	bromide	E.E. Adams and L.W. Gelhar	

従来のADE　vs. 新モデルCTRW

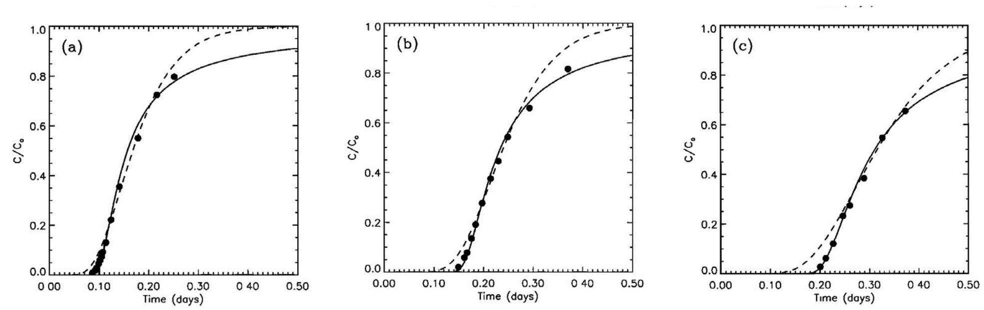

ADE(Advection-Dispersion Equation)

$$\frac{\partial C}{\partial t} = D\frac{\partial^2 C}{\partial x^2} - v\frac{\partial C}{\partial x} \qquad (D = \alpha_L v)$$

■ Scheidegger (1959)
■ systematicなズレ　Systematic Error (known)

連続時間ランダムウォーク(CTRW)

ランダムウォークにおいて
一定だったジャンプ間の待ち時間に分布を与えたモデル

$$R(s,t)=\sum_{s'}\int_0^t \psi(s-s',t-t')R(s',t')dt'$$

待ち時間分布関数$\psi(\tau)$は以下のようになる

$$\psi(\tau)\propto\frac{1}{\left(1+(\tau/\beta)^{\alpha}\right)} \xrightarrow{\text{単純化}} \boxed{\psi(\tau)\propto\tau^{-\alpha} \quad \tau>0}$$

複雑な式を解析的に解くのではなく乱数を用いた
モンテカルロシミュレーションを行う

待ち時間分布

ADEは一定の待ち時間

CTRWは図のように分布を与える

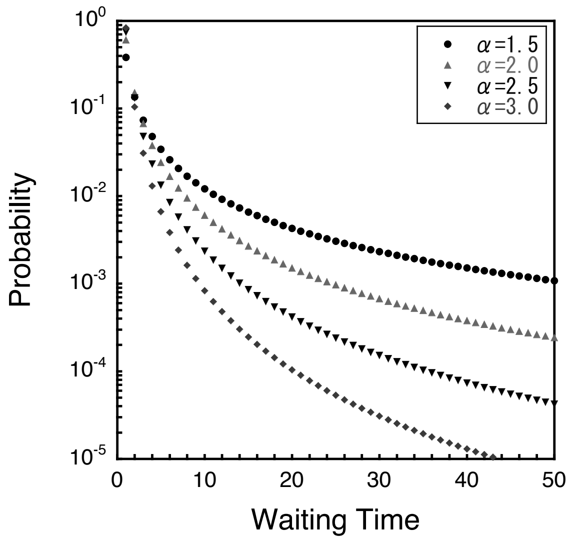

$$\psi(\tau)\propto\tau^{-\alpha}$$

肩の数字 α は「不均質性」に関連

トレーサー実験概要

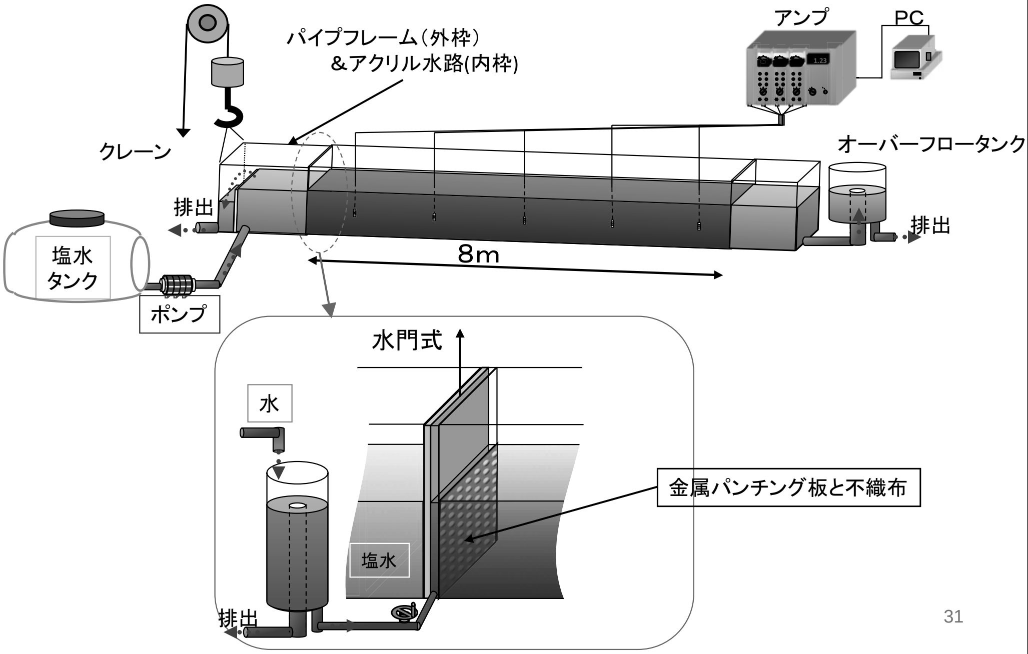

31

実験装置（写真①）

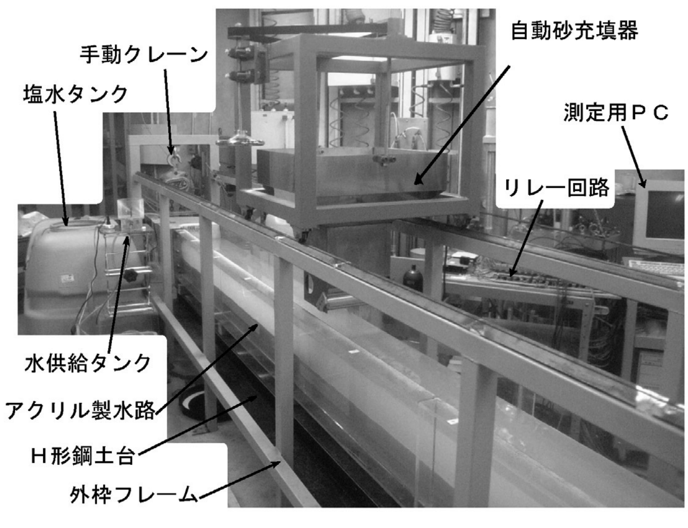

32

実験装置（写真②）

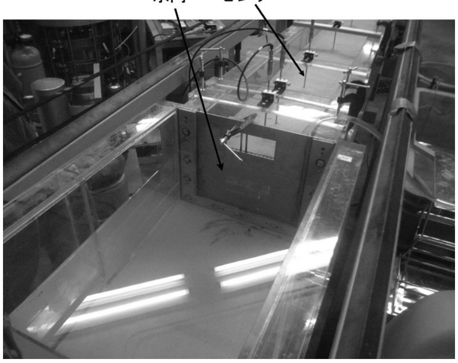

33

LONG-CHANNEL Experiment

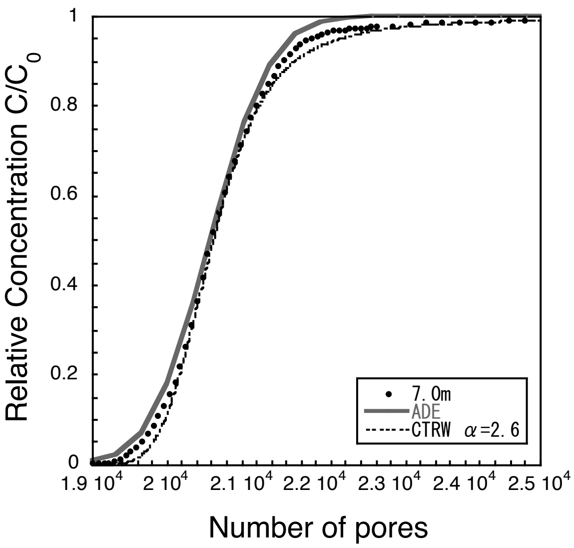

LONG-CHANNEL Experiment

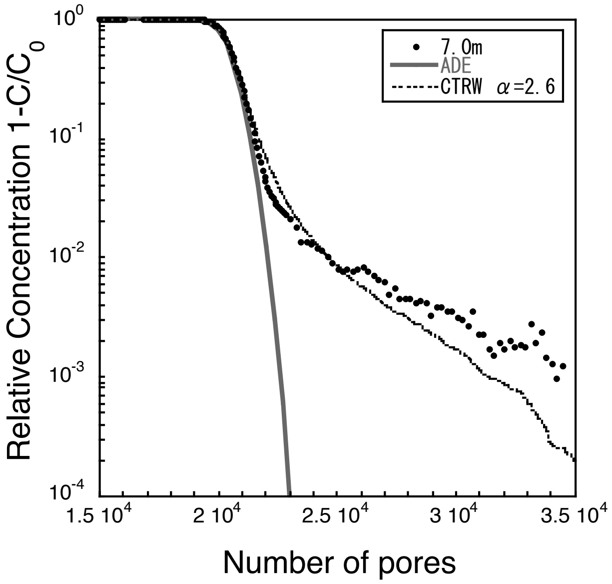

カラム試験 （鉛）
Column Experiment (Pb)

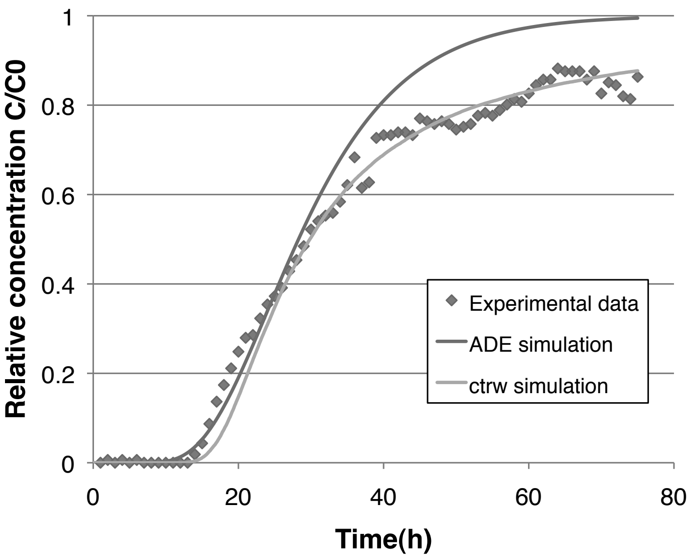

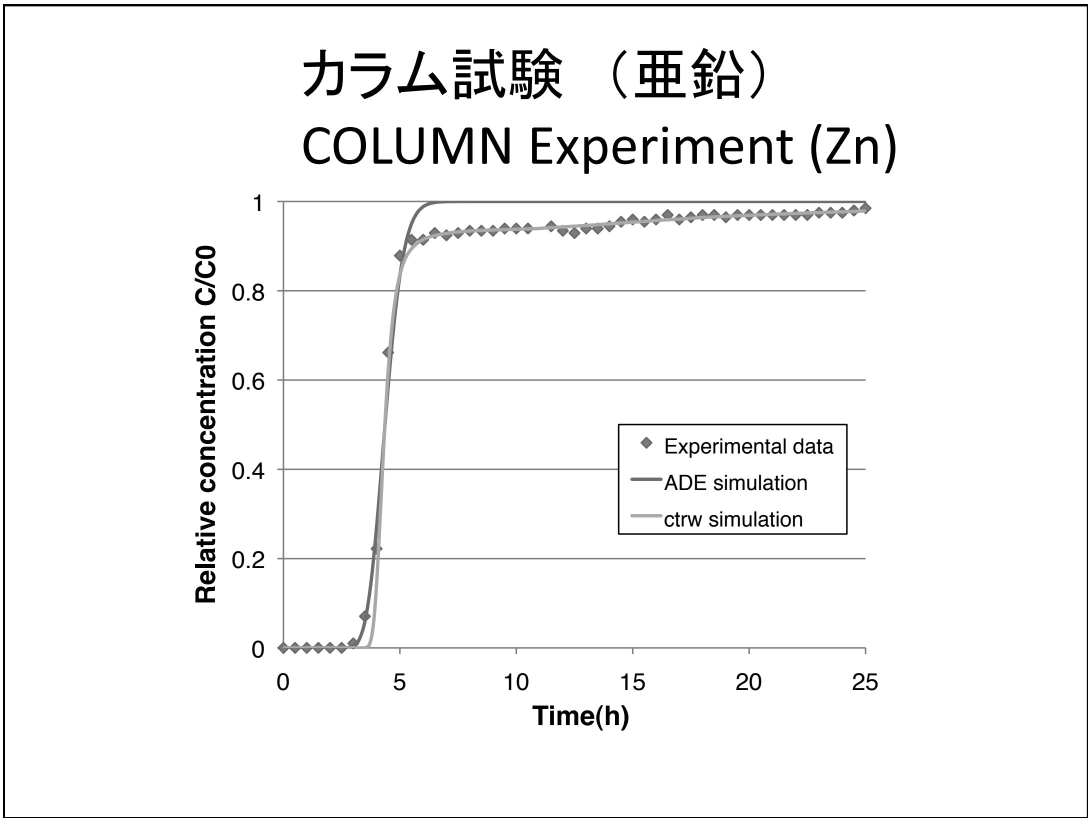
カラム試験　（亜鉛）
COLUMN Experiment (Zn)
Relative concentration C/C0
Time(h)
Experimental data
ADE simulation
ctrw simulation
0
0.2
0.4
0.6
0.8
1
0
5
10
15
20
25

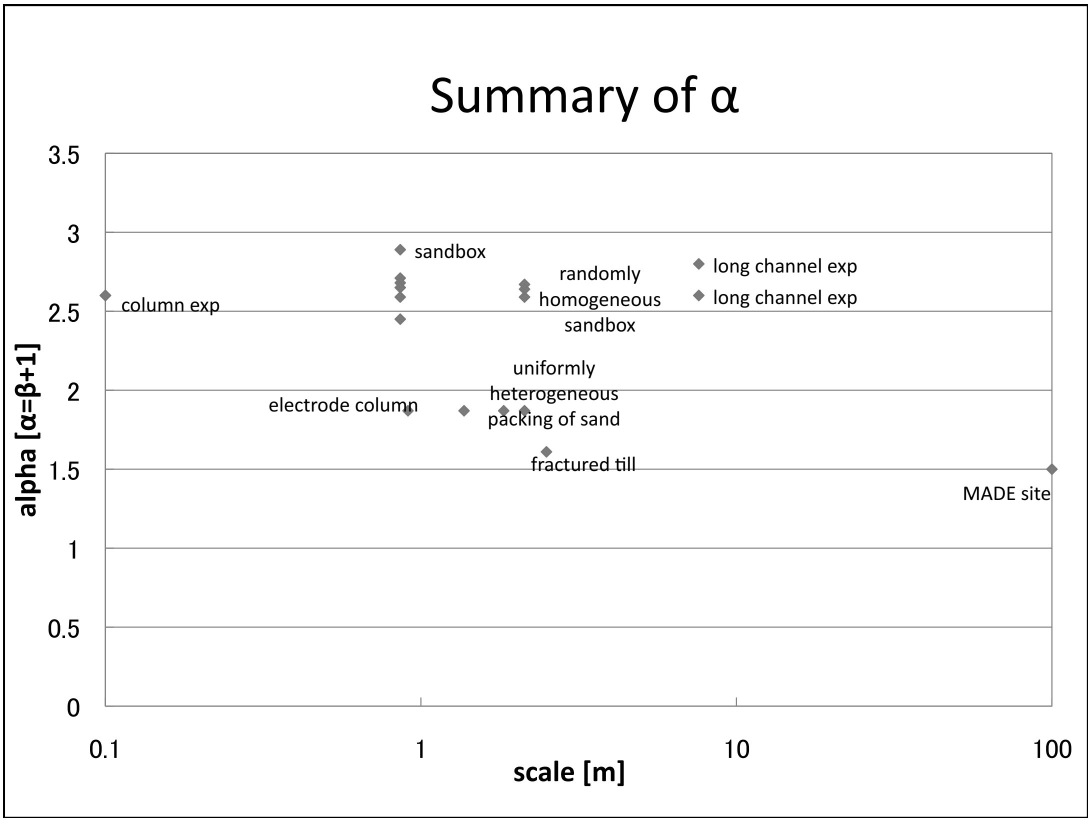
Summary of α
alpha [α=β+1]
scale [m]
sandbox
column exp
randomly homogeneous sandbox
long channel exp
long channel exp
uniformly heterogeneous packing of sand
electrode column
fractured till
MADE site
0
0.5
1
1.5
2
2.5
3
3.5
0.1
1
10
100

CTRWとスケールアップ

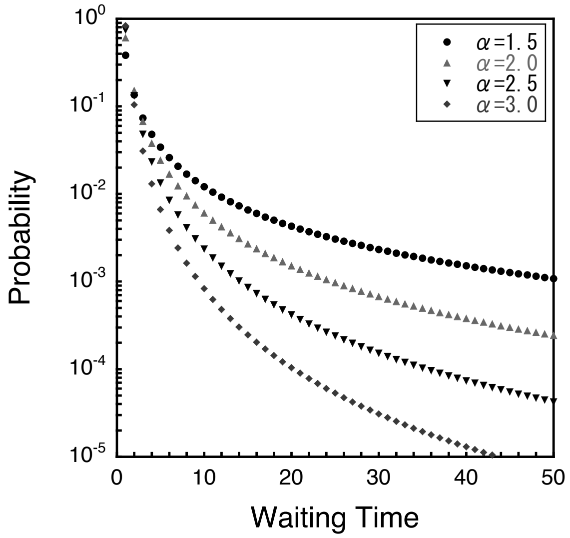

$$\psi(\tau) \propto \tau^{-\alpha}$$

$$\tau > 0$$

スケール不変性

Mathematical theory on perturbation of singular points in continuum mechanics and its application to fracture and to shape optimization

Kohji Ohtsuka *

1 Introduction

The singularity affects the strength of materials greatly. The ideas of this study came from specific studies based on fracture mechanics[54], the continuum theory of lattice defects by Eshelby[13] and conservation laws[6, 33] by Neother's principle[40]. Here, we regard the boundary of material as the set of singular points, that is, the material is described as a system of partial differential equations for the boundary value problems defined in the reference configuration Ω_0 (3-dimensional domain). We consider the boundary $\partial\Omega_0$ as the set of singular points. We think the matrials to be hyperelastic first of all, that is, the strain energy density function $\widehat{W}(x,\varepsilon)$ is written with the strain tensor $\varepsilon = (\varepsilon_{ij}), i,j = 1,2,3$, and the stress tensor $\sigma = (\sigma_{ij}), i,j = 1,2,3$ is given by [10, Chapter 4]

$$\sigma_{ij} = \sigma(x,\varepsilon) = \partial\widehat{W}(x,\varepsilon)/\partial\varepsilon_{ij} \qquad x \in \Omega_0$$

Linear stress-strain relations take the form

$$\sigma_{ij}(x,\varepsilon) = C_{ijkl}(x)\varepsilon_{kl} \tag{1.1}$$

where $C_{ijkl} = C_{jikl} = C_{ijlk} = C_{jilk}$ in view of symmetry $\sigma_{ij} = \sigma_{ji}$, and $C_{ijkl} = C_{klij}$ from the existence of $\widehat{W}$. The equations of motion are

$$\rho\frac{\partial^2 u_i}{\partial t^2} - \partial_j\sigma_{ij} = f_i \quad \text{in } \Omega_0, i = 1,2,3, \quad (\partial_j = \partial/\partial x_j) \tag{1.2}$$

where $\boldsymbol{f} = (f_1, f_2, f_3)$ is the body force per unit volume, $\boldsymbol{u} = (u_1, u_2, u_3)$ the displacement, ρ the mass density. Let Γ_N be the part of $\partial\Omega_0$, on which the force $\boldsymbol{g} = (g_1, g_2, g_3)$ per unit area act with the outward unit normal $\boldsymbol{n} = (n_1, n_2, n_3)$

$$\sigma_{ij}(x,\varepsilon)n_j(x) = g_i(x) \quad x \in \Gamma_N, i,j = 1,2,3 \tag{1.3}$$

On another part $\Gamma_D = \partial\Omega_0 \setminus \overline{\Gamma_N}$, the diplacement $\boldsymbol{u}_D$ is given

$$\boldsymbol{u} = \boldsymbol{u}_D \qquad \text{on } \Gamma_D \tag{1.4}$$

*Hiroshima Kokusai Gakuin University, e-mail:ohtsuka@hkg.ac.jp

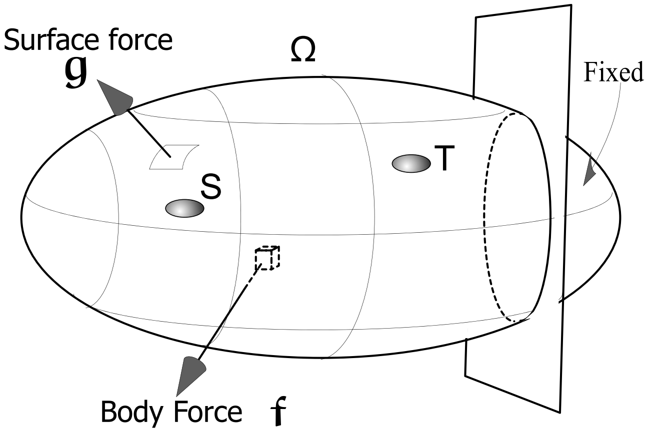

Figure 1: Hyperelastic material with sets S, T of singular points

1.1 Weak formula

The singular points that we consider are the following

Boundary: Seeing from all space $\mathbb{R}^3$, the boundary $\partial\Omega_0$ is the set of singular points. The boundary conditions are; $\boldsymbol{u} = \boldsymbol{u}_D$ on Γ_D, $\sigma(\boldsymbol{u})_{ij}n_j = g_i$ on Γ_N. For simplicity, we study the case that $\boldsymbol{u}_D = 0$.

Fracture: The crack surface Σ is the surface of the discontinuity of displacement when stress is free on Σ. In the crack extension, and strong singularity is on the edge $\partial\Sigma$, in which case the reference configulation is $\Omega = \Omega_0 \setminus \Sigma$. The boundary condition on Σ is

$$\sigma_{ij}(\boldsymbol{u})^{+}\nu_j = \sigma_{ij}(\boldsymbol{u})^{-}\nu_j = 0 \quad \text{on } \Sigma \tag{1.5}$$

where $\sigma_{ij}(\boldsymbol{u}(x))^{\pm} = \lim_{\epsilon\to 0}\sigma_{ij}(\boldsymbol{u}(x+\epsilon\boldsymbol{\nu}^{\pm}(x)))$ with the unit normal $\boldsymbol{\nu}$ oriented from the plus side to the minus side of Σ and $\boldsymbol{\nu}^{-}(x) = -\boldsymbol{\nu}^{+}(x)$

Void(Cavity): The reference configuration is $\Omega = \Omega_0 \setminus \overline{D_c}$ where D_c stands for the void, and the set of singular points is ∂D_c. The boundary condition is

$$\sigma_{ij}(\boldsymbol{u})n_j = 0 \quad \text{on } \partial D_c \tag{1.6}$$

where $\boldsymbol{n}$ is the inward unit normal of ∂D_c.

Inclusion: The reference configuration Ω satisfies that $\overline{\Omega} = \overline{D_o} \cup \overline{D_i}$, $D_i \cap D_o = \emptyset$ Strain energy density has the discontinuity on $\overline{\partial D_i} \cap \overline{D_o}$, that is,

$$\widehat{W}(x, \varepsilon(\boldsymbol{u})) = \begin{cases} \widehat{W}^{i}(x, \varepsilon(\boldsymbol{u}^{i})) & \text{in } D_i \\ \widehat{W}^{o}(x, \varepsilon(\boldsymbol{u}^{o})) & \text{in } D_o \end{cases} \tag{1.7}$$

where $\boldsymbol{u}^i, \boldsymbol{u}^o$ are the displacement on D_i and D_o respcetively. The conditions are

$$\boldsymbol{u}^{o} = \boldsymbol{u}^{i} \quad \text{on } \Gamma_i = \overline{D_i} \cap \overline{D_o} \tag{1.8}$$

$$\sigma^{i}_{ij}(x, \boldsymbol{u}^{i})\boldsymbol{\nu} = \sigma^{o}_{ij}(x, \boldsymbol{u}^{o})\boldsymbol{\nu} \quad \text{on } \Gamma_i \tag{1.9}$$

where $\sigma_{ij}^i = \partial\widehat{W}^i/\partial\varepsilon_{ij}, \sigma_{ij}^o = \partial\widehat{W}^o/\partial\varepsilon_{ij}$ and $\boldsymbol{\nu}$ the unit normarl oriented from D_o to D_i.

Joint parts: The joint part $\overline{\Gamma_D} \cap \overline{\Gamma_N}$ of different boudary conditions is the set of singular points.

The materials with the various singularity stated just above are discribed by the following variational problem over the space $V(\Omega, \Gamma_D)$ in which Ω stands for the reference configuration, that is,

$$V(\Omega, \Gamma_D) = \{\boldsymbol{v} : \overline{\Omega} \to \mathbb{R}^3;\ \boldsymbol{v} = \boldsymbol{u}_D \quad \text{on } \Gamma_D\}$$

In fracture problem, $\Omega = \Omega_0 \setminus \Sigma$; $\Omega = \Omega_0 \setminus \overline{D_c}$ when the void is contained and $\partial D_c \subset \Gamma_N$; if there is inclusion, we adopt (1.7).

The displacement $\boldsymbol{u}$ is given as the minimizer of the functional

$$\mathcal{E}(\boldsymbol{v}; \Omega, f, g) = \int_\Omega \widehat{W}(x, \varepsilon(\boldsymbol{v}))dx - \int_\Omega \boldsymbol{f} \cdot \boldsymbol{v}\, dx - \int_{\Gamma_N} \boldsymbol{g} \cdot \boldsymbol{v} ds \tag{1.10}$$

over $v \in V(\Omega, \Gamma_D)$[10, Theorem 4.1.-2]. In linear elasticity, we can write $V(\Omega, \Gamma_D)$ more precisely as follows

$$V(\Omega, \Gamma_D) = \{\boldsymbol{v} \in W^{1,2}(\Omega, \mathbb{R}^3);\ \boldsymbol{v} = \boldsymbol{u}_D \quad \text{on } \Gamma_D\} \tag{1.11}$$

Here for a domain $\mathcal{O}$ in d-dimensional space $\mathbb{R}^d$ and the vector valued function $\boldsymbol{v} = (v_1, \cdots, v_m), m \geq 0$

$$\begin{aligned}
W^{1,p}(\mathcal{O}; \mathbb{R}^m) &= \left\{\boldsymbol{v} = (v_1, \cdots, v_m) : \sum_{i=1}^m (\|v_i\|_{L^p(\mathcal{O})} + \|\nabla v_i\|_{L^p(\mathcal{O})}) < +\infty\right\} \\
\|\nabla v_i\|_{L^p(\mathcal{O})} &= \sum_{j=1}^d \left\{\int_\mathcal{O} |\partial_j v_i(x)|^p\, dx\right\}^{1/p}, \quad \partial_j = \partial/\partial x_j, j = 1, \cdots, d \\
W^{1,\infty}(\mathcal{O}; \mathbb{R}^m) &= \left\{\boldsymbol{v} = (v_1, v_2, v_3) : \sum_{i=1}^3 (\|v_i\|_{L^\infty(\mathcal{O})} + \|\nabla v_i\|_{L^\infty(\mathcal{O})}) < +\infty\right\} \\
\|v_i\|_{L^\infty(\mathcal{O})} &= \sum_{j=1}^3 \operatorname*{ess\,sup}_{x \in \mathcal{O}} |v_i(x)|
\end{aligned}$$

where $\operatorname{ess\,sup}_{x \in \mathcal{O}} |v_i(x)|$ means the greatest lower bound of $v_i(x)$ almost everywhere (a.e.) on $\mathcal{O}$ (see e.g. [2]). In the case $m = 1$, $\boldsymbol{v}$ stands for *the function.*

1.2 Perturbation of singular points, and vector field $\boldsymbol{\mu}$

Let $\gamma \in \overline{\Omega}$ be a singular point, and $[t \mapsto \phi_t(\gamma) \in \mathbb{R}^3], 0 \leq t \leq \epsilon_0$ the perturbation of γ, which makes the vector field $d\phi_t(\gamma)/dt$. We assume the existence of parallel extension $\boldsymbol{\mu}_\phi(x)$, $x \in \mathbb{R}^3$ of $d\phi_t(\gamma)/dt$, and the path $\varphi_t(x), x \in \mathbb{R}^3$ of $\phi_t(\gamma)$.

1.2.1 Field of view ω

In this paper, we consider the various singular points, so we introduce the concept "field of view" to separate in singular points, that is the open set ω. For

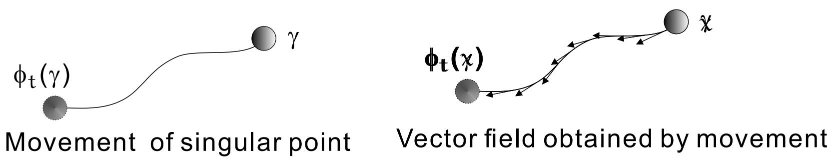

Figure 2: Path by perturbation and vector field of singular points

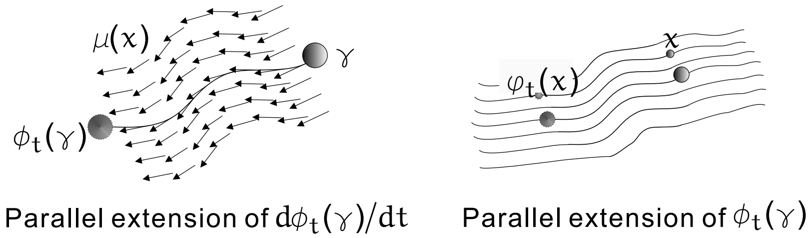

Figure 3: Parallel extension $\boldsymbol{\mu}_\phi(x)$ of $d\phi_t(x)/dt$

examples, if there are sets S, T of singular points as shown in Fig.4, and assume that $S \Subset \Omega$. Let ω_S be an open set such that

$$S \subset \omega_S, \qquad T \subset D \setminus \overline{\omega_S}$$

Let us call ω_S the *field of view focusing on* S.

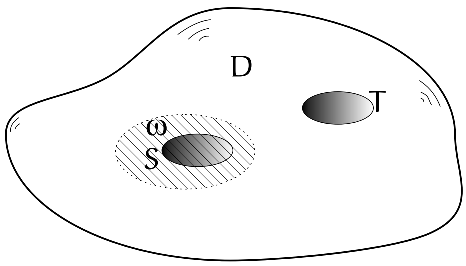

Figure 4: Material containing the sets S, T of singular points

2 Generalized J-integral

The original J-integral is difined by

$$J = \int_C \left[\widehat{W}(x, \varepsilon) dx_2 - \widehat{T}(\boldsymbol{u}) \cdot \partial \boldsymbol{u} / \partial x_1 \, ds \right] \tag{2.1}$$

where C is the closed curve surrounding the crack tip and $\boldsymbol{n}$ the outward unit normal of C (see Fig.5). Since C avoid the crack tip, J take finite value and independent on C. Moreover, J expresses the rate of released energy with respcet to crack extension as shown in (2.2).

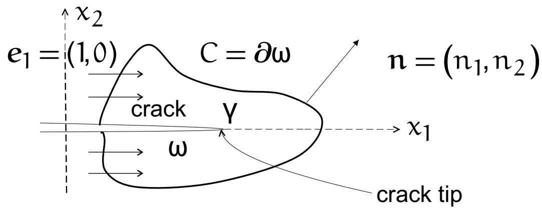

Figure 5: Curve C surrounding the crack tip

Consider the straight crack extension as shown in Fig.6 inside *homogineous* elastic plate when $\boldsymbol{f} = 0$ *near the crack tip*. Here ℓ stands for the crack increment. Denoting $\Omega_{\Sigma(\ell)} = \Omega \setminus \Sigma(\ell)$ with crack surface $\Sigma(\ell)$, we write the energy

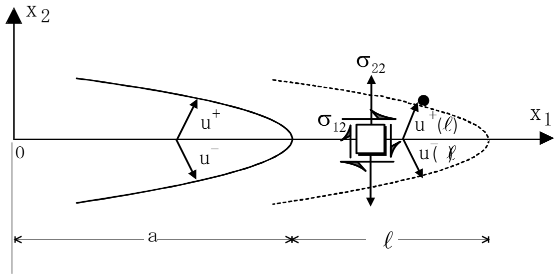

Figure 6: Straight crack extension in 2D fracture

at the crack increment ℓ by

$$\mathcal{E}(\boldsymbol{u}(\ell); \boldsymbol{f}, \Omega_{\Sigma(\ell)}) = \int_{\Omega_{\Sigma(\ell)}} \widehat{W}(\varepsilon(\boldsymbol{u}(\ell)))dx - \int_{\Omega_{\Sigma(\ell)}} \boldsymbol{f} \cdot \boldsymbol{u}(\ell)\, dx$$

G.P.Cherepanov[9] and J. Rice[53] showed that

$$-\frac{d}{d\ell}\mathcal{E}(\boldsymbol{u}(\ell); \boldsymbol{f}, \Omega_{\Sigma(\ell)}) \quad = \quad \int_C \left(\widehat{W}(\nabla \boldsymbol{u})dx_2 - \widehat{T}(\boldsymbol{u})\frac{\partial \boldsymbol{u}}{\partial x_1} ds \right) \qquad (2.2)$$

The left-hand side of (2.2) expresses the released energy per unit crack length.

If Σ is parametrized by arc length s, that is, $\Sigma = \{(x_1(s), x_2(s));\, a \le x \le b\}$, then the outward unit norma $\boldsymbol{n} = (n_1, n_2)$ at $(x_1(s_0), x_2(s_0))$ is equivalent to

$$\boldsymbol{n} = \left(\frac{dx_2}{ds}(s_0), -\frac{dx_1}{ds}(s_0) \right)$$

which means that $dx_2 = n_1 ds = (\boldsymbol{n} \cdot \boldsymbol{e}_1)$ with the unit vector $\boldsymbol{e}_1$ in the x_1-direction. Then we can rewite (2.1) as

$$\begin{aligned} J &= P_\omega(\boldsymbol{u}, \boldsymbol{e}_1) && (2.3) \\ P_\omega(\boldsymbol{u}, \boldsymbol{e}_1) &= \int_C \left\{ \widehat{W}(x, \varepsilon)(\boldsymbol{e}_1 \cdot \boldsymbol{n}) - \widehat{T}(\boldsymbol{u}) \cdot \nabla \boldsymbol{u} \cdot \boldsymbol{e}_1 \right\} ds \end{aligned}$$

where ω is the open set containing the crack tip (see Fig.6).

In 3D fracture, the vector field $\boldsymbol{\mu}_C$ obtained crack extension is not constant, so that $P_\omega(\boldsymbol{u}, \boldsymbol{\mu}_C)$ dependend on ω. Therefore Generalized J-integral is introduced in [43].

Definition 2.1 (GJ-integral) *Let us denote* $\widehat{W}(x, \varepsilon(\boldsymbol{u}))$ *by* $\widehat{W}(x, \nabla \boldsymbol{u}) = \widehat{W}(x, \zeta)|_{\zeta=\nabla u}$ *and write it as* $\widehat{W}(\boldsymbol{u})$ *if there is no ambiguity. For* $\boldsymbol{\mu} \in W^{1,\infty}(\mathbb{R}^3; \mathbb{R}^3)$

$$J_\omega(u, \boldsymbol{\mu}) = P_\omega(\boldsymbol{u}, \boldsymbol{\mu}) + R_\omega(\boldsymbol{u}, \boldsymbol{\mu}) \tag{2.4}$$

$$P_\omega(u, \boldsymbol{\mu}) = \int_{\partial\omega\cap\Omega} \left\{ \widehat{W}(\boldsymbol{u})(\boldsymbol{\mu} \cdot \boldsymbol{n}) - \widehat{T}(\boldsymbol{u}) \cdot (\boldsymbol{\mu} \cdot \nabla u) \right\} ds \tag{2.5}$$

where
$\widehat{T}(\boldsymbol{u}) = \boldsymbol{n} \left(\nabla_\zeta \widehat{W}(x, \nabla u) \right)$

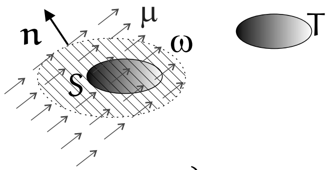

$$\begin{aligned} R_\omega(u, \boldsymbol{\mu}) = &- \int_{\omega\cap\Omega} \left\{ \nabla_x \widehat{W}(x, \nabla \boldsymbol{u}) \cdot \boldsymbol{\mu} + f \cdot (\nabla \boldsymbol{u} \cdot \boldsymbol{\mu}) \right\} dx \\ &+ \int_{\omega\cap\Omega} \left\{ \left(\nabla_\zeta \widehat{W}(x, \nabla \boldsymbol{u}) \right)^T (\nabla \boldsymbol{\mu}^T) \nabla \boldsymbol{u} - \widehat{W}(x, \nabla \boldsymbol{u})(\operatorname{div} \boldsymbol{\mu}) \right\} dx \end{aligned} \tag{2.6}$$

Generalized J-integral (GJ-integral) is defined on wide variety of (nonlinear) materials. But, to push forward a mathematical argument, we introduce next.

2.1 Quasilinear elliptic systems of p-structure

For a mathematical example, we try to take up *quasilinear elliptic systems of p-structure* (see e.g. [30]). Here, we make them general setting.

Assume that $\Omega \subset \mathbb{R}^d \, (2 \le d)$ is decomposed a finite number of pairwise disjoint subdomains $\Omega_i \subset \Omega, i = 1, \cdots, M$ with local Lipschitz property, such that $\overline{\Omega} = \sum_{i=1}^M \overline{\Omega_i}$. For $m \ge 1$ and $1 \le i \le M$, let $\widehat{W}_i(x, \zeta) : x \in \Omega, \zeta \in \mathbb{R}^{m\times d}$ be scalar functions. We consider the mathematical model of composite material (transmission problem): For given functions $\boldsymbol{u}_D, \boldsymbol{f}, \boldsymbol{g}$, find $\boldsymbol{u}, \boldsymbol{u}_i = \boldsymbol{u}|_{\Omega_i}$ such that

$$-\mathrm{div}_x(\nabla_\zeta \widehat{W}_i(x, \nabla \boldsymbol{u}_i(x))) = \boldsymbol{f}(x) \quad x \in \Omega_i, 1 \le i \le M \tag{2.7}$$

$$\boldsymbol{u}_i = \boldsymbol{u}_j \quad \text{on } \Gamma_{ij} = \partial\Omega_i \cap \partial\Omega_j \tag{2.8}$$

$$\nabla_\zeta \widehat{W}(x, \nabla u_i)\boldsymbol{n}_{ij} = -\nabla_\zeta \widehat{W}(x, \nabla u_j)\boldsymbol{n}_{ji} \quad \text{on } \Gamma_{ij} \tag{2.9}$$

$$\boldsymbol{u} = \boldsymbol{u}_D \quad \text{on } \Gamma_D \tag{2.10}$$

$$\nabla_\zeta \widehat{W}(x, \nabla u_i)\boldsymbol{n}_i = \boldsymbol{g} \quad \text{on } \Gamma_N \tag{2.11}$$

where $\boldsymbol{n}_i(x)$ denote the outword unit vector of Ω at $x \in \partial\Omega_i$ and $\boldsymbol{n}_{ij}$ the outward unit normal to Γ_{ij}.

The (k, l)-element of $\nabla_\zeta \widehat{W}_i$ is

$$\left(\nabla_\zeta \widehat{W}_i(x, \zeta) \right)_{k,l} = \frac{\partial \widehat{W}_i(x, \zeta)}{\partial \zeta_{kl}} \quad (1 \le k \le m, 1 \le l \le d)$$

For $\zeta, \tilde{\zeta}, \widehat{\zeta} \in \mathbb{R}^{m\times d}$ and $x \in \Omega_i$

$$
\begin{aligned}
\nabla_\zeta \widehat{W}_i(x,\zeta) : \tilde{\zeta} &= \sum_{k=1}^{m}\sum_{l=1}^{d} \frac{\partial \widehat{W}_i(x,\zeta)}{\partial \zeta_{kl}} \tilde{\zeta}_{kl} \quad (1 \le k \le m, 1 \le l \le d) \\
\left(\mathrm{div}_x(\nabla_\zeta \widehat{W}_i(x, \nabla \boldsymbol{u}_i(x)))\right)_j &= \sum_{l=1}^{d} \left(\frac{\partial}{\partial x_l} \nabla_\zeta \widehat{W}_i(x, \nabla u(x)) \right)_{j,l} \\
\nabla_\zeta^2 \widehat{W}_i(x,\zeta)[\tilde{\zeta}, \widehat{\zeta}] &= \sum_{k,j=1}^{m} \sum_{s,r=1}^{d} \frac{\partial^2 \widehat{W}_i(x,\zeta)}{\partial \zeta_{ks} \partial \zeta_{jr}} \tilde{\zeta}_{ks} \widehat{\zeta}_{jr} \\
\left| \nabla_\zeta^2 \widehat{W}_i(x,\zeta) \right| &= \left(\sum_{k,j=1}^{m} \sum_{s,r=1}^{d} \left(\frac{\partial^2 \widehat{W}_i(x,\zeta)}{\partial \zeta_{ks} \partial \zeta_{jr}} \right)^2 \right)^{1/2}
\end{aligned}
$$

For $1 < p_i < \infty, i = 1, \cdots, M$, let $\boldsymbol{p} = (p_1, \cdots, p_M)$ and $p_{\min} = \min\{p_i, 1 \le i \le M\}$ and define

$$
\begin{aligned}
L^{\boldsymbol{p}}(\Omega) &= \{\boldsymbol{v} \in L^{p_{\min}}(\Omega; \mathbb{R}^m);\ \boldsymbol{v}|_{\Omega_i} \in L^{p_i}(\Omega_i)\} \\
W^{1,\boldsymbol{p}}(\Omega) &= \left\{\boldsymbol{v} \in W^{1,p_{\min}}(\Omega; \mathbb{R}^m);\ \boldsymbol{v}|_{\Omega_i} \in W^{1,p_i}(\Omega_i)\right\} \\
V(\Omega, \Gamma_D) &= \left\{\boldsymbol{v} \in W^{1,\boldsymbol{p}}(\Omega);\ \boldsymbol{v} = \boldsymbol{u}_D \quad \text{on } \Gamma_D\right\}
\end{aligned}
$$

Problem 2.2 **($P(\boldsymbol{f}, \boldsymbol{g}; V(\Omega, \Gamma_D))$)** *For given $\boldsymbol{f} \in L^{\boldsymbol{q}}(\Omega; \mathbb{R}^m), \boldsymbol{q} = (q_1, \cdots, q_M), p_i^{-1} + q_i^{-1} = 1$, $\boldsymbol{u}_D \in W^{1-\frac{1}{\boldsymbol{p}}, \boldsymbol{p}}(\Gamma_D)$ and $\boldsymbol{g} \in L^{\boldsymbol{q}}(\Gamma_N)$, find $\boldsymbol{u} \in V(\Omega, \Gamma_D)$ such that*

$$
\begin{aligned}
\mathcal{E}(\boldsymbol{u}; \boldsymbol{f}, \boldsymbol{g}, \Omega) &= \min_{\boldsymbol{u} \in V(\Omega, \Gamma_D)} \mathcal{E}(\boldsymbol{v}; \boldsymbol{f}, \boldsymbol{g}, \Omega) \\
\mathcal{E}(\boldsymbol{v}; \boldsymbol{f}, \boldsymbol{g}, \Omega) &= \int_\Omega \left(\widehat{W}(x, \nabla v) - \boldsymbol{f} \cdot \boldsymbol{v} \right) dx - \int_{\Gamma_N} \boldsymbol{g} \cdot \boldsymbol{v}\, ds \\
\widehat{W}(x, \nabla u(x)) &= \widehat{W}_i(x, \nabla u_i(x)) \quad \text{if } x \in \Omega_i, \quad 1 \le i \le M
\end{aligned}
$$

Conditions for $\widehat{W}(x,\zeta)$ are necessary to show the existence of the solution $\boldsymbol{u}$ mathematically. For example,

Theorem 2.3 *If $\widehat{W}(x,\zeta)$ satisfy the following properties and the surface measure of Γ_D is positive, then there is a solution $\boldsymbol{u}$.*

(a) *There is a $\beta \in \mathbb{R}$ such that*

$$\beta \le \widehat{W}(x,\zeta) \qquad \text{for all } x \in \Omega, \zeta \in \mathbb{R}^{m\times d}$$

(b) Convexity: *$[\zeta \mapsto \widehat{W}(x,\zeta)]$ is convex for all $x \in \Omega$, i.e.*

$$\widehat{W}(x, \lambda\zeta + (1-\lambda)\tilde{\zeta}) \le \lambda \widehat{W}(x,\zeta) + (1-\lambda)\widehat{W}(x,\tilde{\zeta}) \quad \text{for all } \lambda \in [0,1]$$

(c) Continuity and measurability: *For all $x \in \Omega$, $[\zeta \mapsto \widehat{W}(x,\zeta)]$ is continuous, and $[x \mapsto \widehat{W}(x,\zeta)]$ is measurable for all $\zeta \in \mathbb{R}^{m\times d}$.*

(d) Coerciveness: *There is constants $\alpha > 0$ such that*

$$\widehat{W}(x,\zeta) \ge \alpha|\zeta|^{p_i} + \beta \quad \text{for all } x \in \Omega_i \text{ and for } \zeta \in \mathbb{R}^{m\times d}$$

For the coerciveness (d), we have from $1 < p_{\min} \leq p_i, 1 \leq i \leq M$,

$$\widehat{W}(x, \zeta) \geq \alpha |\zeta|^{p_{\min}} + \beta$$

Then we obtain $\boldsymbol{u} \in W^{p_{\min}}(\Omega; \mathbb{R}^m)$ by [10, Therem 7.3-2]. Using (d) again, we have

$$\alpha \int_{\Omega} |\nabla u_i|^{p_i} dx + \beta \leq \int_{\Omega_i} \widehat{W}(x, \nabla u_i(x)) dx < \infty$$

This means $\boldsymbol{u} \in V(\Omega, \Gamma_D)$. □

Definition 2.4 *We say that* $[\boldsymbol{v} \mapsto \mathcal{E}(\boldsymbol{v}; \boldsymbol{f}, \boldsymbol{g}, \Omega)]$ *is* weakly lower semicontinuous *on* $V(\Omega, \Gamma_D)$ *if*

$$\mathcal{E}(\boldsymbol{v}_0; \boldsymbol{f}, \boldsymbol{g}, \Omega) \leq \lim_{n\to\infty} \inf \mathcal{E}(\boldsymbol{v}_n; \boldsymbol{f}, \boldsymbol{g}, \Omega)$$

for any $\boldsymbol{v}_0 \in V(\Omega, \Gamma_D)$ *and for any sequence* $\{\boldsymbol{v}_n\}_{n=1}^{\infty}$ *of elements of* $V(\Omega, \Gamma_D)$ *such that* $\boldsymbol{v}_n \to \boldsymbol{v}_0$ *weakly as* $n \to \infty$.

In [10, Theorem 7.3-1], it is proven that the condition (a)–(c) derive the weakly lower semicontinuity of $\mathcal{E}(\cdot; \boldsymbol{f}, \boldsymbol{g}, \Omega)$.

The inequality

$$\left(\nabla_\zeta \widehat{W}(x, \zeta) - \nabla_\zeta \widehat{W}(x, \tilde{\zeta})\right) : (\zeta - \tilde{\zeta}) > 0 \quad \text{for all } \zeta, \tilde{\zeta} \in \mathbb{R}^{m\times d}, \zeta \neq \hat{\zeta} \tag{2.12}$$

leads that

$$\int_{\Omega} \left(\nabla_\zeta \widehat{W}(x, \nabla \boldsymbol{v}) - \nabla_\zeta \widehat{W}(x, \nabla \boldsymbol{w})\right) : (\nabla \boldsymbol{u} - \nabla \boldsymbol{w}) > 0$$

for all $\boldsymbol{v}, \boldsymbol{w} \in V(\Omega, \Gamma_D), \boldsymbol{v} \neq \boldsymbol{w}$, which is called *strictly monotone*.

Theorem 2.5 *If* $\widehat{W}(x, \zeta)$ *satisfy the following properties and the surface measure of* Γ_D *is positive, then there is unique solution* $\boldsymbol{u}$.

(a) *There is a* $\beta \in \mathbb{R}$ *such that*

$$\beta \leq \widehat{W}(x, \zeta) \qquad \text{for all } x \in \Omega, \zeta \in \mathbb{R}^{m\times d}$$

(b) $\widehat{W}(x, \zeta)$ *satisfy (2.12).*

See e.g. [16, 26.10] for the proof.

Theorem 2.6 *If* $\widehat{W}(x, \zeta)$ *satisfy the following properties and the surface measure of* Γ_D *is positive, then there is unique solution* $\boldsymbol{u}$. *For each* $1 \leq i \leq M$, $\widehat{W}_i$ *and their derivatives satisfy the following growth properties for* $1 < p_i < \infty$,

H0 $[\zeta \mapsto \widehat{W}_i(x, \zeta)] \in C^1(\mathbb{R}^{m\times d}) \cap C^2(\mathbb{R}^{m\times d} \setminus \{0\})$ *for every* $x \in \Omega_i$. *For fixed* $\zeta \in \mathbb{R}^{m\times d}$, *there is a constant* $L_i > 0$ *such that*

$$\left|\widehat{W}_i(x, \zeta) - \widehat{W}_i(x, \zeta)\right| \leq L_i |x - y| (1 + |\zeta|^{p_i}) \quad \text{for every } x, y \in \Omega_i$$

H1 *There is* $c_0^i \in \mathbb{R}, c_1^i, c_2^i > 0$ *such that for every* $\zeta \in \mathbb{R}^{m\times d}, x \in \Omega_i$,

$$c_0^i + c_1^i|\zeta|^{p_i} \leq \widehat{W}_i(x,\zeta) \leq c_2^i(1+|\zeta|^{p_i})$$

H4 *There is* $c_i > 0$ *and* $\kappa_i \in \{0,1\}$ *such that for every* $\zeta, \tilde{\zeta} \in \mathbb{R}^{m\times d}, \zeta \neq 0, x \in \Omega_i$,

$$\nabla_\zeta^2 \widehat{W}_i(x,\zeta)[\tilde{\zeta},\tilde{\zeta}] \geq c_i(\kappa_i + |\zeta|)^{p_i-2}|\tilde{\zeta}|^2$$

See the proof of [30], it is proven that (2.12) holds from the conditions **H0** and **H4**.

Theorem 2.7 *The domain integral (2.6) take finite value for the solution* $\boldsymbol{u}$ *of Problem 2.2, if* $\widehat{W}(x,\zeta)$ *satisfy the following,*

H2 *There is* $c^i > 0$ *such that for every* $\zeta \in \mathbb{R}^{m\times d}, x \in \Omega_i$,

$$\left|\nabla_\zeta \widehat{W}_i(x,\zeta)\right| \leq c^i\left(1+|\zeta|^{p_i-1}\right) \tag{2.13}$$

Proof. $R_\omega(\boldsymbol{u},\boldsymbol{\mu})$ is decomposed as follows

$$\begin{aligned}
R_\omega(u,\boldsymbol{\mu}) = &-\sum_{i=1}^{M}\int_{\omega\cap\Omega_i}\left\{\nabla_x\widehat{W}_i(x,\nabla\boldsymbol{u}_i)\cdot\boldsymbol{\mu} + f\cdot(\nabla\boldsymbol{u}_i\cdot\boldsymbol{\mu})\right\}dx \\
&+\sum_{i=1}^{M}\int_{\omega\cap\Omega_i}\left\{\left(\nabla_\zeta\widehat{W}_i(x,\nabla\boldsymbol{u}_i)\right)^T(\nabla\boldsymbol{\mu}^T)\nabla\boldsymbol{u}_i - \widehat{W}_i(x,\nabla\boldsymbol{u}_i)(\operatorname{div}\boldsymbol{\mu})\right\}dx
\end{aligned}$$

The first term in the right hand side is finite by **H0**, the second term by $\boldsymbol{f} \in L^q(\Omega;\mathbb{R}^m), \nabla\boldsymbol{u} \in L^p(\Omega;\mathbb{R}^m)$ and the last term by **H1**. We can show that the third term is finite by **H2** using Hölder's inequality(see e.g. [2, 2.4]) as follows,

$$\begin{aligned}
\int_{\omega\cap\Omega_i}\left|\left(\nabla_\zeta\widehat{W}_i(x,\nabla\boldsymbol{u}_i)\right)^T(\nabla\boldsymbol{\mu}^T)\nabla\boldsymbol{u}_i\right|dx &\leq c_0\int_{\Omega_i}(1+|\nabla\boldsymbol{u}|^{p_i-1})|\nabla\boldsymbol{u}|dx \\
&\leq c_0(1+\||\nabla\boldsymbol{u}|^{p_i-1}\|_{L^{q_i}(\Omega_i)})\|\nabla\boldsymbol{u}\|_{L^{p_i}(\Omega_i)} \\
&\leq c_0(1+\|\boldsymbol{u}\|_{L^{p_i}(\Omega_i)}^{p_i-1})\|\nabla\boldsymbol{u}\|_{L^{p_i}(\Omega_i)}
\end{aligned}$$

It is important $R_\omega(\boldsymbol{u},\boldsymbol{\mu})$ *is finite for the (weak) solution* of Problem 2.2, but we need *smoothness of* $\boldsymbol{u}$ *on* $\partial(\omega\cap\Omega)$ *to show that* $P_\omega(\boldsymbol{u},\boldsymbol{\mu})$ *is finite.*

2.2 Properties of GJ-integral

Proposition 2.8 (Green's formula) *If* $\mathcal{O} \subset \mathbb{R}^d$ *is the domain with local Lipschitz property, then the outward unit normal* $\boldsymbol{n}$ *exists allmost every on* $\partial\mathcal{O}$ *and the Green's formula*

$$\int_{\mathcal{O}} g(\partial_i h)dx = \int_{\partial\mathcal{O}} ghn_i ds - \int_{\mathcal{O}}(\partial_i g)hdx \tag{2.14}$$

hold for $g \in W^{1,s}(\mathcal{O}),\ h \in W^{1,q}(\mathcal{O})$ *with* $s^{-1}+q^{-1} \leq (d+1)/d$ *if* $1 \leq s < d, 1 \leq q < d$, *with* $q > 1$ *if* $s \geq d$ *and with* $s > 1$ *if* $q \geq d$.

See [38, Theorem 1.1,Chapter 3] for the proof.

Theorem 2.9 *Now we take the field of view* ω *such that* $\overline{\omega} \subset \Omega_i$ *for some* $0 \le i \le M$. *Assume that the solution* $\boldsymbol{u}$ *of Problem 2.2 has the regularity such as* $\boldsymbol{u}|_\omega \in W^{2,p_i}(\omega)$. *Then the following holds.*

$$J_\omega(\boldsymbol{u}, \boldsymbol{\mu}) = 0 \qquad \forall \mu \in W^{1,\infty}(\mathbb{R}^3; \mathbb{R}^3) \tag{2.15}$$

Proof. By the chain rule,

$$\begin{aligned} \mu_j \frac{\partial}{\partial x_j} \widehat{W}(x, \nabla \boldsymbol{u}) &= \mu_j \frac{\partial}{\partial \xi_j} \widehat{W}(\xi, \nabla \boldsymbol{u}) \Big|_{\xi = x} \\ &\quad + \sum_{k=1}^m \sum_{l=1}^m \mu_j \frac{\partial}{\partial \zeta_{kl}} \widehat{W}(\xi, \zeta) \Big|_{\zeta = \nabla \boldsymbol{u}} \partial_j \partial_l u_k \end{aligned}$$

it follows that $\mu(x) \cdot \nabla_x \widehat{W}(x, \nabla \boldsymbol{u})$ is integrable.

We can apply Green's formula

$$\begin{aligned} \int_\omega (\boldsymbol{\mu} \cdot \nabla) \widehat{W}(\boldsymbol{u}) dx &= \int_{\partial \omega} \widehat{W}(\boldsymbol{u})(\boldsymbol{\mu} \cdot \boldsymbol{n})\, ds \\ &\quad - \int_\omega \widehat{W}(\boldsymbol{u}) \mathrm{div}\, \boldsymbol{\mu}\, dx \end{aligned} \tag{2.16}$$

We can use the *chain rule*

$$\begin{aligned} (\boldsymbol{\mu} \cdot \nabla) \widehat{W}(\boldsymbol{u}) &= (\boldsymbol{\mu} \cdot \nabla_x) \widehat{W}(x, \nabla \boldsymbol{u}) + \nabla_\zeta \widehat{W}(\boldsymbol{u}) : [\nabla(\boldsymbol{\mu} \cdot \nabla u)] \\ &\quad - \nabla_\zeta \widehat{W}(x, \nabla \boldsymbol{u})(\nabla \mu_k) \partial_k \boldsymbol{u}. \end{aligned}$$

Here we used that $\partial_k \partial_j v = \partial_j \partial_k v$. Now, we get by Green's formula

$$\begin{aligned} \int_\omega (\boldsymbol{\mu} \cdot \nabla) \widehat{W}(\boldsymbol{u}) &= \int_\omega \Big\{ (\mu \cdot \nabla_x) \widehat{W}(x, \nabla \boldsymbol{u}) - \nabla_\zeta \widehat{W}(x, \nabla \boldsymbol{u}) \nabla \mu_k \partial_k \boldsymbol{u} \Big\}\, dx \\ &\quad + \int_\omega \nabla_\zeta \widehat{W}(x, \nabla \boldsymbol{u}) : [\nabla(\boldsymbol{\mu} \cdot \nabla \boldsymbol{u})] dx \end{aligned} \tag{2.17}$$

The formula (2.7) holds in distribution sense, we obtain the following by *Green's formula*

$$\int_\Omega \nabla_\zeta \widehat{W}(x, \nabla \boldsymbol{u}) : [\nabla(\boldsymbol{\mu} \cdot \nabla \boldsymbol{u})]\, dx = \int_{\partial \omega} \widehat{T}(\boldsymbol{u}) \cdot (\boldsymbol{\mu} \cdot \nabla \boldsymbol{u}) ds + \int_\omega \boldsymbol{f} \cdot (\boldsymbol{\mu} \cdot \nabla \boldsymbol{u})\, dx \tag{2.18}$$

From (2.16)–(2.18), we get that $J_\omega(\boldsymbol{u}, \boldsymbol{\mu}) = 0$. □

Remark 2.10 *If we take the field of view* ω *to become* $\overline{\Omega} \subset \omega$, *then* $\partial \omega \cap \Omega = \emptyset$ *which means*

$$J_\omega(\boldsymbol{u}, \boldsymbol{\mu}) = R_\Omega(\boldsymbol{u}, \boldsymbol{\mu})$$

Remark 2.11 *Even though* $\boldsymbol{u}|_\omega \notin W^{2,p_i}(\omega)$, *the identity (2.15) hold if* $\boldsymbol{u}$ *satisfies (2.16)–(2.18).*

Corollary 2.12 *Let* $\omega_2 \subset \omega_1$ *be two open sets such that there (2.16)–(2.18) hold in* $\omega_1 \setminus \overline{\omega_2}$. *Then*

$$J_{\omega_1}(\boldsymbol{u}, \boldsymbol{\mu}) = J_{\omega_2}(\boldsymbol{u}, \boldsymbol{\mu}) \tag{2.19}$$

Proof. Since (2.16)–(2.18) hold in $\omega_1\backslash\overline{\omega_2}$

$$\begin{aligned}R_{\omega_1}(\boldsymbol{u},\boldsymbol{\mu})-R_{\omega_2}(\boldsymbol{u},\boldsymbol{\mu}) &= R_{\omega_1\backslash\overline{\omega_2}}(\boldsymbol{u},\boldsymbol{\mu})\\ &= -P_{\omega_1\backslash\overline{\omega_2}}(\boldsymbol{u},\boldsymbol{\mu})\\ &= -P_{\omega_1}(\boldsymbol{u},\boldsymbol{\mu})+P_{\omega_2}(\boldsymbol{u},\boldsymbol{\mu})\end{aligned}$$

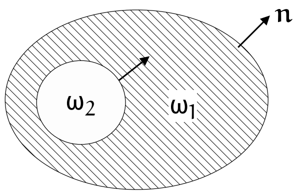

2.3 Examples of variational problems $P(\boldsymbol{f},\boldsymbol{g};V(\Omega,\Gamma_D))$

2.3.1 Elliptic boundary value problem

There is Poisson equation $\widehat{W}(x,\zeta)=|\zeta|^2/2, \quad \zeta\in\mathbb{R}^d \quad (m=1)$ for the simplest example, whose GJ-integral is the form

$$\begin{aligned}P_\omega(u,\boldsymbol{\mu}) &= \int_{\partial\omega\cap\Omega}\left\{\frac{1}{2}|\nabla u|^2(\boldsymbol{\mu}\cdot\boldsymbol{n})-\frac{\partial u}{\partial n}(\boldsymbol{\mu}\cdot\nabla u)\right\}ds,\\ R_\omega(u,\boldsymbol{\mu}) &= -\int_{\omega\cap\Omega}\left\{f(\boldsymbol{\mu}\cdot\nabla u)-(\nabla u\cdot\nabla\mu_k)\partial_k u+\frac{1}{2}|\nabla u|^2\mathrm{div}\boldsymbol{\mu}\right\}dx.\end{aligned}$$

The simplest non-linear problem is p-Poisson, that is, $\widehat{W}(x,\zeta)=|\zeta|^p/p$ for some $1\le p<\infty$, which leads the boundary value problem

$$\begin{aligned}-\mathrm{div}\left(|\nabla u|^{p-2}\nabla u\right) &= f \qquad \text{in } \Omega\\ u &= 0 \qquad \text{on } \Gamma_D\\ \frac{\partial u}{\partial n} &= g \qquad \text{on } \Gamma_N.\end{aligned} \tag{2.20}$$

whose GJ-integral is

$$\begin{aligned}P_\omega(u,\boldsymbol{\mu}) &= \int_{\partial\omega\cap\Omega}\left\{\frac{1}{p}|\nabla u|^p(\boldsymbol{\mu}\cdot\boldsymbol{n})-|\nabla u|^{p-2}\frac{\partial u}{\partial n}(\boldsymbol{\mu}\cdot\nabla u)\right\}ds,\\ R_\omega(u,\boldsymbol{\mu}) &= -\int_{\omega\cap\Omega}\left\{f(\boldsymbol{\mu}\cdot\nabla u)-|\nabla u|^{p-2}(\nabla u\cdot\nabla\mu_k)\partial_k u+\frac{1}{p}|\nabla u|^p\mathrm{div}\boldsymbol{\mu}\right\}dx.\end{aligned}$$

We now consider the case

$$\widehat{W}(x,z,\zeta) \quad x\in\Omega, z\in\mathbb{R}^m,\zeta\in\mathbb{R}^{m\times d}$$

such as, in the linear equation $(m=1)$

$$-\partial_j a_{ij}(x)\partial_i u(x)+b(x)u(x)=f(x) \qquad \text{in } \Omega$$

it become $\widehat{W}(x,z,\zeta)=(a_{ij}\zeta_i\zeta_j+bz^2)/2$. *GJ-integral is the same form, even if*

$\widehat{W} = \widehat{W}(x, z, \zeta)$,

$$\begin{aligned}P_\omega(u, \boldsymbol{\mu}) &= \int_{\partial\omega\cap\Omega} \left\{ \frac{1}{2}(a_{ij}D_j u D_i u + bu^2)(\boldsymbol{\mu}\cdot\boldsymbol{n}) - (n_i a_{ij}\partial_j u)(\boldsymbol{\mu}\cdot\nabla u) \right\} ds, \\ R_\omega(u, \boldsymbol{\mu}) &= -\int_{\omega\cap\Omega} \left\{ \frac{1}{2}((\boldsymbol{\mu}\cdot\nabla a_{ij})\partial_j u \partial_i u + (\boldsymbol{\mu}\cdot\nabla b)u^2) + f(\boldsymbol{\mu}\cdot\nabla u) \right. \\ &\qquad \left. -(a_{ij}\partial_j u \partial_i \mu_k)\partial_k u + \frac{1}{2}(a_{ij}\partial_j u\partial_i u + bu^2)\mathrm{div}\boldsymbol{\mu} \right\} dx.\end{aligned}$$

2.3.2 Linear elasticity

We consider the *linear elastic field* (the case $m = d$) which is given by the following formulae

$$\begin{aligned}&\widehat{W}(x, z, \zeta) = \frac{1}{2}\sigma_{ij}(x, \zeta)e_{ij}(\zeta), \qquad (2.21)\\ &e_{ij}(\zeta) = (\zeta_{i,j} + \zeta_{j,i})/2 \qquad \text{for } 1 \le i,\ j \le d, \\ &c_{ijkl}(x) \text{ denotes Hooke's tensor components, } c_{ijkl} = c_{jikl} = c_{klij}.\end{aligned}$$

The variational problem $P(\boldsymbol{f}, \boldsymbol{g};\ V(\Omega, \Gamma_D))$ corresponding to the space

$$V(\Omega, \Gamma_D) = \left\{ \boldsymbol{v} \in W^{1,2}(\Omega; \mathbb{R}^d);\ \boldsymbol{v} = \boldsymbol{0} \text{ on } \Gamma_D \right\}, \qquad (2.22)$$

implies the boundary value problem

$$\begin{aligned}-\partial_j c_{ijkl} e_{kl}(\boldsymbol{u}) &= f_i \qquad \text{in } \Omega, \qquad i = 1, \cdots, d, \qquad (2.23)\\ \boldsymbol{u} &= \boldsymbol{0} \quad \text{on } \Gamma_D, \qquad \sigma_{ij}(\boldsymbol{u})n_j = g_i \quad \text{on } \Gamma_N. \qquad (2.24)\end{aligned}$$

For uniqueness of the solution to the problem $\mathrm{P}(\boldsymbol{f}, \boldsymbol{g}, V(\Omega, \Gamma_D))$, we assume that the elements c_{ijkl} satisfy the following inequality

$$c_{ijkl}\xi_{ij}\xi_{jk} \ge \alpha\xi_{ij}\xi_{ij} \qquad \text{for all } \xi_{ij} \in \mathbb{R}^1;\ \alpha > 0. \qquad (2.25)$$

GJ-integral is the following

$$\begin{aligned}P_\omega(u, \boldsymbol{\mu}) &= \int_{\partial\omega\cap\Omega} \left\{ \frac{1}{2}\sigma_{ij}(\boldsymbol{u})e_{ij}(\boldsymbol{u})(\boldsymbol{\mu}\cdot\boldsymbol{n}) - \sigma_{ij}n_j(\boldsymbol{\mu}\cdot\nabla u_i) \right\} ds, \\ R_\omega(u, \boldsymbol{\mu}) &= -\int_{\omega\cap\Omega} \left\{ \frac{1}{2}(\boldsymbol{\mu}\cdot\nabla c_{ijkl})e_{kl}(\boldsymbol{u})e_{ij}(\boldsymbol{u}) + \boldsymbol{f}_i(\boldsymbol{\mu}\cdot\nabla u_i) \right. \\ &\qquad \left. - \sigma_{ij}(\boldsymbol{u})\partial_j\mu_k\partial_k u_i + \frac{1}{2}\sigma_{ij}(\boldsymbol{u})e_{ij}(\boldsymbol{u})\mathrm{div}X \right\} dx.\end{aligned}$$

2.3.3 Elasto-plasticity

Consider the case corresponding to elasto-plasticity (see [39, Chapter8]) with Lamé constants λ and ρ

$$\widehat{W}(x, \nabla\boldsymbol{v}) = k(x)\theta^2(\boldsymbol{v})/2 + \int_0^{\Gamma(\boldsymbol{v},\boldsymbol{v})} \rho(x)(x, \sigma)d\sigma, \qquad (2.26)$$

where $\theta(\boldsymbol{v}) = \mathrm{div}\boldsymbol{v}, \Gamma(\boldsymbol{v}, \boldsymbol{w}) = -2\theta(\boldsymbol{v})\theta(\boldsymbol{w})/3 + 2e_{ij}(\boldsymbol{v})e_{ij}(\boldsymbol{w})$. For coercivity, we require $\widehat{W}$ to satisfy the following conditions. Assume that $k \in C^2(\mathbb{R}^d)$,

$\rho \in C^2(\mathbb{R}^d \times [0,\infty))$, and suppose the existence of constants $k_0 > 0, k_1 > 0$ and $\rho_0 > 0, \rho_1 > 0$ such that

$$0 < k_0 \le k(x) \le k_1 < \infty, \quad |\nabla k(x)| \le k_1 < \infty \qquad \text{for all } x \in \mathbb{R}^d, \tag{2.27}$$

$$\begin{aligned} &0 < \rho_0 \le \rho(x,s) \le 3k(x)/2, \\ &|\nabla_x \rho(x,s)| \le \rho_1 < \infty, \quad \text{for all } x \in \mathbb{R}^d \quad \text{and } s \ge 0. \end{aligned} \tag{2.28}$$

We also assume that the inequalities

$$0 < \xi \le \rho(x,s) + 2(\partial\rho(x,s)/\partial s)s \le \xi_1 \tag{2.29}$$

hold with some constants ξ_1, ξ.

The problem $P(\boldsymbol{f}, \boldsymbol{g}; V(\Omega, \Gamma_D))$ implies the equation (2.23) with nonlinear Hooke's tensor

$$c_{ijkl} = \left(k - \frac{3}{2}\mu(\Gamma^2(\boldsymbol{u}))\right)\delta_{ij}\delta_{kl} + \mu(\Gamma^2(\boldsymbol{u}))(\delta_{ik}\delta_{jl} + \delta_{il}\delta_{jk}). \tag{2.30}$$

Here $\Gamma^2(\boldsymbol{u}) = \Gamma(\boldsymbol{u}, \boldsymbol{u})$, δ_{ij} are the elements of Kronecker's symbol, and (2.30) is derived from the consideration of generalized Hooke's law (see [39, Chapter 3]). GJ-integral is the following

$$\begin{aligned} P_\omega(u, \boldsymbol{\mu}) &= \int_{\partial\omega\cap\Omega} \left\{\widehat{W}(x, \nabla\boldsymbol{u})(\boldsymbol{\mu}\cdot\boldsymbol{n}) - (n_j c_{ijkl}(\boldsymbol{u})e_{kl}(\boldsymbol{u}))(\boldsymbol{\mu}\cdot\nabla u_i)\right\} ds, \\ R_\omega(u, X) &= -\int_{\omega\cap\Omega} \Bigg\{(\boldsymbol{\mu}\cdot\nabla k)(\mathrm{div}\boldsymbol{u})^2/2 + \int_0^{\Gamma(\boldsymbol{u},\boldsymbol{u})} \boldsymbol{\mu}\cdot\nabla_x\rho(x,\sigma)d\sigma \\ &\qquad + f_i(\boldsymbol{\mu}\cdot\nabla u_i) - c_{ijkl}(\boldsymbol{u})e_{kl}(\boldsymbol{u})\partial_j\mu_p\partial_p u_i + \widehat{W}(x, \boldsymbol{u})\mathrm{div}X\Bigg\} dx \end{aligned}$$

2.3.4 Micropolar elasticity

Considering the case $d \ne m$, we introduce micropolar continuum mechanics (see [14]). For this material, $d = 3$, $m = 6$. Let $\tilde{\boldsymbol{u}} = (\boldsymbol{u}, \boldsymbol{\psi})$ be six-component vectors, and let $\boldsymbol{u} = (u_1, u_2, u_3), \boldsymbol{\psi} = (\psi_1, \psi_2, \psi_3)$ be defined in the domain $\psi \subset \mathbb{R}^3$. The linearized approximation is called the couple-stress theory, see [34, p. 147], in which (Lamé constants are λ and ρ)

$$\begin{aligned} 2\widehat{W}(\nabla\tilde{\boldsymbol{u}}) &= \{(3\lambda + 2\rho)/3\}|\mathrm{div}\boldsymbol{u}|^2 + (\rho/2)\sum_{i,j}|\partial_j u_i + \partial_i u_j - (2/3)\delta_{ij}\mathrm{div}\boldsymbol{u}|^2 \\ &\quad + (\alpha/2)\sum_{i,j}|\partial_j u_i - \partial_i u_j + 2\varepsilon_{kji}\psi_k|^2 + \{(3\epsilon + 2\upsilon)/3\}|\mathrm{div}\boldsymbol{\psi}|^2 \\ &\quad + (\upsilon/2)\sum_{i,j}|\partial_i\psi_j + \partial_j\psi_i - (2/3)\delta_{ij}\mathrm{div}\boldsymbol{\psi}|^2 \\ &\quad + (\beta/2)\sum_{i,j}|\partial_j\psi_i - \partial_i\psi_j|^2 \end{aligned} \tag{2.31}$$

where $\lambda, \rho, \alpha, \epsilon, \upsilon, \beta$ are constants satisfying the conditions

$$\rho > 0,\ 3\lambda + 2\rho > 0,\ \alpha > 0,\ \upsilon > 0,\ 3\epsilon + 2\upsilon > 0,\ \beta > 0,$$

and ε_{kij} is the permutation tensor. If displacements and rotations are zero on Γ_D and the couple stresses are zero on Γ_N, then

$$V(\Omega,\Gamma_D)=\left\{\tilde{\boldsymbol{v}}=(\boldsymbol{v},\boldsymbol{\psi})\in W^{1,2}(\Omega;\mathbb{R}^6)|\,\tilde{\boldsymbol{v}}=\boldsymbol{0}\text{ on }\Gamma_D\right\}. \tag{2.32}$$

From [44] the following estimate for $\tilde{u}\in V(\Omega;\Gamma_D)$ is obtained,

$$\int_\Omega \widehat{W}(\nabla\tilde{u})dx\geq C_3\|\tilde{u}\|^2_{W^{1,2}(\Omega;\mathbb{R}^6)} \tag{2.33}$$

with a constant $C_3>0$ independent of $\tilde{\boldsymbol{u}}$. Under the conditions (2.31)–(2.32), the variational problem $P(\boldsymbol{f},\boldsymbol{g},V(\Omega,\Gamma_D))$ implies the following boundary value problem with $\boldsymbol{f}=(f_1,f_2,f_3)$, $\boldsymbol{f}_m=(f_4,f_5,f_6)$, for $i=1,2,3$,

$$\left\{\begin{array}{rl}(\rho+\alpha)\Delta\boldsymbol{u}+(\lambda+\rho-\alpha)\mathrm{grad}\,\mathrm{div}\,\boldsymbol{u}+2\alpha\mathrm{rot}\,\psi=-\boldsymbol{f} & \text{in }\Omega,\\ (\upsilon+\beta)\Delta\psi+(\epsilon+\upsilon-\beta)\mathrm{grad}\,\mathrm{div}\,\psi+\mathrm{rot}\,\boldsymbol{u}-4\alpha\psi=-\boldsymbol{f}_m & \text{in }\Omega,\\ \boldsymbol{u}=0,\ \boldsymbol{\psi}=0 & \text{on }\Gamma_D,\\ \lambda n_i\mathrm{div}\,\boldsymbol{u}+(\rho+\alpha)n_j\partial_iu_j+(\rho-\alpha)n_j\partial_ju_i-2\alpha\varepsilon_{ijk}n_j\psi_k=0 & \text{on }\Gamma_N,\\ \epsilon n_i\mathrm{div}\,\boldsymbol{\psi}+(\rho+\beta)n_j\partial_i\psi_j+(\rho-\beta)n_j\partial_j\psi_i=g_i & \text{on }\Gamma_N.\end{array}\right. \tag{2.34}$$

GJ-integral is the following

$$\begin{aligned}P_\omega(u,\boldsymbol{\mu}) &= \int_{\partial\omega\cap\Omega}\Big\{\widehat{W}(\nabla\tilde{\boldsymbol{u}})(\boldsymbol{\mu}\cdot\boldsymbol{n})-(\sigma_{E,ij}(\boldsymbol{u},\psi)n_j)(\boldsymbol{\mu}\cdot\nabla u_i)\\ &\qquad -(\sigma_{R,ij}(\boldsymbol{\psi})n_j)(\boldsymbol{\mu}\cdot\nabla\psi_i)\}\,ds,\\ R_\omega(u,\boldsymbol{\mu}) &= -\int_{\omega\cap\Omega}\Big\{\boldsymbol{f}(\boldsymbol{\mu}\cdot\nabla\tilde{u})-\sigma_{E,ij}(\boldsymbol{u},\boldsymbol{\psi})\partial_j\mu_p\partial_pu_i\\ &\qquad -\sigma_{R,ij}(\boldsymbol{\psi})\partial_j\mu_p\partial_p\psi_i+\widehat{W}(\nabla\tilde{\boldsymbol{u}})\mathrm{div}\boldsymbol{\mu}\Big\}\,dx,\end{aligned}$$

where

$$\begin{aligned}\sigma_{E,ij}(\boldsymbol{u},\boldsymbol{\psi}) &= \lambda\delta_{ij}\mathrm{div}\boldsymbol{u}+(\mu+\alpha)\partial_iu_j+(\mu-\alpha)\partial_ju_i-2\alpha\varepsilon_{ijk}\psi_k,\\ \sigma_{R,ij}(\boldsymbol{\psi}) &= \epsilon\delta_{ij}\mathrm{div}\boldsymbol{\psi}+(\upsilon+\beta)\partial_i\psi_j+(\upsilon-\beta)\partial_j\psi_i.\end{aligned}$$

3 Fundamental theorem

3.1 Historical background

3.1.1 2D Fracture

Let ω' be an open set such that $\Sigma\subset\omega'$ (Fig.7) and $\overline{\omega'}\subset\Omega$. Using the cut-off function $\eta_{\omega'}$ such that $\eta_{\omega'}(x)=1$ near Σ and $\mathrm{supp}\eta_{\omega'}\subset\omega'$, then for the vector field $\boldsymbol{\mu}_C$

$$\begin{aligned}R_\Omega(\boldsymbol{u},\boldsymbol{\mu}_C) &= R_{\Omega\setminus\overline{\omega'}}(\boldsymbol{u},\boldsymbol{\mu}_C)+R_{\omega'}(\boldsymbol{u},\boldsymbol{\mu}_C)\\ &= -P_{\Omega\setminus\overline{\omega'}}(\boldsymbol{u},\boldsymbol{\mu}_C)+R_{\omega'}(\boldsymbol{u},\boldsymbol{\mu}_C)\end{aligned}$$

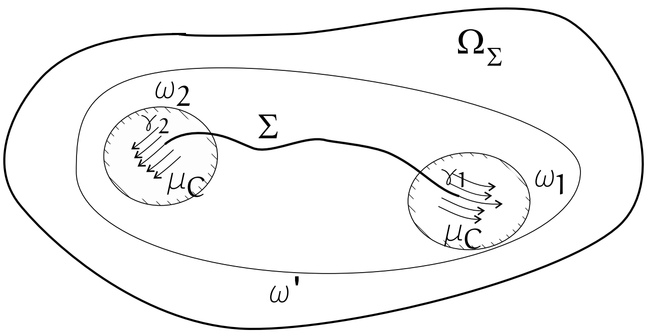

Figure 7: open sets containing the crack tips γ_1, γ_2

Let ω_1, ω_2 be open sets containing the crack tips γ_1, γ_2 (Fig.7), then

$$\begin{aligned} R_{\omega'}(\boldsymbol{u}, \boldsymbol{\mu}_C) &= R_{\omega' \setminus \overline{\omega_1 \cup \omega_2}}(\boldsymbol{u}, \boldsymbol{\mu}_C) + \sum_{l=1}^{2} R_{\omega_l}(\boldsymbol{u}, \boldsymbol{\mu}_C) \\ &= -P_{\omega' \setminus \overline{\omega_1 \cup \omega_2}}(\boldsymbol{u}, \boldsymbol{\mu}_C) + \sum_{l=1}^{2} R_{\omega_l}(\boldsymbol{u}, \boldsymbol{\mu}_C) \\ &= \sum_{l=1}^{2} J_{\omega_l}(\boldsymbol{u}, \boldsymbol{\mu}_C) \end{aligned}$$

Here we used the following: On the crack surface, $\widehat{T}(\boldsymbol{u})^{\pm} = 0$ (stress free) and $\boldsymbol{\mu}_C \cdot \boldsymbol{\nu} = 0$ on Σ where $\boldsymbol{\nu}$ stands for the normal vector directed from '+' to '-'.

$$\int_{\Sigma^{\pm}} \left(\widehat{W}(x, \nabla \boldsymbol{u})(\boldsymbol{\mu}_C \cdot \boldsymbol{\nu}) - \widehat{T}(\boldsymbol{u})(\boldsymbol{\mu}_i \cdot \nabla \boldsymbol{u}) \right) ds = 0$$

From (2.2), we can derive

$$-\frac{d}{dt}\mathcal{E}(\boldsymbol{u}(t); f, \Omega_{\Sigma(t)}) = R_{\Omega}(\boldsymbol{u}, \boldsymbol{\mu}_C) \tag{3.1}$$

3.1.2 Shape Optimization

Consider the Poisson problem

$$-\Delta u = f \quad \text{in } \Omega, \qquad u = 0 \quad \text{on } \partial\Omega$$

with C^2-boundary and Hadamard's perturbation

$$\partial\Omega(t) = \{\gamma + h(\gamma) t \boldsymbol{n}(\gamma) : \gamma \in \partial\Omega\}$$

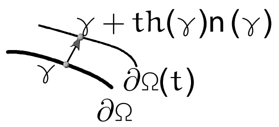

the problem

$$\begin{array}{lll} -\Delta u(t) = f & \text{in} & \Omega(t), \\ u(t) = 0 & \text{on} & \partial\Omega(t) \end{array}$$

$$\left. \frac{d}{dt} \int_{\Omega(t)} |\nabla u(t)|^2 dx \right|_{t=0} = \int_{\partial\Omega} \left(\frac{\partial u}{\partial n} \right)^2 h \, ds \qquad \text{(see e.g. [24, (3.3.58)])}$$

$$\frac{d}{dt}\int_{\Omega(t)}\left(\frac{1}{2}|\nabla u(t)|^2 - fu\right)dx\bigg|_{t=0} = -\int_{\partial\Omega}\left(\frac{\partial u}{\partial n}\right)^2 h\,ds \tag{3.2}$$

because $\int fu(t)\,dx = \int \nabla u(t)\cdot\nabla u(t)\,dx$.

Since $\nabla u = \boldsymbol{n}\cdot\nabla u + \nabla_\tau u$ ($\nabla_\tau = \nabla - (\boldsymbol{n}\cdot\nabla)\boldsymbol{n}$) and $\nabla_\tau u = 0$ on $\partial\Omega$, the right-hand side of (3.2) become as follows

$$-\int_{\partial\Omega}\left(\frac{\partial u}{\partial n}\right)^2 h\,ds = \int_{\partial\Omega}\left(\frac{1}{2}|\nabla u|^2 - \boldsymbol{n}\cdot\nabla u(\boldsymbol{n}\cdot\nabla)u\right)h\,ds$$

Therefore we arrive at the following

$$\frac{d}{dt}\mathcal{E}(u(t);f)\bigg|_{t=0} = P_\Omega(u,h\boldsymbol{n}) \tag{3.3}$$

$$\mathcal{E}(u(t);f.\Omega(t)) = \int_{\Omega(t)}\left(\frac{1}{2}|\nabla u(t)|^2 - fu(t)\right)dx$$

let ω be an open set such that $\partial\Omega\subset\omega$ and $\tilde{\boldsymbol{n}}(x), x\in\omega$ the extension of $\boldsymbol{n}(x), x\in\partial\Omega$. Consider the cut-off function η_ω. In this case, $u\in W^{2,2}(\Omega)$, which leads from Theorem 2.9 that

$$0 = J_\Omega(u,h\boldsymbol{n}) = P_\Omega(u,h\boldsymbol{n}) + R_\Omega(u,h\eta_\omega\tilde{\boldsymbol{n}})$$

We arrive at the following identity

$$\frac{d}{dt}\mathcal{E}(u(t);f,\Omega(t))\bigg|_{t=0} = -R_\Omega(u,h\eta_\omega\tilde{\boldsymbol{n}}) \tag{3.4}$$

3.1.3 Hadamard's variational formula[23]

Let Ω be a domain in $\mathbb{R}^2$ with C^2-boundary and $G(x,y,t), x,y\in\Omega$, $0\le t\le t_0$ Green function, i.e. for $y\in\Omega(t)$

$$-\Delta_x G(x,y,t) = \delta(x-y),\quad G(x,y,t)=0\quad \forall x\in\partial\Omega(t)$$
$$\partial\Omega(t) = \{x + th(\gamma)\boldsymbol{n}(\gamma) : \gamma\in\partial\Omega\}$$

Hadamard's variational formula is

$$\frac{dG(w,y,t)}{dt}\bigg|_{t=0} = \int_{\partial\Omega}\frac{\partial}{\partial\boldsymbol{n}_x}G(x,y)\frac{\partial}{\partial\boldsymbol{n}_x}G(x,w)h(x)\,ds_x \tag{3.5}$$

For a function $f\in C_0^\infty(\Omega)$,

$$u(x,t) = \int_{\Omega(t)} G(x,y,t)f(y)\,dy$$

satisties the boundary value problem

$$-\Delta_x u(x,t) = f(x)\quad x\in\Omega;\qquad u(x,t)=0\quad x\in\partial\Omega$$

For a function $\theta\in C_0^\infty(\Omega)$, we have

$$\begin{aligned}\langle u(t),\theta\rangle &= \int_\Omega u(x,t)\theta(x)\,dx\\ &= \int_{\Omega_x}\int_{\Omega_y} G(x,y,t)f(y)dy\theta(x)dx\end{aligned}$$

Now we obtain

$$
\begin{aligned}
\frac{d}{dt}\langle u(t),\theta\rangle\Big|_{t=0} &= \int_{\Omega_x}\int_{\Omega_y}\frac{d}{dt}G(x,y,t)\Big|_{t=0} f(y)dy\theta(x)dx \\
&= \int_{\Omega_x}\int_{\Omega_y}\int_{\partial\Omega_\xi}\frac{\partial G(\xi,y)}{\partial \boldsymbol{n}_\xi}\frac{\partial G(\xi,x)}{\partial \boldsymbol{n}_\xi}h(\xi)\,ds_\xi f(y)dy\theta(x)dx \\
&= \int_{\partial\Omega}\frac{\partial u}{\partial n}(x)\frac{\partial u_\theta}{\partial n}(x)h(x)ds_x
\end{aligned}
$$

where $\boldsymbol{u}_\theta$ is the solution of the problem

$$
-\Delta u_\theta = \theta \quad \text{in } \Omega; \qquad u_\theta = 0 \quad \text{on } \partial\Omega
$$

For $\epsilon > 0$, we have

$$
\begin{aligned}
P_\Omega(u+\epsilon u_\theta, h\boldsymbol{n}) - P_\Omega(u, h\boldsymbol{n}) &= \int_{\partial\Omega}\left\{\nabla u\cdot\nabla u_\theta - 2\frac{\partial u}{\partial n}\frac{\partial u_\theta}{\partial n}\right\}h\,ds + O(\epsilon^2) \\
&= -\epsilon\int_{\partial\Omega}\frac{\partial u}{\partial n}\frac{\partial u_\theta}{\partial n}h\,ds + O(\epsilon^2)
\end{aligned}
$$

Here we used that $u=0, u_\theta = 0$ on $\partial\Omega$.

We now arrive at the following

$$
\begin{aligned}
\frac{d}{dt}\langle u(t),\theta\rangle &= -\delta P_\Omega(u,u_\theta;h\boldsymbol{n}) \qquad (3.6) \\
\delta P_\Omega(u,u_\theta;h\boldsymbol{n}) &= \lim_{\epsilon\to 0}\epsilon^{-1}\left\{P_\Omega(u+\epsilon u_\theta, h\boldsymbol{n}) - P_\Omega(u,h\boldsymbol{n})\right\}
\end{aligned}
$$

From Theorem 2.9, it follows that

$$
\begin{aligned}
\frac{d}{dt}\langle u(t),\theta\rangle &= \delta R_\Omega(u,u_\theta;h\boldsymbol{n}) \qquad (3.7) \\
\delta R_\Omega(u,u_\theta;h\boldsymbol{n}) &= \lim_{\epsilon\to 0}\epsilon^{-1}\left\{R_\Omega(u+\epsilon u_\theta, h\boldsymbol{n}) - R_\Omega(u,h\boldsymbol{n})\right\}
\end{aligned}
$$

We call the formula (3.7) *the generalization of Hadamard formula (GJ-Hadamard formula).*

Let $\boldsymbol{u}(t)$ be minimizers of functionals

$$
\mathcal{E}(\boldsymbol{v};\Omega(t),\boldsymbol{f},\boldsymbol{g}) = \int_{\Omega(t)}\widehat{W}(x,\nabla\boldsymbol{v})dx - \int_{\Omega(t)}\boldsymbol{f}\cdot\boldsymbol{v}\,dx \qquad (3.8)
$$

over the spaces

$$
V_0(\Omega(t),\Gamma(t)_{D(t)}) = \left\{\boldsymbol{v}\in W^{1,p}(\Omega(t);\mathbb{R}^3) : \boldsymbol{v}=0 \quad \text{on } \Gamma(t)_{D(t)}\right\}
$$

3.1.4 3D Fracture

In 3-dimensional brittle fracture problem (linear case), the relation

$$
-\frac{d}{dt}\mathcal{E}(\boldsymbol{u}(t);\boldsymbol{f},\boldsymbol{g},\Omega_{\Sigma(t)}) = J_\omega(\boldsymbol{u},\boldsymbol{\mu}_\phi) \qquad (3.9)
$$

is proven[43], where $\Omega_{\Sigma(t)} = \Omega\setminus\Sigma(t)$ with the crack surfaces $\Sigma(t)$ and $\boldsymbol{\mu}_\phi$ the vector field obtained from crack extension.

We now introduce the set $SC(\Sigma(t)|\Pi)$ of smooth crack extensions.

SC1 There is a smooth 2-dimensional manifold Π embedded in $\mathbb{R}^3$ such that $\Sigma(t) \subset \Pi, 0 \le t \le T$.

SC2 $\Sigma = \Sigma(0) \subset \Sigma(t) \subset \Sigma(t')$ if $0 < t < t'$.

SC3 For each $t \in [0, T]$, there is a C^∞-diffeomorphism $\phi_t : \partial\Sigma \to \partial\Sigma(t)$ such that the map $[t \mapsto \phi_t] \in C^\infty([0, T]; C^\infty(\partial\Sigma; \Pi))$.

SC4 The limit $\lim_{t\to 0} t^{-1}|\Sigma(t)-\Sigma|$ exists and non zero, where $|\Sigma(t)-\Sigma|$ denote the surface area of $\Sigma(t) - \Sigma$.

The vector field $\boldsymbol{\mu}_\phi$ is constructed as follows.

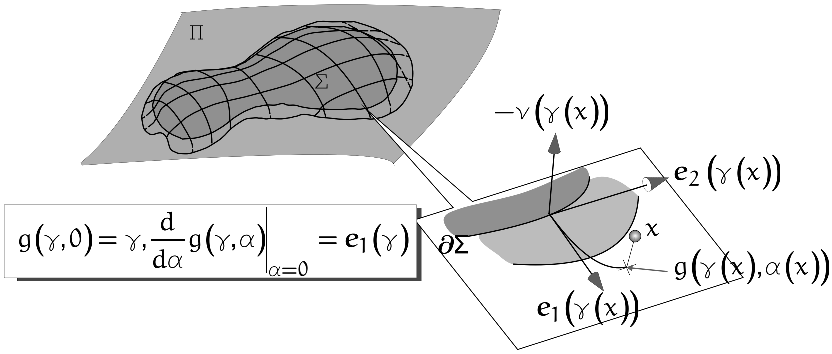

Figure 8: Smooth crack extension of Σ

1. Let $\boldsymbol{e}_1(\gamma), \boldsymbol{e}_2(\gamma)$ be tangential vector fields at $\gamma \in \partial\Sigma$ on Π such that $|\boldsymbol{e}_1(\gamma)| = |\boldsymbol{e}_2(\gamma)| = 1$, $\boldsymbol{e}_2(\gamma)$ tangent along the curve $\partial\Sigma$, let us take $\boldsymbol{e}_1$ in the crack extension direction and $\boldsymbol{e}_1(\gamma) \perp \boldsymbol{e}_2(\gamma)$

2. There is a neiborhood $U(\partial\Sigma)$ of $\partial\Sigma$ such that there is only one nearest point $\mathcal{P}(x) \in \Pi$ for all $x \in U(\partial\Sigma)$. Let us denote the distance from x to $\mathcal{P}(x) \in \Pi$ by $\lambda_3(x)$, that is,

$$x = \mathcal{P}(x) + \lambda_3(x)\boldsymbol{e}_3(\mathcal{P}(x)) \qquad \boldsymbol{e}_3(p) = -\boldsymbol{\nu}(p),\ p \in \Pi$$

   where $\boldsymbol{\nu}(p)$ is the unit normal vector at $p \in \Pi$ in the direction from plus side to minus side of Π.

3. There is a unique geodesic curve through $\mathcal{P}(x)$ on Π crossing at $\gamma(\mathcal{P}(x)) \in \partial\Sigma$ perpendicularly [35, Lemma 10.2]; for each $\gamma \in \partial\Sigma$ the geodesic curve $[\lambda \mapsto g(\gamma, \lambda)]$ satisfy the second order differential equation (the geodesic equation [35, §10]) with the initial conditions

$$g(\gamma, 0) = \gamma, \quad \frac{dg}{d\alpha}(\alpha, 0) = \boldsymbol{e}_1(\gamma)$$

   We now write the length of the geodesic curve from $\gamma(\mathcal{P}(x)) \in \partial\Sigma$ to $\mathcal{P}(x) \in \Pi$ by $\lambda_1(x)$.

4. There is a number $\delta > 0$ so that the mapping

$$F_{\partial\Sigma} : (\gamma, \lambda_1, \lambda_3) \mapsto c(\gamma, \lambda_1) + \lambda_3 \boldsymbol{e}_3(c(\gamma, \lambda_1)) \tag{3.10}$$

become 1-1 mapping from $\partial\Sigma \times (-\delta, \delta)^2$ into $\mathbb{R}^3$. Now we replace $U(\partial\Sigma)$ with $F_{\partial\Sigma}(\partial\Sigma \times (-\delta, \delta)^2)$. Then $F_{\partial\Sigma}$ become the diffeomorphism from $\partial\Sigma \times (-\delta, \delta)^2$ onto $U(\partial\Sigma)$.

5. Take ω so that $\overline{\omega} \subset U(\partial\Sigma)$.

6. $\frac{d}{dt}\phi_t|_{t=0} \mapsto J_\omega(\boldsymbol{u}, \boldsymbol{\mu}_\phi)$ depend only on [43, Theorem 5.4]

$$v_\phi(\gamma)\boldsymbol{e}_1(\gamma), \quad v_\phi(\gamma) = \left\langle \frac{d}{dt}\phi_t(\gamma)\bigg|_{t=0}, \boldsymbol{e}_1(\gamma) \right\rangle \tag{3.11}$$

where $\langle , \rangle$ stands for the inner product in $\mathbb{R}^3$. We call v_ϕ the *velocity of crack extension.*

7. $\boldsymbol{\mu}_\phi(x) = v_\phi(\gamma(\mathcal{P}(x)))\boldsymbol{e}_1(\gamma(\mathcal{P}(x)))$.

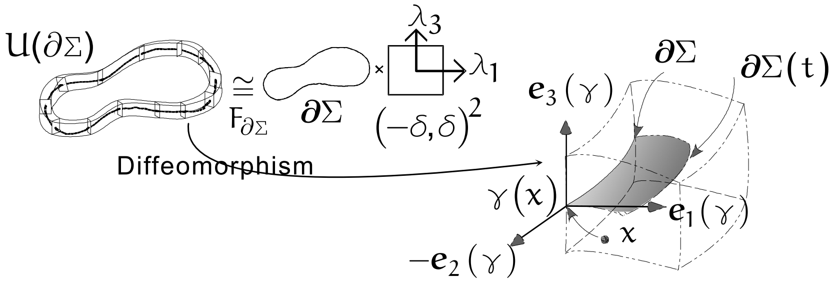

Figure 9: Tubular neighborhood of $\partial\Sigma$

The identity (3.9) is rewritten as follows

$$\frac{d}{dt}\mathcal{E}(\boldsymbol{u}(t); \boldsymbol{f}, \boldsymbol{g}, \Omega_{\Sigma(t)}) = -R_\Omega(\boldsymbol{u}, \eta_{\omega_0}\boldsymbol{\mu}_\phi) \tag{3.12}$$

where $\overline{\omega} \subset \omega_0$ and $\eta_{\omega_0} = 1$ on ω. Indeed, there is no singularity inside $\Omega \setminus \overline{\omega}$ except $\Sigma \cap \Omega \setminus \overline{\omega}$, however

$$\int_{\Sigma\cap(\Omega\setminus\overline{\omega})} \left\{ \widehat{W}(x, \nabla \boldsymbol{u})^\pm (\boldsymbol{\mu}_\phi \cdot \boldsymbol{\nu}) - \widehat{T}(\boldsymbol{u})^\pm (\nabla \boldsymbol{u} \cdot \boldsymbol{\mu}_\phi \right\} = 0$$

because $\boldsymbol{\mu}_\phi$ tanget to Σ leads that $\boldsymbol{\mu}_\phi \cdot \boldsymbol{\nu} = 0$ and $\widehat{T}(\boldsymbol{u})^\pm = 0$ on Σ. Hence by Theorem 2.9

$$\begin{aligned} R_\Omega(\boldsymbol{u}, \eta_{\omega_0}\boldsymbol{\mu}_\phi) &= R_{\Omega\setminus\omega}(\boldsymbol{u}, \eta_{\omega_0}\boldsymbol{\mu}_\phi) + R_\omega(\boldsymbol{u}, \eta_{\omega_0}\boldsymbol{\mu}_\phi) \\ &= -P_{\partial\Omega}(\boldsymbol{u}, \eta_{\omega_0}\boldsymbol{\mu}_\phi) + J_\omega(\boldsymbol{u}, \eta_{\omega_0}\boldsymbol{\mu}_\phi) \\ &= J_\omega(\boldsymbol{u}, \eta_{\omega_0}\boldsymbol{\mu}_\phi) \qquad (\eta_{\omega_0} = 0 \quad \text{on } \partial\Omega) \end{aligned}$$

3.1.5 Shape sensitivity analysis

For $[t \mapsto \varphi_t(x)] \in C^\infty([0,\epsilon], C^2(\mathbb{R}^d,\mathbb{R}^d))$ and linear elliptic boundary value problem

$$
\begin{aligned}
\mathcal{E}(\boldsymbol{v};\boldsymbol{f},\Omega(t)) &= \int_{\Omega(t)} \left\{\widehat{W}(x,\nabla\boldsymbol{v}) - \boldsymbol{f}\cdot\boldsymbol{v}\right\} dx \\
\forall\boldsymbol{v}\in V_0(\Omega(t),\Gamma(t)_{D(t)}) &= \left\{\boldsymbol{v}\in W^{1,2}(\Omega(t),\mathbb{R}^m);\ \boldsymbol{v}=0 \quad \text{on } \Gamma(t)_D(t)\right\}
\end{aligned}
$$

where $\Omega(t)=\varphi_t(\Omega)$, $\Gamma(t)_{D(t)}=\varphi_t(\Gamma_D)$, it is proven in [44] that

$$
\begin{aligned}
\frac{d}{dt}\mathcal{E}(\boldsymbol{u}(t);\boldsymbol{f},\Omega(t))\bigg|_{t=0} &= -R_\Omega(\boldsymbol{u},\boldsymbol{\mu}_\varphi) \\
\boldsymbol{\mu}_\varphi &= \frac{d}{dt}\varphi_t|_{t=0}
\end{aligned}
$$

in the case that $\boldsymbol{f}=0$ near $\partial\Omega$. In the proof, the coercivity with $\alpha>0$

$$
\int_\Omega \nabla_\varsigma\widehat{W}(x,\nabla\boldsymbol{v}) : \nabla\boldsymbol{v}\,dx \ge \alpha\|\boldsymbol{v}\|_{1,\Omega} \quad \forall v\in V_0(\Omega,\Gamma_D)
$$

is essential, and key estimation is that

$$
\|\boldsymbol{u}-\varphi_t^*\boldsymbol{u}(t)\|_{1,\Omega} \le Ct\|\boldsymbol{f}\|_{0,\mathbb{R}^3} \quad \text{with } C>0
$$

where $\varphi_t^*\boldsymbol{u}(t)$ is the pullback $\varphi_t^*\boldsymbol{u}(x,t) = \boldsymbol{u}(\varphi_t(y),t), y\in\Omega$ (slightly changed form [44]).

3.2 Fundamental theorem of GJ-integral

From 3.1 Historical background, we have the following conjecture:

Conjecture 3.1 (Fundamental theorem) *Assume that the extension φ_t of perturbation of singularities is 1-1 mapping from $\mathbb{R}^d$ onto $\mathbb{R}^d$ for each t and $[t\mapsto\varphi_t]\in C^1([0,\epsilon);W^{1,\infty}(\mathbb{R}^d;\mathbb{R}^d))$. Let $\boldsymbol{u}(t)$ be the minimizer of the potential energy functional*

$$
\mathcal{E}(\boldsymbol{v};\boldsymbol{f},\Omega(t)) = \int_{\Omega(t)} \left\{\widehat{W}(x,\nabla\boldsymbol{v}) - \boldsymbol{f}\cdot\boldsymbol{v}\right\} dx
$$

over $V_0(\Omega(t),\Gamma(t)_{D(t)})$. Then the following will hold

$$
\begin{aligned}
\frac{d}{dt}\mathcal{E}(\boldsymbol{u}(t);\boldsymbol{f},\Omega(t))\bigg|_{t=0} &= -R_\Omega(\boldsymbol{u},\boldsymbol{\mu}_\varphi) - \int_{\partial\Omega}\boldsymbol{f}\cdot\boldsymbol{u}(\boldsymbol{\mu}_\varphi\cdot\boldsymbol{n})ds && (3.13) \\
\boldsymbol{\mu}_\varphi(x) &= \frac{d}{dt}\varphi_t(x)\bigg|_{t=0} && (3.14)
\end{aligned}
$$

In [48], (3.13) is proven when $[t\mapsto\varphi_t]\in C^2([0,T],W^{2,\infty}(\mathbb{R}^3;\mathbb{R}^3))$.

In [28, 29], (3.13) is proven for linear problem when $[t\mapsto\varphi_t]\in C^1([0,T],W^{1,\infty}(\mathbb{R}^3;\mathbb{R}^3))$ using the following theorem.

Theorem 3.2 *Let X and M be real Banach spaces. For $\mathcal{U}_0 \subset X$ and an open subset $\mathcal{O}_0 \subset M$, we consider a real valued functional $J : \mathcal{U}_0 \times \mathcal{O}_0 \to \mathbb{R}$ and a map $u : \mathcal{O}_0 \to \mathcal{U}_0$. We define $\mathcal{J}_*(\mu) = \mathcal{J}(u(\mu), \mu)$ for $\mu \in \mathcal{O}_0$. We suppose the following conditions.*

1. *$\mathcal{J} \in C^0(\mathcal{U}_0 \times \mathcal{O}_0)$, $[\mu \mapsto \mathcal{J}(w, \mu)] \in C^1(\mathcal{O}_0)$ for $w \in \mathcal{U}_0$, and $\partial_M \mathcal{J} \in C^0(\mathcal{U}_0 \times \mathcal{O}_0, M')$.*

2. *$u \in C^0(\mathcal{O}_0, X)$ and $u(\mu)$ is a global minimizer of $\mathcal{J}(\cdot, \mu)$ in $\mathcal{U}_0$ for each $\mu \in \mathcal{O}_0$.*

Then we have $\mathcal{J}_* \in C^1(\mathcal{O}_0)$ and

$$\mathcal{J}_*'(\mu) = \partial_M \mathcal{J}(u(\mu), \mu) \qquad (\mu \in \mathcal{O}_0). \tag{3.15}$$

3.3 Fundamental theorem in nonlinear case

In fracture mechanics, it was shown that (2.2) will hold in nonlinear problems. There are some mathematical results[30, 31, 32] and the results in [44, 28, 29] are applicable to nonlinear case (nearly linear). Before proof, we prepare for an abstract result.

Under the same assumption in Theorem 3.2, for $u \in \mathcal{U}_0$ and $w \in X$, the Gâteaux derivative $\delta_X \mathcal{J}(v, \mu)[w] \in \mathbb{R}$ is defined as

$$\delta_X \mathcal{J}(u, \mu)[w] = \frac{d}{dt} \mathcal{J}(u + tw, \mu)\bigg|_{t=0},$$

where ∂_X, ∂_M are partial Fréchet derivative operators for $\mathcal{J}(u, \mu)$ with respect to $u \in X$ and $\mu \in M$. Assume the following.

(F1) $[\mu \mapsto \mathcal{J}(w, \mu)] \in C^1(\mathcal{O}_0)$ for all $w \in \mathcal{U}_0$, and $\partial_M \mathcal{J} : \mathcal{U}_0 \times \mathcal{O}_0 \to M'$ is continuous at $(u(\mu_0), \mu_0)$.

(F2) The Banach space X is reflexive and $\mathcal{U}_0$ is closed and convex in X.

(F3) For the functional $[v \mapsto \mathcal{J}(v, \mu_0)]$, u_0 is a unique minimizer over $\mathcal{U}_0$.

(F4) The functional $[v \mapsto \mathcal{J}(v, \mu_0)]$ is sequentially lower semicontinuous with respect to the weak topology of X.

(F5) There is a monotone nondecreasing function β_0 defined on $[0, \infty)$ with $\lim_{s\to\infty} \beta_0(s) = \infty$ such that

$$\beta_0(\|v\|_X) \le \mathcal{J}(v, \mu) \qquad (v \in \mathcal{U}_0,\ \mu \in \mathcal{O}_0).$$

(F6) For any $\varepsilon > 0$ and $R > 0$, there exists $\delta > 0$ such that

$$\begin{aligned} &|\mathcal{J}(v, \mu) - \mathcal{J}(v, \mu_0)| \le \varepsilon \\ &\quad (v \in \mathcal{U}_0,\ \|v\|_X \le R,\ \ \mu \in \mathcal{O}_0,\ \|\mu - \mu_0\|_M \le \delta). \end{aligned}$$

(F7) For $v \in \mathcal{U}_0$, the function $[t \mapsto \mathcal{J}(u_0 + t(v - u_0), \mu_0)]$ belongs to $C^1((0, 1])$. Moreover, for a sequence $\{u_n\}_n \subset \mathcal{U}_0$ which weakly converges to u_0 as $n \to \infty$, the condition $\overline{\lim}_{n\to\infty} \delta_X \mathcal{J}(u_n, \mu_0)[u_n - u_0] \le 0$ implies that $u_n \to u_0$ strongly in X as $n \to \infty$.

In particular, under the condition (F7),

$$\delta_X \mathcal{J}(v,\mu_0)[v-u_0] = \frac{d}{dt}\mathcal{J}(u_0+t(v-u_0),\mu_0)\bigg|_{t=1}$$

exists for all $v \in \mathcal{U}_0$. The condition (F7) is often called the (S_+)-property.

Theorem 3.3 *Under the conditions (F1)–(F7), $[\mu \mapsto \mathcal{J}_*(\mu)]$ is Fréchet differentiable at $\mu = \mu_0$ and the following holds.*

$$D_\mu[\mathcal{J}(u(\mu_0),\mu_0)] = \partial_M \mathcal{J}(u(\mu_0),\mu_0) \tag{3.16}$$

where the D_μ denotes the Fréchet differential operator with respect to $\mu \in M$.

Now, we apply Theorem 3.3 with $X = W^{1,\boldsymbol{p}}(\Omega), M = W^{1,\infty}(\mathbb{R}^d;\mathbb{R}^d)$ to prove Conjecture 3.1 for the solution $\boldsymbol{u}(t) \in W^{1,1}(\Omega,\mathbb{R}^m)$ of Problem 2.2 over $V_0(\Omega(t),\Gamma(t)_{D(t)})$ with $\boldsymbol{g} = 0$ when $[t \mapsto x + t\boldsymbol{\mu}] \in C^\infty([0,T];W^{1,\infty}(\mathbb{R}^d;\mathbb{R}^d))$. Here we notice that

$$\begin{aligned} R_\omega(u,\boldsymbol{\mu}) = &-\sum_{i=1}^{M}\int_{\omega\cap\Omega_i}\left\{\nabla_x \widehat{W}_i(x,\nabla\boldsymbol{u}_i)\cdot\boldsymbol{\mu} + f\cdot(\nabla\boldsymbol{u}_i\cdot\boldsymbol{\mu})\right\}dx \\ &+\sum_{i=1}^{M}\int_{\omega\cap\Omega_i}\left\{\left(\nabla_\zeta \widehat{W}_i(x,\nabla\boldsymbol{u}_i)\right)^T(\nabla\boldsymbol{\mu}^T)\nabla\boldsymbol{u} - \widehat{W}_i(x,\nabla\boldsymbol{u}_i)(\operatorname{div}\boldsymbol{\mu})\right\}dx \end{aligned} \tag{3.17}$$

Assume the additional condition for $\widehat{W}_i$ in Theorem 2.7.

H0' $\widehat{W}_i$ satisfy **H0** and $[x \mapsto \widehat{W}_i(x,\zeta)] \in C^1(\Omega_i)$ for all $\zeta \in \mathbb{R}^{m\times d}$.

Now, we consider the case that $\varphi_t(x) = x + t\boldsymbol{\mu}(x)$ for any $\boldsymbol{\mu} \in W^{1,\infty}(\mathbb{R}^d;\mathbb{R}^d)$. For a function $\boldsymbol{v} \in W^{1,1}(\Omega;\mathbb{R}^m)$, we define the *pushforward*

$$\varphi_{t*}\boldsymbol{v}(x) = \boldsymbol{v}(\varphi_t^{-1}(x)) \quad x \in \Omega(t)$$

which satisfy the following

$$\begin{aligned} [\nabla(\varphi_{t*}v)]\circ\varphi_t &= A(\varphi_t)\nabla v \quad \text{a.e in } \Omega \quad \text{for } v \in W^{1,1}(\Omega) \\ A(\varphi) &= \left(\nabla\varphi^T\right)^{-1} \in L^\infty(\mathbb{R}^d,\mathbb{R}^{d\times d}) \\ \nabla\varphi^T(x) &= \left(\frac{\partial\varphi_j}{\partial x_i}(x)\right)_{1\le i\le d, 1\le j\le d} \in \mathbb{R}^{d\times d} \quad \text{for } x \in \mathbb{R}^d \\ \int_{\Omega(t)}(\varphi_{t*}v)(y)dy &= \int_\Omega \boldsymbol{v}(x)\kappa(\varphi_t)(x)dx \quad \text{for } v \in L^1(\Omega) \\ \kappa(\varphi) &= \det\nabla\varphi^T \in L^\infty(\mathbb{R}^d,\mathbb{R}) \end{aligned}$$

The mapping $\varphi_{t*} : \boldsymbol{v} \mapsto \varphi_{t*}v$ become 1-1 mapping from $V_0(\Omega,\Gamma_D)$ onto $V_0(\Omega(t),\Gamma(t)_{D(t)})$. Then $\boldsymbol{u}(t) = \varphi_{t*}\boldsymbol{u}_0$,

$$\begin{aligned} \mathcal{E}(\boldsymbol{u}(t);\boldsymbol{f},\Omega(t)) &= \min_{\boldsymbol{v}\in V_0(\Omega(t),\Gamma(t)_{D(t)})} \mathcal{E}(\boldsymbol{v};\boldsymbol{f},\Omega(t)) \\ \mathcal{E}(\boldsymbol{u}_0;\boldsymbol{f},\Omega,\varphi_t) &= \min_{\boldsymbol{v}\in V(\Omega,\Gamma_D)} \widetilde{\mathcal{E}}(\boldsymbol{v};\boldsymbol{f},\varphi_t) \end{aligned}$$

where

$$\begin{aligned}\widetilde{\mathcal{E}}(\boldsymbol{v};\boldsymbol{f},\varphi_t) &= \int_{\Omega(t)} \left\{\widehat{W}(x,\nabla(\varphi_{t*}\boldsymbol{v})) - \boldsymbol{f}\cdot\varphi_{t*}\boldsymbol{v}\right\} dx \\ &= \sum_{i=1}^{M}\int_{\Omega_i}\left\{\widehat{W}_i(\varphi_t(x),A(\varphi_t)\nabla\boldsymbol{v}_i) - \varphi_t^*\boldsymbol{f}\cdot\boldsymbol{v}_i\right\}\kappa(\varphi_t)dx \quad (3.18)\end{aligned}$$

The differentiability of $[t\mapsto \widetilde{\mathcal{E}}(\boldsymbol{v};\boldsymbol{f},\varphi_t)]$ is given by the following [29, Theorem 3.3].

Proposition 3.4

1. *$[\varphi\mapsto\kappa(\varphi)]\in C^\infty(W^{1,\infty}(\mathbb{R}^d,\mathbb{R}^d),L^\infty(\mathbb{R}^d))$. More precisely, the $(d+1)$-th Fréchet derivative of κ vanishes, i.e., $\kappa^{(d+1)}=0$. In particular, we have*

$$\left.\frac{d}{dt}\kappa(x+t\boldsymbol{\mu})\right|_{t=0} = \mathrm{div}\boldsymbol{\mu} \quad \textit{for } \boldsymbol{\mu}\in W^{1,\infty}(\mathbb{R}^d,\mathbb{R}^d)$$

2. *We define an open subset of $W^{1,\infty}(\mathbb{R}^d,\mathbb{R}^d)$,*

$$\mathcal{O}_0(\mathbb{R}^d) = \{\varphi\in W^{1,\infty}(\mathbb{R}^d,\mathbb{R}^d);\ \text{ess-}\inf_{\mathbb{R}^d}\kappa(\varphi)>0\}$$

Then we have $[\varphi\mapsto A(\varphi)]\in C^\infty(\mathcal{O}_0(\mathbb{R}^d),L^\infty(\mathbb{R}^d,\mathbb{R}^{d\times d}))$. In particular,

$$\left.\frac{d}{dt}A(x+t\boldsymbol{\mu})\right|_{t=0} = -\nabla\mu^T \quad \textit{for } \boldsymbol{\mu}\in W^{1,\infty}(\mathbb{R}^d,\mathbb{R}^d)$$

Here we notice that

$$A(x+t\boldsymbol{\mu})(I+t\nabla\boldsymbol{\mu}^T) = I \quad (I:\ \text{identity matrix of degree } d)$$

we have

$$\frac{d}{dt}A(x+t\boldsymbol{\mu})|_{t=0} = -A(x)\nabla\boldsymbol{\mu}^T = -\nabla\boldsymbol{\mu}^T$$

We now arrive at the following for $\boldsymbol{f}\in W^{1,q_{\min}}(\Omega;\mathbb{R}^m)$, $q_{\min}^{-1}+p_{\min}^{-1}=1$

$$\begin{aligned}I_{\Omega_i}(\boldsymbol{v},x+t\boldsymbol{\mu}) &= \int_{\Omega_i}\left\{\widehat{W}_i(x+t\boldsymbol{\mu},A(x+t\boldsymbol{\mu})\nabla\boldsymbol{v}) - \varphi_t^*\boldsymbol{f}\cdot\boldsymbol{v}\right\}\kappa(x+t\boldsymbol{\mu})dx \\ \left.\frac{d}{dt}I_{\Omega_i}(\boldsymbol{v},x+t\boldsymbol{\mu})\right|_{t=0} &= \int_{\Omega_i}\left\{\nabla_x\widehat{W}_i(x,\nabla\boldsymbol{v})\cdot\boldsymbol{\mu} - (\nabla_\varsigma\widehat{W}_i(x,\nabla\boldsymbol{v}))^T(\nabla\boldsymbol{\mu}^T)\nabla\boldsymbol{v}\right\}dx \\ &\quad + \int_{\Omega_i}\widehat{W}_i(x,\nabla\boldsymbol{v})\mathrm{div}\boldsymbol{\mu}dx \\ &\quad - \int_{\Omega_i}((\nabla\boldsymbol{f}\cdot\boldsymbol{\mu})\cdot\boldsymbol{v}+\boldsymbol{f}\cdot\boldsymbol{v}\mathrm{div}\boldsymbol{\mu})\,dx \qquad (3.19)\end{aligned}$$

By Green's formula, it follows that, if $\boldsymbol{f}\in W^{1,\boldsymbol{q}}(\mathbb{R}^d;\mathbb{R}^m)$

$$\begin{aligned}\int_{\Omega_i}\boldsymbol{f}\cdot\boldsymbol{v}\partial_j\mu_j\,dx &= \int_{\Gamma_i}\boldsymbol{f}\cdot\boldsymbol{v}\mu_j n_{ij}\,ds - \int_{\Omega_i}\partial_j(\boldsymbol{f}\cdot\boldsymbol{v})\mu_j\,dx \\ &= \int_{\Gamma_i}\boldsymbol{f}\cdot\boldsymbol{v}\mu_j n_{ij}\,ds - \int_{\Omega_i}\{\partial_j\boldsymbol{f}\cdot\boldsymbol{v}+\boldsymbol{f}\cdot\partial_j\boldsymbol{v}\}\mu_j dx\end{aligned}$$

where $\boldsymbol{n}_i = (n_{i1}, \cdots, n_{id})$ stands for the outward unit normal to $\partial\Omega_i$. This means that

$$\begin{aligned}
\int_{\Omega} \{\boldsymbol{f}\cdot\boldsymbol{v}\mathrm{div}\boldsymbol{\mu} + (\nabla\boldsymbol{f}\cdot\boldsymbol{\mu})\cdot\boldsymbol{v}\}\,dx &= \sum_{i=1}^{M}\int_{\Omega_i}\{\boldsymbol{f}\cdot\boldsymbol{v}\mathrm{div}\boldsymbol{\mu} + (\nabla\boldsymbol{f}\cdot\boldsymbol{\mu})\cdot\boldsymbol{v}\}\,dx \\
&= \sum_{i=1}^{M}\int_{\Gamma_i} f\cdot\boldsymbol{v}(\boldsymbol{\mu}\cdot\boldsymbol{n}_i)ds - \int_{\Omega}\boldsymbol{f}\cdot(\nabla\boldsymbol{u}\cdot\boldsymbol{\mu})dx \\
&= \int_{\partial\Omega} f\cdot\boldsymbol{v}(\boldsymbol{\mu}\cdot\boldsymbol{n})ds - \int_{\Omega}\boldsymbol{f}\cdot(\nabla\boldsymbol{u}\cdot\boldsymbol{\mu})dx \quad (3.20)
\end{aligned}$$

Here we used that $\boldsymbol{v}_i = \boldsymbol{v}_j$ on Γ_{ij} because $\boldsymbol{v}\in W^{1,p_{\min}}(\Omega)$, and $n_{ij} = -n_{ij}$ on $\Gamma_{ij} = \Gamma_i\cap\Gamma_j, i\neq j$ and $\boldsymbol{f}\in W^{1,q_{\min}}(\Omega)$.

By combining (3.18)-(3.20), we have the folloing

$$\begin{aligned}
\frac{d}{dt}\widetilde{\mathcal{E}}(\boldsymbol{v};\boldsymbol{f},\varphi_t)\Big|_{t=0} &= \sum_{i=1}^{M}\int_{\Omega_i}\left\{\nabla_x\widehat{W}_i(x,\nabla\boldsymbol{v})\cdot\boldsymbol{\mu} - \sum_{i=1}^{M}(\nabla_\varsigma\widehat{W}_i(x,\nabla\boldsymbol{v}))^T(\nabla\boldsymbol{\mu}^T)\nabla\boldsymbol{v}\right\}dx \\
&\quad + \int_{\Omega}\left\{\widehat{W}_i(x,\nabla\boldsymbol{v})\mathrm{div}\boldsymbol{\mu}dx + \boldsymbol{f}\cdot(\nabla\boldsymbol{v}\cdot\boldsymbol{\mu})\right\}dx \\
&\quad - \int_{\partial\Omega}\boldsymbol{f}\cdot\boldsymbol{v}(\boldsymbol{\mu}\cdot\boldsymbol{n})ds \\
&= -R_\Omega(\boldsymbol{v},\boldsymbol{\mu}) - \int_{\partial\Omega}\boldsymbol{f}\cdot\boldsymbol{v}(\boldsymbol{\mu}\cdot\boldsymbol{n})ds \qquad (3.21)
\end{aligned}$$

$$R_\Omega(\boldsymbol{v},\boldsymbol{\mu}_j) - \int_{\partial\Omega}\boldsymbol{f}\cdot\boldsymbol{v}(\boldsymbol{\mu}_j\cdot\boldsymbol{n})ds \to R_\Omega(\boldsymbol{u},\boldsymbol{\mu}_0) - \int_{\partial\Omega}\boldsymbol{f}\cdot\boldsymbol{v}(\boldsymbol{\mu}_0\cdot\boldsymbol{n})ds$$

as $j\to\infty$ for $\boldsymbol{\mu}_j, j = 1,\cdots,\infty$ such that $\boldsymbol{\mu}_j\to\boldsymbol{\mu}_0$ in $W^{1,\infty})(\mathbb{R}^d;\mathbb{R}^d)$.

We now check (F1)–(F7) in Theorem 3.3.

(F1) $\partial_\varphi\widetilde{\mathcal{E}}(\boldsymbol{v};\boldsymbol{f},\varphi)$ exists and continuous at $\varphi_0(x) = x$.

(F2) $W^{1,\boldsymbol{p}}(\Omega), 1 < p_i < \infty, 1\leq i\leq M$ is rerlexive and $V_0(\Omega,\Gamma_D)$ is closed and convex in $W^{1,\boldsymbol{p}}(\Omega)$.

(F3) The unique minimizer is shown in Thoerem 2.5.

(F4) (2.12) leads that $[\boldsymbol{v}\mapsto\widetilde{\mathcal{E}}(\boldsymbol{v};\boldsymbol{f},\varphi_0)]$ is sequentially lower semiconinuous in $W^{1,\boldsymbol{p}}(\Omega)$.

(F5) By **H1**, there is a constant c_0

$$\begin{aligned}
\beta_0(\|\boldsymbol{v}\|_{1,\boldsymbol{p}}) &= c_0\sum_{i=1}^{M}\|\boldsymbol{v}\|^{p_i}_{W^{1,p_i}(\Omega)} \\
\widetilde{\mathcal{E}}(\boldsymbol{v};\boldsymbol{f},\varphi) &\geq \beta_0(\|\boldsymbol{v}\|)
\end{aligned}$$

for φ near φ_0.

(F6) From **H1** and **H2**, we have the estimation

$$|\widetilde{\mathcal{E}}(\boldsymbol{v};\boldsymbol{f},\varphi) - \widetilde{\mathcal{E}}(\boldsymbol{v};\boldsymbol{f},\varphi_0)| \leq c_1\|\varphi-\varphi_0\|_{1,\infty,\mathbb{R}^d}\left(\sum_{i=1}^{M}\|\boldsymbol{v}\|^{p_i}_{W^{1,p_i}(\Omega_i)}\right)$$

(F7) If $p_i \geq 2$, then from **H4** we can derive the following with constants $c_i > 0, 1 \leq i \leq M$ such that

$$(\nabla_\zeta \widehat{W}(x,\zeta) - \nabla_\zeta \widehat{W}(x,\tilde{\zeta})) : (\zeta - \tilde{\zeta}) \geq c_i |\zeta - \tilde{\zeta}|^{p_i} \tag{3.22}$$

so we can derive

$$\int_{\Omega_i} \left(\nabla_\zeta \widehat{W}(x,\nabla \boldsymbol{v}) - \nabla_\zeta \widehat{W}(x,\nabla \boldsymbol{w})\right) : (\nabla \boldsymbol{v} - \nabla \boldsymbol{w}) dx \\ \geq c_i' \|\nabla \boldsymbol{v} - \nabla \boldsymbol{w}\|_{0,p_i,\Omega_i}^{p_i}$$

with $c_i' > 0$, which implies (S_+)-property.

Detail in (F7): For a sequence $\boldsymbol{v}_n, n = 1, \cdots$ converging to v_0 such that

$$\begin{aligned} &\delta_X \mathcal{E}(\boldsymbol{v}_n, \boldsymbol{f}, \varphi_0)[\boldsymbol{v}_n - \boldsymbol{v}_0] \\ &\quad = \sum_{i=1}^{M} \int_{\Omega_i} \left\{\nabla_\zeta \widehat{W}_i(x,\nabla \boldsymbol{v}_n) : (\nabla \boldsymbol{v}_n - \nabla \boldsymbol{v}_0) - \boldsymbol{f} \cdot (\boldsymbol{v}_n - \boldsymbol{v}_0)\right\} dx \\ &\overline{\lim_{n\to\infty}} \delta_X \mathcal{E}(\boldsymbol{v}_n, \boldsymbol{f}, \varphi_0)[\boldsymbol{v}_n - \boldsymbol{v}_0] \leq 0 \end{aligned}$$

we can derive $\boldsymbol{v}_n \to \boldsymbol{v}_0$ as $n \to \infty$ strongly in $L^p(\Omega_i;\mathbb{R}^d)$ by Rellich-Kondrachov theorem[2], this means

$$\int_{\Omega_i} \boldsymbol{f} \cdot (\boldsymbol{v}_n - \boldsymbol{v}_0) dx \to 0$$

$$\int_{\Omega_i} \nabla_\zeta \widehat{W}_i(x,\nabla \boldsymbol{v}_0) : (\nabla \boldsymbol{v}_n - \nabla \boldsymbol{v}_0) dx \to 0$$

as $n \to \infty$.

$$\begin{aligned} &\overline{\lim}_{n\to\infty} \int_{\Omega_i} \left\{\nabla_\zeta \widehat{W}_i(x,\nabla \boldsymbol{v}_n) : (\nabla \boldsymbol{v}_n - \nabla \boldsymbol{v}_0) - \boldsymbol{f} \cdot (\boldsymbol{v}_n - \boldsymbol{v}_0)\right\} dx \\ &\quad = \overline{\lim}_{n\to\infty} \int_{\Omega_i} \nabla_\zeta \left(\widehat{W}_i(x,\nabla \boldsymbol{v}_n) - \widehat{W}_i(x,\nabla \boldsymbol{v}_0)\right) : (\nabla \boldsymbol{v}_n - \nabla \boldsymbol{v}_0) dx \\ &\quad \geq c_i' \overline{\lim}_{n\to\infty} \|\nabla \boldsymbol{v}_n - \nabla \boldsymbol{v}_0\|_{0,p_i,\Omega_i}^{p_i} \end{aligned}$$

Assumption $\overline{\lim}_{n\to\infty} \delta_X \mathcal{E}(\boldsymbol{v}_n, \boldsymbol{f}, \varphi_0)[\boldsymbol{v}_n - \boldsymbol{v}_0] \leq 0$ implies

$$\overline{\lim}_{n\to\infty} \|\nabla \boldsymbol{v}_n - \nabla \boldsymbol{v}_0\|_{0,p_i,\Omega_i}^{p_i} \leq 0$$

This means $\nabla \boldsymbol{v}_n \to \nabla \boldsymbol{v}_0$ as $n \to \infty$ strongly in $L^{p_i}(\Omega;\mathbb{R}^d)$. Therefore $\boldsymbol{v}_n \to \boldsymbol{v}_0$ as $n \to \infty$ in $W^{1,\boldsymbol{p}}(\Omega)$ strongly.

Theorem 3.5 *For the perturbation* $x + t\boldsymbol{\mu}$, $\boldsymbol{\mu} \in W^{1,\infty}(\mathbb{R}^d, \mathbb{R}^d)$, $\boldsymbol{f} \in W^{1,\boldsymbol{q}}(\mathbb{R}^d;\mathbb{R}^m)$ *and* $\boldsymbol{g} = 0$, *let* $\boldsymbol{u}(t)$ *be the solution of Problem 2.2 with the conditions* ***H0', H1, H2, H4*** *and* $p_{\min} \geq 2$ *over* $V_0(\Omega(t), \Gamma(t)_{D(t)})$. *Then the following hold*

$$\left.\frac{d}{dt}\mathcal{E}(\boldsymbol{u}(t);\boldsymbol{f},\Omega(t))\right|_{t=0} = -R_\Omega(\boldsymbol{u},\boldsymbol{\mu}) - \int_{\partial\Omega} \boldsymbol{f} \cdot \boldsymbol{u}(\boldsymbol{\mu} \cdot \boldsymbol{n}) ds \tag{3.23}$$

For the energy $\mathcal{E}(\boldsymbol{u}(t) : \boldsymbol{f}, \boldsymbol{g}, \Omega(t))$, Theorem 3.5 is valid if $\boldsymbol{\mu} = 0$ on the closure of $\{x; \boldsymbol{g}(x) \neq 0\}$.

Remark 3.6 *In the case* $1 < p_i < 2$ *for some* $i, 1 \le i \le M$, *then we cannot derive (3.22) in general. Notice that (F7) will hold even if* $1 < p_i < 2$ *in some case, for example, p-Poisson equation as shown in [52].*

In 3D-fracure problem, it is difficult that

$$\Sigma(t) = \{x + t\boldsymbol{\mu}(x) : x \in \Sigma\} \quad \text{for some } \boldsymbol{\mu} \in W^{1,\infty}(\mathbb{R}^d, \mathbb{R}^d)$$

In 3D-fracture problem, we consider the mapping for $h \in C^1(\partial\Sigma)$

$$\varphi_h(x) = \begin{cases} F_{\partial\Sigma}(\gamma(x), \lambda_1(x) + \eta_\omega h(\gamma(x)), \lambda_3(x)) & \text{for } x \in U(\partial\Sigma) \\ 0 & \text{for } x \notin U(\partial\Sigma) \end{cases} \tag{3.24}$$

Then $\widetilde{\mathcal{E}}(\boldsymbol{v}; \boldsymbol{f}, \varphi_h) = \widetilde{\mathcal{E}}(\boldsymbol{v}; \boldsymbol{f}, h)$ and

$$\left.\frac{d}{dt}\widetilde{\mathcal{E}}(\boldsymbol{v}; \boldsymbol{f}, th)\right|_{t=0} = -R_\Omega(\boldsymbol{v}; \boldsymbol{f}, \eta_\omega \boldsymbol{\mu}_h)$$

where $\boldsymbol{\mu}_h(x) = h(\gamma(x))$.

Theorem 3.7 *Let* Σ *be a 2-dimensional surface such that* $\Sigma \subset \Omega_k$ *for some* $1 \le k \le M$. *With* $h \in C^1(\partial\Sigma)$, *consider the crack extension given in (3.24). For* $\boldsymbol{f} \in W^{1,\boldsymbol{q}}(\Omega; \mathbb{R}^d), \boldsymbol{g} = 0$, *let* $\boldsymbol{u}(t)$ *be the solution of Problem 2.2 with the conditions **H0', H1, H2, H4** and* $p_{\min} \ge 2$, *which is minimizer of energy functional over* $V_0(\Omega_{\Sigma(t)}, \Gamma_D)$.

$$\left.\frac{d}{dt}\mathcal{E}(\boldsymbol{u}(t); \boldsymbol{f}, \Omega_{\Sigma(t)})\right|_{t=0} = -R_{\Omega_\Sigma}(\boldsymbol{u}, \boldsymbol{\mu}_h) \tag{3.25}$$

with $\boldsymbol{\mu}_h = d\varphi_{th}/dt|_{t=0}$.

For a smooth crack extension $\{\Sigma(t)\}_{0 \le t \le T}, \Sigma(t) \subset \Pi$, h is the velocity (3.11).

3.4 GJ-Hadamard formula

Under the same assumption in Theorem 3.5 in the case of *Problem 2.2 is linear,* $M = 1$ *and* $\boldsymbol{g} = 0$, let $\boldsymbol{\vartheta} \in W^{1,2}(\mathbb{R}^d; \mathbb{R}^m)$ and the solution $\boldsymbol{u}_\vartheta(t)$ such that

$$\mathcal{E}(\boldsymbol{u}_\vartheta(t); \boldsymbol{\vartheta}, \Omega(t)) = \min_{\boldsymbol{v} \in V_0(\Omega(t), \Gamma(t)_{D(t)})} \mathcal{E}(\boldsymbol{v}; \boldsymbol{\vartheta}, \Omega(t))$$

Writing $\boldsymbol{\mu} = \boldsymbol{\mu}_\varphi$ for simplicity, we then have

$$\left.\frac{d}{dt}\mathcal{E}(\boldsymbol{u}_\vartheta(t); \boldsymbol{\vartheta}, \Omega(t))\right|_{t=0} = -R_\Omega(\boldsymbol{u}_\vartheta, \boldsymbol{\mu}_\varphi) - \int_{\partial\Omega} \boldsymbol{\vartheta} \cdot \boldsymbol{u}_\vartheta (\boldsymbol{\mu} \cdot \boldsymbol{n})\, ds \tag{3.26}$$

We assumed that Problem 2.2 is linear, so that $\boldsymbol{u} + \epsilon\boldsymbol{u}_\vartheta$ is the solution, we then have we have

$$\begin{aligned} \mathcal{E}(\boldsymbol{u}(t) + \epsilon\boldsymbol{u}_\vartheta(t); \boldsymbol{f} + \epsilon\boldsymbol{\vartheta}, \Omega(t)) &= \min_{\boldsymbol{v} \in V_0(\Omega(t), \Gamma(t)_{D(t)})} \mathcal{E}(\boldsymbol{v}; \boldsymbol{f} + \epsilon\boldsymbol{\vartheta}, \Omega(t)) \\ \left.\frac{d}{dt}\mathcal{E}(\boldsymbol{u}(t) + \epsilon\boldsymbol{u}_\vartheta(t); \boldsymbol{f} + \epsilon\boldsymbol{\vartheta}, \Omega(t))\right|_{t=0} &= -R_\Omega(\boldsymbol{u} + \epsilon\boldsymbol{u}_\vartheta, \boldsymbol{\mu}) \\ &\quad - \int_{\partial\Omega} (\boldsymbol{f} + \epsilon\boldsymbol{\vartheta}) \cdot (\boldsymbol{u} + \epsilon\boldsymbol{u}_\vartheta)(\boldsymbol{\mu} \cdot \boldsymbol{n})\, ds \end{aligned}$$

By linearity it follows that

$$\widehat{W}(x,\nabla\boldsymbol{u}(t)+\epsilon\nabla\boldsymbol{u}_\vartheta(t))=\widehat{W}(x,\nabla\boldsymbol{u}(t))+\epsilon\nabla_\zeta\widehat{W}(x,\nabla\boldsymbol{u}(t)):\nabla\boldsymbol{u}_\vartheta(t)+\epsilon^2\widehat{W}(x,\nabla\boldsymbol{u}_\vartheta(t))$$

This implies the following

$$\begin{aligned}
&\mathcal{E}(\boldsymbol{u}(t)+\epsilon\boldsymbol{u}_\vartheta(t);\boldsymbol{f}+\epsilon\boldsymbol{\vartheta},\Omega(t))\\
&=\int_{\Omega(t)}\left\{\widehat{W}(x,\boldsymbol{u}(t)+\epsilon\boldsymbol{u}_\vartheta(t))-\left(\boldsymbol{f}\cdot\boldsymbol{u}(t)+\epsilon\boldsymbol{f}\cdot\boldsymbol{u}_\vartheta(t)+\epsilon\boldsymbol{\vartheta}\cdot\boldsymbol{u}(t)+\epsilon^2\boldsymbol{\vartheta}\cdot\boldsymbol{u}_\vartheta\right)\right\}dx\\
&=\mathcal{E}(\boldsymbol{u}(t);\boldsymbol{f},\Omega(t))+\epsilon\int_{\Omega(t)}\left\{\nabla_\zeta\widehat{W}(x,\nabla\boldsymbol{u}(t)):\nabla\boldsymbol{u}_\vartheta(t)-\boldsymbol{f}\cdot\boldsymbol{u}_\vartheta(t)\right\}dx\\
&\qquad-\epsilon\int_{\Omega(t)}\boldsymbol{\vartheta}\cdot\boldsymbol{u}(t)\,dx+\epsilon^2\int_{\Omega(t)}\left\{\widehat{W}(x,\boldsymbol{u}_\vartheta)-\boldsymbol{\vartheta}\cdot\boldsymbol{u}_\vartheta\right\}dx
\end{aligned}$$

Hence we can derive

$$\begin{aligned}
-\epsilon\int_{\Omega(t)}\boldsymbol{\vartheta}\cdot\boldsymbol{u}(t)\,dx &= \mathcal{E}(\boldsymbol{u}(t)+\epsilon\boldsymbol{u}_\vartheta(t);\boldsymbol{f}+\epsilon\boldsymbol{\vartheta},\Omega(t))-\mathcal{E}(\boldsymbol{u}(t);\boldsymbol{f},\Omega(t))\\
&\quad+\epsilon^2\mathcal{E}(\boldsymbol{u}_\vartheta(t);\boldsymbol{\vartheta},\Omega(t))\\
-\frac{d}{dt}\epsilon\int_{\Omega(t)}\boldsymbol{\vartheta}\cdot\boldsymbol{u}(t)\,dx\bigg|_{t=0} &= \frac{d}{dt}\mathcal{E}(\boldsymbol{u}(t)+\epsilon\boldsymbol{u}_\vartheta(t);\boldsymbol{f}+\epsilon\boldsymbol{\vartheta},\Omega(t))\bigg|_{t=0}\\
&\quad-\frac{d}{dt}\mathcal{E}(\boldsymbol{u}(t);\boldsymbol{f},\Omega(t))\bigg|_{t=0}+\epsilon^2\frac{d}{dt}\mathcal{E}(\boldsymbol{u}_\vartheta(t);\boldsymbol{\vartheta},\Omega(t))\bigg|_{t=0}\\
&= -R_\Omega(\boldsymbol{u}+\epsilon\boldsymbol{u}_\vartheta,\boldsymbol{\mu})-\int_{\partial\Omega}(\boldsymbol{f}+\epsilon\boldsymbol{\vartheta})\cdot(\boldsymbol{u}+\epsilon\boldsymbol{u}_\vartheta)(\boldsymbol{\mu}\cdot\boldsymbol{n})ds\\
&\quad+R_\Omega(\boldsymbol{u},\boldsymbol{\mu})+\int_{\partial\Omega}\boldsymbol{f}\cdot\boldsymbol{u}(\boldsymbol{\mu}\cdot\boldsymbol{n})ds\\
&\quad-\epsilon^2\left\{R_\Omega(\boldsymbol{u}_\vartheta,\boldsymbol{\mu})+\int_{\partial\Omega}\boldsymbol{\vartheta}\cdot\boldsymbol{u}_\vartheta(\boldsymbol{\mu}\cdot\boldsymbol{n})ds\right\}
\end{aligned}$$

Therefore we have the following

$$\begin{aligned}
\frac{d}{dt}\int_{\Omega(t)}\boldsymbol{\vartheta}\cdot\boldsymbol{u}(t)\,dx\bigg|_{t=0} &= \epsilon^{-1}\left\{R_\Omega(\boldsymbol{u}+\epsilon\boldsymbol{u}_\vartheta,\boldsymbol{\mu})-R_\Omega(\boldsymbol{u},\boldsymbol{\mu})\right\}\\
&\quad+\int_{\partial\Omega}\boldsymbol{\vartheta}\cdot\boldsymbol{u}(\boldsymbol{\mu}\cdot\boldsymbol{n})ds+\int_{\partial\Omega}\boldsymbol{f}\cdot\boldsymbol{u}_\vartheta(\boldsymbol{\mu}\cdot\boldsymbol{n})ds\\
&\quad+o(\epsilon) \qquad (3.27)\\
&= \delta R_\Omega(\boldsymbol{u},\boldsymbol{u}_\vartheta;\boldsymbol{\mu})\\
&\quad+\int_{\partial\Omega}\left\{\boldsymbol{\vartheta}\cdot\boldsymbol{u}+\boldsymbol{f}\cdot\boldsymbol{u}_\vartheta\right\}(\boldsymbol{\mu}\cdot\boldsymbol{n})ds \qquad (3.28)\\
\delta R_\Omega(\boldsymbol{u},\boldsymbol{u}_\vartheta;\boldsymbol{\mu}) &= \lim_{\epsilon\to0}\epsilon^{-1}\left\{R_\Omega(\boldsymbol{u}+\epsilon\boldsymbol{u}_\vartheta,\boldsymbol{\mu})-R_\Omega(\boldsymbol{u},\boldsymbol{\mu})\right\}
\end{aligned}$$

Theorem 3.8 (GJ-Hadamard) *Consider the case that $M=1$. For any $\vartheta\in C^\infty\left(\overline{\Omega};\mathbb{R}^m\right)$, $\boldsymbol{f}\in W^{1,\boldsymbol{q}}(\mathbb{R}^d;\mathbb{R}^m)$ and $\boldsymbol{g}=0$, let $\boldsymbol{u}(t)$ be the solution of the problem 2.2 in the case of linear.*

$$\mathcal{E}(\boldsymbol{u}(t);\boldsymbol{f},\Omega(t))=\min_{\boldsymbol{v}\in V_0(\Omega(t),\Gamma(t)_{D(t)})}\mathcal{E}(\boldsymbol{v};\boldsymbol{f},\Omega(t))$$

Then the following generalization of (3.7) holds

$$\left.\frac{d}{dt}\int_{\Omega(t)} \boldsymbol{\vartheta}\cdot\boldsymbol{u}(t)\,dx\right|_{t=0} = \delta R_\Omega(\boldsymbol{u},\boldsymbol{u}_\vartheta;\boldsymbol{\mu}_\varphi) + \int_{\partial\Omega}\{\boldsymbol{\vartheta}\cdot\boldsymbol{u}+\boldsymbol{f}\cdot\boldsymbol{u}_\vartheta\}(\boldsymbol{\mu}_\varphi\cdot\boldsymbol{n})ds \tag{3.29}$$

Theorem is proven in [48].

We now find the form $R_\omega(\boldsymbol{u},\boldsymbol{u}_\vartheta)$. Writing

$$\delta\widehat{W}(x,\nabla\boldsymbol{u})[\boldsymbol{u}_\vartheta] = \lim_{\epsilon\to 0}\frac{1}{\epsilon}\left\{\widehat{W}(x,\nabla\boldsymbol{u}+\epsilon\nabla\boldsymbol{u}_\vartheta) - \widehat{W}(x,\nabla\boldsymbol{u})\right\}$$

we have

$$\begin{aligned}\delta R_\omega(\boldsymbol{u},\nabla\boldsymbol{u}_\vartheta;\boldsymbol{\mu}) \;=\; & -\int_{\omega\cap\Omega}\left\{\nabla_x\delta\widehat{W}(x,\nabla\boldsymbol{u})[\nabla\boldsymbol{u}_\vartheta]\cdot\boldsymbol{\mu} + f\cdot(\nabla\boldsymbol{u}_\vartheta\cdot\boldsymbol{\mu})\right\}dx \\ & + \int_{\omega\cap\Omega}\left(\nabla_\zeta\delta\widehat{W}(x,\nabla\boldsymbol{u})[\nabla\boldsymbol{u}_\vartheta]\right)^T(\nabla\boldsymbol{\mu}^T)\nabla\boldsymbol{u}\,dx \\ & + \int_{\omega\cap\Omega}\left(\nabla_\zeta\widehat{W}(x,\nabla\boldsymbol{u})\right)^T(\nabla\boldsymbol{\mu}^T)\nabla\boldsymbol{u}_\vartheta\,dx \\ & - \int_{\omega\cap\Omega}\delta\widehat{W}(x,\nabla\boldsymbol{u})[\nabla\boldsymbol{u}_\vartheta](\mathrm{div}\,\boldsymbol{\mu})dx\end{aligned} \tag{3.30}$$

If $\boldsymbol{u}(t)=\boldsymbol{u}(x,t), x\in\Omega(t)$ is smooth, we define the *material derivative* and *shape derivative* as follows.

Definition 3.9 *The material derivative* $\dot{\boldsymbol{u}}$ *of* $\boldsymbol{u}(t)$ *in the direction of a vector field* $\boldsymbol{\mu}$ *is defined by*

$$\dot{\boldsymbol{u}}(x) = \lim_{t\to 0}\frac{1}{t}\{\boldsymbol{u}(\varphi_t(x),t)-\boldsymbol{u}(x)\}\quad \textit{for } x\in\Omega \tag{3.31}$$

The shape derivative $\boldsymbol{u}'$ *of* $\boldsymbol{u}(t)$ *in the direction* $\boldsymbol{\mu}$ *is defined by*

$$\boldsymbol{u}'(x) = \dot{\boldsymbol{u}}(x) - \nabla\boldsymbol{u}(x)\cdot\boldsymbol{\mu}(x) \tag{3.32}$$

Lemma 3.10 *If* $\boldsymbol{u}(t)$ *is smooth, we have*

$$\left.\frac{d}{dt}\int_{\Omega(t)}\boldsymbol{\vartheta}\cdot\boldsymbol{u}(t)\,dx\right|_{t=0} = \int_\Omega \boldsymbol{\vartheta}\cdot\boldsymbol{u}'dx + \int_{\partial\Omega}\boldsymbol{\vartheta}\cdot\boldsymbol{u}(\boldsymbol{\mu}_\varphi\cdot\boldsymbol{n})ds \tag{3.33}$$

Proof. Putting $\boldsymbol{u}(t)\circ\varphi_t(x)=\boldsymbol{u}(\varphi_t(x),t)$, $\omega(t)=\det\nabla\varphi_t$

$$\begin{aligned}\left.\frac{d}{dt}\int_{\Omega(t)}\boldsymbol{\vartheta}\cdot\boldsymbol{u}(t)\,dx\right|_{t=0} &= \left.\frac{d}{dt}\int_\Omega \boldsymbol{\vartheta}\circ\varphi_t\cdot\boldsymbol{u}(t)\circ\varphi_t\,\omega(t)dx\right| \\ &= \int_\Omega\left\{\boldsymbol{\vartheta}\cdot\dot{\boldsymbol{u}} + (\nabla\boldsymbol{\vartheta}\cdot\boldsymbol{\mu}_\varphi)\cdot\nabla\boldsymbol{u} + \boldsymbol{\vartheta}\cdot\boldsymbol{u}\mathrm{div}\boldsymbol{\mu}_\varphi\right\}dx \\ \int_\Omega(\nabla\boldsymbol{\vartheta}\cdot\boldsymbol{\mu}_\varphi)\cdot\nabla\boldsymbol{u}\,dx &= \int_{\partial\Omega}\boldsymbol{\vartheta}\cdot\boldsymbol{u}(\boldsymbol{\mu}_\varphi\cdot\boldsymbol{n})ds - \int_\Omega\left\{\boldsymbol{\vartheta}\cdot(\nabla\boldsymbol{u}\cdot\boldsymbol{\mu}_\varphi) + \boldsymbol{\vartheta}\cdot\boldsymbol{u}\mathrm{div}\boldsymbol{\mu}_\varphi\right\}dx\end{aligned}$$

Therefore, we can derive (3.33). $\square$

If $\boldsymbol{u}(t)$ is smooth, it follows that

$$\begin{aligned}\int_{\Omega}\boldsymbol{\vartheta}\cdot\boldsymbol{u}'dx+\int_{\partial\Omega}\boldsymbol{\vartheta}\cdot\boldsymbol{u}(\boldsymbol{\mu}_{\varphi}\cdot\boldsymbol{n})ds &= \delta R_{\Omega}(\boldsymbol{u},\boldsymbol{u}_{\vartheta};\boldsymbol{\mu}_{\varphi}) \\ &\quad+\int_{\partial\Omega}\left\{\boldsymbol{\vartheta}\cdot\boldsymbol{u}+\boldsymbol{f}\cdot\boldsymbol{u}_{\vartheta}\right\}(\boldsymbol{\mu}_{\varphi}\cdot\boldsymbol{n})ds\end{aligned}\tag{3.34}$$

which implies the following theorem.

Theorem 3.11 *Under the same condition in Theorem 3.8, the shape derivative $\boldsymbol{u}'\in L^2(\Omega;\mathbb{R}^m)$ exist, and*

$$\int_{\Omega}\boldsymbol{\vartheta}\cdot\boldsymbol{u}'\,dx=R_{\Omega}(\boldsymbol{u},\boldsymbol{u}_{\vartheta};\boldsymbol{\mu}_{\varphi})+\int_{\partial\Omega}\boldsymbol{f}\cdot\boldsymbol{u}_{\vartheta}(\boldsymbol{\mu}_{\varphi}\cdot\boldsymbol{n})\,ds\tag{3.35}$$

Proof For any $\vartheta\in C_0^\infty(\Omega;\mathbb{R}^m)$, we have by Theorem 3.8,

$$\left.\frac{d}{dt}\int_{\Omega(t)}\boldsymbol{\vartheta}\cdot\boldsymbol{u}(t)\,dx\right|_{t=0}=\delta R_{\Omega}(\boldsymbol{u},\boldsymbol{u}_{\vartheta};\boldsymbol{\mu}_{\varphi})+\int_{\partial\Omega}\boldsymbol{f}\cdot\boldsymbol{u}_{\vartheta}(\boldsymbol{\mu}_{\varphi}\cdot\boldsymbol{n})\,ds$$

Since $[\vartheta\mapsto\boldsymbol{u}_{\vartheta}]$ is continuous linear mapping from $L^2(\Omega;\mathbb{R}^m)$ to $W^{1,2}(\Omega;\mathbb{R}^m)$, we have the estimation with a constant $C>0$

$$\begin{aligned}&\left|\delta R_{\Omega}(\boldsymbol{u},\boldsymbol{u}_{\vartheta};\boldsymbol{\mu}_{\varphi})+\int_{\partial\Omega}\boldsymbol{f}\cdot\boldsymbol{u}_{\vartheta}(\boldsymbol{\mu}_{\varphi}\cdot\boldsymbol{n})\,ds\right|\\ &\qquad\le C\|\boldsymbol{\mu}_{\varphi}\|_{1,\infty,\mathbb{R}^d}\left(\|\boldsymbol{u}\|_{1,2,\Omega}+\|\boldsymbol{f}\|_{0,2,\Omega}\right)\|\boldsymbol{u}_{\vartheta}\|_{1,2,\Omega}\end{aligned}$$

Then tere is a function $\boldsymbol{K}\in L^2(\Omega;\mathbb{R}^m)$ such that

$$\int_{\Omega}\boldsymbol{\vartheta}\cdot\boldsymbol{K}\,dx=\delta R_{\Omega}(\boldsymbol{u},\boldsymbol{u}_{\vartheta};\boldsymbol{\mu}_{\varphi})+\int_{\partial\Omega}\boldsymbol{f}\cdot\boldsymbol{u}_{\vartheta}(\boldsymbol{\mu}_{\varphi}\cdot\boldsymbol{n})\,ds$$

for any $\boldsymbol{\vartheta}\in C_0^\infty(\Omega;\mathbb{R}^m)$. From Lemma 3.10, $\boldsymbol{K}$ is the natural extension of $\boldsymbol{u}'$. From (3.34), we can prove (3.35). $\square$

From Theorem 2.9, the following holds.

Corollary 3.12 *If $\boldsymbol{u}\in W^{2,2}(\Omega;\mathbb{R}^m)$, then*

$$\begin{aligned}\left.\frac{d}{dt}\int_{\Omega(t)}\boldsymbol{\vartheta}\cdot\boldsymbol{u}(t)\,dx\right|_{t=0} &= -\delta P_{\Omega}(\boldsymbol{u},\boldsymbol{u}_{\vartheta};\boldsymbol{\mu}_{\varphi})+\int_{\partial\Omega}\left\{\boldsymbol{\vartheta}\cdot\boldsymbol{u}+\boldsymbol{f}\cdot\boldsymbol{u}_{\vartheta}\right\}(\boldsymbol{\mu}_{\varphi}\cdot\boldsymbol{n})ds\\ \textit{with }\delta P_{\Omega}(\boldsymbol{u},\boldsymbol{u}_{\vartheta};\boldsymbol{\mu}) &= \lim_{\epsilon\to0}\frac{1}{\epsilon}\left\{P_{\Omega}(\boldsymbol{u}+\epsilon\boldsymbol{u}_{\vartheta},\boldsymbol{\mu})-P_{\Omega}(\boldsymbol{u},\boldsymbol{\mu})\right\}\end{aligned}\tag{3.36}$$

$$\begin{aligned}\delta P_{\Omega}(\boldsymbol{u},\boldsymbol{u}_{\vartheta};\boldsymbol{\mu}) &= \int_{\partial\Omega}\Big\{\delta\widehat{W}(x,\boldsymbol{u})[\boldsymbol{u}_{\vartheta}](\boldsymbol{\mu}_{\varphi}\cdot\boldsymbol{n})\\ &\quad-\widehat{T}(x,\boldsymbol{u})(\nabla\boldsymbol{u}_{\vartheta}\cdot\boldsymbol{\mu}_{\varphi})-\widehat{T}(x,\boldsymbol{u}_{\vartheta})(\nabla\boldsymbol{u}\cdot\boldsymbol{\mu}_{\varphi})\Big\}\,ds\end{aligned}$$

In the case that boundary condition is mixed, non-smooth boundary, we use Green kernel by Schwartz's theorem of kernels therem (see e.g.[12, Appendix,§3,12]), there is a $G_t \in \mathcal{D}'_{xy}$ such that

$$\begin{aligned} \boldsymbol{u}(\xi,t) &= \langle \boldsymbol{G}_t(\xi,x), \boldsymbol{f}(x)\rangle_{\Omega(t),x} \qquad \text{for } \boldsymbol{f} \in C_0^\infty(\Omega;\mathbb{R}^m) \\ \boldsymbol{u}_\vartheta(\xi,t) &= \langle \boldsymbol{G}_t(\xi,y), \boldsymbol{\vartheta}(y)\rangle_{\Omega(t),y} \qquad \text{for } \boldsymbol{\vartheta} \in C_0^\infty(\Omega;\mathbb{R}^m) \end{aligned}$$

and the following hold for $\mathcal{D} = C_0^\infty(\Omega;\mathbb{R}^m)$,

$$\begin{aligned} \delta R_\Omega(\boldsymbol{u}, \boldsymbol{u}_\vartheta; \boldsymbol{\mu}_\varphi) &= \delta R_\Omega(\langle \boldsymbol{G}(\xi,\cdot), \boldsymbol{f}(\cdot)\rangle_{\Omega,x}, \langle \boldsymbol{G}(\xi,\cdot), \boldsymbol{\vartheta}(\cdot)\rangle_{\Omega,y}; \boldsymbol{\mu}_\varphi) \\ &= \left\langle \delta R_\Omega(\boldsymbol{G}(\cdot,x), \boldsymbol{G}(\cdot,y); \boldsymbol{\mu}_\varphi)\boldsymbol{f}(x), \boldsymbol{\vartheta}(y)\right\rangle_{\mathcal{D}_x\times\mathcal{D}_y} \end{aligned}$$

Theorem 3.13 *Under the same condition in Theorem 3.8, the material derivative of Green's kernel $\boldsymbol{G}_t$ is*

$$\boldsymbol{G}'(x,y) = \delta R_\Omega(\boldsymbol{G}(\cdot,x), \boldsymbol{G}(\cdot,y); \boldsymbol{\mu}_\varphi)$$

Moreover, if all solutions are in $W^{2,2}(\Omega)$, then

$$\boldsymbol{G}'(x,y) = -\delta P_\Omega(\boldsymbol{G}(\cdot,x), \boldsymbol{G}(\cdot,y); \boldsymbol{\mu}_\varphi)$$

3.5 Finite Element Analysis

In this paper, we assume the existence of singular points. Because solutions may not be smooth, attention is necessary about finite element method.

3.5.1 FEM solution

In this section, we consider the linear elasticity, that is, Hooke's tensor $C_{ijkl}(x)$ exist such as $\sigma_{ij}(\boldsymbol{u}) = C_{ijkl}\varepsilon_{kl}(\boldsymbol{u})$ Consider the bilinear form

$$a(\boldsymbol{u},\boldsymbol{v}) = \int_\Omega \sigma_{ij}(\boldsymbol{u})\varepsilon_{ij}(\boldsymbol{v})\,dx$$

The displacement $\boldsymbol{u}$ satisfy

$$a(\boldsymbol{u},\boldsymbol{v}) = \int_\Omega \boldsymbol{f}\cdot\boldsymbol{v}\,dx + \int_{\Gamma_N} \boldsymbol{g}\cdot\boldsymbol{v}ds \qquad \forall \boldsymbol{v} \in V(\Omega,\Gamma_D)$$

and is approximated by the piesewize linear function $\boldsymbol{u}_h$, that is *P1-element* $V_h(\Omega,\Gamma_D)$. Here we assume that Ω is the polygonal/polyhedral domain for simplicity. By Céa's lemma [15, Lemma 2.28] we have estimation with a constant $C_0 > 0$,

$$\|\boldsymbol{u} - \boldsymbol{u}_h\|_{1,\Omega} \le C_0 \inf_{\boldsymbol{v}_h\in V_h} \|\boldsymbol{u} - \boldsymbol{v}_h\|_{1,\Omega} \qquad V_h = V_h(\Omega,\Gamma_D)$$

Let P_h be the orthogonal projection from V_h into $V(\Omega,\Gamma_D)$. If $\boldsymbol{v} \in H^2(\Omega;\mathbb{R}^3)$, then (see e.g.[15, Corollary 1.141]

$$\|\boldsymbol{v} - P_h\boldsymbol{v}\|_{1,\Omega} \le C_1 h\|v\|_{2,\Omega}$$

with a constant C_1 independent h, and for $\boldsymbol{v} \in H^1(\Omega;\mathbb{R}^3)$ we have

$$\|\boldsymbol{v} - P_h\boldsymbol{v}\|_{1,\Omega} \le \|\boldsymbol{v}\|_{1,\Omega}$$

They means that the operator norm of $I - P_h$ is $C_1 h$ when $I - P_h$ is linear operator $H^2(\Omega, \Gamma_D) \cap V(\Omega, \Gamma_D)$ to $V(\Omega, \Gamma_D)$, and is 1 on $H^1(\Omega, \Gamma_D) \cap V(\Omega, \Gamma_D)$ to $V(\Omega, \Gamma_D)$. Then using the interpolation of operator[2, 7.23], we have

$$\|\boldsymbol{v} - P_h \boldsymbol{v}\|_{1,\Omega} \leq C_2 h^{s-1} \|\boldsymbol{v}\|_{s,\Omega}$$

for any $\boldsymbol{v} \in H^s(\Omega; \mathbb{R}^3) \cap V(\Omega, \Gamma_D)$ for $1 \leq s \leq 2$. Using the Céa's lemma, we arrive at the estimation

$$\|\boldsymbol{u} - \boldsymbol{u}_h\|_{1,\Omega} \leq C_2 C_0 h^{s-1} \|\boldsymbol{u}\|_{s,\Omega} \tag{3.37}$$

if the solution $\boldsymbol{u}$ is in $W^{s,2}(\Omega, \mathbb{R}^m)$ with $s > 1$.

3.5.2 Numerical calculation of GJ-integral

$$J_\omega(u_h, \boldsymbol{\mu}) = P_\omega(u_h, \boldsymbol{\mu}) + R_\omega(u_h, \boldsymbol{\mu})$$

By singularity, in usual FEM, we can only prove that $\|u - u_h\|_{1,\Omega} \to 0$, so it is difficult that $P_\omega(u_h, \boldsymbol{\mu}) \to P_\omega(u, \boldsymbol{\mu})$ as $h \to 0$.

Let η_ω be the cut-off function such that

$$\eta_\omega = 1 \quad \text{on } \omega' \quad \overline{\omega'} \subset \omega$$
$$\text{supp}\eta_\omega \subset \omega$$

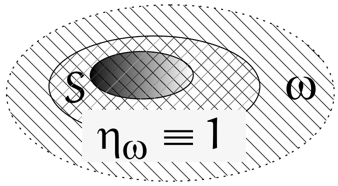

$$\begin{aligned} J_\omega(u, \boldsymbol{\mu}) &= J_{\omega'}(u, \boldsymbol{\mu}) = J_{\omega'}(u, \eta_\omega \boldsymbol{\mu}) \\ &= J_\omega(u, \eta_\omega \boldsymbol{\mu}) = R_\omega(u, \eta_\omega \boldsymbol{\mu}) \end{aligned}$$

The functional $R_\omega(u, \eta_\omega \boldsymbol{\mu})$ is bounded in $W^{1,p}(\Omega)$-norm, so we can prove that $R_\omega(u_h, \eta_\omega \boldsymbol{\mu}) \to R_\omega(u, \eta_\omega \boldsymbol{\mu})$ as $h \to 0$.

4 Fracture Problem

4.1 Energy release rate

The elastic body with a crack Σ is described as the boundary value problem:

$$\begin{aligned} -\partial_j \sigma_{ij}(\boldsymbol{u}) = f & \qquad \text{in } \Omega_\Sigma (= \Omega \setminus \Sigma) \\ \nu_j \sigma_{ij}(\boldsymbol{u})^+ = \nu_j \sigma_{ij}(\boldsymbol{u})^- = 0 & \qquad \text{on } \Sigma \\ \boldsymbol{u} = 0 \quad \text{on } \Gamma_D \quad n_j \sigma_{ij}(\boldsymbol{u}) = g & \qquad \text{on } \Gamma_N \end{aligned}$$

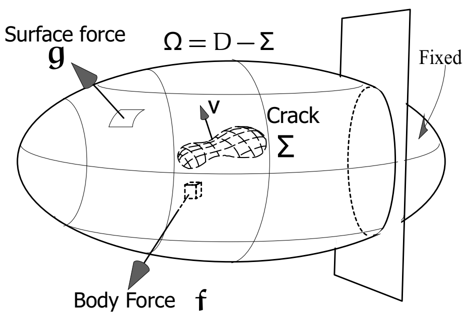

Let us denote by $C(\Sigma(t)|\Pi)$ the crack extension, that is,

(C1) Π is a part of the boundary of domain D_Π with local Lipschitz property.

(C2) $\Sigma(t) \subset \Pi$ and $\Sigma = \Sigma(t) \subset \Sigma(t')$ if $0 < t < t'$.

Dviding Ω_Σ into $\Omega_+ = \Omega \setminus \overline{D_\Pi}$, $\Omega_- = \Omega \cap D_\Pi$ and using Green's formula (2.14), we can prove the existence of the displacement $\boldsymbol{u}(t)$ as the minimizer of energy functional

$$\mathcal{E}(\boldsymbol{v}; \Omega_{\Sigma(t)}, \boldsymbol{f}, \boldsymbol{g}) \quad = \quad \int_{\Omega_{\Sigma(t)}} \left\{ \widehat{W}(x, \nabla \boldsymbol{v}) - \boldsymbol{f} \cdot \boldsymbol{v} \right\} dx - \int_{\Gamma_N} \boldsymbol{g} \cdot \boldsymbol{v} \, ds$$

over the space

$$V_0(\Omega_{\Sigma(t)}, \Gamma_D) = \left\{ \boldsymbol{v} \in W^{1,2}(\Omega_{\Sigma(t)}; \mathbb{R}^3) : \boldsymbol{v} = 0 \quad \text{on } \Gamma_D \right\}$$

Because $V_0(\Omega_{\Sigma(t_1)}, \Gamma_D) \subset V_0(\Omega_{\Sigma(t_2)}, \Gamma_D)$ if $t_1 < t_2$, the following inequality holds

$$\mathcal{E}(\boldsymbol{u}(t_1); \Omega_{\Sigma(t_1)}, \boldsymbol{f}, \boldsymbol{g}) \geq \mathcal{E}(\boldsymbol{u}(t_2); \Omega_{\Sigma(t_2)}, \boldsymbol{f}, \boldsymbol{g}) \tag{4.1}$$

Then the released energy will serve as the drivinig force for the crack extension if the released energy exceeds the fracture resistance, that is, the crack Σ will grow if $\mathcal{F}(\Omega_{\Sigma(t)}, \boldsymbol{f}, \boldsymbol{g}) \geq 0$

$$\mathcal{F}(\Sigma(\cdot), \boldsymbol{f}, \boldsymbol{g}) \quad = \quad \mathcal{E}(\boldsymbol{u}(t); \Omega_{\Sigma(t)}, \boldsymbol{f}, \boldsymbol{g}) - \mathcal{E}(\boldsymbol{u}; \Omega_\Sigma, \boldsymbol{f}, \boldsymbol{g}) - \int_{\Sigma(t) \setminus \Sigma} \gamma_R \, ds \tag{4.2}$$

where γ_R is the resistance force per unit surface.

Remark 4.1 *Griffith[20, 21] considered a through thickness crack of lenghth ℓ, subjected to a uniform tensile stress σ_∞, at infinity. Griffith get the released strain energy W_1 by the crack*

$$W_1 = \frac{\pi \ell^2 \sigma_\infty^2}{4E} \begin{cases} 1 - \nu^2 & \textit{plain strain} \\ 1 & \textit{plain stress (generalized)} \end{cases}$$

where E is Young's modulus and ν Poisson ratio (see also [55]). Using the energy balance

$$\frac{\partial}{\partial \ell} W_1 = \gamma_R \quad \Leftrightarrow \quad \frac{\ell \pi \sigma_\infty^2}{2E} = 2\gamma_S$$

where he used $\gamma_R = 2\gamma_S$ (surface energy). He get the length of crack

$$\ell = \frac{4\pi \gamma_S}{\sigma_\infty^2} \tag{4.3}$$

He substituted $\gamma_S = 5.6 \times 10^{-4} kg/cm$, $E = 7 \times 10^5 kg/cm^2$ and $\sigma_\infty = 700 kg/cm^2$ to ed the surface energy γ_S on the crack surface $\Sigma(t) \setminus \Sigma$ and set $\gamma_R = 2\gamma_S$ to (4.3) and get the rough size of $\ell \sim 1 \times 10^{-3} cm$.

We now introduce the concept of *energy release reate*

$$\mathcal{G}(\mathcal{L}; \Sigma(\cdot)) = \lim_{t \to +0} \frac{\mathcal{E}(\boldsymbol{u}; \Omega, \mathcal{L}) - \mathcal{E}(\boldsymbol{u}(t); \Omega_{\Sigma(t)}, \mathcal{L})}{|\Sigma(t) \setminus \Sigma|}, \quad \mathcal{L} = (\boldsymbol{f}, \boldsymbol{g}) \tag{4.4}$$

Now we call

$$V_\Sigma(t+0) = \lim_{\delta t \downarrow 0} |\Sigma(t+\delta t) \setminus \Sigma(t)|$$

the *speed of crack extension* $\{\Sigma(t)\}_{0\le t\le T}$ and using (4.4) we can rewrite (4.2) with

$$\mathcal{F}(\Sigma(\cdot),\mathcal{L}) \simeq t(\mathcal{G}(\mathcal{L};\Sigma(\cdot)) - \gamma_R)V_\Sigma(+0) \tag{4.5}$$

Definition 4.2 (Crack initiation) *Assume that the crack is at a stop in $t<0$. If $V_\Sigma(0+)>0$, then the crack Σ grow at $t=0$.*

Griffith's criterion is the following.

If $\mathcal{G}(\mathcal{L};\Sigma(\cdot)) \ge \gamma_R$, then $V_\Sigma(+0)>0$.

Remark 4.3 *The inequality (4.1) is valid only if $\mathcal{L}(t)=\mathcal{L}$ for $t\ge 0$, where $\mathcal{L}(t)=(\boldsymbol{f}(t),\boldsymbol{g}(t))$. Because we can construct examples in which (4.1) holds and the stress intensity $K_I(t)$ decrease when $\mathcal{L}(t)\neq\mathcal{L}$. By this reason, Griffith's criterion is true in crack initiation, but*

Theorem 4.4

$$\mathcal{G}(\mathcal{L};\Sigma(\cdot)) = J_\omega(\boldsymbol{u},\boldsymbol{\mu}_\phi)\left(\int_{\partial\Sigma} v_\phi(\gamma)\,d\gamma\right)^{-1} \tag{4.6}$$

where

$$v_\phi(\gamma) = \left\langle \frac{d\phi_t}{dt}(\gamma)\bigg|_{t=0}, \boldsymbol{e}_1(\gamma)\right\rangle_\Pi$$

and $\boldsymbol{\mu}_\phi$ the parallel extension

$$\boldsymbol{\mu}_\phi(x) = F_{\partial\Sigma}(\gamma(x), \lambda_1(x)+v_\phi(\gamma(x)), \zeta(x))$$

where $<\cdot,\cdot>_\Pi$ denote the inner product on tangent space of Π.

Refer [43] in linear case, and use Theorem 3.3 in non-linear case when $h_t(\gamma) = h(\gamma)t$.

Since the mappings for $h\in C^1(\partial\Sigma)$

$$\begin{array}{rcl} h & \mapsto & \boldsymbol{\mu}_h(x) = F_{\partial\Sigma}(\gamma(x),\lambda_1(x)+h(\gamma(x)),\lambda_3(x)) \\ \boldsymbol{\mu}_h & \mapsto & J_\omega(\boldsymbol{u},\boldsymbol{\mu}_h) \end{array}$$

are linear, we can write

$$[h\mapsto J_\omega(\boldsymbol{u},\boldsymbol{\mu}_h)] = \langle \mathcal{K}(\gamma), h(\gamma)\rangle_{\partial\Sigma}$$

We assume that $\mathcal{K}\in C(\partial\Sigma)$. The dual space of $C(\partial\Sigma)$ is Radon measure on $\partial\Sigma$, since $\partial\Sigma$ is compact[5, Chap.III-2.2]. containig

$$\delta_{\lambda_0} = \begin{cases} 1 & \text{if } \lambda=\lambda_0 \\ =0 & \text{if } \lambda\neq\lambda_0 \end{cases} \qquad \int_{\partial\Sigma}\delta_{\lambda_0}\,d\gamma = 1$$

We put $Ra(\partial\Sigma) = \left\{\lambda:\ \lambda \text{ is radon measure on } \partial\Sigma,\ \int_{\partial\Sigma}\lambda\,d\gamma = 1\right\}$. The criterion become; Find $\lambda_{\max}\in Ra(\partial\Sigma)$ such that

$$\langle\mathcal{K}(\gamma),\lambda_{\max}(\gamma)\rangle_{\partial\Sigma} = \max_{\lambda\in Ra(\partial\Sigma)}\langle\mathcal{K}(\gamma),\lambda(\gamma)\rangle_{\partial\Sigma} \ge R_C$$

We can easily show by taking $\lambda=\gamma_{\max}$ the following

$$\max_{\lambda\in Ra(\partial\Sigma)}\langle\mathcal{K}(\gamma),\lambda(\gamma)\rangle_{\partial\Sigma} = \mathcal{K}(\gamma_{\max}), \mathcal{K}(\gamma_{\max}) = \max_{\gamma\in\partial\Sigma}\mathcal{K}(\gamma)$$

This means that the crack extends if $\mathcal{K}(\gamma_{\max})\ge\gamma_R$.

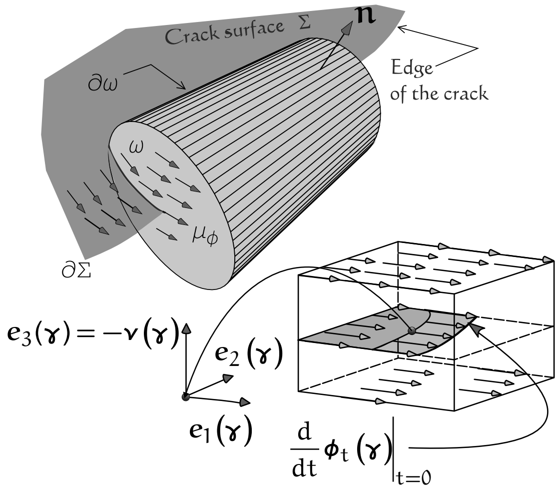

Figure 10: field of view ω and vector field $\boldsymbol{\mu}_\phi$

4.2 Griffith-Irwin theory

In fracture mechanics, they consider the stress near the edge $\partial\Sigma$ will behave like the plate which is perpendicular to $\partial\Sigma$. By 2-dimensional analysis, they derive 3 modes near $\partial\Sigma$, as follows.

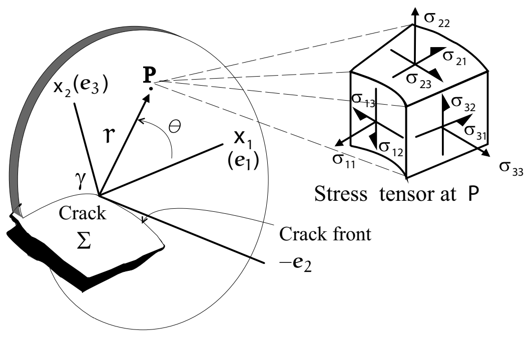

At the point $(\lambda, \boldsymbol{x}')$, $\boldsymbol{x}' = (x_1, x_2)$ on the plate, the following exapansion will hold

$$\begin{aligned} \boldsymbol{u}(\gamma, \boldsymbol{x}') &= \sum_{i=1}^{3} \boldsymbol{S}_i^C(\gamma, (r, \theta)) + \text{higher order of } r, && (4.7) \\ \boldsymbol{S}_i^C(\gamma, (r, \theta)) &= \frac{K_i(\gamma)}{2\mu}\sqrt{\frac{r}{2\pi}}\boldsymbol{\Phi}_i(\theta) \quad \text{for } i = 1, 2; && (4.8) \\ \boldsymbol{S}_3^C(\gamma, (r, \theta)) &= \frac{2K_3(\gamma)}{\mu}\sqrt{\frac{r}{2\pi}}\Phi_3(\theta)\boldsymbol{e}_2 && (4.9) \end{aligned}$$

where the constant $K_i(\gamma)$ for $\gamma \in \partial\Sigma$ are called the *stress intensity factors* and

$$\mathbf{\Phi}_1(\theta) = \begin{bmatrix} \varphi_{11}(\theta) \\ \varphi_{12}(\theta) \\ 0 \end{bmatrix} = \begin{bmatrix} \cos\frac{\theta}{2}\left(\kappa - 1 + 2\sin^2\frac{\theta}{2}\right) \\ \sin\frac{\theta}{2}\left(\kappa + 1 - 2\cos^2\frac{\theta}{2}\right) \\ 0 \end{bmatrix} \tag{4.10}$$

$$\mathbf{\Phi}_2(\theta) = \begin{bmatrix} \varphi_{21}(\theta) \\ \varphi_{22}(\theta) \\ 0 \end{bmatrix} = \begin{bmatrix} \sin\frac{\theta}{2}\left(\kappa + 1 + 2\cos^2\frac{\theta}{2}\right) \\ -\cos\frac{\theta}{2}\left(\kappa - 1 - 2\sin^2\frac{\theta}{2}\right) \\ 0 \end{bmatrix} \tag{4.11}$$

$$\Phi_3(\theta) = \sin\frac{\theta}{2} \tag{4.12}$$

where $\kappa = (3-\nu)/(1+\nu)$ with the Poisson radio ν.

The constants $K_i(\gamma)$, $i = 1, 2, 3$ for each $\gamma \in \partial\Sigma$ exress the modes of following manner.

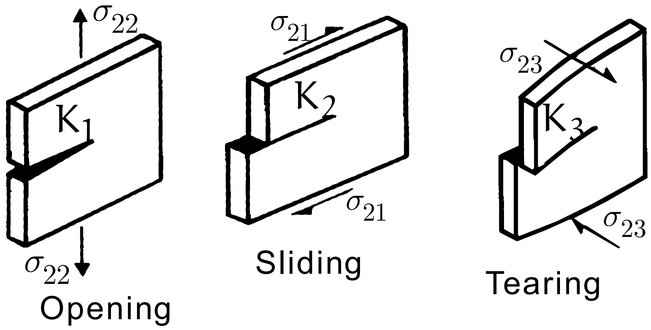

Using the asymptotic expansions in (4.7), we can derive under rough consideration

$$\mathcal{K}(\gamma) \simeq \frac{1}{E}\left(K_1^2(\gamma) + K_2^2(\gamma)\right) + \frac{1}{2G}K_3^2(\gamma) \quad \gamma \in \partial\Sigma$$

where E, G denotes Young's modulus and shear modulus, respectively. Here $\simeq$ become $=$ in the case of the homogeneous isotropic elastic plane stress (see e.g.[54] and [19, 46] for mathematical result).

Remark 4.5 *The calculations in (4.7)-(4.12) are made in 2D case (homogeneous isotropic elastic plane), so asymptotic expansion in 3-dimensional case will be open in mathematical view point.*

4.3 Crack path

In fracture mechanics, crack paths are calculated by means of broken line paths, that is, we need the *direction* and length (See [56, Chapter 7] for detail). We discuss them with the following simple example: For the straight initial crack Σ and the virtual kinked crack extension

$$\Sigma_\alpha(t) = \Sigma \cup \delta\Sigma(t), \quad \delta\Sigma^\alpha(t) = \{(x, y);\ x = l\cos\alpha,\ y = l\sin\alpha,\ 0 \le l \le t\},$$

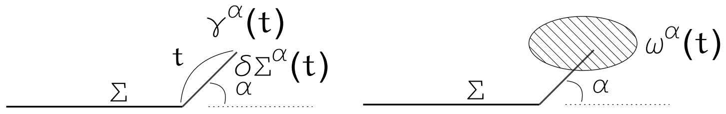

Figure 11: Kinked crack extension

There are famous criterions for the direction of crack extension:

Maximum energy release rate criterion: Find α^* which take the maximum value of $[\alpha \mapsto \mathcal{G}(\mathcal{L}; \Sigma^\alpha(\cdot))]$ on $-\pi < \alpha < \pi$.

Local symmetry criterion: Find the angle $\alpha^\#$ that satisfies the condition $K_{2,\alpha^\#}(\gamma(+0)) = 0$.

Maximum stress criterion: Find α^{**} such that

$$\sigma_{\alpha^{**}} = \max_\theta \sigma_\theta \quad \text{and } \sigma_{r\alpha^{**}} = 0. \tag{4.13}$$

Consider the open neighborhood $\omega^\alpha(t)$ of the crack tip $\gamma^\alpha(t) = (t\cos\alpha, t\sin\alpha)$ as shown in Fig.11.

By mean value theorem, there is a number $0 < \tau < t$ such that

$$\begin{aligned} \mathcal{E}(\boldsymbol{u}; \Omega_\Sigma, \mathcal{L}) - \mathcal{E}(\boldsymbol{u}^\alpha(t); \Omega_{\Sigma^\alpha(t)}, \mathcal{L}) &= tJ_{\omega^\alpha(\tau)}(\boldsymbol{u}^\alpha(\tau), \boldsymbol{\mu}_\alpha) \\ \boldsymbol{\mu}_\alpha &= \boldsymbol{e}_1\cos\alpha + \boldsymbol{e}_2\sin\alpha \end{aligned}$$

Hence we have the relation

$$\begin{aligned} \mathcal{G}_\Omega(\mathcal{L}; \Sigma(\cdot)) &= \lim_{\tau\to 0} \lim_{|\omega^\alpha(\tau)|\to 0} J_{\omega^\alpha(\tau)}(\boldsymbol{u}(\tau); \boldsymbol{\mu}_\alpha) \\ &= \lim_{\tau\to 0} \frac{1}{E'}\left(K_1(\gamma^\alpha(\tau))^2 + K_2(\gamma^\alpha(\tau))^2\right) \\ &= \frac{1}{E'}\left(K_1(\gamma,\alpha)^2 + K_2(\gamma,\alpha)^2\right) \end{aligned}$$

where $K_l(\gamma, \alpha) = \lim_{\tau\to 0} K_l(\gamma^\alpha(\tau)), l = 1, 2$. By Maximum energy release rate criterion, we have

$$0 = K_1(\gamma, \alpha^*)\frac{d}{d\alpha}K_1(\gamma, \alpha^*) + K_2(\gamma, \alpha^*)\frac{d}{d\alpha}K_2(\gamma, \alpha^*)$$

If $\alpha^* \simeq 0$, then $K_l(\gamma, \alpha^*) \simeq \tilde{K}_l(\gamma, \alpha^{**}), l = 1, 2$, where α^{**} is the angle obtained by Maximun stess criterion and $\tilde{K}_l(\gamma, \alpha)$ is introduced in [49]

$$\tilde{K}_1(\gamma, \alpha) = \lim_{r\to 0}(2\pi r)^{-1/2}\sigma_\theta(\boldsymbol{u})|_{\theta=\alpha}, \quad \tilde{K}_2(\gamma, \alpha) = \lim_{r\to 0}(2\pi r)^{-1/2}\sigma_{r\theta}(\boldsymbol{u})|_{\theta=\alpha}, \tag{4.14}$$

which is expressed as follows,

$$\begin{aligned}
\tilde{K}_l(\gamma,\alpha) &= \tilde{F}_{l1}(\alpha)K_1(\gamma)+\tilde{F}_{l2}(\alpha)K_2(\gamma), \quad l=1,2, \\
\tilde{F}_{11}(\theta) &= \frac{3}{4}\cos(\theta/2)+\frac{1}{4}\cos(3\theta/2), \\
\tilde{F}_{12}(\theta) &= -\frac{3}{4}\sin(\theta/2)-\frac{3}{4}\sin(3\theta/2), \\
\tilde{F}_{21}(\theta) &= \frac{1}{4}\sin(\theta/2)+\frac{1}{4}\sin(3\theta/2), \\
\tilde{F}_{22}(\theta) &= \frac{1}{4}\cos(\theta/2)+\frac{3}{4}\cos(3\theta/2).
\end{aligned} \tag{4.15}$$

Maximum stress criterion is equivalent to find α^{**} such that

$$\tilde{K}_1(\gamma,\alpha^{**})=\max_{-\pi\le\alpha\le\pi}\tilde{K}_1(\gamma,\alpha), \qquad K_2(\gamma,\alpha^{**})=0$$

Moreover

$$\begin{aligned}
\frac{d}{d\alpha}\left(\tilde{K}_1(\gamma,\alpha)^2+\tilde{K}_2(\gamma,\alpha)^2\right)\Big|_{\alpha=\alpha^{**}} &= 2\tilde{K}_1(\gamma,\alpha^{**})\,\frac{d}{d\alpha}\tilde{K}_1(\gamma,\alpha)\Big|_{\alpha=\alpha^{**}} \\
&\quad +2\tilde{K}_2(\gamma,\alpha^{**})\,\frac{d}{d\alpha}\tilde{K}_2(\gamma,\alpha)\Big|_{\alpha=\alpha^{**}}=0
\end{aligned}$$

The difference between $K_l(\alpha,\gamma)$ and $\tilde{K}_l(\gamma,\alpha)$ will be

$$K_l(\alpha,\gamma)-\tilde{K}_l(\gamma,\alpha)=O(\alpha^2),\ l=1,2$$

using the result[1].

5 Shape optimization

In this section, we consider the perturbation $\Gamma(t)=\partial\Omega(t)$ of boundary and Joint $\Gamma(t)_{D(t)}\cap\Gamma(t)_{N(t)}$.

5.1 Mixed boundary value problem

Let us consider Poisson equation with Dirichlet condition on $\Gamma_D\subset\Gamma$ and Neumann condition on $\Gamma_N=\Gamma\setminus\overline{\Gamma_D}$, and perturbation $\Gamma(t)=\{\phi_t(x);\ x\in\Gamma\}$

$$\begin{aligned}
-\Delta u(t) &= f \quad \text{in } \Omega(t) \\
u(t) &= 0 \quad \text{on } \Gamma_D(t) \\
\frac{\partial u(t)}{\partial n} &= 0 \quad \text{on } \Gamma_N(t)
\end{aligned}$$

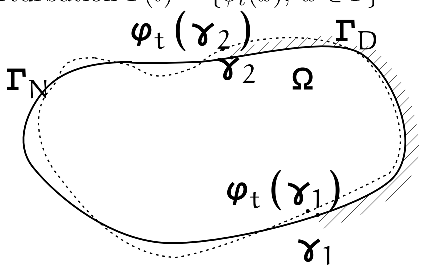

$u(t)$ is disintegrated by singular and regular terms

$$\sum_{j=1}^{2} K(\gamma_j(t))\eta_j(r_j)S(r_j(t),\theta_j(t)) \\ +u_R(t), \qquad (5.1) \\ u_R(t) \in H^2(\Omega(t)) \\ S(r,\theta) = \sqrt{r}\sin(\theta/2).$$

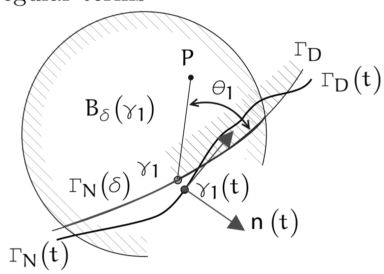

$K(\gamma_i), i = 1,2$: constants depending on Γ, f etc.
$(r_i(t), \theta_i(t))$, $i = 1,2$: local polar coordinate with origin at $\gamma_i(t)$ and $\gamma_i = \gamma_i(0)$

$$\begin{aligned} R_\Omega(\boldsymbol{u},\boldsymbol{\mu}_\varphi) &= R_{\Omega\setminus(B_\delta(\gamma_1)\cup B_\delta(\gamma_2))}(\boldsymbol{u},\boldsymbol{\mu}_\varphi) + \sum_{j=1}^{2} R_{B_\delta(\gamma_j)}(\boldsymbol{u},\boldsymbol{\mu}_\varphi) \\ &= -P_{\Omega\setminus(B_\delta(\gamma_1)\cup B_\delta(\gamma_2))}(\boldsymbol{u},\boldsymbol{\mu}_\varphi) + \sum_{i=1}^{2} J_{B_\delta(\gamma_j)}(\boldsymbol{u},\boldsymbol{\mu}_\varphi) \\ P_{B_\delta(\gamma_i)}(\boldsymbol{u},\boldsymbol{\mu}_\varphi) &= \frac{\pi}{8}K(\gamma_i)^2 \mathrm{sgn}_D\boldsymbol{\tau}(\gamma_i)(\boldsymbol{\mu}_\varphi(\gamma_i)\cdot\boldsymbol{\tau}(\gamma_i)) \end{aligned}$$

where $\boldsymbol{\tau}$ denotes the unit tangential vector along $\partial\Omega$.

Theorem 5.1 *If the domain Ω has tha smooth boundary Γ, then*

$$\begin{aligned} &\frac{d}{dt}\mathcal{E}(u(t); f, \Omega(t))\Big|_{t=0} \\ &\quad = \lim_{\delta\to 0}\frac{1}{2}\int_{\Gamma_N(\delta)} (\partial_\tau u)^2(\boldsymbol{\mu}_\varphi\cdot\boldsymbol{n})ds \\ &\quad - \lim_{\delta\to 0}\frac{1}{2}\int_{\Gamma_D(\delta)} (\partial_n u)^2(\boldsymbol{\mu}_\varphi\cdot\boldsymbol{n})ds - \int_{\Gamma_N} fu(\boldsymbol{\mu}_\varphi\cdot\boldsymbol{n})ds \\ &\quad -\frac{\pi}{8}\sum_{i=1}^{2} K(\gamma_i)^2\mathrm{sgn}_D\boldsymbol{\tau}(\gamma_i)(\boldsymbol{\mu}_\varphi(\gamma_j)\cdot\boldsymbol{\tau}(\gamma_i)). \end{aligned}$$

where $\boldsymbol{\tau}$ stands for the unit tangent vector on Γ corresponds to the natural orientation on Γ, $\partial_\tau u = \nabla u - (\partial_n u)\boldsymbol{n}$ and $\mathrm{sng}_D\boldsymbol{\tau}(\gamma_i) = 1$ if $\boldsymbol{\tau}(\gamma_i)$ has the direction from Γ_N to Γ_D and otherwise $\mathrm{sng}\boldsymbol{\tau}(\gamma_i) = -1$.

5.2 Shape optimization

For a given domain Ω^0, let $u(\Omega^0)$ be the solution of boundary value problem. For domains Ω, consider the cost functional

$$J(\Omega) = \int_\Omega \hat{j}(x, u(\Omega), \nabla u(\Omega)) \quad \hat{j} \in C^2(\mathbb{R}^d, \mathbb{R}^m, \mathbb{R}^{m\times d})$$

Under the constraint $J^c(\Omega) = \text{constant}$, find the domain Ω^o

$$J(\Omega^{opt}) \le J(\Omega^0)$$

The problem is to find *better shape* Ω^{opt} than Ω^0 using the const function. In real problem, there would be many constraints, so that we can find unique minimizer. However, in mathematical situation, we suppose only few constraints, for example, the volume(area) $|\Omega|$ of Ω is constant.

5.2.1 Procedure

1. Shape sensitivity: For perturbation $\Omega(t) = \varphi_t(\Omega^0), 0 \le t \ll 1$, find the shape gradient $G(\Omega^0)$,

$$\frac{d}{dt}J(\Omega(t)) = \langle G(\Omega^0), \boldsymbol{\mu}_\varphi \rangle$$

2. Minimum search: H1 gradient method(Azegami's method): Find the vector field $\boldsymbol{\mu}^0$ such that

$$\begin{aligned} b_{\Omega^0}(\boldsymbol{\mu}, \boldsymbol{\eta}) &= \int_{\Omega^0} \sum_{i=1}^{d} \{\nabla \mu_i \nabla \eta_i + \mu_i \eta_i\} \qquad \forall \boldsymbol{\mu}, \boldsymbol{\eta} \in H^1(\mathbb{R}^d; \mathbb{R}^d) \\ b_{\Omega^0}(\boldsymbol{\mu}^0, \boldsymbol{\eta}) &= -\langle G(\Omega^0), \boldsymbol{\eta} \rangle \quad \forall \boldsymbol{\eta} \in H^1(\Omega^0; \mathbb{R}^d) \cap \{\text{fix condi.}\} \end{aligned}$$

3. Constraint: Use Lagrange multiplier λ, such as

$$\begin{aligned} b_{\Omega^0}(\boldsymbol{\mu}^c, \boldsymbol{\eta}) &= -\langle G^c(\Omega^0), \boldsymbol{\eta} \rangle \quad \forall \boldsymbol{\eta} \in H^1(\Omega^0; \mathbb{R}^d) \cap \{\text{fix condi.}\} \\ \Omega^{opt} &= \{x + \epsilon_0 \boldsymbol{\mu}^{opt}(x) : x \in \Omega^0\} \quad \boldsymbol{\mu}^{opt} = \boldsymbol{\mu}^0 + \lambda \boldsymbol{\mu}^c \end{aligned}$$

5.3 Energy optimization

Problem: Find the solution $\boldsymbol{u}^{i-1}$ such that

$$\int_\Omega \delta\widehat{W}(x, u^{i-1}, \nabla u^{i-1})[v]dx = \int_\Omega fv\, dx \quad \forall v \in V(\Omega, \Gamma_D)$$

Azegami's method[4]: Find a vector field $\boldsymbol{\mu}_0^i$ such that

$$\begin{aligned} b_{\Omega^{i-1}}(\boldsymbol{\mu}_0^i, \boldsymbol{\eta}) &= R_{\Omega^{i-1}}(\boldsymbol{u}^{i-1}, \boldsymbol{\eta}) + \int_{\Gamma_N} f u^{i-1}(\boldsymbol{\eta} \cdot \boldsymbol{n}) ds \quad \forall \boldsymbol{\eta} \\ b_{\Omega^{i-1}}(\boldsymbol{\mu}, \boldsymbol{\eta}) &= \int_\Omega \{\nabla \boldsymbol{\mu} : \nabla \boldsymbol{\eta} + \boldsymbol{\mu} \cdot \boldsymbol{\eta}\}\, dx \\ &\quad \text{with conditions for } \boldsymbol{\mu}_0^i \end{aligned}$$

Find $\boldsymbol{\mu}_1^i$ for the constraint with same conditions for $\boldsymbol{\mu}_1^i$,

$$b_{\Omega^{i-1}}(\boldsymbol{\mu}_1^i, \boldsymbol{\eta}) = -\int_{\Omega^{i-1}} \mathrm{div} \boldsymbol{\eta}\, dx \quad \forall \boldsymbol{\eta}$$

Lagrange multiplier: $\lambda = -(J^1(\Omega^{i-1}) - J^1(\Omega^0) + \ell_0)/\ell_1$

$$\ell_0 = \int_{\Omega^{i-1}} \mathrm{div} \boldsymbol{\mu}_0^i\, dx, \quad \ell_1 = \int_{\Omega^{i-1}} \mathrm{div} \boldsymbol{\mu}_1^i\, dx$$

Better shape: $\boldsymbol{V}^i = \boldsymbol{\mu}_0^i + \lambda\boldsymbol{\mu}_1^i$, put the new shape with a small number $0 < \epsilon^i$

$$\Omega^i = \{\boldsymbol{x} + \epsilon^i \boldsymbol{V}^i(\boldsymbol{x}) : \boldsymbol{x} \in \Omega^{i-1}\} \tag{5.2}$$

By Tayler's expansion w.r.t. $\Omega(\epsilon) = \{x + \epsilon\boldsymbol{\mu}_0^i(x) : x \in \Omega^{i-1}\}$

$$\begin{aligned}
\mathcal{E}(u^i; f, \Omega^i) &= \mathcal{E}(u; f, \Omega^{i-1}) + t\frac{d}{d\epsilon}\mathcal{E}(u(\epsilon); f, \Omega(\epsilon))\Big|_{\epsilon=0} + o(\epsilon) \\
&= \mathcal{E}(u^{i-1}; f, \Omega^{i-1}) - tb_{\Omega^{i-1}}(\boldsymbol{\mu}_0^i, \boldsymbol{\mu}_0^i) + o(\epsilon) \\
&= \mathcal{E}(u^{i-1}; f, \Omega^{i-1}) - t\|\boldsymbol{\mu}_0^i\|_{1,\Omega^{i-1}} + o(\epsilon)
\end{aligned}$$

5.3.1 Example (Energy optimization)

Consider the domain Ω^0

$$\Omega_0 = \left\{(x_1, x_2) : x_1^2 + x_2^2 < 1\right\}, \Gamma_D = \{(x_1, x_2) : x_1^2 + x_2^2 = 1, x_2 > 0\}$$

We calculate two cases: *Case1*: Γ_D is fixed. *Case2*: Γ_D is changed.

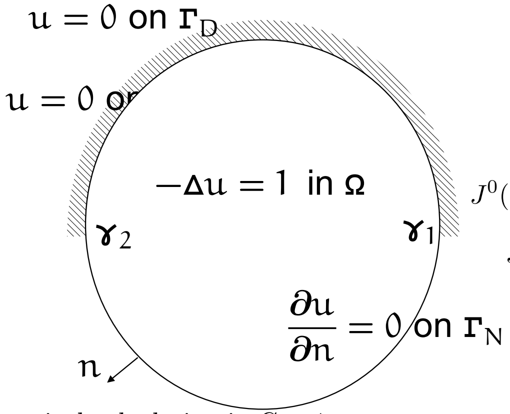

$$\begin{aligned}
J^0(u(\Omega)) &= \int_\Omega \left\{\frac{1}{2}|\nabla u|^2 - u\right\} dx \\
J^1(\Omega) &= |\Omega| \quad \text{(constant)}
\end{aligned}$$

Numerical calculation in Case1:

contour map of u^0

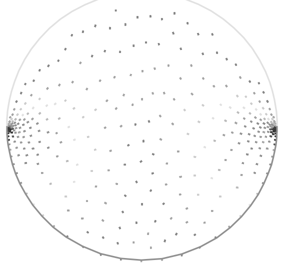

vector diagram of V^0

contour map of u^1

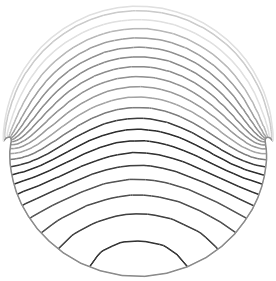

contour map of u^{10}

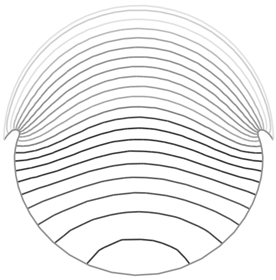

contour map of u^{20}

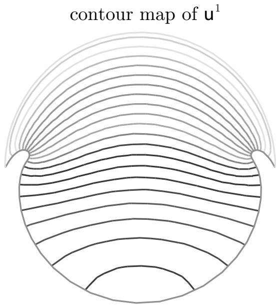

contour map of u^{30}

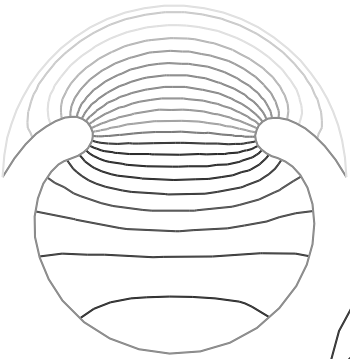

contour map of u^{70}

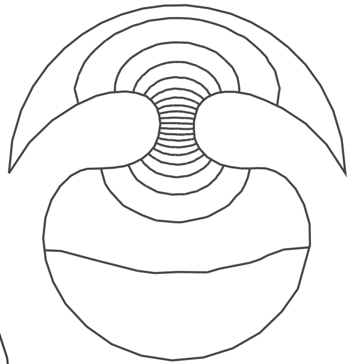

contour map of u^{90}

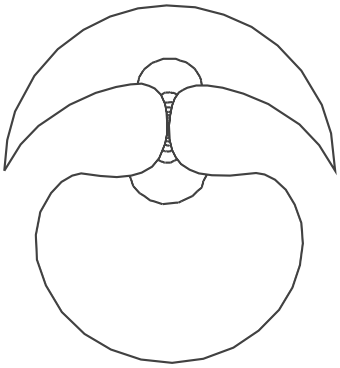

contour map of u^{93}

Numerical calculation in Case2:

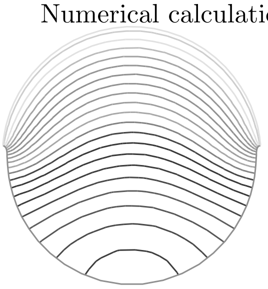

contour map of u^{5}

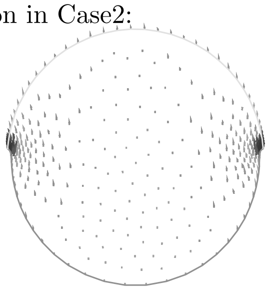

vector diagram of V^{5}

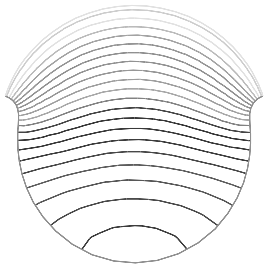

contour map of u^{20}

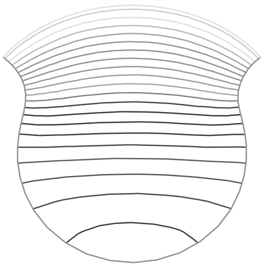

contour map of u^{40}

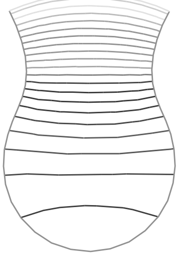

contour map of u^{60}

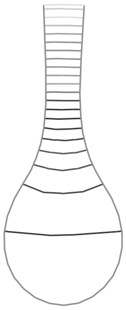

contour map of u^{75}

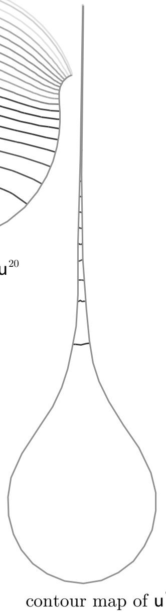

contour map of u^{78}

5.4 Mean compliance problem

The problem is considered in the variational problem

$$\begin{aligned} a_\Omega(u(\Omega), v) &= \ell_\Omega(v) \qquad \forall v \in v(\Omega) \\ \mathcal{E}(u(\Omega); \Omega, \ell) &= \tfrac{1}{2} a_\Omega(u(\Omega), u(\Omega)) - \ell_\Omega(u(\Omega)) \end{aligned}$$

and means a stiffness maximization problem for the shape optimization with respect to $J(\Omega) = \ell_\Omega(u(\Omega))$. The cost function is equal to

$$J(\Omega) = -2\mathcal{E}(u(\Omega); \Omega, \ell)$$

by which we can use GJ-integral at shape sensitivity

$$\begin{aligned} \frac{d}{dt} J(\Omega(t))\bigg|_{t=0} &= -2\,\frac{d}{dt}\mathcal{E}(u(\Omega(t)); \Omega, \ell)\bigg|_{t=0} \\ &= 2R_\Omega(u, \boldsymbol{\mu}_\varphi) + 2\int_{\partial\Omega} f \cdot u,\, dx \end{aligned}$$

Here, in the case that $\ell(v) = \int_{\Gamma_N} g \cdot v\, ds$, the part Γ_N is fixed, that is, $\boldsymbol{\mu}^0 = \boldsymbol{\mu}^c = \boldsymbol{\eta} = 0$ on Γ_N

Elasticity: Find the displacement $\boldsymbol{u}^{i-1}$ in the reference configuration Ω^{i-1}.
Azegami's method : Find a vector field $\boldsymbol{\mu}_0^i$ such that

$$b_{\Omega^{i-1}}(\boldsymbol{\mu}_0^i, \boldsymbol{\eta}) = -2R_{\Omega^{i-1}}(\boldsymbol{u}^{i-1}, \boldsymbol{\eta}) - 2\int_{\Gamma_N} f u^{i-1}(\boldsymbol{\eta}\cdot\boldsymbol{n}) ds \quad \forall\boldsymbol{\eta}$$

with conditions for $\boldsymbol{\mu}_0^i$

Find $\boldsymbol{\mu}_1^i$ for the constraint with same conditions for $\boldsymbol{\mu}_1^i$,

$$b_{\Omega^{i-1}}(\boldsymbol{\mu}_1^i, \boldsymbol{\eta}) = -\int_{\Omega^{i-1}} \mathrm{div}\boldsymbol{\eta}\, dx \quad \text{for all } \boldsymbol{\eta}$$

Lagrange multiplier: $\lambda = -(J^1(\Omega^{i-1}) - J^1(\Omega^0) + \ell_0)/\ell_1$

$$\ell_0 = \int_{\Omega^{i-1}} \mathrm{div}\boldsymbol{\mu}_0^i\, dx, \quad \ell_1 = \int_{\Omega^{i-1}} \mathrm{div}\boldsymbol{\mu}_1^i\, dx$$

Better shape: $\boldsymbol{V}^i = \boldsymbol{\mu}_0^i + \lambda\boldsymbol{\mu}_1^i$, put the new shape with a small number $0 < \epsilon^i$

$$\Omega^i = \{\boldsymbol{x} + \epsilon^i \boldsymbol{V}^i(\boldsymbol{x}) : \boldsymbol{x} \in \Omega^{i-1}\} \tag{5.3}$$

5.4.1 Example (cantilever)

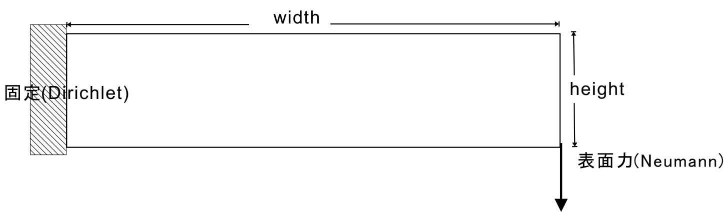

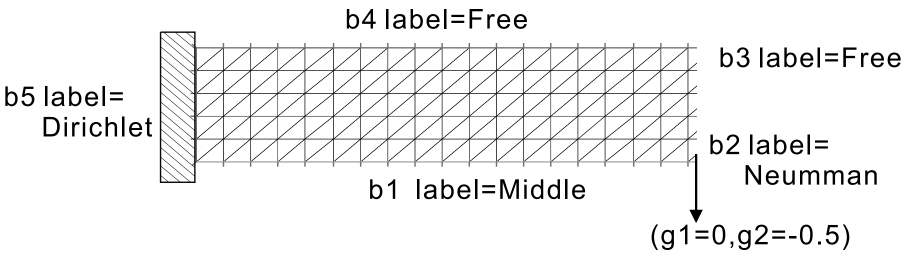

Iteration 4, Compliance 1.5809, Volume 10.0498

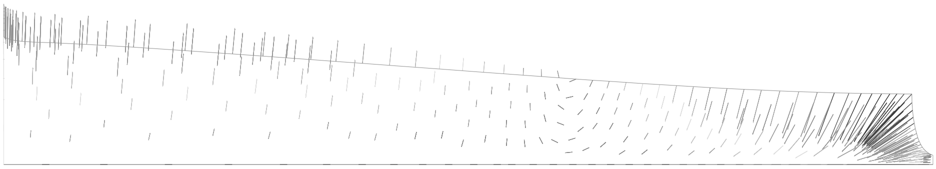

Iteration 5, Compliance 1.5174, Volume 10.0555

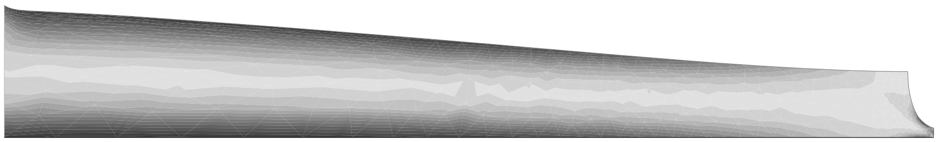

Iteration 47, Compliance 1.38367, Volume 10.0687

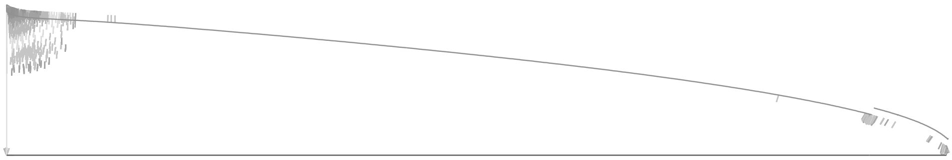

Iteration 48, Compliance 1.38367, Volume 10.0687

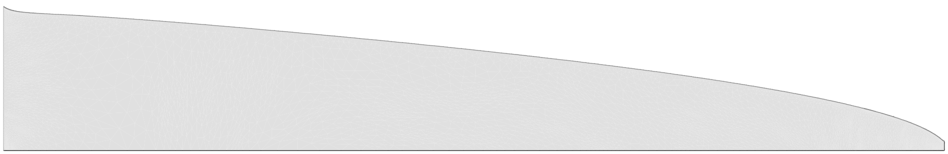

5.4.2 Example (cantilever by Allier[3])

Initial shape, Compliance 5.49664, Volume 39.8569

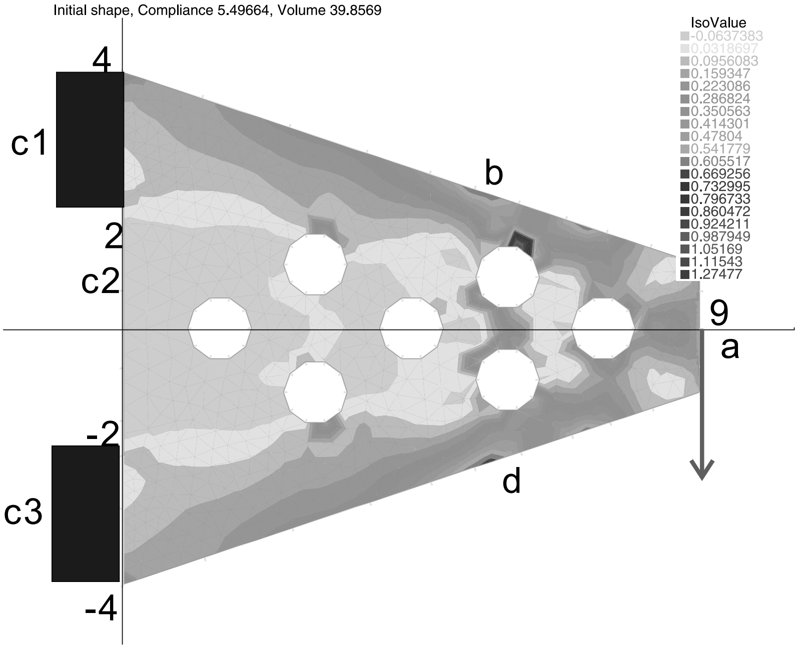

5.4.3 Example (cantilever by Allier[3], no hole)

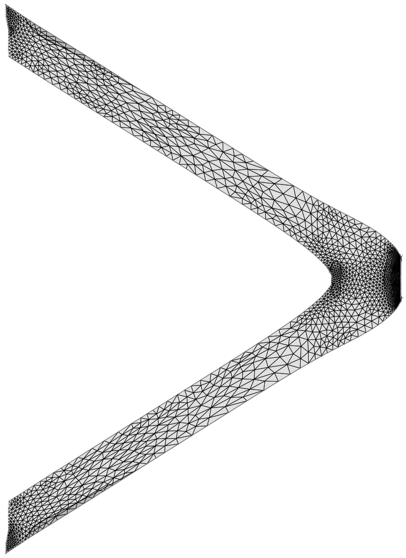

5.4.4 Example (cantilever by Allier[3], 7 holes)

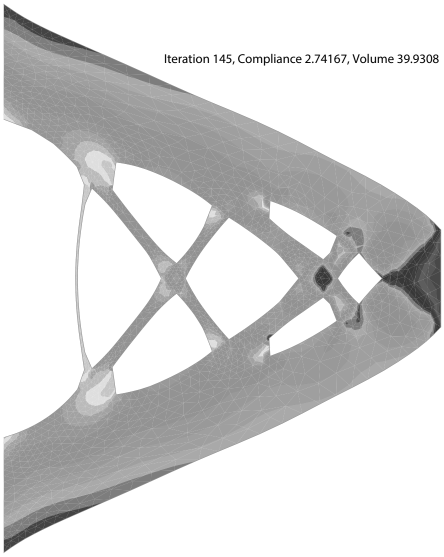

5.5 Other cost functionals

Cost functional is given by the density $\hat{j}(z)$, $z \in \mathbb{R}^m$

$$J(\Omega) = \int_\Omega \hat{j}(u(\Omega))dx$$

For example, to find $\Omega^{opt}, u(\Omega^{opt})$ becomes near to $u_d(m=1)$, in this case, we put $\hat{j}(z)=(z-u_d)^2$

$$
\begin{aligned}
\left.\frac{d}{dt}J(\Omega(t))dx\right|_{t=0} &= \left.\frac{d}{dt}\int_{\Omega(t)}\hat{j}(u(t))\right|_{t=0} \\
&= \int_\Omega \left\{\nabla_z\hat{j}(u)\hat{j}(u)(\mu_\varphi\cdot n)dotu+\hat{j}(u)\mathrm{div}\boldsymbol{\mu}_\varphi)\right\}dx \\
&= \int_\Omega \left\{\nabla_z\hat{j}(u)(\dot{u}-\nabla u\cdot\boldsymbol{\mu}_\varphi\right\}dx+\int_{\partial\Omega^0}\hat{j}(u)(\mu_\varphi\cdot n)ds \\
&= \int_{\Omega^0}(\nabla_z\hat{j})(u)\cdot u' dx+\int_{\partial\Omega^0}\hat{j}(u)(\mu_\varphi\cdot n)ds
\end{aligned}
$$

For example, $\hat{j}(z)=(z-u_d)^2$, $\nabla\hat{j}=\hat{j}'=2z$.

5.5.1 Shape optimizer (adjoint variable method)

Let u^j be the solution of ajoint problem

$$
a_{\Omega^0}(u^j,v) = \int_{\Omega^0}(\nabla\hat{j})(u)\cdot v\,dx \qquad \forall v\in V(\Omega)
$$

then from Theorem 3.11 we have

$$
\begin{aligned}
\int_\Omega(\nabla\hat{j})(u)\cdot u'\,dx &= \delta R_{\Omega^0}(u,u^j;\boldsymbol{\mu}_\varphi)+\int_{\partial\Omega^0}f\cdot u^j(\boldsymbol{\mu}_\varphi\cdot n)\,ds \\
J'(\Omega^0) &= \delta R_{\Omega^0}(u,u^j;\boldsymbol{\mu}_\varphi)+\int_{\partial\Omega^0}\left\{f\cdot u^j+\hat{j}(u)\right\}(\boldsymbol{\mu}_\varphi\cdot n)\,ds
\end{aligned}
$$

5.5.2 Example ($\hat{j}(z)=z^2$)

Dirichlet condition on upper semicircle, and Neumann condition on lower semicircle. All circle change is permitted.

$$
\begin{aligned}
-\Delta u &= 2 && \text{in } \Omega \\
u &= 0 && \text{on upper semicircle} \\
\partial u/\partial n &= 0 && \text{on lower semicircle}\Gamma_N
\end{aligned}
$$

$i = 1$

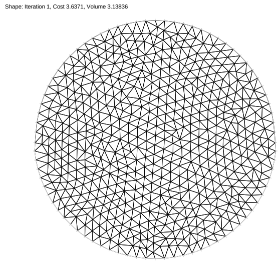

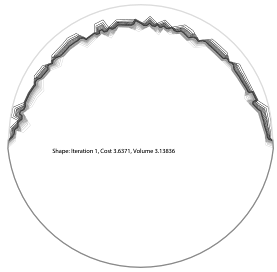

Ω^1 $\{\boldsymbol{x} : -0.2 < u(\boldsymbol{x}) < 0.2\}$

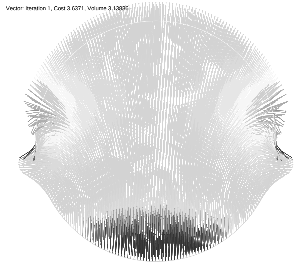

Vector field $\boldsymbol{\mu}^{opt}$
Cost= 3.6371

$i = 1000$

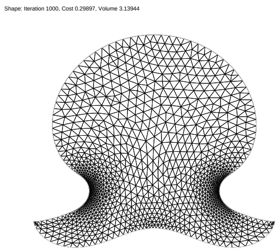

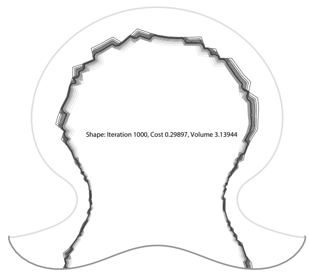

Ω^{1000} $\{\boldsymbol{x} : -0.2 < u(\boldsymbol{x}) < 0.2\}$

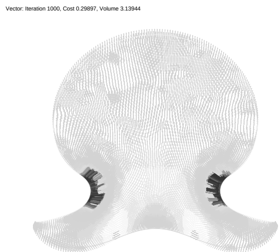

Vector field $\boldsymbol{\mu}^{opt}$
Cost= 0.29897
0.355013 when $i = 800$.

$i = 1000$

5.5.3 Example ($\hat{j}(z) = z^2$)

Upper semicircle is fixed.

$$\begin{aligned} -\Delta u &= 2 && \text{in } \Omega \\ u &= 0 && \text{on upper semicircle} \\ \partial u/\partial n &= 0 && \text{on lower semicircle}\Gamma_N \end{aligned}$$

$i = 1000$

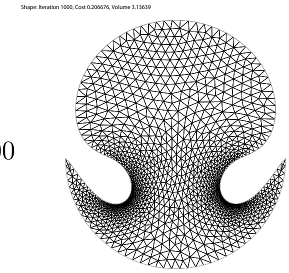

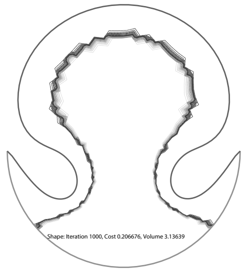

Ω^{1000} $\{\boldsymbol{x} : -0.2 < u(\boldsymbol{x}) < 0.2\}$

Vector field $\boldsymbol{\mu}^{opt}$
Cost= 0.206676
0.250123 when $i = 800$.

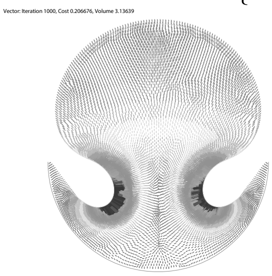

$i = 1000$

My deepest appreciation goes to Prof. Kimura, because joint work founded the new prospects to non-linear problems. I also owe a very important debt to Prof. Azegami who provided the knowledge on shape optimization.

References

[1] Amestoy, M. and Leblond J.B.: Crack paths in plane situation – II, Int. J. Solids Structures, 29(1992), 465–501.

[2] Adams, A.: Sobolev spaces (second ed.), Academic Press, 2003.

[3] Allaire, G. and Pantz, O.: Structural Optimization with FreeFem++, Structural and Multidisciplinary Optimization, 32(2006), 173–181. http://www.cmap.polytechnique.fr/ãllaire/freefem_en.html

[4] Azegami, H. and Wu, Z.: Domain Optimization Analysis in Linear Elastic Problems: Approach Using Traction Method, JSME International Journal Series A, 39 (2)(1996), 272-278.

[5] Bourbaki, N.: Elements of mathematics. Integration, Addison-Wesley, 1975.

[6] Budiansky, B. and J. R. Rice: Conservation laws and energy release rates, J. Appl. Mech., 40(1973), 201–203.

[7] Bui, H.D.: Fracture Mechanics, Springer, 2006.

[8] Chen, F. and R. T. Shield: Conservation laws in elasticity of the J-integral type, J. Appl. Math. Phys., 28(1977), 1–22.

[9] Cherepanov, G.P.: On Crack propagation in continuous media, Prikl. Math. Mekh., 31(1967), 476–493.

[10] Ciarlet, P.G.: Mathematical Elasticity Vol. 1. Three-Dimensional Elasticity, North-Holland, 1988.

[11] Dacorogna, B.: Direct methods in the calculus of variations 2nd Ed., Springer, 2008.

[12] Dautray, R. and Lions, J.-L.: Functional and Variational Methods, in Mathematical analysis and numerical methods for science and technology, Vol.2, Springer, 1985.

[13] Eshelby, J.D.: The continuum theory of lattice defects, Solid State Physics, 3(1956), pp. 79–144.

[14] Eringen, A.C.: Theory of micropolar elasticity, "Fracture" Vol. 2, Ed. by H. Liebowitz, Academic Press, New York·San Francisco·London, 621–729, 1968.

[15] Ern, A. and Guermond, J.-L.: Theory and Practice of Finite Elements, Springer, 2004.

[16] Fučik, S. and Kufner, A.: Nonlinear differential equations, Elsevier, 1980.

[17] Gelfand, I.M. and Fomin, S.V.: Calculus of Variations, English translation by R.A. Silverman. Englewood Cliffs, N.Y.: Prentice-Hall 1963.

[18] Grisvard, P.: Elliptic Problems in Non-smooth Domains, Pitman, Boston 1985.

[19] Grisvard, P.: Singularities in boundary value problems, Springer, 1992.

[20] Griffith, A. A.: The phenomena of rupture and fiow in solids, Phil. Trans. Ray. Soc. London, Series A(1920), 221, 163.

[21] Griffith, A. A.: The theory of rupture, Proc. of first Int. Ccng. for Applied Mechanics, Delft, 1924.

[22] Günther, W.: Über einige Randintegrale der Elastomechanik, Abh. Braunschw Wiss. Ges., 14(1962), 53-72.

[23] Hadamard, J.: Mémoire sur le probleme d'analyse relatif a l'equilibre des plaques élastiques encastrées, Oeuvres, 2(1968), 515–631.

[24] Haug, E.J., Choi, K.K.,Komkov V.: Design sensitivity analysis of structural systems, Academic Press, 1986.

[25] Hecht, F., Pironneau, O., Morice, J. Hyaric, A. Le and Ohtsuka, K.: FreeFem++, `http://www.freefem.org/ff++/`.

[26] Kaizu, S. and Azegami, H.: Optimal Shape Problems and Traction Method, Transactions of the Japan Society for Industrial and Applied Mathematics, 16(3)(2006) 277-290.

[27] Khludnev, A., Ohtsuka,K. and Sokolowski, J.: On derivative of energy functional for elastic bodies with cracks and unilateral conditions, Quarterly of Applied Mathematics, Vol. LX (2002), 99 – 109.

[28] Kimura, M. and Wakano, I.: New mathematical approach to the energy release rate in crack extension, Trans. Japan Soc. Indust. Appl. Math., 16(2006) 345–358. (in Japanese)

[29] Kimura, M. and Wakano, I.: Shape derivative of potential energy and energy release rate in fracture mechanics, Journal of Math-for-industry, 3(2011), A, 21–31.

[30] Knees, D.: Regularity results for quasilinear elliptic systems of power-law growth in nonsmooth domains –Boundary, transmission and crack problems–, PhD thesis, University of Stuttgart, 2005.

[31] Knees, D.: Griffith-formula and J-integral for a crack in a power-law hardening material, Math. Models Methods Appl. Sci., 16 (2006), 1723.

[32] Knees, D.: On the Energy Release Rate in Finite-Strain Elasticity, Mechanics of Advanced Materials and Structures, 15 (2008), 421–427.

[33] Knowles, J. and Sternberg, E.: On a class of conservation laws in linearized and finite elasticities, Arch. Rat. Mech. Anal., 44(1972), 187–211, 1972.

[34] Kupradze, V.D, Gegelia T. G., Basheleishvili M. O. and Burchuladze T. V.: Three-Dimeneional Problems of the Mathematical Theory of Elasticity and Thermoelasticity, North Holland, Amsterdam 1979.

[35] Milnor, J.: Morse theory, Princeton University Press, 1963.

[36] Nazarov, S. A.: Principle of virtual work and Rice weighting integrals. Mech. Solids, 1980, 64 – 67.

[37] J. Nečas, On domains of type N, Czechslovak Math. J. 12(1962), 274-287.

[38] Nečas, J.: Méthodes Directes en Th' eorie des Équations Elliptiques, Masson Éditeur, Paris, 1967

[39] Nečas, J. and Hlaváček,I.: Mathematical Theory of Elastic and Elasto-Plastic Bodies, An introduction, Elsevier, Amsterdam·Oxford·New York, 1981.

[40] Noether, E.: Invariante Variationsprobleme, Göttinger Nachrichten, Mathematisch-Physikalische Klasse, 2(1918), 235–257.

[41] Olver, P. J.: Conservation laws in elasticity I. General Results, Arch. Rat. Mech. Anal., 85(1984), 111–129.

[42] Olver, P. J.: Conservation laws in elasticity II. Linear homogeneous isotropic elasticitcs, Arch. Rat. Mech. Anal., 85(1984), 131–160.

[43] Ohtsuka, K: Generalized J-integral and three-dimensional fracture mechanics I. Hiroshima Math. J., Vol.11 (1981), 21-52.

[44] Ohtsuka, K.: Generalized J-integral and its applications I – Basic theory –. Japan J. Appl. Math. Vol.2, No.2 (1985), 329-350.

[45] Ohtsuka, K.: Generalized J-integral and three-dimensional fracture mechanics. II. Surface crack problems, Hiroshima Math. J., 1986, 16, no. 2, 327–352.

[46] Ohtsuka, K.: Mathematical aspects of fracture mechanics, Lecture Notes in Num. Appl. Anal., 13(1994), 39–59.

[47] 大塚厚二, 楕円型混合境界値問題における境界及び接合点に関する形状微分とその数値解析, 日本応用数理学会論文誌, 9(1999), pp.77–94

[48] Ohtsuka, K. and Khludnev,A.: Generalized J-integral method for sensitivity analysis of static shape design. Control & Cybernetics, Vol.29 (2000), 513-533.

[49] Ohtsuka, K.: Comparison of criteria on the direction of crack extension, Jour. Comp. Appl. Math., 149(2002), pp.335–339.

[50] 大塚厚二, グリーン関数の亀裂進展変分, 第 54 回理論応用力学講演会　講演論文集

[51] Ohtsuka, K., Shape optimization for partial differential equations/system with mixed boundary conditions, 講究録 1791, 2012, pp.172–181.

[52] Ohtsuka, K. and Kimura, M.: Differentiability of potential energies with a parameter and shape sensitivity analysis for nonlinear case: the p-Poisson problem, Japan J. Indust. Appl. Math., 29, 2012

[53] Rice, J.R.: A path-independent integral and the approximate analysis of strain concentration by notches and cracks, J. Appl. Mech., 35(1968), 379–386.

[54] Rice, J.R.: Mathematical analysis in the mechanics of fracture, in Chapter 3 of Fracture II (ed. H.Liebowitz), Academic Press, 192–311, 1968.

[55] Sih, G.C. and Liebowitz, H.: Mathematical theories of brittle fracture, in Chapter 1 of Fracture II (ed. H.Liebowitz), Academic Press, 67–190, 1968.

[56] Sumi, Y.: Mathematical and computational analysis of cracking formation, Springer, 2014.

「マス・フォア・インダストリ研究」シリーズ刊行にあたり

本シリーズは，平成 23 年 4 月に設立された九州大学マス・フォア・ インダストリ研究所(IMI)が，平成 25 年 4 月に共同利用・共同研究拠点「産業数学の先進的・基礎的共同研究拠点」として，文部科学大臣より認定を受けたことにともない刊行するものである．本シリーズでは，主として，マス・フォア・インダストリに関する研究集会の会議録，共同研究の成果報告等を出版する．　各巻はマス･フォア･インダストリの最新の研究成果に加え，その新たな視点からのサーベイ及びレビューなども収録し，マス・フォア・インダストリの展開に資するものとする．

平成 26 年 10 月
マス・フォア・インダストリ研究所
所長 福本康秀

Collaboration between theory and practice in inverse problems

マス・フォア・インダストリ研究 No.2, IMI, 九州大学
ISSN 2188-286X
発行日　2015 年 3 月 12 日
編　集　滝口孝志，藤原宏志
発　行　九州大学マス・フォア・インダストリ研究所
〒819-0395 福岡市西区元岡 744
九州大学数理・IMI 事務室
TEL 092-802-4402　FAX 092-802-4405
URL http://www.imi.kyushu-u.ac.jp/
印　刷　社会福祉法人　福岡コロニー
〒811-0119　福岡県糟屋郡新宮町緑ケ浜 1 丁目 11 番 1 号
TEL 092-962-0764　FAX 092-962-0768

シリーズ既刊

Issue	Author ／ Editor	Title	Published
マス・フォア・インダストリ研究　No.1	穴田 啓晃 安田 貴徳 Xavier Dahan 櫻井 幸一	Functional Encryption as a Social Infrastructure and Its Realization by Elliptic Curves and Lattices	26 February 2015

Institute of Mathematics for Industry
Kyushu University

九州大学マス・フォア・インダストリ研究所

〒819-0395 福岡市西区元岡744
URL http://www.imi.kyushu-u.ac.jp/